*Phil. Trans. R. Soc. Lond.* B **307**, 399–455 (1985) [ 399 ]
*Printed in Great Britain*

# THE GLIAL CELLS AND GLIA–NEURON RELATIONS IN THE BUCCAL GANGLIA OF *PLANORBIS CORNEUS* (L.): CYTOLOGICAL, QUALITATIVE AND QUANTITATIVE CHANGES DURING GROWTH AND AGEING

By V. W. PENTREATH[1], T. RADOJCIC,[1] L. H. SEAL[2] and E. K. WINSTANLEY[1]

[1] *Department of Biology, School of Life Sciences, University of Salford, Salford M5 4WT, U.K.*
[2] *Department of Biological Sciences, Manchester Polytechnic, Manchester M1 5GD, U.K.*

(*Communicated by E. G. Gray, F.R.S.* – *Received* 16 *December* 1983)

[Plates 1–15]

## CONTENTS

Buccal ganglia from snails ranging from embryos to 5.5 g adults (approximately five years old) were examined by light and electron microscopy. The glial cells are principally located around the neuron perikarya, between the blood and the neurons. Relatively few glial cells are located in the axon tracts and areas of neuropil within the core of the ganglion. The glia–neuron relations are established early in embryonic life and remain relatively constant throughout the life of the animal. The glial cells contain increased numbers of lysosomes and lipofuscin material with age. Some glial cells make up a distinct subpopulation that is specialized for the phagocytic ingestion of debris and nerve terminals in the core of the ganglion. These cells appear to degrade the ingested material to lipofuscin residues, and migrate to the edges of the ganglia where they aggregate in localized clumps. The phagocytic glial cells and the peripheral lipofuscin residues increase in numbers with age. The glial cells phagocytose nerve endings labelled with radioactive serotonin.

The glial cells around the neuron perikarya contain varying numbers of glycogen particles, gliagrana and lipid droplets. Haemoglobin is present in the glial cell cytoplasm. The pigment appears identical to that present in the blood and other peripheral tissues, and may act as an oxygen store or facilitate diffusion of oxygen to the neurons when the animal is submersed. Light and electron microscopic histochemical studies of glucose-6-phosphatase and 5′-nucleotidase localization demonstrated reactive sites along the glial cell membranes, except where they face the basement membrane surrounding the ganglia. Relatively few reactive sites were present on neuronal membranes.

The glial cells actively accumulate tritiated nucleosides and bind them within their cytoplasm. The bound material is not measurably associated with DNA–RNA–protein mechanisms. Glial uptake of nucleosides has been previously reported in other nervous systems although the physiological significance is not yet clear. Two of the nucleosides

were employed as selective anatomical markers for the different components of the ganglia (glia, neurons, connective tissue). [$^3$H]Uridine labels the glial cytoplasm and connective tissue, and [$^3$H]adenosine, under the appropriate experimental conditions, distinguishes the neuronal and glial nuclei. Serial-section radioautographs were analysed by computer image analysis, and the components of the ganglia measured quantitatively throughout the life span of the animal. The following have been established.

(i) The percentage volumes of the ganglia occupied by neuronal perikarya (33%) and glial cells (43%), and the ratio of the volumes of neuronal perikarya to glial cells remain constant.

(ii) Glial cell numbers increase significantly (18%; mean number 391 cells per ganglion). The increase is chiefly due to the increase in phagocytic glial cells. There appears to be little or no turnover of glial cells.

(iii) The major change responsible for the increased volume of the ganglion (approximately fourfold) and increased volumes of the neurons (approximately fourfold) is the growth and proliferation of axonal and dendritic processes.

(iv) Neuronal 'fallout' does not occur in the buccal ganglion (mean number 298 neurons per ganglion).

The cytological, quantitative and functional properties of the glial cells and glia–neuron relations are discussed in relation to glial cells in other nervous systems.

## 1. Introduction

The arrangements of the non-myelin-forming glial cells of the nervous system were elegantly portrayed by Cajal, Golgi and Del Rio Hortega. The subsequent electron microscopic studies, principally of the mammalian brain but also on some other vertebrate and invertebrate nervous systems, have described the extents of the relationships that the cells form with the neurons. Throughout the literature neuroanatomists have tended to depict glial form and distribution as consequential to that of the neurons; terms such as interweaving, entwining, filling, wrapping and ensheathing occur frequently. In turn many suggestions about their functions appear to have been based on the intuition that they are subservient to the neurons; for example roles in protecting, guiding, insulating, maintaining and nursing have been proposed repeatedly.

The physiological evidence now available begins to substantiate these earlier suggestions. However, it also seems clear that the neurons may be dependent upon the glial cells and that the two cell types should interact in harmony for the normal functioning of the nervous system. Important directions are being established in ion homeostasis, transmitter uptake and cycling, macromolecular transfer, neuronal growth and development, and trophic and metabolic interactions and the means by which they are controlled. Detailed descriptions of these topics have been presented in the reviews by Kuffler & Nicholls (1966) and Varon & Somjen (1979), and in the volumes edited by Treherne (1981) and Sears (1982).

In the invertebrates many of the different types of glial cells have only been partly described, and the relationships of the different types are unclear (Radojcic & Pentreath 1979; Lane 1981). Comparatively little is known about the physiological functions of the cells, with the exception of a few animals where detailed studies have been made of some neuron–glial phenomena; these include ionic and metabolic interactions in the leech (Kuffler & Nicholls 1966, 1976) and the insect (Coles & Tsacopoulos 1981; Treherne & Schofield 1981), and macromolecular transfer and transmitter interactions between the giant axons and their glial sheaths in the squid and crayfish (Lasek & Tytell 1981; Bittner 1981; Villegas 1981). The arrangement and properties

of the glial cells in the nervous tissue of these animals have allowed some types of experiment to be made which are not possible in the mammalian brain.

The large neurons in the ganglia of some gastropods are well known for the success with which they have been used to study neuron physiology. On the other hand comparatively little is known about the properties of the glial cells in these animals; their relatively small size has made them less attractive for study. The cells are located around and between the neuron perikarya, and to a lesser extent along nerve trunks and within areas of neuropil. Information about their structure is scattered in the literature, where it is generally included as secondary to descriptions of the neurons (see Nicaise (1973) and Radojcic & Pentreath (1979) for reviews of molluscan glia). The following account is of the glial cells and the glio-neuronal interrelations in the buccal ganglion of the pond snail *Planorbis corneus*. The emphasis is on the cytological and quantitative changes in the glial population with growth and ageing. Other related topics studied are the localization of haemoglobin, phosphatase enzymes and calcium within the glial cell processes, and the roles of the cells in phagocytosis and degeneration within the ganglia. A part of the work on the quantitative measurement of glial cells has been published previously (Radojcic & Pentreath 1981).

## 2. Materials and methods

Adult specimens of *Planorbis corneus* were collected from an isolated pond at Alderly Edge, Cheshire, and were maintained in well-aerated aquaria. Egg-laying begins in March, continues throughout the spring and summer months, and finishes in late July and August. The eggs were normally deposited on the walls of the aquaria in a mass of jelly, each containing between 10 and 40 eggs (figure 1, plate 1). In approximately two weeks, the eggs hatch. Like other pulmonate gastropods, *Planorbis* does not pass through a larval stage, but the adult body plan develops directly in the egg case before hatching (figures 3 and 4).

### 2.1. *Electron microscopy*

Snail embryos aged 11 and 14 days after egg deposition were removed from their egg cases and fixed for 2 h in 1% glutaraldehyde (by mass) in 0.02 M cacodylate buffer (pH 7.2). Post fixation was carried out for 1 h in osmium tetroxide (10 g $l^{-1}$) in 0.1 M phosphate buffer. Other snails two to three days after hatching were processed in the same way. The fixed specimens were dehydrated through an ethanol series, passed through epoxy propane and embedded in Araldite. Serial sections of 1 μm were cut with an LKB ultratome, beginning at the head of the animal. These survey sections were stained with toluidine blue and examined under a light microscope. At the level of the perioesophageal ganglion complex, sections were cut for examination with the electron microscope. The sections were mounted on copper grids and stained in Reynolds' lead citrate and uranyl acetate.

Since it has not been possible to rear laboratory bred specimens of *Planorbis corneus* to an age greater than 2.5 years, the investigation of the age-related changes of the glial cells were carried out on specimens collected from the wild. These animals were arranged in a size series ranging from 0.5 g to 5.5 g in mass (figure 5). From observations made on laboratory-bred animals, the ages were calculated to range from one year to about four or five years (see Szabo 1935; Comfort 1964). Size has been fairly widely used as an index of age in gastropods (see, for

example, Peretz & Lukowiak 1975). The buccal ganglia were dissected from the animal and processed in glutaraldehyde and osmium solutions as described above.

Some ganglia were processed in 1% glutaraldehyde (by mass) in 0.02 M cacodylate buffer containing 1 mM $CaCl_2$; this procedure has been shown to reduce disruption of membrane structures in nervous tissue (Glauert 1975).

To obtain information on the cytological changes that take place with neuronal damage and degeneration, and on any similarities or differences between such changes and ageing, individual large neuronal perikarya were ablated with a fine needle (one cell per buccal ganglion) and the preparations maintained for 2.5–12 h in fresh saline. In other experiments intact ganglia were isolated in saline for 12, 24 and 48 h before being examined by electron microscopy.

Measurements of the extracellular space and its changes with age were obtained by point counting of electron micrographs by using the Delesse principle (Delesse 1847; see also Williams 1977).

X-ray analytical electron microscopic techniques were used to study $Ca^{2+}$ localization in the neurons and glial cells. Freshly dissected ganglia were quenched in liquid propane and freeze-dried for 24 h at $10^{-3}$ Torr, −35 °C, and vacuum-embedded in Araldite. Sections of 150 nM were briefly stained (for 30 s) in lead citrate and examined in an AEI EMMA-4 microscope, using probe size areas of 0.2–1 μM. Some analyses were made of sections of material prepared by the aqueous fixation methods described above.

### 2.2. *Histochemical studies*

Histochemical staining procedures were used to clarify the localization of certain substances within the neurons or glial cells, or both, and any changes in their distribution during the life of the animal.

The distribution of lipofuscin was studied by the ferric–ferricyanide method of Schmorl (see Drury & Wallington (1980) for a detailed description). This is dependent upon the reduction of ferricyanide to ferrocyanide, with the production of dark blue ferric ferrocyanide (Prussian blue).

The distribution of haemoglobin was analysed by the technique described by Dunn & Thompson (1945; see also Drury & Wallington 1980). Non-circulatory haemoglobin, located intracellularly within the tissues, is present in *Planorbis* and many other molluscs (figures 2 and 6). The experiments were made to determine its location within the nervous tissue.

Glucose-6-phosphatase localization was studied at the light and electron microscope level by the lead phosphate technique described in Lewis & Knight (1977). For this isolated buccal ganglia were fixed for 1, 2, 4 and 8 min in 1% glutaraldehyde (by mass) in 0.02 M cacodylate buffer pH 7.2, rinsed thoroughly in several changes of 0.2 M Tris–maleate buffer pH 6.5, and incubated for 1 h at room temperature in the following medium: 60 mM Tris–maleate pH 6.5, 2.5 mM lead nitrate, 4 mM disodium glucose-6-phosphate. The ganglia were then rinsed in several changes 0.2 M Tris–maleate buffer 7.2, further fixed for 1 h in 1% glutaraldehyde (by mass) in 0.02 M cacodylate buffer pH 7.2, dehydrated in ethanol and embedded in wax or Araldite. By using brief fixation time and intact ganglia enzyme inactivation was minimized in the peripheral regions of the ganglia, where many glial cell processes are located, although the cores of the ganglia were poorly preserved. Enzyme specificity was controlled for by using β-glycerophosphate as the incubation substrate.

5′-Nucleotidase distribution was determined at the light and electron microscope level by

the technique described by Wachstein & Meisel (1957) (see also Barka & Anderson 1963; Lewis & Knight 1977). The method is similar to that for glucose-6-phosphatase, using lead ions to localize sites of activity. Isolated ganglia were fixed for 1, 2, 4 and 8 min in 1% glutaraldehyde (by mass) in 0.02 cacodylate buffer pH 7.2, rinsed in several changes of Tris–maleate buffer pH 7.2 and incubated for 1 h at room temperature in the following medium: 0.2 M Tris–maleate buffer, pH 7.2 (4 ml), 0.02 M lead nitrate (4 ml), 0.05 M manganous chloride (2 ml), adenosine-5′-monophosphate (25 mg), distilled water (10 ml). Control incubation media contained no AMP, or additional $10^{-4}$ nickel sulphate with the Tris–maleate buffer replaced by 0.2 M acetate buffer, pH 7.2. Nickel ions have been reported to specifically inhibit 5′-nucleotidase (see Barka & Anderson 1963). The ganglia were rinsed in several changes of 0.2 M Tris–maleate buffer pH 7.2, fixed for 1 h in 1% glutaraldehyde (by mass) in 0.02 cacodylate buffer pH 7.2, dehydrated through an ethanol series and embedded in wax or Araldite.

### 2.3. *Radiolabelled tracer studies*

Radioactive tracers were used in conjunction with radioautography to study properties of the neuron–glia relations.

Attempts to measure the turnover of the glial cells in normal and experimentally damaged ganglia were made by exposing the ganglia to 6-[$^3$H]thymidine (27 Ci mmol$^{-1}$) (Radiochemical Centre, Amersham) in *Planorbis* saline (Berry 1972) at final concentration 2 μg ml$^{-1}$ for 15 min to 1 h, at varying times (0–5 h) after their isolation or damage. The ganglia were then rinsed in saline (5 min), fixed for 2 h in 1% glutaraldehyde (by mass) in 0.02% cacodylate buffer (pH 7.2), dehydrated through a graded ethanol series, cleared in xylene and embedded in paraffin wax.

For light microscope radioautography 8 μm serial sections were mounted on glass slides, de-waxed (xylene), coated with Kodak AR.10 stripping film and stored in the dark for two weeks at 4 °C. The slides were developed in Kodak D-19 (2.5 min at 22 °C), fixed in Unifix (Kodak) for 10 min, rinsed in distilled water and mounted in Farrant's medium.

To provide a basis for quantitative studies of the cellular components within the ganglia it was necessary to develop consistently reliable anatomical markers that could then be measured by morphometric techniques. Tritiated nucleosides were used for this; the reason for choosing these compounds arose from unpublished experiments in which they were being tested as possible selective markers for individual *Planorbis* neurons, but which radioautography subsequently revealed to mark the glial cells.

Isolated paired buccal ganglia were incubated in solutions of snail saline containing 2-[$^3$H]adenosine (22 Ci mmol$^{-1}$), 5-[$^3$H]uridine (5 Ci mmol$^{-1}$), 5,6-[$^3$H]uridine (48 Ci mmol$^{-1}$), 5-[$^3$H]thymidine (12.8 Ci mmol$^{-1}$), 6-[$^3$H]thymidine (27 Ci mmol$^{-1}$), 5-[$^3$H]cytidine (28 Ci mmol$^{-1}$) and 8-[$^3$H]guanosine (8 Ci mmol$^{-1}$) (purchased from the Radiochemical Centre, Amersham). Each solution was made to concentrations of 0.1, 1.0, 2.0 and 5.0 μg ml$^{-1}$. Ganglia from a range of snail sizes (0.1–5.5 g total animal mass) were incubated separately for 15 min, 30 min, 1, 2 or 3 h in each of the solutions at room temperature, rinsed in fresh saline (5 min) and processed for light microscope radioautography. The serial radioautographs were assessed for optimal labelling of the glial cell cytoplasm and nuclei, of the neurons and of the connective tissue.

Electron microscope radioautography was used to determine whether the activity observed over the glial components after [$^3$H]uridine and [$^3$H]adenosine exposure provided an accurate

and uniform marking, or whether the label was associated with any particular organelle. Ganglia were incubated in 2.0 μg $ml^{-1}$ 5,6-[$^3$H]uridine (48 Ci $mmol^{-1}$) or 5.5 μg $ml^{-1}$ 2-[$^3$H]adenosine (22 Ci/mmol) for 15 min, rinsed in fresh saline, fixed for 1 h in 1% glutaraldehyde (by mass) in 0.02 M cacodylate buffer (pH 7.2), post-fixed for 1 h in osmium tetroxide (10 g $l^{-1}$) in 0.1 M phosphate buffer (pH 7.2), dehydrated through an ethanol series and embedded in Araldite. Gold sections were stained with lead citrate and uranyl acetate and coated with 2–5 nm evaporated carbon. The grids were coated with Ilford L 4 emulsion by a loop technique (Caro *et al.* 1962) and stored in the dark at 4 °C for one month. Radioautographs were developed in Kodak Microdol-X (5 min at 22 °C) and fixed in 30% sodium thiosulphate (1.5 min at 22 °C).

The possibility of transfer of material from the glial cells to the neurons was investigated by loading the ganglia with labelled nucleoside for 15 min, briefly rinsing in fresh saline, and subsequently maintaining the ganglia in saline for 1–10 h at room temperature. The ganglia were then prepared for light microscopy, and grain distribution carefully compared with material processed immediately after the load period.

The role of the glial cells in the removal of degenerating serotonergic nerve terminals was investigated by exposing the buccal ganglia *in situ*, on the buccal mass, to 0.1 μM 5-hydroxy G-[$^3$H]tryptamine creatinine sulphate (15 Ci $mmol^{-1}$; Radiochemical Centre, Amersham) in snail saline for 1 h, and then maintaining the tissues in fresh saline for 1–24 h. The buccal ganglia were then studied by light and electron microscope radioautography.

### 2.4. *Properties of the selective marking of glial cells by nucleosides*

The DNA, RNA and protein fractions of the nervous tissue were separated (method of Ogur & Rosen 1950) to determine the extent of nucleoside tracer incorporation into these components. Batches of ten freshly dissected buccal ganglia were incubated in saline containing 5.0 μg $ml^{-1}$ [$^3$H]thymidine, 5.5 μg $ml^{-1}$ [$^3$H]adenosine, 2.0 μg $ml^{-1}$ [$^3$H]uridine or 2.1 μg $ml^{-1}$ [$^3$H]cytidine, for periods of 15 min at room temperature. The sets of ganglia were homogenized in 1.5 ml cold 1 M $HClO_4$, then centrifuged at 1800 $g_{av}$ for 10 min to separate the precipitated DNA, RNA and protein fractions from the acid-soluble small molecules and lipids. A 0.2 ml sample of each supernatant was counted by liquid scintillation. The precipitates were dissolved in tissue solubilizer (Protosol, New England Nuclear) and re-extracted at 4 °C with 1.5 ml of 1 M $HClO_4$ (18 h). After centrifugation (1800 $g_{av}$ for 30 min) the supernatant (containing the RNA and RNA products) was counted by liquid scintillation. The precipitates were treated with two changes of 1 M $HClO_4$ (each 30 min at 80 °C) and re-centrifuged (2000 $g_{av}$ for 30 min) to separate the DNA components (supernatant) from the protein residues (precipitate). Both fractions were counted by liquid scintillation.

Some ganglia were exposed to the radioactive nucleosides as described above, fixed in Carnoy's fluid (1 h) and incubated separately in solutions of RNaseA, DNase I and II (Sigma) and 5% TCA (Singer & Green 1968; Schick *et al.* 1978). The tissues were then briefly re-fixed in 1% glutaraldehyde (by mass), embedded in wax and prepared for light microscope radioautography. The radioautographs were compared with those of material not treated with the digestive enzymes.

To test whether the uptake of the nucleosides was by an active or passive process some ganglia were exposed to 0.2 mM 2,4-dinitrophenol before and during the incubation in the nucleoside tracer.

### 2.5. *Quantitative analysis*

Specimens of *Planorbis* were arranged in a size series ranging from 0.5 to 5.5 g in approximately 0.5 g steps. All but some of the smallest (0.5 g) were sexually mature. laboratory-bred animals attain this size and sexual maturity at the age of one year. The largest animals were estimated to be three to five years old (see also Comfort 1964). However, it is likely that there is some individual variation in growth rate, and the size range may not strictly coincide with age.

Freshly dissected paired buccal ganglia were incubated in the tritiated nucleoside solutions described above. [$^3$H]Uridine (2 μg ml$^{-1}$ for 15 min) provided a particularly useful anatomical marker for the cytoplasm of the glial cells; [$^3$H]adenosine (5.5 μg ml$^{-1}$ for 30 min) was valuable for marking the nuclei of the glial cells. The ganglia were serially sectioned (8 μm) and prepared for light microscope radioautography. Each radioautograph was photographed and printed to a standard size. The following measurements were made.

(i) *Cell counts*

*Number of neurons* ($N_n$). The neurons were counted from sets of photographs of the [$^3$H]uridine- and [$^3$H]adenosine-labelled ganglia. Care was taken to avoid re-counting individual neurons by tracing them through superimposed successive sections.

*Number of glial cells* ($N_g$). Glial cell nuclei were counted from the serial section micrographs of the [$^3$H]adenosine labelled ganglia.

(ii) *Volume measurements*

*Ganglion volumes* ($V_{ga}$). The area of the ganglion in each photograph (sets of [$^3$H]uridine labelled material) was measured by planimeter. The product of the areas ($A_{ga}$, in square centimetres) the section thickness ($T_s$; 8 μm), and the magnification of the micrograph ($M$; standard at 79.33) were derived for each section. The values were summed for each set, and the volume of the ganglion in cubic millimetres obtained by dividing by the cubic magnification factor ($M^3$).

*Core* ($V_{cr}$) *and cortical* ($V_c$) *volumes.* (The central regions of the ganglia of gastropods and many other invertebrates are frequently referred to as neuropil. This is inaccurate because only a small proportion of the central region is neuropil, but a large proportion is composed of axon tracts and some glial cells. Areas of neuropil are arranged between axon tracts. The term core is more appropriate.) Measurements were made from micrographs of [$^3$H]uridine-labelled material. Core areas ($A_{cr}$) were obtained by planimetric measurements; cortical areas by subtracting core areas from the ganglion areas ($A_{ga}$) in each section. Volumes were derived as described above.

*Glial* ($V_g$) *and neuronal* ($V_n$) *volumes.* These were obtained with a Joyce–Loebl Magiscan Image Analysis System. By this procedure the radioautographs or their photographs were displayed on a television screen (the television camera attached to the microscope, or placed in front of the photomicrographs). The black areas (silver grains) were computed as percentages of the ganglion section, which was circumscribed by a light-pen attachment. Adjustments were made to compensate for variations in the exposure of individual radioautographs (figure 83, plate 15). Minor corrections such as additions or deletions (for example, occasional neuronal nuclei labelled with [$^3$H]uridine) were made on the television screen by a light-pen. The Magiscan

provided a print-out of the percentage of the labelled regions of each section (glia, % $G$). The [$^3$H]uridine radioautographs were principally employed for these measurements (see figures 81–83).

Each section of a serial set though a ganglion was analysed and the data correlated with individual section volumes. The products of percentage glia, area of the photographic section, and corrected ganglion thickness of all the sections were added to obtain the total glial volume of the ganglion. This result was then scaled down to determine actual volumes within the ganglion. Neuronal percentage volumes (% $N$) were obtained by subtracting glial percentage from 100 %. Neuronal volume was obtained by the same arithmetical means as that described for glial volume. Thus

$$V_{ga} = \Sigma(A_{ga} \times 8\ \mu m \times M)/M^3 \quad (M = 79.33),$$
$$V_{cr} = \Sigma(A_{cr} \times 8\ \mu m \times M)/M^3,$$
$$V_c = \Sigma(A_{ga} - A_{cr}) \times 8\ \mu m \times M)/M^3,$$
$$V_g = \Sigma(A_{ga} \times 8\ \mu m \times M \times \%\ G)/M^3,$$
$$V_n = \Sigma(A_{ga} \times 8\ \mu m \times M \times (100\% - \%\ G)/M^3$$

and volume of perikarya ($V_p$) was obtained by

$$V_p = V_n - V_{cr}.$$

## 3. Results

### 3.1. *The glial–neuron relations*

The buccal ganglia are located on the posterior surface of the buccal mass, at the point where the oesophagus arises. Each ganglion is oval, connected with each other by a commissure and to the perioesophageal complex by connectives, and sends several nerves to the buccal musculature (figures 2 and 6, plate 1; figure 7). The ganglia are not supplied internally by blood vessels; the blood permeates through the connective tissue spaces surrounding the surface of the tissue (see Pentreath & Cottrell 1970). The neuronal perikarya and most of the glial cells are located in the outer layers of the ganglia. In the living tissue the perikarya appear

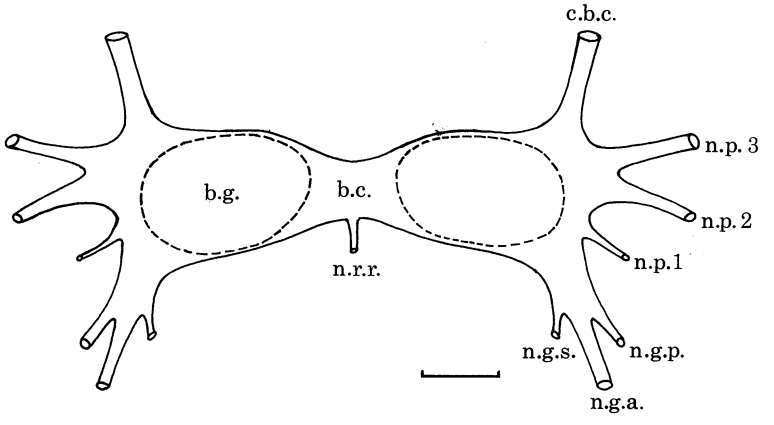


FIGURE 7. The buccal ganglia and associated nerves of *Planorbis corneus*. The neuron perikarya are located in the central areas contained within the dashed lines. The scale would represent approximately 0.1 mm in a 5.0 g snail. b.c., Buccal commissure; b.g., buccal ganglion; c.b.c., cerebro-buccal connective; n.g.a., n. gastricus anterior; n.g.p., n. gastricus posterior; n.g.s., n. glandulae salvalis; n.p.1, n. pharyngealis primus; n.p.2, n. pharyngealis secundus; n.p.3, n. pharyngealis tertius; n.r.r., n. receptaculus radulae.

white to pale yellow in colour, embedded in the glial tissue that varies from pink to bright red (figures 2 and 6). The red colour is due to the presence of haemoglobin within the glial cells (§3.5). The neurons, together with glial processes, project into the core of the ganglion. The core of the ganglion consists of axon tracts, areas of neuropil, and a relatively small amount of glial tissue (figure 8). The distribution of the glial tissue can be clearly visualized in material exposed to radiolabelled nucleosides (for example, figure 81, §3.8).

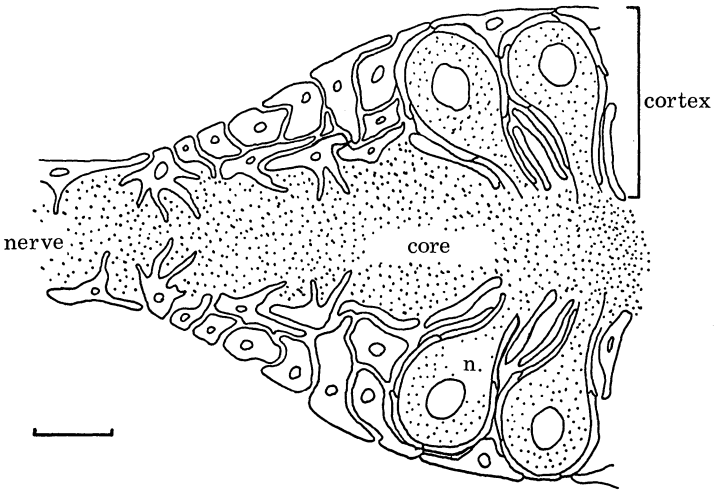


FIGURE 8. The distribution of the glial cells and the glia–neuron relations in the buccal ganglia of *Planorbis corneus*. The neurons are stippled. The glial cells in the cortex form sheets, which surround the ganglion and ensheath the neuron perikarya (one labelled n.) in lamellated and shingled arrangements, frequently penetrating them to form a trophospongium (see also figures 22 and 36). Glial cells are rarely found in the core of the ganglion, especially in areas of neuropil. In the nerves the glial cells form sheets that wrap individual axons or bundles of axons. The arrangement of the glial cells is similar in the circumoesophageal ganglia. The scale represents 50 μm.

In the adult animal 40–50% of the ganglion is composed of glial tissue. The glial cells surround, encapsulate and send processes into the neuronal perikarya, into the axon hillocks and the major axon branches (figures 9, 11 and 12, plate 2). Large neurons were commonly surrounded by large numbers of glial processes which varied in appearance from thin lamellae to thicker shingled processes (figures 9, 11, 16 and 18), while smaller neurons were associated with comparatively few glial processes (figures 14 and 15). In the pre-hatched animal glial cells were also chiefly associated with the neuronal perikarya, but the glial processes were thicker than those in the adult (figures 23 and 25, plate 5). In all animals examined neuronal perikarya were usually completely surrounded by glial cell processes, and only rarely were regions of adjacent perikarya observed to make close contact, without intervening glial processes. Such perikarya were of small diameter (figure 15). Because the perikarya are spherical, the areas between them are varied in shape, in some places being expanded and filled with glial cells and their processes interwoven into a complex network (figures 9, 16 and 26). These regions contained many glial cell nuclei and were most extensive in older animals.

The connective tissue capsule covering the ganglion is underlain by a basement membrane (figures 9–13, plate 2). Glial cell processes lie against this, forming a layer separate from the neurons, but which is occasionally penetrated by presumed neurosecretory structures. The neurosecretory structures may be obviously terminal (figures 14 and 47), but sometimes are

of large diameter, contain fewer electron-dense granules, and may be close to the cell's perikaryon (figure 12). The basement membrane is sometimes reduced or eliminated by the neurosecretory terminals (figure 14). Some terminals extend into and ramify within the connective sheath (figures 20 and 27). This type of arrangement has been observed in the closely related freshwater snails, *Lymnaea* (Wendelaar Bonga 1970; Swindale & Benjamin 1976*a*, *b*) and *Bulinus* (Boer *et al.* 1977), and in the ganglia of some other invertebrates (for example, the cerebral ganglia of the earthworm, Aros *et al.* 1977).

Individual glial cells radiate processes from their nuclear regions outwards to the basement membrane, and inwards alongside the axon hillocks and major axonal processes that enter the ganglion core (summarized in figures 22 and 36). The glial processes divide and form sheets and fins that interdigitate with those from other glial cells and with the neurons. An important question is whether or not each glial cell makes contact with the basement membrane so as to have close access to the blood supply. There are approximately 400 glial cells in each ganglion (§3.9), and the number of processes abutting the basement membrane exceeds this by several orders of magnitude, thus the likelihood seems great. By semi-serial sectioning it was established that some of the peripheral glia may project to the basement membrane at several different places, but the method was found impractical for tracing the deeper glial cells. On the other hand, a small proportion of glial cells, which appear to be a different type specialized for nerve-ending phagocytosis and which are located in the core of the ganglion (see §3.3), did not appear to send processes to the basement membrane. Thus contact with the basement membrane seems a likely generality for the peripheral glial cells, but may not include all the glial cells in the ganglion.

The glial cells project processes into the neuronal perikarya, their axon hillocks and large-diameter axonal processes, forming a trophosphongium (figures 9, 11, 12, 18, 19 and 22). Glial processes also accompany varicose nerve terminals, which are sometimes found penetrating the perikarya, forming possible synaptic contacts (figure 19). The general rule that synapses are absent from the somata of molluscan neurons is apparently excepted in these cases. The glial processes incompletely surround the varicose terminals, being absent from presumed sites of synaptic contact (figures 19 and 27).

In the core of the ganglion, glial cell nuclei were rarely observed. However, glial sheets extend from the cortex of the ganglia and wrap around individual axons or bundles of axonal and dendritic processes. The larger axons were associated with glial processes, often arranged in complex overlapping layers (figures 29–33, plate 6). It appeared that the layers were contributed to by several glial cells. The glial layering became reduced as axons and dendrites decreased in diameter with branching. Individual small axons and dendrites were frequently unaccompanied by glial processes (figures 29, 30 and 33). The glial sheets also become attenuated when they surrounded bundles of axonal and dendritic processes. Some fine glial processes penetrated areas of neuropil where they separated different regions of synaptic intermingling (figures 34 and 35, plate 7). However, glial tissue was generally absent from large areas of neuropil (figure 35), except in cases of suspected phagocytosis (see §3.3, figures 43–46, plate 9). The comparative lack of glial tissue in the core of the ganglion is clearly demonstrated in the autoradiographic marking experiments (§3.8; see, for example, figure 82). Some features of the arrangement of the neuropil are summarized in figure 37.

In the nerves and connectives the majority of the glial cells are arranged at the periphery, close to the connective tissue. Glial cell nuclei are uncommon in the axon tracts in the mid-regions

## Description of plate 1

The development of *Planorbis corneus* and the appearance of the adult nervous system.

Figure 1. The eggs are deposited in a gelatinous mass which is attached to the surface of pond weed or bottom stones. The time span from egg deposition to hatching averages 15 d in the laboratory at room temperature. This egg mass is 7 d old. The scale is 1 mm.

Figure 2. The buccal ganglia on the ventral surface of the buccal mass, at the point where the oesophagous (oes.) arises. Individual neuron perikarya, of varying sizes, appear pale yellow and are surrounded by glial tissue, which is pale red. Individual glial cells cannot be resolved. The red colour is due to the presence of haemoglobin in the glial cells. See also figures 6–8. The scale is 100 μm.

Figure 3. At day 14 the body plan of the snail, and its movements within the egg case, resemble those of the adult. The eyes, located at the base of the tentacles, are pigmented. There are two adjacent empty egg cases. The scale is 0.2 mm.

Figure 4. The snail hatches by continual feeding action, which eventually ruptures the egg case. At hatching the animal is approximately 1 mm long with the foot fully extended. The snail begins feeding on algae and becomes progressively pigmented. The animal shown here is 20 d old. The scale is 0.2 mm.

Figure 5. Snails ranging in mass from 0.6 to 5.4 g (estimated age range 1–5 years). The animals are retracted within their shells. The scale is 1.0 cm.

Figure 6. The central nervous system of *Planorbis*. The oesophagus, which passes through the oesophageal ring of ganglia (o.r.), has been cut and placed to the anterior, between the salivary glands (s.g.). The buccal ganglia (b.g.) supply nerves to the buccal mass (b.m.), and are connected to the cerebral ganglia (c.g.) by connectives (see figure 7). Neuron perikarya within the different ganglia appear as pale spheres in a red matrix. The red colour is due to haemoglobin within the glial cells. Haemoglobin is also present within the buccal musculature, but is less obvious within the nerves and connectives. r.s., Radula sac. The scale is 400 μm.

## Description of plate 2

The arrangement of the glial cells in the periphery of the buccal ganglia.

Figure 9. Several layers of glial cell processes separate a neuron perikaryon (n.) from the basement membrane (b.) and outer connective tissue collagen (c.). The tissue was fixed in the presence of elevated calcium (5 mM), which causes a darkening of many of the outer glial cell processes. The tissue is from a snail weighing 4.7 g. Fairly extensive extracellular lacunae separate some glial cells (short arrows). Other empty spaces within the glial cytoplasm may be due to loss of material (for example, gligrana) during histological processing. The arrow at top left marks a lipid droplet. The asterisk marks a glial cell process penetrating the neuron. Magn. ×8200.

Figure 10. There are no barriers preventing access of small molecules to the extracellular spaces within the ganglion. The two glial cell processes at the edge of the ganglion (basement membrane, b.) are separated by an extracellular channel of average width 12 nm (see also figure 13). Magn. ×56000.

Figure 11. Glial cell processes form a trophospongium within the neuron pereikaryon (n.) at the right of the micrograph. The neuron lies close to the basement membrane (b.), but is separated from it by the glial cell processes. At the left of the micrograph glial cell processes run into the ganglion between adjacent neurons. Lacunae separate many of the glial cell processes, but do not occur between the glial cells and neurons. The connective tissue sheath (c.) contains muscle cells (m.). The tissue is from a snail weighing 3.3 g. Magn. ×8200.

Figure 12. Trophospongium within a neuron perikaryon (n.) located on the ventral surface of a buccal ganglion from a 2.0 g snail. The glial sheets encapsulate areas of somatoplasm (for example, top arrows). This neuron appears to make contact with the basement membrane (b.) at several points (for example, bottom arrows), which is an unusual feature, generally restricted to presumed neurosecretory structures (see figure 14). The neuron contains electron-dense granules, which suggests that it may be neurosecretory. c., Connective tissue. Magn. ×8200.

Figure 13. Glial cell processes in a buccal ganglion from a young snail (mass 1.7 g). The glial processes are thick in comparison with those in the older animals (cf. figures 9 and 21). Extracellular spaces of mean width 15 nm, without membrane specializations, separate large areas of adjacent cells (for example, arrow). Extracellular dilatations comparable to those in the older animals (cf. figures 9 and 21) are not present. c., Connective tissue. Magn. ×23000.

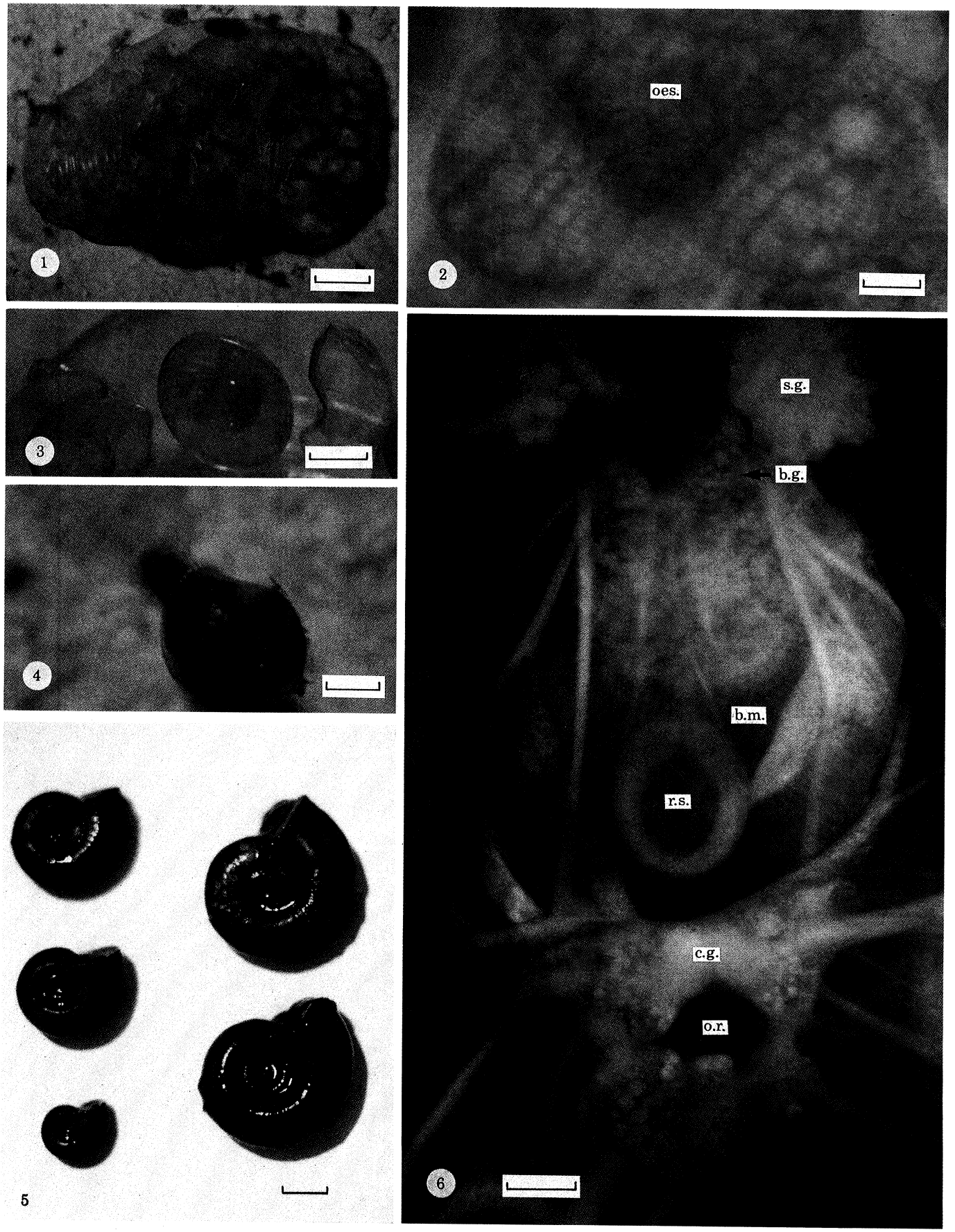


FIGURES 1–6. For description see opposite.

(*Facing p.* 410)

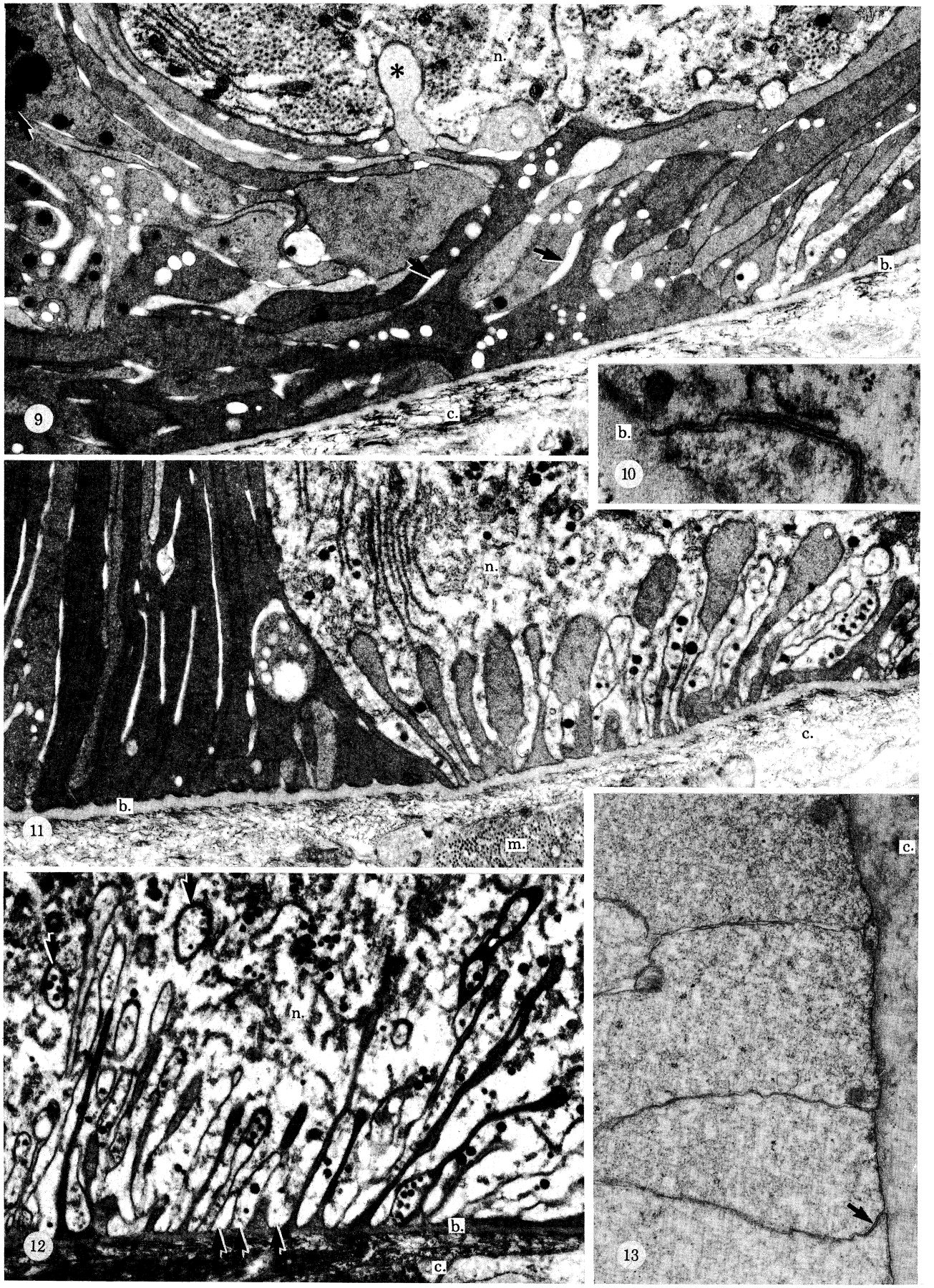


FIGURES 9–13. For description see p. 410.

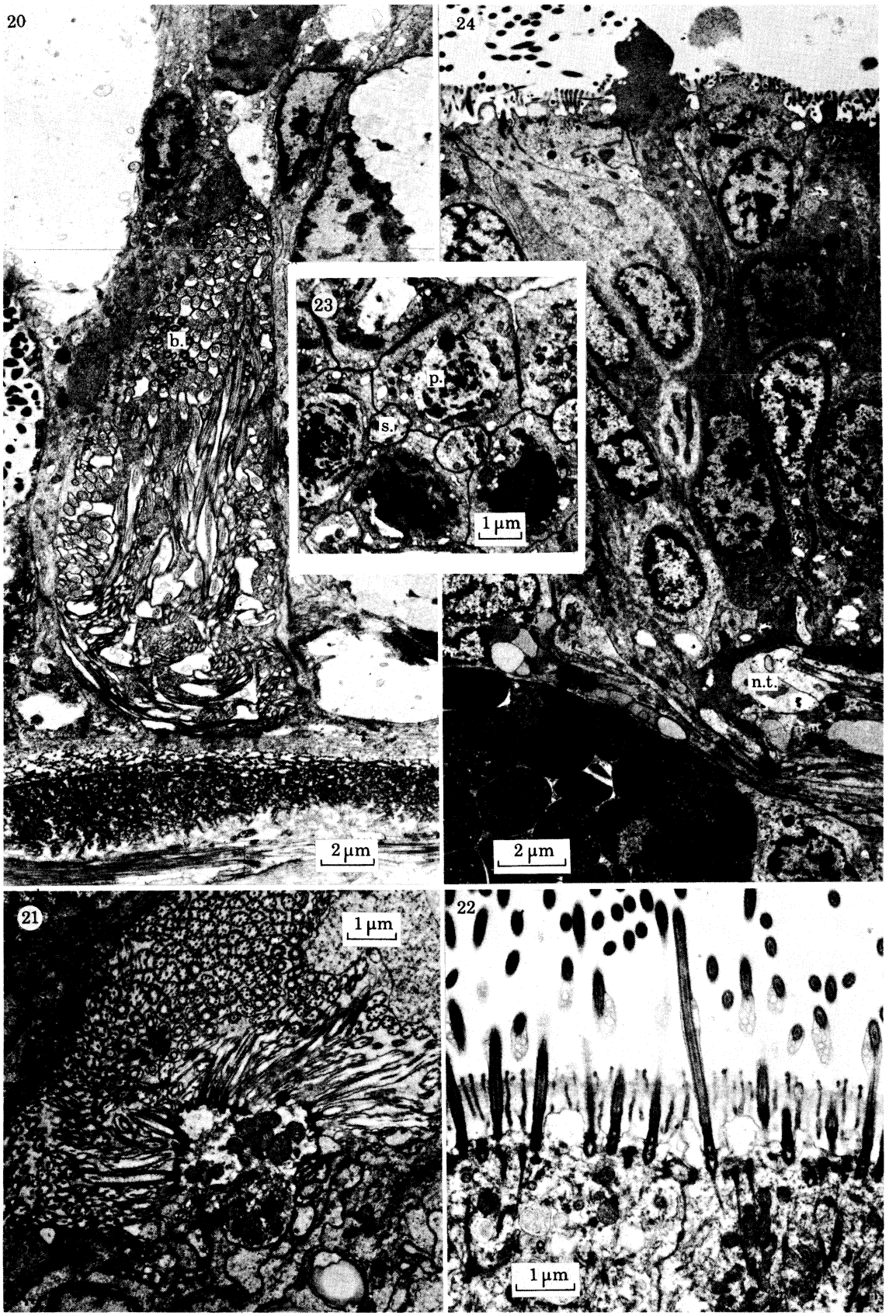


FIGURES 20–24. b., Basal bodies; n.t., nervous tissue; p., pigment body; s., process of sensory cell.

FIGURE 20. *Haliotis lamellosa*; cilia bottle.

FIGURE 21. *Patella coerulea*: cilia star cell (osphradial ganglion).

FIGURE 22. *Diodora italica*: extended ciliary membranes (central ciliated zone).

FIGURE 23. *Nerita plicata*: horizontally sectioned part of the central zone.

FIGURE 24. *Puperita pupa*: special cell 'y'.

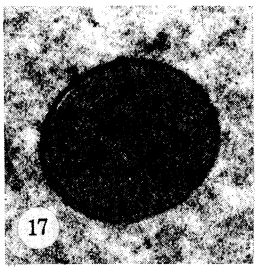





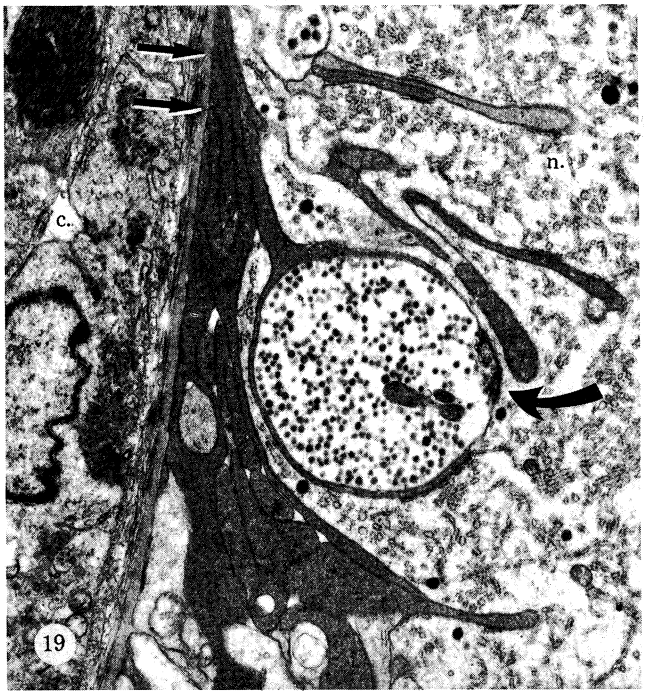



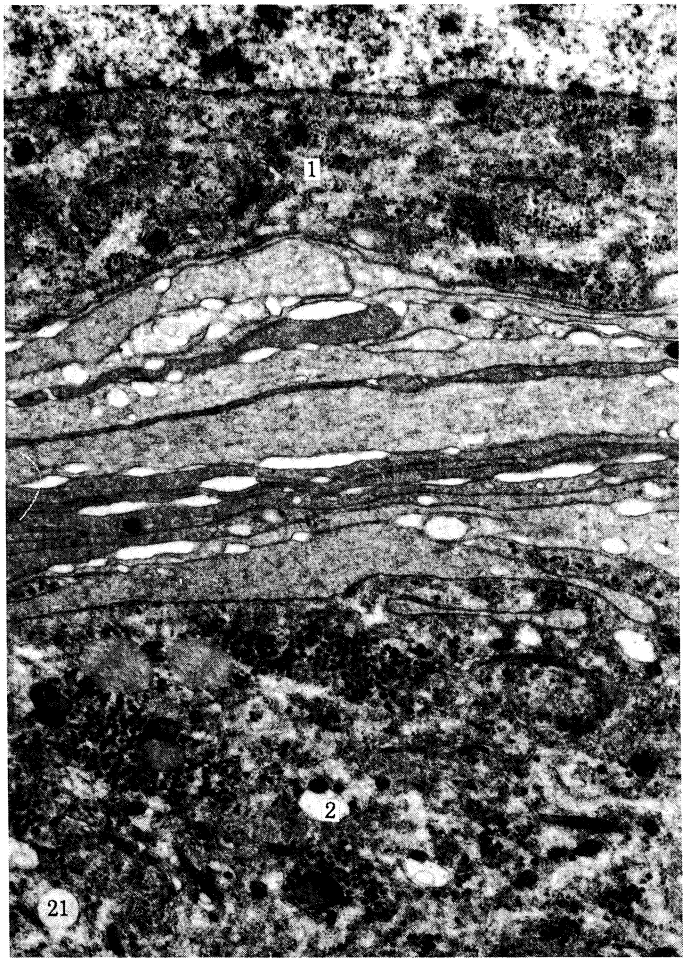


FIGURES 17–21. For description see opposite.

of the nerves. Sheet-like glial processes extend around the edges of each nerve, underneath the basement membrane and amongst the axons (figures 38 and 40, plate 8). Large axons (that is, diameter greater than 5 μm) were often covered with multiple glial wrappings (figures 38 and 40), smaller axons were wrapped in bundles (see figure 41). Analysis of semi-serial and longitudinal sections of buccal nerves showed that the axons and glial cells wandered along the nerve; thus it is likely that axons which appear isolated from glial cells in any particular cross section are contacted at other levels in the nerve.

The architecture of the ganglion is established before the animal hatches. The overall glial–neuronal relations and the appearance of the glial cells, was similar in animals of all ages. However, progressive alterations were observed in certain features. First, the glial processes around the neuron perikarya, which are relatively thick (2–5 μm) at hatching, become more numerous and thinly lamellated as the size of the neurons increases (figures 13, 23, 25 and 26, cf. figures 9, 16, 18 and 21). Secondly, there was an increased appearance of phagocytic glial

## Description of plate 3

The glial–neuron relationship in the periphery of the buccal ganglia.

Figure 14. A neurosecretory process lies against the connective tissue (c.) on the ventral surface of the ganglion. The basement membrane is reduced or lacking, and the glial processes are displaced between the neurosecretory terminal and the adjacent neuron (nucleus, n.). The glial layers completely surround the neuron soma, but in places are very thin (for example, at the large arrows they are approximately 30 nm wide). The small arrows mark Golgi structures within the neuron. The material is from a snail of mass 3.5 g. Magn. × 10000.

Figure 15. Two small-diameter perikarya (1, 2) make close contact and are unseparated by glial cell processes (arrows). This unusual situation was only observed for the smallest diameter neurons, located relatively deep within the ganglion, away from the connective tissue. The ganglia were from a snail of mass 3.5 g. Magn. × 8200.

Figure 16. Glial cell processes, of varying opacities, located between the neuron perikarya (one marked n.) on the dorsal surface of a buccal ganglion from a 4.1 g snail. The arrows at left mark some of the lacunae between the glial cell processes. The glial cells contain numbers of gliagrana (one cluster in centre labelled g.). Lipid drops (l.) are present within the neuron. Magn. × 7500.

## Description of plate 4

The glial–neuron relations in the periphery of the buccal ganglia.

Figure 17. An individual gliagrana, surrounded by a unit membrane, containing an electron-dense matrix of unknown composition or function(s). Magn. × 60000.

Figure 18. Glial cell processes wrapping a neuron perikaryon (nucleus, n.; animal mass 4.0 g). The glial processes contain numerous gliagrana (one cluster marked g.). Lacunae occur between adjacent glial cells, but not between the neurons and glial cells. Magn. × 10000.

Figure 19. The axonal process containing dense-cored vesicles passes through the neuron soma (n.), accompanied by glial cell processes which extend from the basement membrane (arrows). The axon terminal is surrounded by the glial processes, except on its inner face, where small clear vesicles are clustered (arrow). The structure may be termed synaptic on the grounds of its similarity with the other relatively non-specialized synapses that are widespread in areas of neuropil in the snail ganglia. Terminal processes extend through and around neuron perikarya to reach the basement membrane and connective tissue sheath (see also figures 20 and 27). c., Connective tissue. Magn. × 10000.

Figure 20. Varicose axonal processes containing a variety of granules and different types of vesicle are common in the connective sheath. The processes do not appear to be innervating muscles within the sheath, but are probably neurosecretory, releasing substances into the blood sinuses around the ganglion. The axons are not surrounded by glial processes, and may have somata located in the buccal ganglia or within the connective tissue sheath. n., Nucleus of fibroblast. Magn. × 8200.

Figure 21. Two neurons (numbered 1 and 2), on the dorsal surface of the buccal ganglion from a snail weighing 4.5 g, are separated by approximately ten relatively thin glial lamellae. Extracellular lacunae are located between the glial processes, but not between the neurons and glial cells. Magn. × 8500.

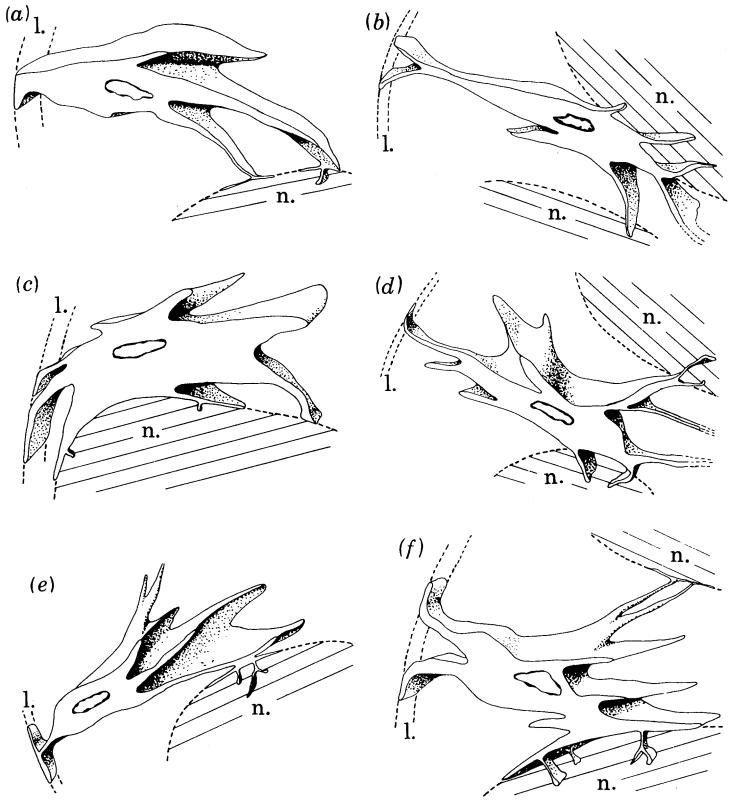


FIGURE 22. The relations between the glial cells, the neurons (n.), and the basal lamina (l.), in the cortex of the buccal ganglion. Each diagram shows the arrangement for a 5 μm slice in the nuclear region of a glial cell. The glial cells vary greatly in complexity, but each cell appears to make at least one contact with the basal lamina. A single glial cell may make contact with a small part of a neuron (*a*), (*e*), or may wrap a relatively large part of it (*c*). A glial cell may also contact one neuron (*a*), (*c*), (*e*), or several neurons (*b*), (*d*), (*f*). Some of the ensheathing glial processes penetrate the neurons, forming a trophospongium (*d*)–(*f*). Different processes from an individual glial cell may extend deep within the ganglion, in addition to contacting several neuron perikarya (*d*) (see also figure 36). The scale is 10 μm.

cells in the core of the ganglion. Thirdly, and of greater apparent significance, there were marked increases in the size of the extracellular spaces between the glial cells in the cortex of the ganglion. In young animals the spaces were of a fairly uniform width of 10–20 nm, but there was progressive increase in local regions of expansion that reached 0.2 μm in older animals (figures 13, 23, 25 and 26, cf. figures 9, 16, 18 and 21). These dilatations formed an interconnecting system of lacunae between adjacent glial cell processes, but not between the glial cells and the neurons (figures 18 and 21). Point-counting analysis of micrographs showed that their volume made up approximately 15 % of the non-neuronal cortex of the buccal ganglia in snails weighing 4 g. Even larger expansions were observed in other central ganglia that were of greater size or ganglia maintained for up to 36 h in unoxygenated saline (figure 52). For example, in the right pedal ganglia of 4.0 g snails they made up 20 % of the non-neuronal volume. The findings therefore indicate that the size of the spaces were proportional to the size of the ganglion.

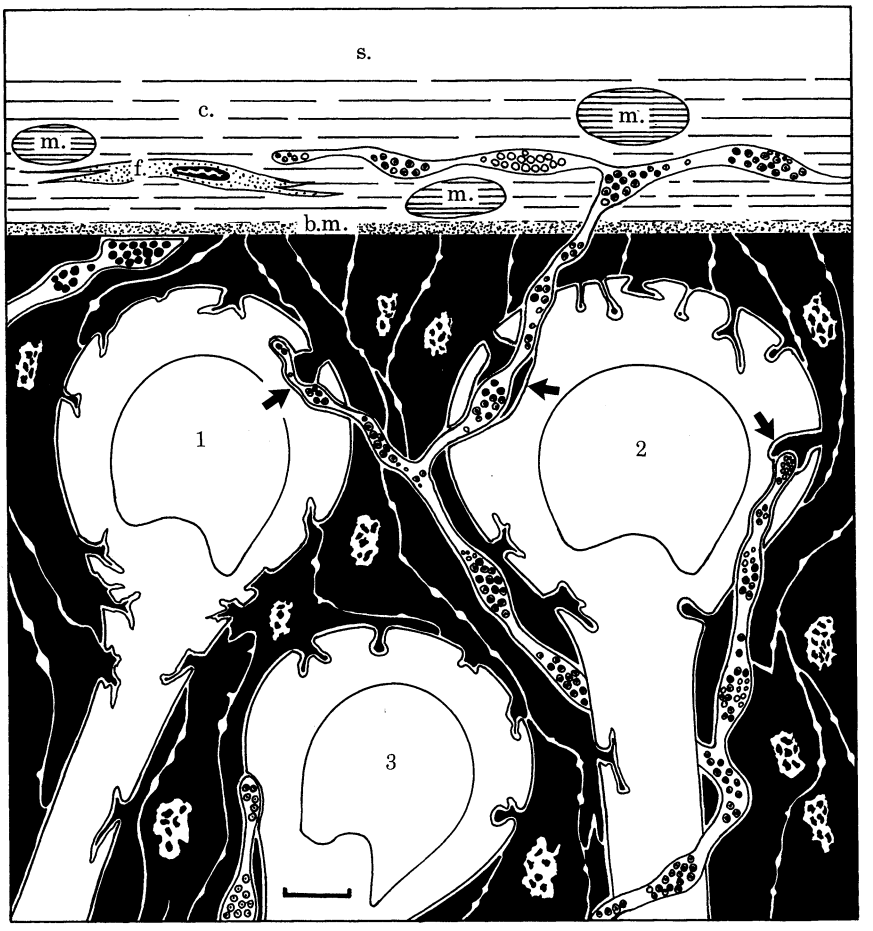


FIGURE 27. Features of the glial–neuron relations in the cortex of the adult buccal ganglion. Three neurons (nuclei, 1–3) and surrounded by glial cells (black). The glial cell processes are separated from each other and from the neurons by extracellular spaces 10–20 nm wide. The extracellular spaces between glial cell processes, but not between the neurons and glial cells are periodically expanded into lacunae. There are no occluding junctions between the glial cells; low molecular mass substances have access from the blood sinuses (s.), through the connective tissue sheath which is largely composed of collagen (c.) and muscle cells (m.), across the basement membrane (b.m.) to the extracellular spaces within the ganglion. Varicose axonal processes, sometimes containing neurosecretory granules, pass over and through the cellular components of the cortex. Some axonal processes terminate against the basement membrane (for example, left-hand side of diagram), others terminate or form *en passant* contacts with the neuron somata and axon hillocks. Glial processes frequently accompany the penetrating axonal processes (arrows). Varicose axonal processes pass through the glial cells and into the connective tissue sheath, where other terminal arborizations are formed. No obvious specialized synaptic contacts have been observed between the axonal varicosities and the glial cells, nor between the varicosities and the neurons. This widespread peripheral distribution of varicosities may coordinate activity in neurons and glial cells, and has also been noted in the closely related snail *Lymnaea stagnalis* by Roubos & Moorer-van Delft (1979). The neuron perikarya are normally completely surrounded by glial tissue; only very exceptionally do they make contact with each other or with the basement membrane. f., Fibroblast. The scale is 10 μm.

### 3.2. *The anatomy of the glial cells*

The glial cells in the buccal ganglia, and also the other central ganglia, did not contain extensive aggregates of organelles and fibrous material such as occurs in the glial cells of some other invertebrates. The glial cytoplasm contained a matrix which appeared relatively uniform within individual cells, but which varied in electron density in different cells (figures 16, 18

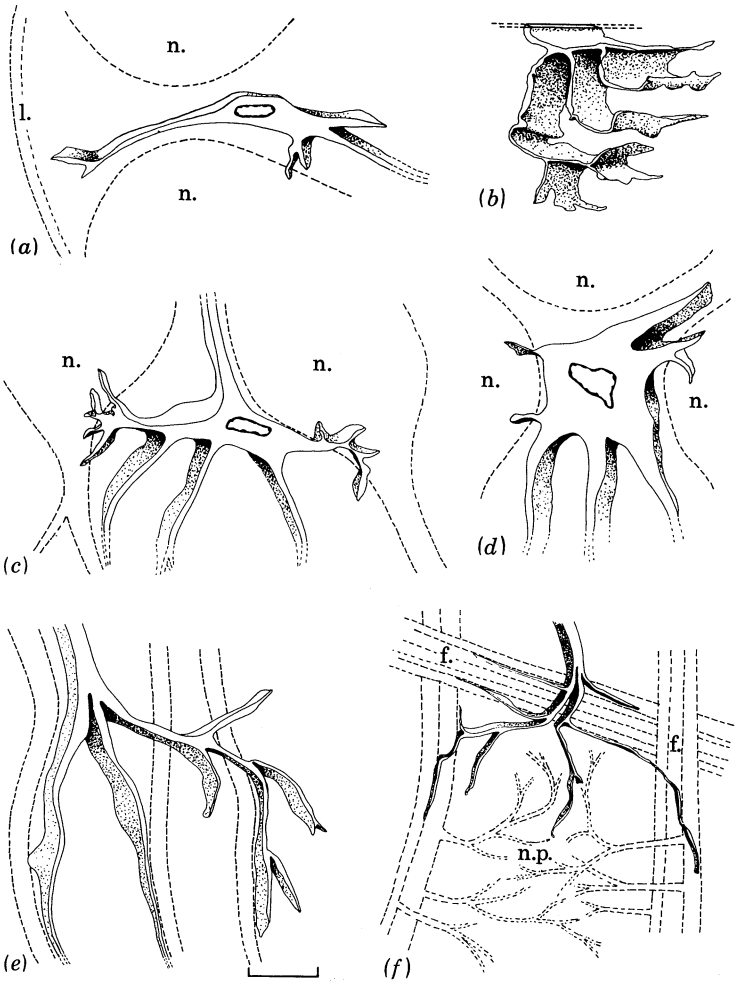


FIGURE 36. Relations between the glial cells and the neurons in the subcapsular cortex (*a*) and core (*b*)–(*f*) of the buccal ganglion. Each drawing shows the arrangement for a slice of glial tissue 5 μm thick. Glial cells located around the neuron perikarya (n.) project processes into the neurons, forming a trophospongium, and other processes towards the basal lamina (l.), or the core of the ganglion (*a*), (*c*), (*d*). It is not known whether every glial cell projects at least one process to the basal lamina, or whether occasional cells may fail to make contact with it (*a*). The glial processes run within the axon tracts (*f*) in the core of the ganglion, wrapping the axons in bundles (*e*), (*f*). In these situations, as well as in the buccal nerves and connectives, the glial tissue is arranged in sheets (*b*). A few attenuated glial processes enter areas of neuropil (n.p.), (*f*). The scale is 10 μm.

and 26). In some cells the cytoplasm appeared relatively empty. The cytological features and their changes with age were as follows.

(i) *Nuclei*

The glial cell nuclei in the adult buccal ganglia were rounded to oval in shape, sometimes more elongated in the nerves (figures 26, 38 and 40). They contained peripheral chromatin, multiple nucleoli, and the nuclear membrane was sometimes studded with attached ribosomes. The adult distribution of chromatin and nucleoli develops between 14 days after egg laying and hatching; before this the nuclei lack nucleoli and have dispersed chromatin. The glial nuclei became increasingly lobed in aged and in experimentally damaged ganglia (figure 50). This change could be correlated with the increased occurrence of lysosomes within the glial cells,


FIGURE 37. Features of the neuropil in the buccal ganglion. Glial processes are black. Two dendritic processes (1 and 2; stippled) are surrounded by large numbers of vesicle-filled, terminal profiles. The terminal processes are more rounded than the post-synaptic structures, and synaptic specializations are frequently lacking (for example, the terminals marked with an asterisk). Areas of limited membrane thickening are sometimes present (arrows on 1), and these normally have 50 nm diameter clear vesicles clustered against the presynaptic thickening. The presynaptic terminals contain a great variety of vesicle types. In comparison with the axon tracts and cortex of the ganglion, only a relatively small amount of glial tissue is located within the neuropil. The scale is 1 μm.

and was most marked in cells containing lipofuscin material. Thus the change was apparently associated with increased phagocytic activity. Similar observations have been reported in mouse brain (Lemkey-Johnson *et al.* 1976). Degenerating glial cells were occasionally observed in ganglia from older snails, and more frequently in damaged ganglia. However, pycnotic glial nuclei such as have been observed in the mammalian brain (Sturrock 1974*c*) were not observed in any experimental animal.

(ii) *Organelles and cytoplasm*

The mitochondria, rough endoplasmic reticulum, and occasional Golgi structures were generally confined to the perinuclear region of the glial cells (figure 26). In adult animals fibrous

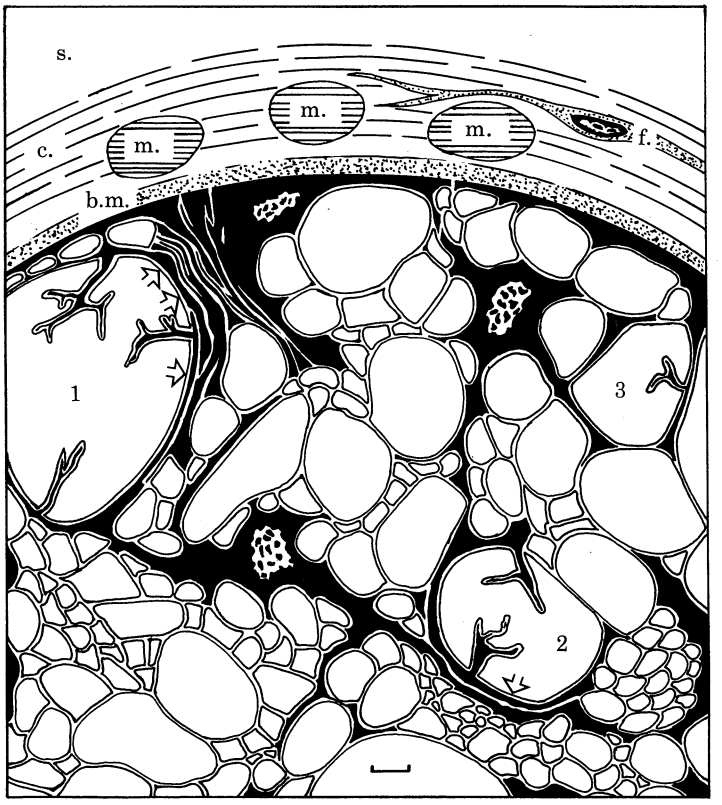


1. Features of the glial–neuron relations in the nerves and connectives. Three glial cells are shown, with their processes black. The general rule is that the large-diameter axons are surrounded by more glial cell processes than the small-diameter axons, which are wrapped in bundles. Large-diameter axons may be penetrated by a trophospongium (axons 1–3), and be surrounded by multiple glial layers (arrows in 1, 2). The axons are separated from the basement membrane (b.m.) by glial tissue. Small molecules have access from the blood sinuses (s.) across the connective tissue (c.) and basement membrane, to the extracellular spaces in the nerve. m., Muscle fibres; f., fibroblast. The scale is 1 μm.

material was present within some of the processes of the glial cells in the nerves and connectives (figures 39 and 40), and to a lesser extent in the glial processes within the ganglia. The fibres were prominent in the lamellate glial wrappings of some axons (figure 31). The fibrous material showed a significant increase with the age of the animal, being absent in the pre-hatched form. In the oldest animals fibres were observed in most glial processes within nerves, sometimes extending to the perinuclear regions of the glial cells (figure 39). A less marked increase with age in fibre content, and also in rough endoplasmic reticulum and granular material was found in the cells of the cortex of the ganglion. Age-related increases in fibrous and reticular material within mammalian glial cells have been reported on several occasions (for example, Vaughan & Peters 1974; Roberts & Goldberg 1976; Mervis 1981). No changes were observed in the number or distribution of organelles in ganglia in which degeneration was induced by ablating individual neurons or by maintaining the isolated ganglia for up to 36 h in saline, although these caused marked neuronal changes (for example, extensive swelling and vacuolation), and increases in the lacunae between the glial cells (figure 52).

The cytoplasm of each glial cell contained a matrix which, after the preparative conditions employed here, varied from weak to moderate electron density. However, local variations in

density were observed in cells at the periphery of the ganglion in material that had been fixed in the presence of elevated $Ca^{2+}$ (5 mM). In these cells there was a progressive darkening of the processes near the connective tissue boundary (figure 9). To test the possibility that $Ca^{2+}$ was becoming bound to the glial matrix sections were examined by electron microscope X-ray analysis. This revealed that the glial cell cytoplasm contained low but significant $Ca^{2+}$. However, as far as could be judged from the spectral analysis the glial cytoplasm of tissues preserved in the absence of high $Ca^{2+}$ contained very similar levels of the element (figure 42),

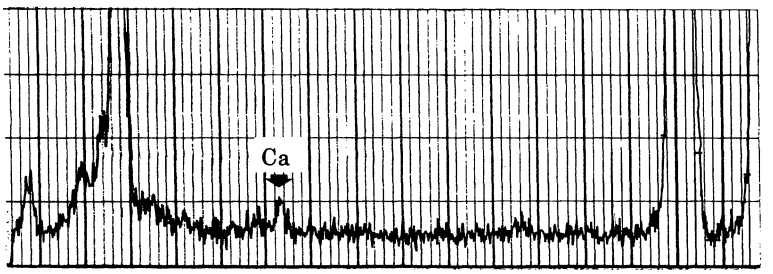


FIGURE 42. Elemental spectrum from analysis of glial cytoplasm in the cortex of the dorsal side of a buccal ganglion (animal mass 4.5 g). The tissue was fixed in glutaraldehyde and osmium solutions and embedded in Araldite. The glial cytoplasm contains significant calcium, which was not detectable in adjacent neurons. The large peak to the left is due to the osmium within the section, that to the right is caused by copper scatter from the supporting grid.

thus increased $Ca^{2+}$-binding could not account for the increased electron density. The significance of the changes in electron opacity caused by $Ca^{2+}$, together with its presence in the normal tissue in a bound state that resists processing for electron microscopy, are not clear. We were unable to detect $Ca^{2+}$ by X-ray analysis within the neurons adjacent to the glial processes, nor did significantly more $Ca^{2+}$ appear to be bound within glial cell inclusions.

Specialized contacts or attachment sites were not observed between adjacent glial cells (figures 10 and 13, plate 2), nor between glial cells and neurons. Such sites, especially desmosomes, are common in some other invertebrates. Synaptic contacts onto glial cells have been reported in *Aplysia* (Colonnier *et al.* 1979) and *Glossodoris* (Nicaise 1967). Varicose axonal processes containing dense-cored vesicles or presumed neurosecretory granules, or both, were frequently observed meandering through the glial cells (figures 39 and 47) as they were through the neuronal perikarya (figure 19) and some large diameter axons (figure 28). However, no synaptic contacts onto the glial cells were observed in *Planorbis*. These features are summarized in figure 27.

(iii) *Inclusions*

Several types of inclusions occur commonly in most glial cells in the buccal and other ganglia, and their associated nerves. They showed variation in number and distribution in the different cells and their processes, and in animals of different ages and states of induced degeneration, as has been described in vertebrates (see, for example, Aune 1976). To aid interpretation they are described under separate headings, but it should be borne in mind that *in vivo* they may be transient structures, perhaps changing from one type to another. Furthermore, structures were sometimes observed which did not fit readily into any category.

*Lipid drops.* These were identified by the criteria of their regular rounded shape and their

strong osmiophilic properties. The diameters ranged from 0.3 to 1.0 μm. They were common in the glial cells in the nerves and connectives, especially in the pre-hatched animal, but very rare in the glial cells in the adult ganglia (figure 9).

*Gliagrana.* These inclusions differ from the lipid drops in being of smaller size (0.2–0.3 μm) and less reactive with osmium (Nicaise 1973). It has been suggested that this type of structure may store metals (for example, Na, K, Ca, P; Nicaise 1973; see also Brown 1982). In *Planorbis* they were common in the glial cells in the cortex of the buccal ganglion as well as in the nerves and connectives (figures 16–18, 38 and 47). The numbers of these structures increased with age. X-ray microanalysis of fixed and resin-embedded material showed that small amounts of $Ca^{2+}$ could be detected inside them; however, this represents material sufficiently well bound to withstand extraction, and *in vivo* they may contain relatively large amounts of this or other metals.

## Description of plate 5

The glial cells in the pre-hatched and young animal.

Figure 23. Tissue from a ten-day (pre-hatched) snail. The neuron on the left (nucleus, n.) is surrounded by a glial cell (g.). The neuronal cytoplasm contains large numbers of ribosomes and dense-core vesicles. The glial cell cytoplasm also contains much ribosomal material, which is a feature not observed in the adult. The glial nucleus (g.n.) also differs from the adult in having very diffuse chromatin, except for a thin band close to the nuclear membrane (see also figures 25 and 26). With one possible exception, marked by the arrow, gliagrana are absent. Magn. × 18700.

Figure 24. Tissue from a 20 d old snail. The two neurons (numbered 1 and 2) are separated by a thin glial process. Neuron 1 contains aggregates of glycogen. Magn. × 18700.

Figure 25. Part of a buccal ganglion in a 14-day embryo. The glial nucleus (g.n.) has no condensed chromatin (cf. the neuronal nuclei, n.), except for a thin band at the nuclear membrane. A few gliagrana (arrows) are present in the glial cytoplasm. Magn. × 8700.

Figure 26. Tissue from a 0.5 g snail (approximate age three months). The micrograph shows an area of glial cells located between neuron perikarya. The nuclear chromatin has become condensed (cf. figures 23 and 25), and mitochondria (m.) are clustered close to the nuclear region. The glial processes are relatively thick compared with old animals. Some of the processes contain gliagrana (large arrows). The extracellular glial lacunae are few and small compared to animals greater than 2.0 g mass. Magn. × 13000.

## Description of plate 6

The glial–neuron relations in the core of the buccal ganglion. The tissue was taken from adult animals (mass range 3–5 g).

Figure 28. The vesicle-filled axonal process runs within the cytoplasm of a neuron axon hillock region (n.). The glial processes on the left contact both neuron elements but do not penetrate the axon hillock. The arrow marks an expansion of the extracellular space between the glial cell processes. Magn. × 35000.

Figure 29. The relatively large-diameter axon running diagonally across the micrograph is covered by a single glial wrapping which in some regions (for example, short arrows) is reduced in thickness to approximately 100 nm. Most of the adjacent small-diameter axons are not associated with glial cell processes. The long arrows mark two glial processes. Magn. × 8500.

Figure 30. Several layers of glial processes (between arrows) run alongside the left-hand axons, separating them from groups of smaller axons on the right of the micrograph. The axon bundle marked by an asterisk is wrapped by a glial process which does not penetrate the middle of the bundle. Magn. × 8500.

Figure 31. Multiple glial wrappings around a relatively large-diameter axon within an axon tract in the centre of the ganglion. Many of the glial processes contain fibrous material. Magn. × 15000.

Figure 32. Multiple glial wrappings separating a relatively large-diameter axon (left) from small-diameter axons (right). Magn. × 15000.

Figure 33. The group of axons on the right are separated from the axons on the left by sheets of glial processes. The glial processes do not penetrate among the axons on the right. Many of the axons are vesicle-filled and appear to be terminal regions. The arrows indicate some of the clumps of glycogen particles present among the synaptic vesicles. Magn. × 15200.

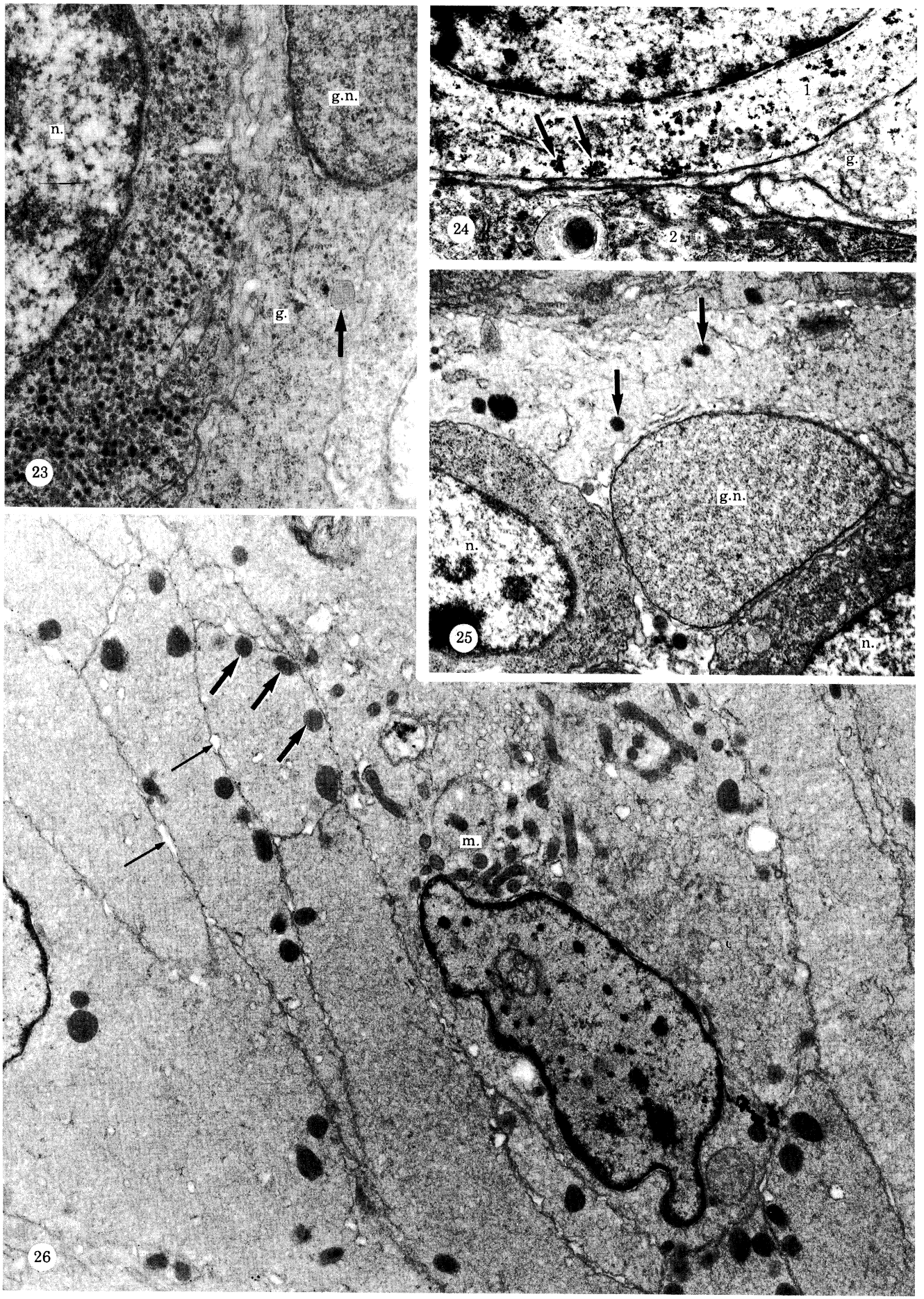


FIGURES 23–26. For description see opposite.

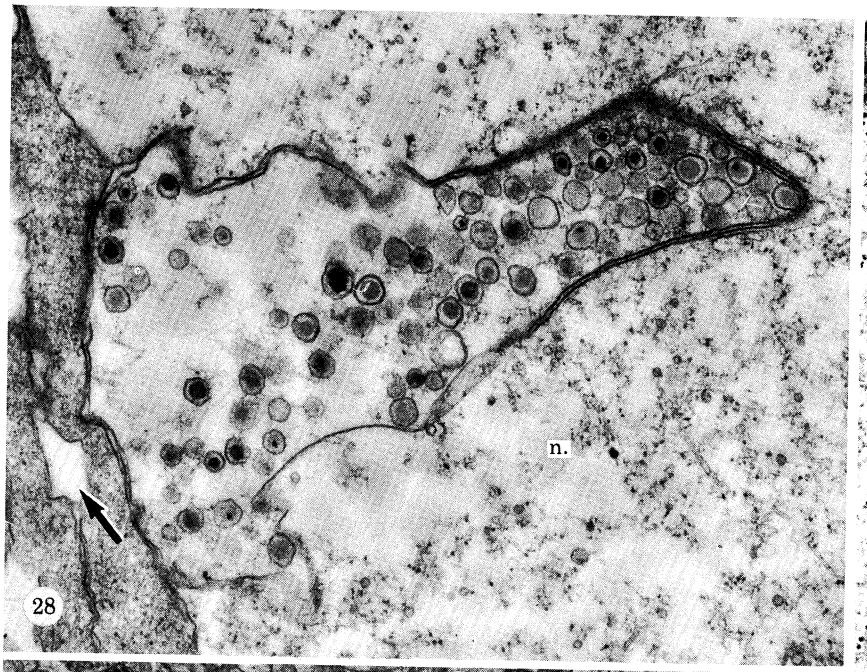



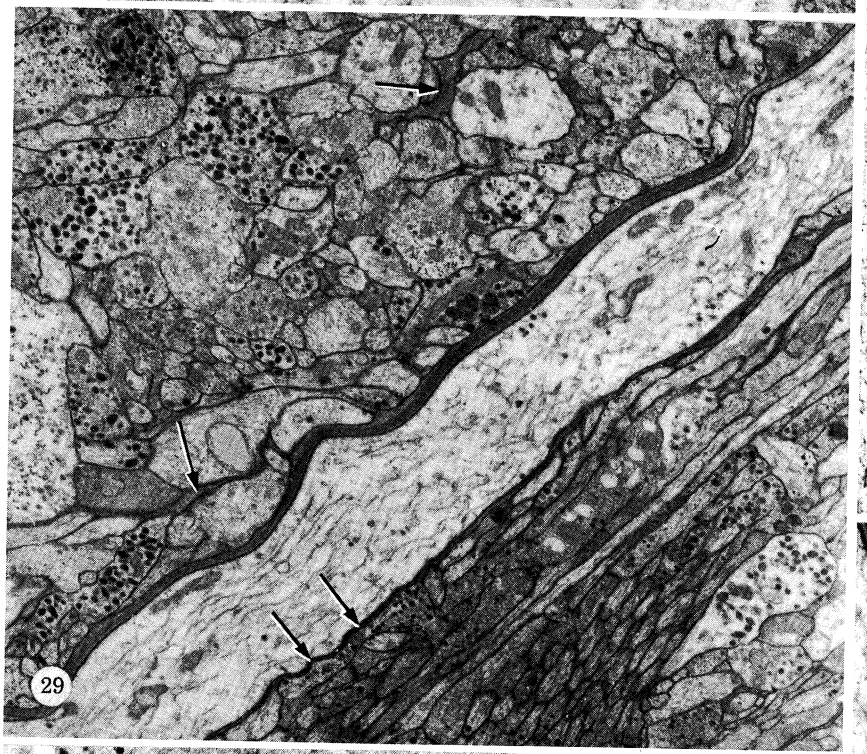


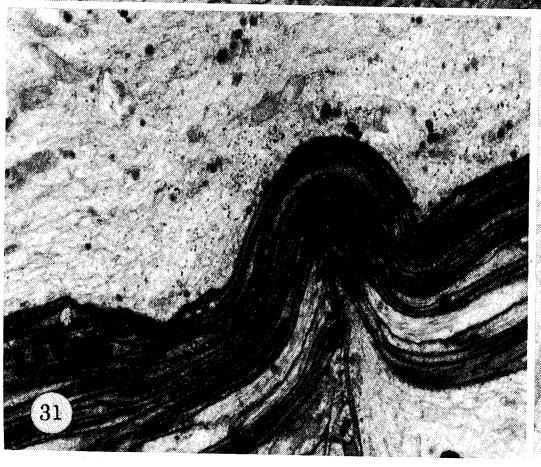




FIGURES 28–33. For description see p. 418.

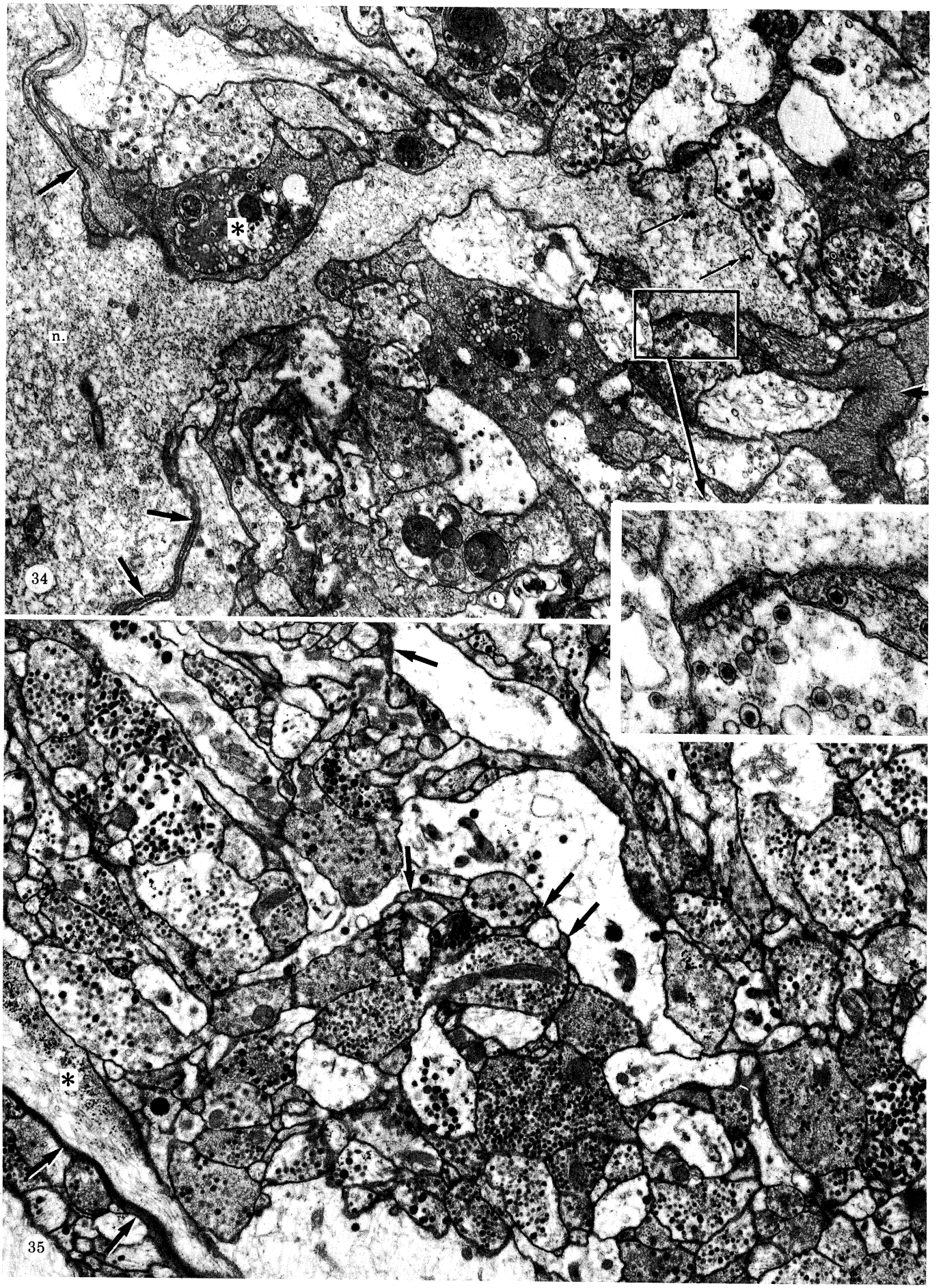


FIGURES 34 AND 35. For description see opposite plate 8

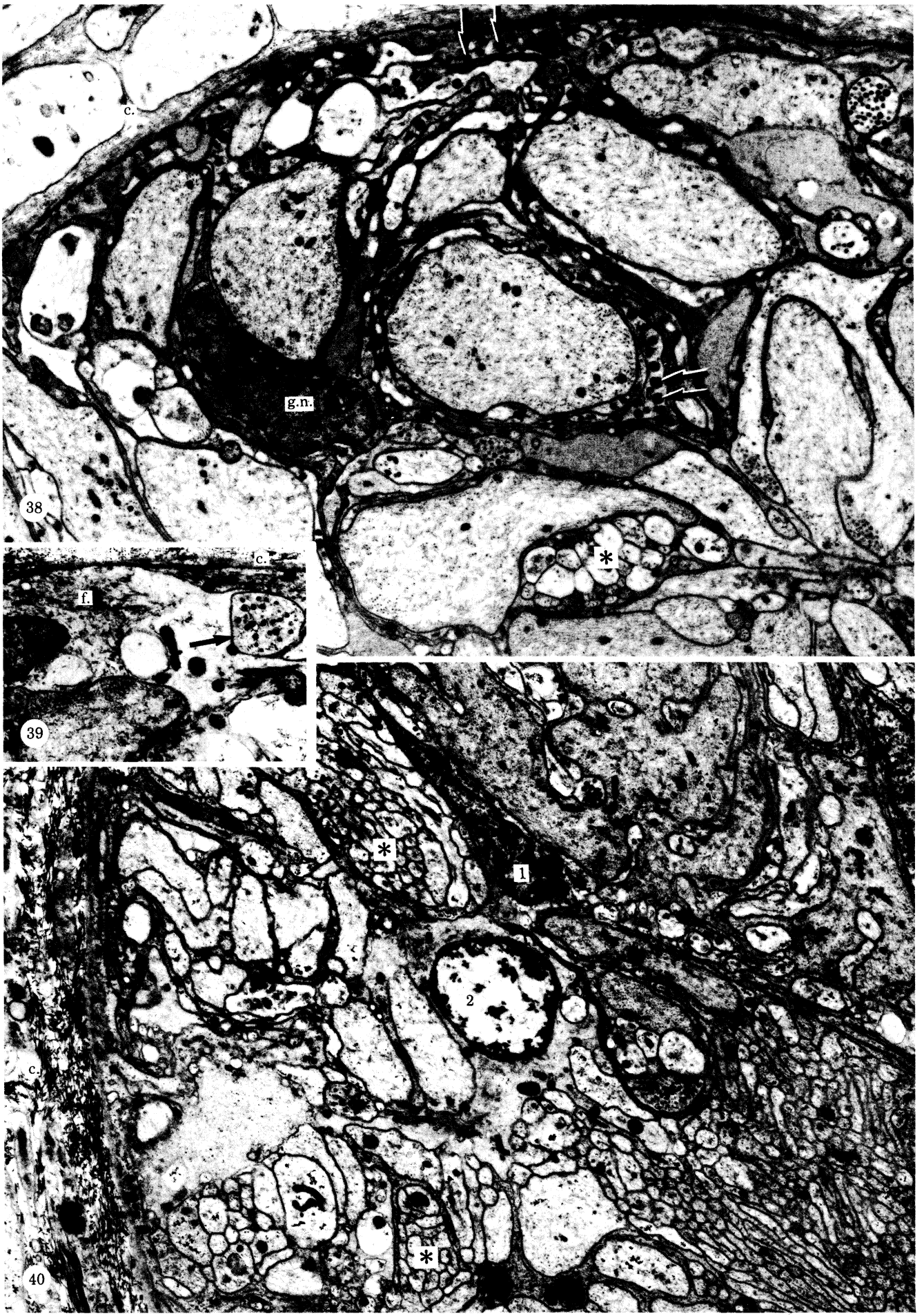


FIGURES 38–40. For description see opposite.

## Description of plate 7

The glial–neuron relations in the neuropil of the buccal ganglion.

Figure 34. A relatively large-diameter axon, n., on the left, projects a process into an area of neuropil. The process contains a few dense-cored vesicles (small arrows), but appears to be dendritic because it is surrounded by numerous vesicle-filled terminal axonal processes. The boxed area, enlarged in the inset, shows a possible synaptic contact onto the dendrite. The major axon is wrapped by glial tissue (arrows at left) but the dendritic branch in the neuropil is not. The asterisk marks nerve terminal material ingested within a glial process. Another glial process is arrowed on the right of the micrograph. Magn. × 10000, inset, × 41000.

Figure 35. Terminal axonal processes, filled with vesicles, intermingle with preterminal or dendritic processes, which are relatively empty. Structures that can be interpreted as glial are indicated by arrows. There is only a very small quantity of glial tissue in neuropil, compared with the cortex of the ganglion. The asterisk marks an axon process containing glycogen particles dispersed amongst the vesicles. The terminal processes contain a great variety of vesicle and granule structures. Magn. × 10000.

## Description of plate 8

The glial–neuron relations in the buccal nerves.

Figure 38. Part of the buccal commissure in a 2.5 g snail. (Axon diameter and shape vary widely.) Some of the larger axons (for example, axon in centre of micrograph) are wrapped by several layers of glial processes, but groups of small-diameter axons are wrapped in bundles (for example, asterisk). Axons do not touch the basement membrane underlying the connective tissue sheath (c.); they are separated by a layer of glial cell processes. The arrows mark some of the gliagrana within the glial cells. g.n., Elongate glial cell nucleus. Magn. × 10200.

Figure 39. In large snails (buccal commissure from an animal weighing 5.0 g) fibre bundles (f.) occur within the glial cells. An axonal profile containing dense-cored vesicles passes through the edge of the glial cell (arrow). c., Connective tissue. Magn. × 11500.

Figure 40. Two glial cell nuclei (1, 2) at the periphery of the cerebrobuccal connective in a 4.5 g animal. The larger glial cell (2) contains scattered fibres and glycogen particles, and wraps adjacent axons. Small-diameter axons are wrapped in bundles (for example, asterisks). Magn. × 10200.

## Description of plate 9

The phagocytic glial cells in the core of the buccal ganglion from a snail of mass 5.0 g.

Figure 43. Phagocytic glial cell (nucleus, n.) containing perinuclear secondary lysosomes (arrows). Magn. × 14500.

Figure 44. The phagocytic glial cell on the left of the micrograph (nucleus, n.) contains numerous autophagic vacuoles, multivesicular bodies and secondary lysosomes. Some of secondary lysosomes are residual bodies (r.). The glial cell projects a process (arrow) which radiates into an area of neuropil (small arrows) but which does not contain lysosome aggregates. Magn. × 10200.

Figure 45. A phagocytic glial cell in an axon tract in the core of the ganglion. A group of secondary lysosomes lies very close to the nucleus (n.). Magn. × 9500.

Figure 46. Phagocytic glial cell (nucleus, n.) lying by an area of neuropil (bottom of micrograph). The cell contains a heterogenous mixture of lysosomes, one of which (arrow) is surrounded by a double membrane, suggesting it may be in the process of being engulfed. Magn. × 9500.

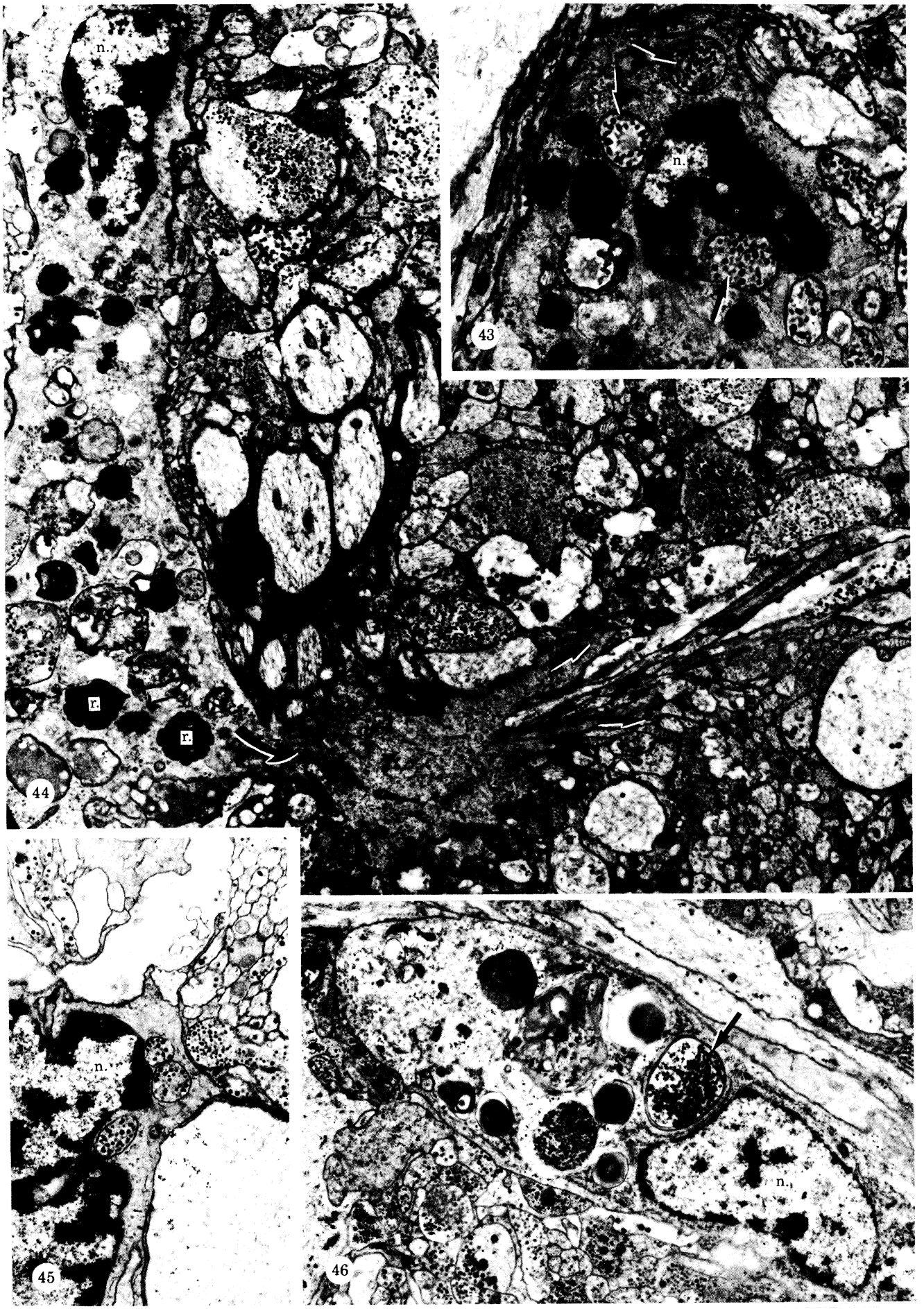


FIGURES 43–46. For description see opposite plate 8.

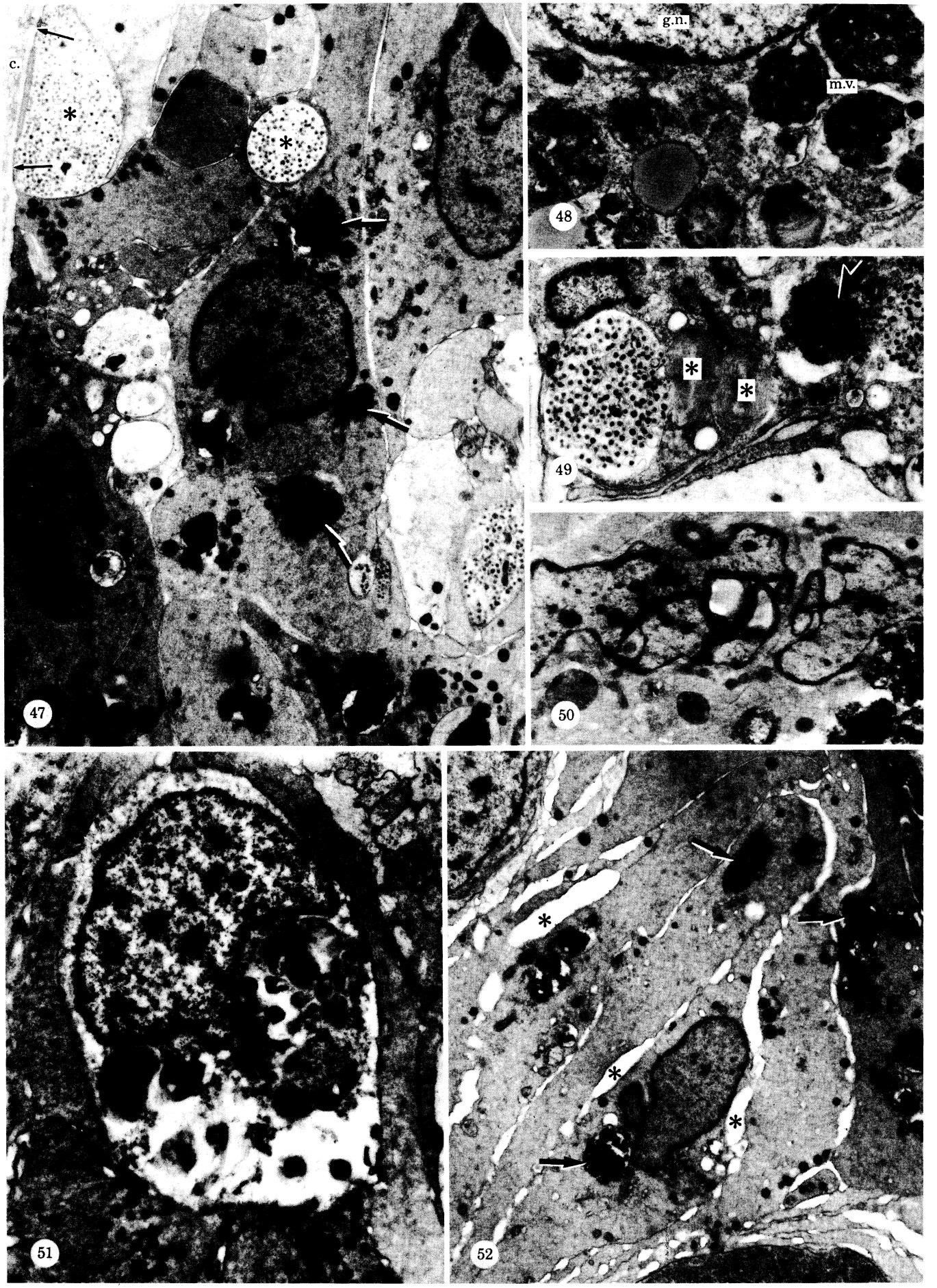


FIGURES 47–52. For description see p. 419.

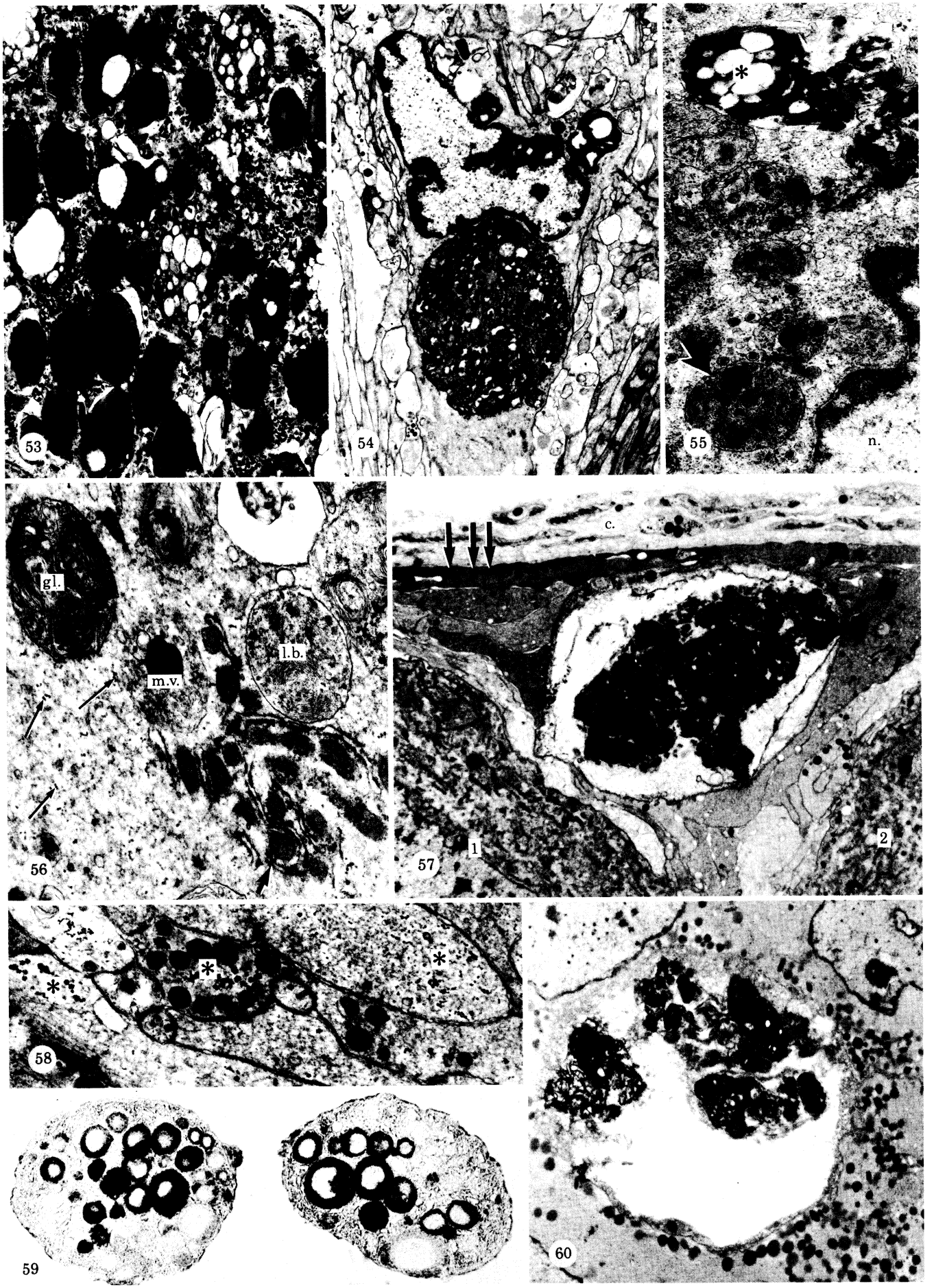


FIGURES 53–60. For description see opposite.

## Description of plate 10

Lysosomes and lipofuscin in the glial cells of the buccal ganglia during ageing and degeneration.

Figure 47. Part of the ventral cortex from a snail of mass 3.8 g showing a group of glial cells which contain numbers of gliagrana, and accumulations of residual bodies. Some of the residual bodies, composed of lipofuscin, in the glial cell in the centre of the micrograph are marked with arrows. Two terminal axonal profiles, perhaps belonging to the same axonal processes, pass through the glial cell processes at the top (asterisks). One of the axonal processes lies against the basement membrane of the connective tissue capsule (c.), without intervening glial tissue (small arrows). Magn. × 8000.

Figure 48. Part of a glial cell (nucleus, g.n.) from the core of a buccal ganglion which had been incubated for 10 h in unoxygenated saline before fixation (animal mass 4.0 g). The cell contains numerous secondary lysosomes, some of which are multivesicular bodies (m.v.), which represent different stages in the breakdown of engulfed nerve terminals. Magn. × 12000.

Figure 49. Part of a glial cell from the core of a buccal ganglion which had been incubated for 14 h in unoxygenated saline before fixation (animal mass 3.7 g). Lamellated bodies (asterisks) are probably secondary lysosomes, as is the multivesicular body to their left. The residual body (arrow) has greater electron density. Magn. × 12000.

Figure 50. The lobed nucleus of a glial cell in a buccal ganglion (animal mass 3.6 g), which had been damaged by ablation of a group of neuron perikarya with a needle tip, then maintained for 12 h in saline. Lipofuscin material is aggregated to the right beneath the nucleus. Magn. × 10000.

Figure 51. A glial cell in a buccal ganglion (animal mass 4.1 g) which had been incubated for 14 h in unoxygenated saline before fixation. The glial cytoplasm is vacuolated and contains aggregates of secondary lysosomes and residual bodies. The glial cell is probably beginning to degenerate. Magn. × 8500.

Figure 52. Part of the cortex of the ventral surface of a buccal ganglion (animal mass 2.0 g) which had been incubated in unoxygenated saline for 36 h before histological processing. The extracellular spaces between some of the glial processes have become swollen (for example, asterisks). The arrows point to some of the residual bodies. The glial processes also contain numbers of gliagrana. Magn. × 7500.

## Description of plate 11

Distribution of lipofuscin and glycogen in the buccal ganglia.

Figure 53. Axon hillock region of a neuron on the ventral surface of a buccal ganglion (animal mass 4.2 g). Large numbers of rounded lipofuscin granules are interspersed with aggregates of glycogen (for example, in the region labelled g.). Magn. × 12000.

Figure 54. A glial cell in the core of a buccal ganglion from a snail mass 5.3 g. The cell contains a few secondary lysosomes above the nucleus, but the most obvious feature is a large residual mass of lipofuscin, which fills most of the cell's cytoplasm. Magn. × 7500.

Figure 55. Lipfuscin aggregate (asterisk) and secondary lysosomes (arrow) in the cytoplasm of a neuron (nucleus, n.) from a snail weight 5.3 g. Magn. × 24000.

Figure 56. Inclusions in the cytoplasm of a glial cell in the cortex of the buccal ganglion of a snail of mass 5.2 g. The variation in appearance of secondary lysosomes is illustrated by the structures termed gliosome (gl.), multivesicular body (m.v.) and lamellated body (l.b.). Some of these may arise from autophagy. In the region indicated by the large arrow a mitochondrion is surrounded by a fold of endoplasmic reticulum, which Holtzman (1976) regards as one of the primary stages of cellular autophagy. Similar lysosome structures have been reported to occur in certain disease states of the human nervous system. The small arrows mark glycogen particles. Magn. × 30000.

Figure 57. A large peripheral mass of lipofuscin in the subcapsular cortex of a snail of mass 3.4 g. The mass is contained within a larger membrane-bound structure, with areas of relatively empty cytoplasm in the periphery. The structure is surrounded by other glial processes, which appear healthy, and two adjacent neuron perikarya (numbered 1 and 2). One of the peripheral glial processes, that lies by the connective tissue capsule (c.), contains gliagrana (arrows). See also figure 60. Magn. × 7500.

Figure 58. Glial cell processes in the ganglion cortex of a snail of mass 4.2 g. Three of the processes, marked by asterisks, contain glycogen deposits. The deposits in the right-hand process are more disperse than in the other two. The glycogen deposits in the middle process are surrounded by gliagrana. Magn. × 17000.

Figure 59. Light microscope radioautograph of a vertical section through a pair of buccal ganglia (snail of mass 3.4 g), previously exposed to [$^3$H]2-deoxyglucose for 1 h and fixed in glutaraldehyde solution. The label is retained in the tissue, incorporated within glycogen (see Kai-Kai & Pentreath 1981*a*). The neuron perikarya are labelled to different extents. The glial cells contain a relatively even grain distribution, but are not labelled as intensely as some of the neurons. Magn. × 120.

Figure 60. A mass of lipofuscin located between a group of healthy glial cells in the cortex of a ganglion from a 4.2 g snail. The section was taken parallel to and just beneath the connective tissue capsule, and shows the relatively large areas of empty cytoplasm that surround the lipofuscin mass. It is not clear whether the empty area contained lipofuscin that was lost during the histological processing, or whether it represents a fluid-filled space of unknown function. The glial cells to the right of the lipofuscin mass contain numerous gliagrana. Magn. × 8000.

*Lysosomes and lipofuscin.* Many structures were recognized as different lysosome stages, according to the features outlined by Holtzman (1976). Phagocytic inclusions and multivesicular bodies (both forms of secondary lysosomes), apparently derived from the neurons, were present in large numbers in some glial cells in the buccal ganglia and nerves (figures 43–46, plate 9, figures 47–52, plate 10, figures 53–56, plate 11; see § 3.3). These inclusions were rarely observed in the glial cells of pre-hatched animals. However, their numbers increased dramatically in ganglia from older animals, and in ganglia which had been damaged to induce degeneration.

Residual bodies also increased in aged and degenerate ganglia. This type of inclusion is membrane-bound and contains lamellate, fibrillar, granular or lipid-like material. They are usually electron-dense, arise from the breakdown of secondary lysosomes (such as phagocytic–pinocytotic vesicles and autophagic vacuoles), and are resistant to further degradation (Holtzman 1976). Structures of this type that occur in insect glial cells have been called gliosomes (Scharrer 1939; Pipa *et al.* 1962). In *Planorbis* the structures were present in both neurons and glial cells and varied from small aggregates approximately 1 μm in diameter, to large masses about 10 μm across (figures 47, 52–55, 57 and 60). The material within these masses appeared directly similar to the well-documented descriptions of vertebrate lipofuscin (Samorajski *et al.* 1964, 1965; Bourne 1973; Glees & Hasan 1976; Schlote & Boellaard 1983). The size and number of the structures increased significantly in the glial cells at the edges of the ganglia in older animals (figures 57 and 60).

The distribution of lipofuscin was investigated using Schmorl's light microscope histochemical technique. Positively reacting sites were observed in both neurons and glial cells. The sites were localized in patches, and showed obvious correspondence with the deposits seen by electron microscopy. A seemingly significant feature was the absence of neuronal lipofuscin when it was present in adjacent glial cells. The reacting sites showed progressive increase in older snails, where strongly reacting sites were located at the edges of the ganglia, among the subcapsular glial cells. In unstained sections these regions appeared as accumulations of yellow-brown pigment. Thus some peripheral glial cells in the buccal ganglia became increasingly filled with residual bodies containing aggregates of lipofuscin as the animals grew older.

*Glycogen.* The distribution of glycogen in the buccal ganglia was mapped with tritium-labelled 2-deoxyglucose and radioautography using aqueous histological processing (Kai-Kai & Pentreath 1981*a*). The glial cells contained a relatively uniform distribution compared with the neurons, where large amounts were frequently present (figure 59). With the electron microscope particles were identified as glycogen because of their size, shape and electron opacity. They were present in many glial processes surrounding the neuronal perikarya (figures 56 and 58). Extensive accumulations were present in some neuronal perikarya and nerve endings (figures 24, 33, 35 and 53).

### 3.3. *The phagocytic glial cells*

The majority of the glial cells in the cortex and nerves of the buccal ganglia contained different amounts of organelles, inclusions and fibres, but no anatomical differences were observed that could warrant their subdivision into separate cell types. The differences in content, although sometimes marked, both in the same animal (for example, fibre content) and in animals of different ages (for example, residual bodies) fitted within a spectrum of characteristics that appeared to belong to the same population. The differences presumably correlate with local variations in previous or present functional requirements; for example, the

progressive increase in fibres in the glial cells in the nerves, which was not apparent in some of the glial cells in the cortex of the ganglia, is probably associated with increased support.

However, some altered glial cells were observed in mature and more commonly, aged animals, but not in embryos or juveniles, which appeared specialized for phagocytic activity. The cells were located in relatively small numbers in the neuropil and in the cortex among the common glial cells. The cells were distinguished by the large numbers of lysosomes and phagocytic inclusions of neuronal origin present in their cytoplasm (figures 43–46, plate 9; figures 48–51, plate 10). Sometimes the cells appeared laden with nerve terminals, apparently accumulated from the adjacent neuropil, and lysosomes sequestering terminals in progressive stages of degradation. In other situations the cells contained numbers of residual bodies. The cells containing residual bodies were chiefly aggregated in the subcapsular cortex and showed deterioration of their organelles and cell membranes (figures 57 and 60). The residual bodies reacted positively to stains that are selective for lipofuscin and increased in number with the age of the animal.

The incidence of the phagocytic glial cells increased markedly after inducing degeneration by mechanical damage to groups of neuron cell bodies. Since the ganglia were isolated from the blood supply, the cells must have derived from within the ganglion. To obtain information on the origin of these cells, damaged ganglia were incubated for 15 min in saline containing [$^3$H]thymidine, followed by 1 h in fresh saline, and processed for radioautography. This caused a significant rise in the number of labelled glial cells in the core of the ganglion (from two or three labelled cells in the undamaged controls to 15–20 labelled cells in the experimental ganglia). However, it is not clear whether the phagocytic glial cells arise from the division of a small stock of specialized scavenger cells that occur in the core of the ganglion, or whether they originate from the division, or transformation of the common glial type that are situated predominantly around the neuron perikarya. Induced degeneration caused relatively fewer morphological alterations in the majority of the glial cells in the ganglion. There was an increase in the size of the extracellular dilatations between the glial cells, but the numbers and distributions of the organelles appeared unaffected. Furthermore the use of [$^3$H]thymidine as an indicator of cell turnover in the buccal ganglia is limited because of the general uptake of this substance by the glial cells (see §3.8). In some parts of the mammalian brain a steady glial turnover has been proposed (Smart & Leblond 1961; Kraus-Ruppert *et al.* 1973; Sturrock 1974*a*, *b*).

The evidence therefore shows that the phagocytic cells increase in the core of the ganglion in response to neuronal degeneration. They engulf inactive or damaged neuronal processes and terminals. The cells become packed with phagocytic vesicles and their breakdown products, residual bodies and lipofuscin, and migrate to the subcapsular region of the cortex, where they occur in aggregations. The fate of these cells is not clear. Their progressive increase in the periphery of the ganglia suggests that they may reside there, neither leaving nor being removed from the ganglia. However, the location of the lipopigment remnants in the periphery would ensure that they do not interfere with the vital functions of the neuropil.

### 3.4. *Phagocytosis of serotonergic nerve terminals*

To obtain information on the nature of the nerve terminals removed by the glial cells, and the frequency of occurrence, in undamaged buccal ganglia, use was made of the ability of 5-HT-containing nerve terminals to selectively accumulate 5-HT (Pentreath & Berry 1978).

The buccal ganglia, intact on the buccal mass, were exposed to [$^3$H]5-hydroxytryptamine for 1 h, and the preparations were maintained in fresh oxygenated saline for up to 24 h. At 10 and 24 h the buccal ganglia were isolated and processed for light and electron microscopy.

A small proportion (less than 1 %) of the axonal processes in the neuropil were labelled after 1 h exposure to [$^3$H]5-HT (figure 61, plate 12). The number and distribution of the labelled processes, as visualized in light microscope radioautographs, was generally the same 24 h after incubation in saline. The labelled terminal processes contained a mixture of granular and agranular vesicles, and were frequently varicose, without specialized synaptic thickenings (see Pentreath & Berry (1978) for a description of the characteristics of the serotonergic nerve terminals). However, 10 h after incubation, and more noticeably at 24 h after incubation, some labelled terminals were observed that were apparently being phagocytosed by glial cells (figures 62–64, plate 12). The increased incidence was difficult to evaluate accurately because the terminals involved could only be identified by electron microscope radioautography. However, the following example indicates the type of change involved. The number of labelled serotonergic profiles and labelled serotonergic inclusions within glial processes in one complete section (excluding grid bar area) of the core of the buccal ganglion were counted in radioautographs from a ganglion processed immediately after exposure to [$^3$H]5-HT (control) and from a ganglion post-incubated for 24 h in fresh saline. In each case approximately 100 labelled profiles were observed; in the control five were associated with glial cells, in the experimental, 14. The labelled profiles in the glial cells were sometimes swollen, with disrupted membranes and vesicle content (figures 62–64), suggesting breakdown. However, no silver grains were observed over secondary lysosomes, nor over electron-dense breakdown products, either because insufficient time had elapsed for the serotonergic terminals to be degraded to these stages, or because the tritium label was lost from ingested material during its degradation. At 24 h after incubation some of the labelled serotonergic processes not associated with glial cells also showed signs of degeneration. Lysosomes containing presumed serotonergic vesicles were present in some of these processes. The serotonergic processes thus possess some autolytic capability, perhaps associated with recycling of the serotonergic vesicles (see Pentreath *et al.* 1982).

The findings therefore show that the fate of many degenerating serotonergic terminals is removal by the phagocytic activity of the glial cells. The large numbers and variety of non-serotonergic nerve terminals also ingested by the glial cells indicates that the reaction is potentially common to all the axonal processes in the neuropil. Moreover, the serotonergic processes did not appear more susceptible to degeneration than other types of process during the course of the experiments, because in many situations apparently healthy labelled profiles were situated close to degenerating non-labelled profiles.

### 3.5. *Haemoglobin in the glial cells*

*Planorbis*, like several other gastropods, contains haemoglobin. The pigment is dissolved in the circulating haemolymph, which appears bright red, and is also present in the animals' tissues, especially the buccal musculature and the nervous system, which also are coloured red. The physiological properties and the significance of the vascular haemoglobin have been extensively studied. The substance is present in aggregates of molecular mass 1 634 000 Da (Svedberg 1933; Svedberg & Hedenius 1934) and has very high oxygen affinity (Mačela & Seliškar 1925). The works by Jones (1961, 1964) have shown that the substance facilitates long

diving periods for bottom-foraging (cf. another pulmonate, *Lymnaea stagnalis*, which has no blood haemoglobin and which occupies a surface ecological niche alongside *Planorbis*). However, the roles of the haemoglobin in the tissues are not clearly understood, although it has been suggested that it may facilitate the diffusion of oxygen (for example, Wittenberg 1966). In *Aplysia* ganglia a similar pigment is localized within the neurons; haemoprotein-containing granules within these cells have been detected and studied by Arvanitaki & Chalazonitis (1952; see also Chalazonitis & Arvanitaki 1951, 1963). In freshly dissected *Planorbis* ganglia, on the other hand, the neuron somata appear as relatively pale areas embedded in a red background (figures 2 and 6, plate 1). The characteristics of the red colour are identical to the haemolymph. On examination under a binocular microscope at high magnification, it is evident that the pigment is chiefly contained within the glial cells surrounding the neuron perikarya. The substance appears distributed evenly among the glial cells; the areas between the perikarya are generally of high red intensity because of the multiple glial layers. The nerve trunks appeared pale yellow to white, which correlates with the relatively low density of thin glial processes.

The distribution of haemoglobin in sections of the buccal ganglia was studied by the method described by Dunn & Thompson (1945). Positive-reacting sites, stained a pale green colour, were present in many of the glial cells surrounding the neuron perikarya (figure 65). Some deposits were also observed in the neuron perikarya, especially their peripheral regions, although these are probably partly located within the glial trophospongium. Some reaction product was also located in the axon hillocks and primary axonal processes of some neurons. Very little positive staining was observed in the nerves or connective tissue.

The observed distribution of the endogenous red pigment indicated that the haemoglobin was distributed relatively evenly throughout many of the glial cell processes. The only organelle present in sufficient numbers to possibly sequester the pigment were the gliagrana (§3.2). However, these structures were not distributed evenly throughout the glial cells and were present in high concentrations in the glial processes in the nerves, which contained very little haemoglobin and therefore appear unlikely to contain the pigment. In some other molluscs the gliagrana are thought to bind metals (Nicaise 1973; Brown 1982). Alternatively it seems most likely that the matrix distributed throughout the cytoplasm of the glial cells surrounding the neuron perikarya, which varies in electron density in different cells but which appears relatively constant within any particular cell (for example, figures 16 and 18), may be a residue of the pigment. This matrix is an unusual feature of the *Planorbis* glial cells, not described in other invertebrates (Radojcic & Pentreath 1979), which appears very similar to the content of mammalian erythrocytes. The intracellular localization of *Planorbis* haemoglobin adds another possible role (that is, oxygen store, or facilitated oxygen supply to the neurons) to the growing list of suggested functions of glial cells.

### 3.6. *Glucose-6-phosphatase localization*

There are two pathways through which glucose and other substances may reach the neurons in the ganglia of the snail: paracellularly through the extracellular spaces, or transcellularly through the glial cells. The relative contributions of each are not known. There do not appear to be any significant barriers restricting the movement of small molecules along the extracellular spaces, because some radioactive tracers (for example, 5-HT) rapidly accumulate in some axonal processes within the neuropil. On the other hand the neuron perikarya in the ganglia and the axons in the nerves are generally separated from the blood sinuses that are located

outside the basal lamina by a layer of glial cell processes, and some control or modification of some substances reaching the neurons either via the extracellular spaces or through the glial cells seems likely. Once inside cells glucose is phosphorylated, and so becomes unable to diffuse back across the cell membranes to the extracellular spaces. If redistribution of glucose between glial cells and neurons, perhaps from local glycogen stores, should take place during nerve activity, it could be predicted that glucose-6-phosphatase be present in the cells where the

## Description of plate 12

Removal of radiolabelled serotonergic processes by the phagocytic glial cells in the core of the buccal ganglia.

Figure 61. Labelled axon profile in the core of a ganglion from a 4.5 g snail, processed for radioautography immediately following 1 h exposure to [$^3$H]5-HT. The axon contains a mixture of granular and agranular vesicles which are characteristic of terminal and preterminal serotonergic axons. Magn. ×32000.

Figures 62–64. Labelled serotonergic profiles in the buccal ganglia from a snail mass 4.4 g. Both buccal ganglia were exposed to [$^3$H]5-HT for 1 h, then individually incubated in fresh saline for 10 h (figure 62) or 24 h (figures 63–64) before processing for radioautography.

Figure 62. The labelled process has been engulfed alongside other, unlabelled, axon profiles. The serotonergic process shows possible early signs of degradation, that is, outer membrane breakdown (arrow), but its vesicle content appears normal. Magn. ×25000.

Figure 63. Several serotonergic profiles in the cytoplasm of a phagocytic glial cell (nucleus, g.n.). The heavily labelled profile nearest the nucleus contains large numbers of vesicles, which are partly masked by silver grains. The larger central profile (asterisk) is overlain by a small cluster of grains apparently associated with a single dense-core vesicle (arrow). The process may be a serotonergic axon. The labelled process at the bottom of the micrograph shows clear signs of degradation, that is, swollen membrane whorls, but two dense-core vesicles are still intact (arrows). Magn. ×18000.

Figure 64. Two serotonergic profiles contained within a glial cell. The bottom profile contains clumps of vesicle material, which appear to be in the process of degradation. Magn. ×21000.

## Description of plate 13

Cytochemistry of haemoglobin (figure 65) and glucose-6-phosphatase (figures 66–72) in the buccal ganglia of adult snails (tissues from snails weight 4.0–5.0 g).

Figure 65. Light micrograph of a part of the dorsal surface of the ganglion. The reaction product is chiefly localized over the glial cells to the right of the neuron perikarya (n.). Relatively little stain is present in the core (asterisk). s., Blood sinus outside the connective tissue capsule. Magn. ×180.

Figure 66. Electron micrograph of sites of glucose-6-phosphatase activity at the edges of the glial cell processes between two neuron perikarya (n.). Magn. ×20000.

Figure 67. Sites of enzyme activity located along the inner membranes of the glial cells, but not their outer membranes, facing the connective tissue capsule (c.). s., Blood sinus. Magn. ×7300.

Figure 68. Reaction product clustered within a neuron perikaryon. It is not possible to resolve the structures underneath the lead deposits, but their shapes and distribution suggest that may be glycogen aggregates. Magn. ×16000.

Figure 69. Glucose-6-phosphatase sites along the membrane of a glial process (arrow), which penetrates a neuron perikaryon (n.). Magn. ×20000.

Figure 70. A group of glial cell processes on the dorsal surface of a buccal ganglion. Sites of enzyme activity are localized along the glial cell membranes, outlining their shapes. Occasional sites of reaction product are located within the glial cells (for example, arrows), possibly associated with glycogen deposits. g., Group of gliagrana. Magn. ×15000.

Figure 71. Axon tract in the core of the ganglion. Enzyme sites are chiefly localized on the glial cell membranes (for example, areas marked by asterisks) but are relatively rare on the axonal membranes (for example, at the arrows where two axons are not separated by glial processes). Magn. ×16000.

Figure 72. Part of an axon tract in the core of the ganglion, illustrating the sparse distribution of reaction product on the axonal membrane (for example, arrows, where two adjacent axons border each other) in contrast to the glial cell membranes in the cortex of the ganglion. Magn. ×16000.

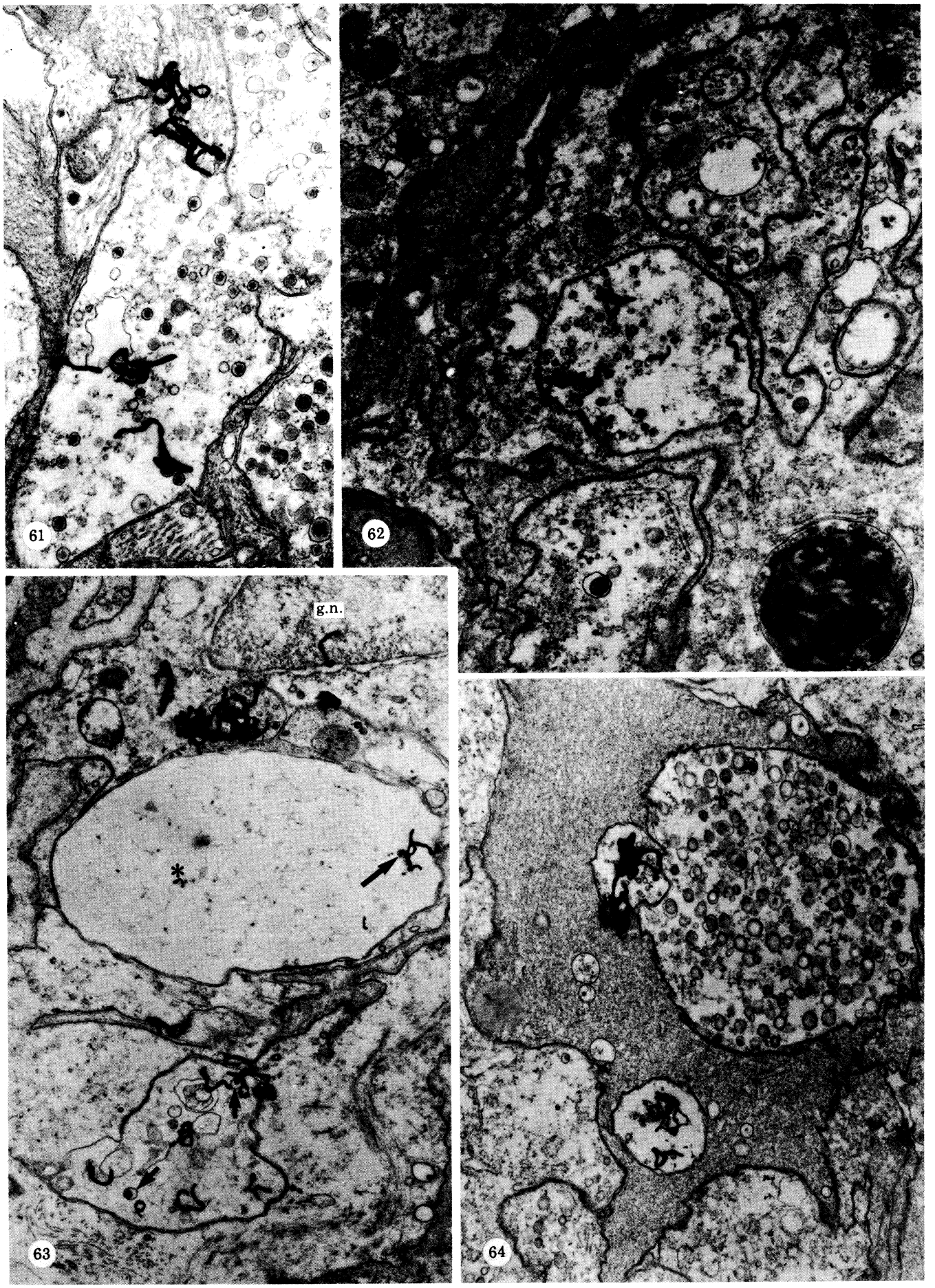


FIGURES 61–64. For description see opposite.

(*Facing p.* 424)

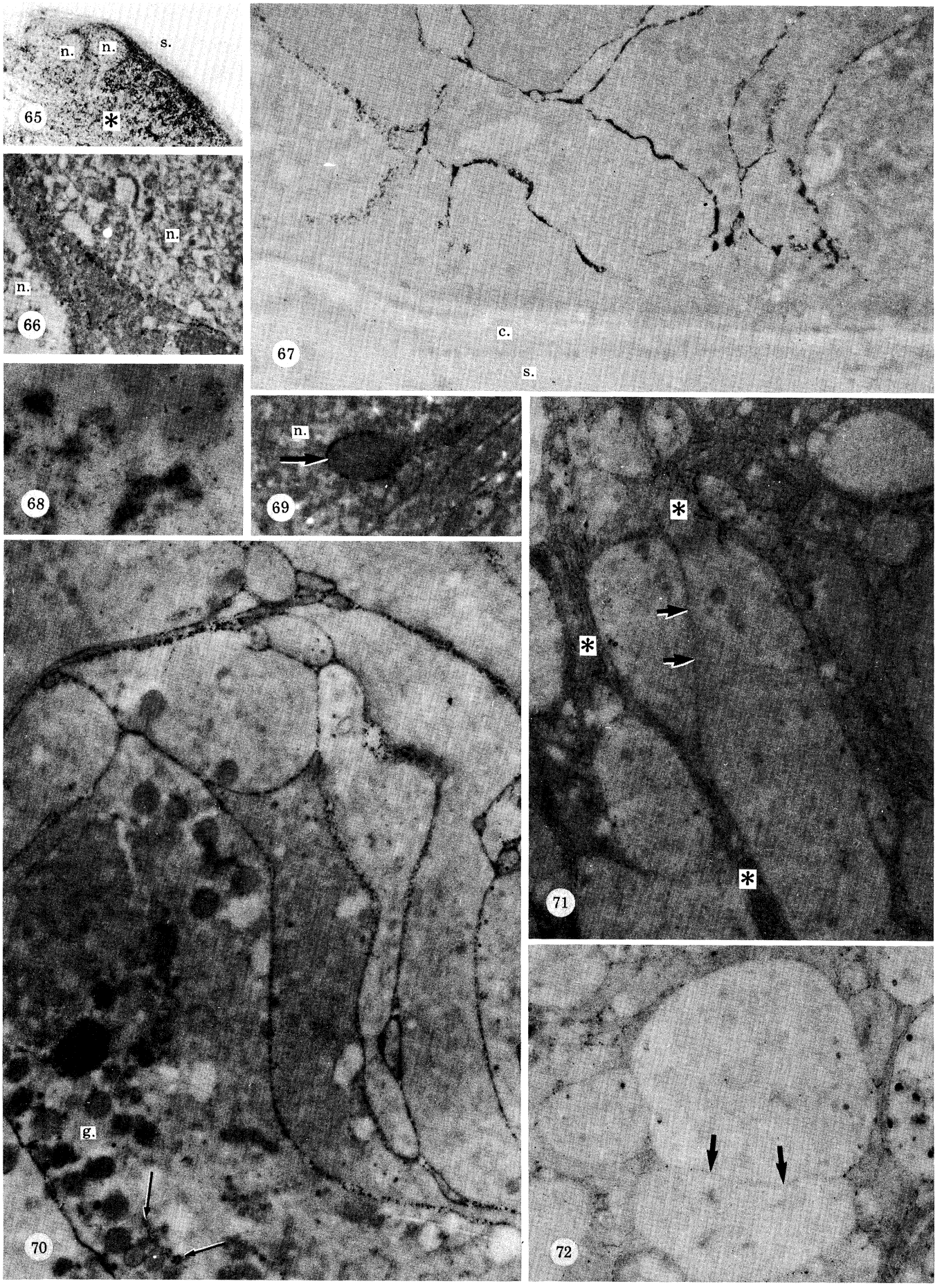


FIGURES 65–72. For description see p. 424.

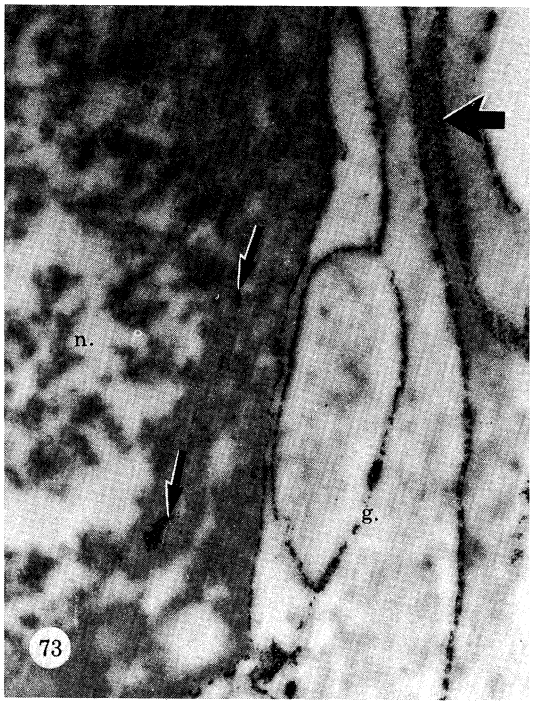


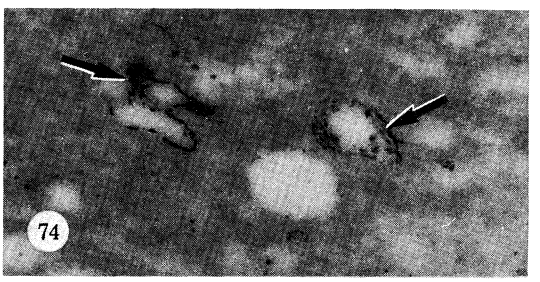


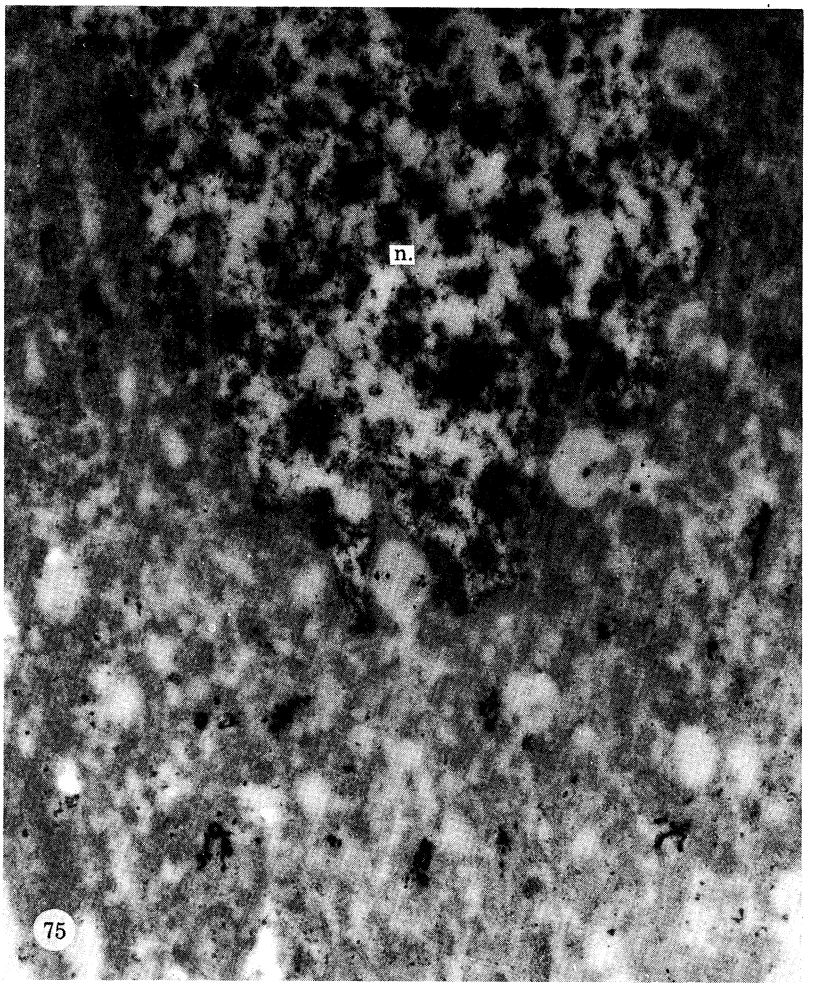


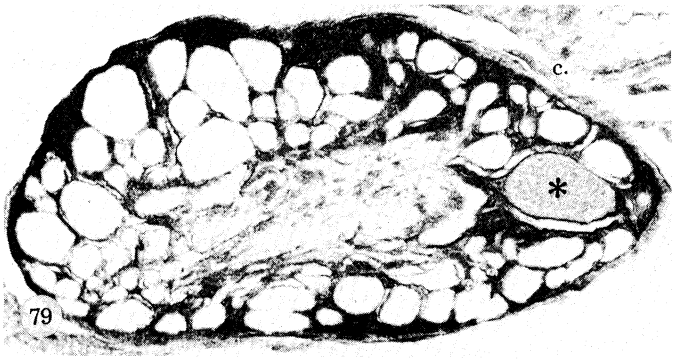


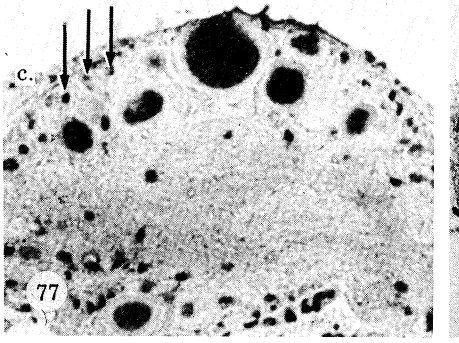


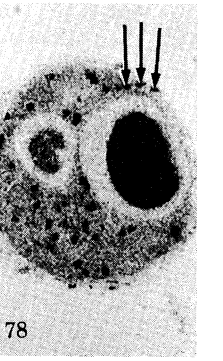


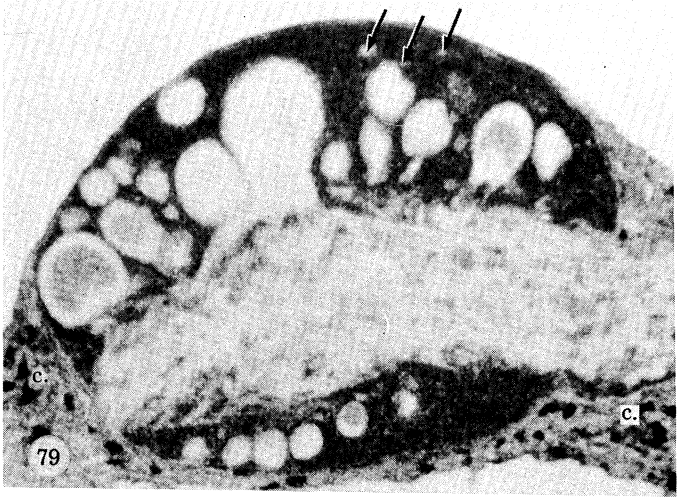


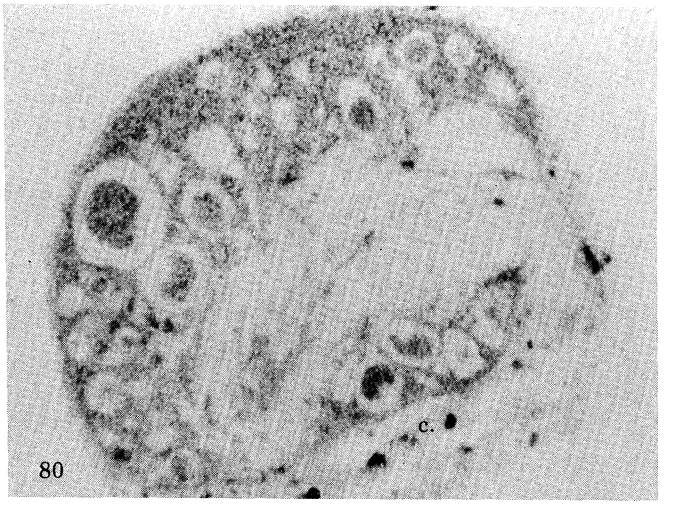


FIGURES 73–80. For description see p. 425.

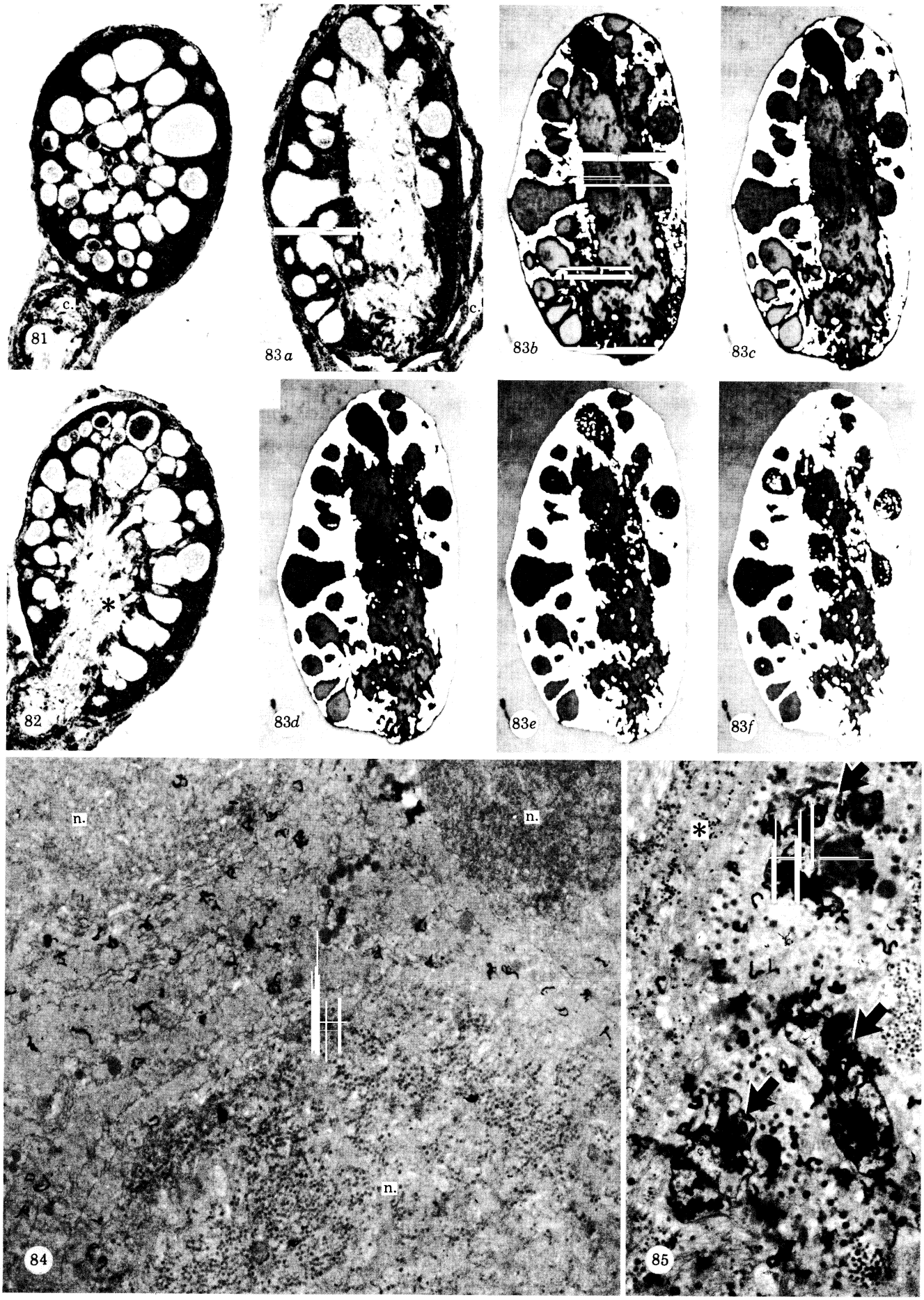


FIGURES 81–85. For description see opposite.

## Description of plate 14

Localization of 5′-nucleotidase (figures 73–75) and uptake of radiolabelled nucleosides (figures 76–80) in the buccal ganglia of adult *Planorbis* (animals mass 4.0–5.0 g).

Figure 73. Sites of reaction product for 5′-nucleotidase on the membranes of glial cell processes (g.), surrounding a neuron (nucleus, n.). The large arrow marks an area of glial membrane sectioned obliquely, where the distribution of the enzyme sites is evident. Two areas of activity are present in the neuron's cytoplasm (small arrows). Magn. × 21000.

Figure 74. Enzyme activity associated with glial processes (arrows) penetrating a neuron soma. Magn. × 20000.

Figure 75. Distribution of 5′-nucleotidase in part of a neuron perikaryon (nucleus, n.) on the dorsal surface of the buccal ganglion. The pattern of distribution indicates a possible association with endoplasmic reticulum or Golgi structures. Note the absence of activity from the nucleus. Magn. × 20000.

Figure 76. Light microscope radioautograph of a buccal ganglion that had been exposed for 15 min to radiolabelled thymidine. The glial tissue surrounding the neuron perikarya in the cortex of the ganglion is heavily labelled. The neurons are unlabelled, with the exception of one marked with an asterisk, which has been evenly but weakly labelled. In this neuron no difference of grain density between nucleus or cytoplasm can be distinguished, nor was evident in adjacent sections. It is possible that the neuron is degenerating and label is being bound in some artefactual manner. Connective tissue structures (c.) are moderately labelled, as are a few structures, presumed glial cell processes, in the core of the ganglion. Magn. × 150.

Figure 77. Radioautograph of material exposed to [$^3$H]adenosine for 15 min. The glial cell nuclei (for example, small arrows) and neuronal nuclei are heavily labelled. Fibroblast nuclei in the connective tissue sheath (c.) are also labelled. Note the absence of glial nuclei in the core of the ganglion. Magn. × 180.

Figure 78. Radioautograph of a section of peripheral cortex of a buccal ganglion incubated in [$^3$H]adenosine for 15 min. Large numbers of glial cell nuclei can be counted between and around the neuron perikarya (for example, arrows). The glial cytoplasm is moderately labelled. Magn. × 180.

Figure 79. Radioautograph of a section of a buccal ganglion incubated for 15 min in [$^3$H]cytidine. The glial cell cytoplasm, but not the nuclei (for example, arrows) is heavily labelled. Some neuronal nuclei and structures in the connective tissue (c.) are also labelled. Scattered, labelled glial processes are present in the core of the ganglion. Magn. × 200.

Figure 80. Radioautograph of material exposed for 15 min to [$^3$H]guanosine. The glial cells and neuronal nuclei are weakly to moderately labelled. Structures within the connective tissue (c.) are also covered by silver grains. Magn. × 200.

## Description of plate 15

Uptake of radiolabelled nucleosides and the use of the Magiscan Image Analysis System for quantitative radioautography.

Figures 81 and 82. Radioautographs of semi-adjacent sections of a buccal ganglion exposed for 15 min to [$^3$H]uridine. The glial tissue is heavily labelled. Silver grains also mark some neuronal nuclei, and structures within the connective tissue (c.). Note the absence of labelling from many parts of the ganglion core (asterisk), which is also evident in figure 83*a*. Both figures magn. × 120.

Figure 83. The radioautograph of a section of [$^3$H]uridine-labelled tissue (*a*) is displayed on a television screen (*b*)–(*f*). This is achieved by placing the television camera in front of the radioautographic photograph, or by attaching the camera directly onto the microscope to view the radioautograph slide. The connective tissue (c.) is removed by cutting from the photograph before placing in front of the camera, or by means of a light pen attachment in front of the television screen. The Magiscan system 'sees' the labelled parts of the radioautograph as the white areas in (*a*)–(*f*), which are then computed as a percentage of the section area. The level at which a particular grain density is included in the percentage can be set by a grey level adjustment. A series of such settings is illustrated in (*a*)–(*f*). The setting must be adjusted to give the most accurate match to the labelled glial cells. The setting shown in (*d*) gives the most satisfactory match of the series; this gives a glial cell measure of 44%. The readings range from 34% for (*b*) to 54% for (*f*). Each magn. × 120.

Figure 84. Electron microscope radioautograph of part of the cortex of a buccal ganglion exposed for 15 min to [$^3$H]uridine. 96% of the silver grains are localized over the glial cell processes which are located around and between three neuron perikarya (n.). Magn. × 5000.

Figure 85. Electron microscope radioautograph of tissue exposed to [$^3$H]adenosine for 15 min. Three glial cell nuclei (arrows) are heavily labelled. Silver grains are also present over the glial cell cytoplasm and gliagrana, but relatively few are present over the neuronal processes to the left of the micrograph (asterisk). Magn. × 10000.

redistribution occurs. To test this we studied the localization of the enzyme by the lead phosphate technique at pH 6.5 (Lewis & Knight 1977).

Positive reacting sites were observed with the light microscope, located in thin bands around the neuronal perikarya and glial cells, and occasionally in small aggregates (diameter 1–3 μm) within the neurons. Stained deposits were also present, but less marked, in the core of the ganglion. The weaker staining may have been because the fixative or incubation mixtures were unable to penetrate sufficiently far during our experimental application of the technique to intact ganglia (the method is normally applied to fresh frozen sections or sections of material that has been briefly pre-fixed, but both procedures may cause translocation of the enzyme and poor preservation). The distribution of reacting sites was revealed clearly by electron microscopy (figures 66–72, plate 13). A striking feature was the association of the activity with the glial cell membranes. The lead reaction product, consisting of fine granules, was deposited intermittently along the membrane of the cells, outlining their shapes (figures 67 and 70). In some places the granules were overlapping and clustered together, forming an apparent unbroken line, which masked the membranes of the adjacent glial cells. In other places the deposits occurred separately, with distances between deposits varying from a few nanometres to approximately 1 μm. The deposits extended along the trophospongia at the edges of the neuron perikarya (figure 69). However, no reaction product was observed at the edges of the glial cell processes that bordered the basement membrane surrounding the ganglion (figure 67). Inside the glial cells sites of activity were uncommon, and not apparently associated with any particular organelle (figure 70).

Less activity was associated with the neurons than with the glial cells. Some deposits were located on their cell membranes, and these were frequently difficult to distinguish from the adjacent glial cell membranes. Deposits were sparsely located along axonal membranes in the core of the ganglion (figures 71 and 72), although as mentioned above, this may have been because access of the incubation mixture was restricted. Inside the neurons sites of activity were observed in small clumps which sometimes appeared to be associated with glycogen particles (figure 68). Reaction sites were significantly reduced in ganglia incubated with sodium β-glycerophosphate as a control substrate, but lead granules were still observed on some glial cell membranes. This indicated that not all the sites of enzyme activity could be considered specific for glucose-6-phosphatase. However, the enzyme is now known to have multiple activities apart from the original single role postulated in liver tissue of the formation of free glucose (see Ryman & Whelan (1971) for review). In beef brain it has in fact been demonstrated that glucose-6-phosphatase hydrolyses β-glycerophosphate (Kornguth & Stubbs 1965) and consequently the control may not be appropriate for nervous tissue. The biochemical and histochemical activities of the enzyme in *Planorbis* ganglia require detailed analysis; however, our results demonstrate that a form of the enzyme with activity for glucose-6-phosphate is distributed along the glial cell membranes (apart from the membranes facing the basement membrane, at the edges of the ganglia) and to a lesser extent, on the neuronal membranes.

### 3.7. *5′-Nucleotidase localization*

5′-Nucleotidase has a widespread distribution on the plasma membranes of many different cell types (see, for example, Solyom & Trams 1973). However, in mammalian central nervous tissue the enzyme is associated with myelin, where it is thought to be particularly important during myelination (see Cammer & Zimmerman 1981; Snyder *et al.* 1983), and has been

localized histochemically on the cell membranes of oligodendrocytes, astrocytes, microglial cells and on the myelin sheath but not on neuronal plasma membranes (Vercelli-Retta *et al.* 1976; Bernstein *et al.* 1978; Kreutzberg *et al.* 1978). A major role of 5′-nucleotidase is the hydrolysis of adenosine-5-monophosphate (AMP), producing adenosine. Because of the importance of adenosine as a modulator of many events in nervous tissue (Stone 1981; Schubert *et al.* 1982), the preferential localization of the enzyme on the plasma membranes of glial cells argues for metabolic interactions between neurons and glial cells. Nucleotides are released from neurons during activity (see reviews by Stone (1981) and Schubert *et al.* (1982)) but cannot penetrate cell membranes. The glial membrane 5′-nucleotidase is appropriately localized from the production of extracellular adenosine which may then exert local modulatory effects, for example stimulation of cyclic AMP via receptors, or be taken up by different cell types. [$^3$H]Adenosine is selectively accumulated by the glial cells in *Planorbis* (§3.8). To determine the distribution of 5′-nucleotidase in the buccal ganglia we used the technique described by Wachstein & Meisel (1957).

The light and electron microscopical cytochemistry showed that reactive sites were mainly associated with the glial cell membranes. Lead deposits were generally localized in a patchy fashion, but sometimes continuously over distances of several micrometres of cell membrane (figures 73–75). The distribution was similar to the glucose-6-phosphatase, with the glial cells clearly outlined, but with no marked sites at the edges of the cells bordering the connective tissue capsule. Deposits were very infrequent over the glial cells cytoplasm and were not observed over any glial cell nucleus. Enzyme-positive sites were rarely observed on neuronal membranes, although these were often masked by deposits on the adjacent glial cell membranes. However, significant sites were located within the cytoplasm of many neuron perikarya (figure 75). The distribution of these sites suggested that they were associated with endoplasmic reticulum or perhaps Golgi structures. No deposits were present in neuronal nuclei. The specificity of the technique for 5′-nucleotidase is considered to be high with insignificant activity owing to unspecific phosphatases (Scott 1965). Substrate-lacking controls, or substrate with added nickel ions were negative in these experiments.

### 3.8. *Uptake of radiolabelled nucleosides*

It has frequently been observed that suitable biochemical, molecular and morphological 'markers' for glial cells would greatly aid studies of their functions and distribution in both normal and diseased states. Some progress has recently been made in discovering these; for example, non-neuronal enolase (Schmechel 1978) glial acidic fibrillary protein (GFA), S-100 protein, carbonic anhydrase and glutamine synthetase are thought to be located to a significant extent in astrocytes (see Varon & Somjen (1979) and Roots (1981) for references). Gamma-aminobutyricacid (GABA) and its analogue DABA, are taken up selectively by non-neuronal cells (Kelly & Dick 1976), and [$^3$H]β-alanine uptake has been employed to distinguish neuroglia from neurons and vascular elements, and has confirmed the 'non-neuroglial' nature of the microglial cells (Schon & Kelly 1975; Dick & Kelly 1977; Soreide *et al.* 1978).

For the purpose of providing a means for accurately quantifying the cellular components of the buccal ganglia we developed selective anatomical markers for the following: the neurons and their nuclei and cytoplasm, the glial cells and their nuclei and cytoplasm, and the connective tissue sheath. The tritiated nucleosides adenosine, uridine, cytidine, thymidine and guanosine 'labelled' the components in different ways. While each nucleoside uniformly

labelled the glial cytoplasm, they varied in their labelling of the different cell nuclei and the connective tissue capsule. The variability was due to three factors: firstly, the concentration of the nucleoside; secondly, the length of the incubation time; and thirdly, the different uptake and binding properties for the different substances.

(i) *Glial labelling*

Each nucleoside uniformly labelled the glial cytoplasm (table 1, figures 76–80, plate 14; figures 81 and 82, plate 15). The density of labelling was generally increased by increasing nucleoside bath concentration as well as incubation time, although after incubation times exceeding 1 h increased accumulation was less noticeable. [$^3$H]Thymidine and [$^3$H]uridine produced heavy labelling of the glial cytoplasm at 15 min; [$^3$H]adenosine and [$^3$H]guanosine gave weaker marking (table 1, figures 76–82). However, radioautographs that could be

TABLE 1. PROPERTIES OF THE LABELLING OF THE GLIAL CELLS AND NEURONS IN THE BUCCAL GANGLIA BY [$^3$H]NUCLEOSIDES

(The ganglia were exposed to the radiolabelled nucleosides for 15 min at room temperature. Grain densities over the different cellular compartments were compared at the different nucleoside concentrations.)

| | concentration μg ml$^{-1}$ | glial nuclei | glial cytoplasm | neuronal nuclei | neuronal cytoplasm | connective tissue |
|---|---|---|---|---|---|---|
| cytidine | 0.1 | − | / | / | − | + |
| | 1.0 | − | / | + | − | + |
| | 2.1* | / | + | + | − | + |
| | 4.2 | / | + | + | − | + |
| uridine | 0.1 | − | / | / | − | − |
| | 1.0 | − | + | / | − | + |
| | 2.0* | / | ++ | / | − | ++ |
| guanosine | 0.1 | − | − | − | − | − |
| | 1.0 | − | − | − | − | − |
| | 4.0 | − | − | − | − | / |
| | 8.0 | / | / | − | − | / |
| | 16.0* | / | + | / | − | / |
| thymidine | 0.1 | − | − | − | − | − |
| | 1.3 | / | / | − | − | − |
| | 2.5 | + | ++ | − | − | / |
| | 5.0* | + | ++ | − | − | + |
| adenosine | 0.1 | − | − | − | − | − |
| | 1.0 | / | / | / | − | / |
| | 2.7 | + | / | + | / | / |
| | 5.5* | +++ | + | ++ | / | + |

−, Trace or no labelling; /, sparse, occasional or uneven labelling; +, moderate labelling; ++, heavy labelling; +++, maximal labelling.

* Concentrations of the nucleosides giving maximum definition of the different cellular compartments.

relatively easily interpreted were obtained for each substance after 15 min exposure, and this period was selected for the quantitative analysis. Uptake of all nucleosides was blocked by 2,4-dinitrophenol, indicating that uptake took place by an active process.

Glial nuclear marking was variable; the nuclei were not always distinguishable from the surrounding glial cytoplasm. Uptake of thymidine and uridine by glial nuclei was particularly difficult to resolve because of the heavy cytoplasmic labelling. Adenosine, however, was strongly

and evenly accumulated by glial nuclei until they were readily discernable within the glial cytoplasm (figures 77 and 78).

The distribution of the [$^3$H]adenosine and [$^3$H]uridine label within the glial cells was studied by electron microscope radioautography (figures 84 and 85). There was no apparent preferential association of either label with any structure in the nuclei or the cytoplasm; the silver grains were distributed relatively evenly over both compartments. However, the electron microscope work confirmed the accuracy of the labelling of the nuclei and cytoplasmic compartments made visible with the light microscope.

(ii) *Neuronal labelling*

The cytoplasm of most neurons was unlabelled by any of the nucleosides after 15 min exposure to a range of concentrations (table 1). However with increased periods of exposure (up to 3 h) the neuronal cytoplasm became progressively labelled, especially with [$^3$H]adenosine, which eventually equalled the density of the nuclear labelling. An exception was [$^3$H]thymidine, which rarely produced any grains over any neuron in the buccal ganglia, under any of the experimental concentrations or incubation times (figure 76).

Many neuronal nuclei were also labelled by [$^3$H]adenosine or [$^3$H]cytidine, especially after 1 h incubation, and weakly labelled by elevated concentrations of [$^3$H]guanosine. [$^3$H]Uridine produced a selective and heavy marking of a small proportion of the neuronal nuclei at all times of incubation; however, the majority were weakly marked or unlabelled (figures 81 and 82). [$^3$H]Thymidine was not observed to label any neuronal nuclei. The labelling with some nucleosides of certain neuronal nuclei, and after extended time periods (that is, up to 3 h) the cytoplasm of some neurons is an interesting phenomenon that has been described in several other molluscs, and also observed in vertebrates and man (see Pevzner (1979) for references), but the significance is not yet clear.

(iii) *Connective tissue labelling*

The radiolabelled nucleosides labelled the connective tissue layer ensheathing the buccal ganglia. This layer consists chiefly of collagen fibres and fibroblasts. Both cellular and extracellular elements appeared labelled (figures 76–82). The labelling characteristics of the nuclei and cytoplasm of the fibroblasts with the different tracers were very similar to that of the glial cells.

(iv) *The possibility of glia–neuron transfer*

Prolonged incubation of the ganglia in each nucleoside except thymidine caused progressive labelling of the neuronal cytoplasm. The question arises of whether this resulted from direct uptake by the neurons, or whether it is partly through transfer of nucleosides, RNA or protein products from the glial cells that are the first cells to become labelled. In an attempt to clarify this, ganglia were given a 15 min pulse of nucleoside followed by 1 h post-incubation in fresh saline. The results, summarized in table 2, did show a slight increase in neuronal labelling with cytidine and uridine which indicated transfer. However, we were unable to obtain more positive proof because the possibility could not be excluded that the neuronal labelling was due to slow conversion of substance or substances normally washed out during the histological processing, to insoluble metabolites during the post-incubation. There were, furthermore, increases in the labelling of the glial cell cytoplasm which would most likely be accounted for by such a slow

TABLE 2. DISTRIBUTION OF LABEL IN THE BUCCAL GANGLIA 1 H AFTER EXPOSURE TO [$^3$H]NUCLEOSIDES

(The ganglia were exposed to the radiolabelled nucleosides for 15 min at room temperature, then maintained in fresh saline for 1 h. Grain densities over the different cellular compartments were compared at the different times.)

| | glial nuclei | glial cytoplasm | neuronal nuclei | neuronal cytoplasm | connective tissue |
|---|---|---|---|---|---|
| cytidine (2.1 μg ml$^{-1}$) | | | | | |
| 15 min load | / | + | + | − | + |
| 1 h post-incubation | / | ++ | ++ | / | + |
| uridine (2.0 μg ml$^{-1}$) | | | | | |
| 15 min load | / | ++ | / | − | ++ |
| 1 h post-incubation | / | +++ | + | / | ++ |
| guanosine (16.0 μg ml$^{-1}$) | | | | | |
| 15 min load | / | + | / | − | / |
| 1 h post-incubation | / | + | + | − | / |
| thymidine (5.0 μg ml$^{-1}$) | | | | | |
| 15 min load | + | ++ | − | − | + |
| 1 h post-incubation | + | +++ | − | − | + |
| adenosine (5.5 μg ml$^{-1}$) | | | | | |
| 15 min load | +++ | + | ++ | / | + |
| 1 h post-incubation | +++ | / | ++ | / | + |

−, Trace or no labelling; /, sparse, occasional or uneven labelling; +, moderate labelling; ++, heavy labelling; +++, maximal labelling.

conversion during the post-incubation period. Attempts to demonstrate transfer by dry-mount radioautography of freeze-dried and wax-embedded material were unsuccessful.

(v) *Properties of the label within the glial cells*

The glial cells take up and bind the nucleosides when they are present in low extracellular concentrations (1–5 μg ml$^{-1}$ of incubating solution). The uptake was blocked by the addition of 2,4-dinitrophenol; thus, the uptake was an active process. As nucleosides retained in tissues after processing for radioautography are frequently associated with RNA and DNA production and with protein synthesis (for example, Angelier *et al.* 1976; Lasek *et al.* 1977), we employed the method of Ogur–Rosen (1950) for the separation of DNA, RNA and protein fractions of ganglia exposed to each of the nucleosides (except for guanosine). Tracer concentration and incubation times were selected to optimize nucleoside uptake to the glia (see table 1), although even under these conditions there was some uptake by the neuronal nuclei. This procedure showed that most activity (96%) was associated with the small molecular and lipid fractions of the ganglion. Approximately 2.0% of the activity was detected in the RNA, 0.5% in the DNA and 1.5% in the protein fractions. These findings were confirmed using several techniques of radioautographic investigation of sections incubated in DNase I and II, RNase A and TCA after incubation in nucleoside (Singer & Green 1968; Schick *et al.* 1978). None of these treatments caused any noticeable alteration of silver grain density over the glial cytoplasm, although some label was removed from the neuronal and glial nuclei.

Thus, the results generally show that the nucleosides are selectively and actively taken up and bound to some small molecule or molecules within the glial cytoplasm, and that a small proportion of tracer is taken up into neuronal and glial nuclei, where it is presumably incorporated into RNA and DNA. The distribution of the bound nucleosides is uniform throughout the glial cytoplasm. The present experiments also raise the possibility that some of the labelled material may subsequently be transferred to neurons. At the appropriate

concentration and time of exposure the nucleosides provide useful and versatile markers of the different cellular components of the buccal ganglia. In particular [$^3$H]uridine is a valuable marker for the glial cytoplasm; [$^3$H]adenosine for the glial nuclei.

### 3.9. *Quantitative changes during development and ageing*

Since the late 19th century much effort has been directed towards understanding the changes that occur in the nervous system, chiefly in higher animals, during the processes of development, ontogenesis and ageing. Many studies are concerned with cytological changes, but quantitative investigations have been undertaken on the mass, volume and cellular make-up of different regions of the central nervous system (summaries by Blinkov & Glezer 1968; Hanley 1974; Berlin & Wallace 1976). A wide variety of approaches have been employed, including sophisticated homogenization and separation techniques (Johnson & Erner 1972; Howard 1973; Franks *et al.* 1974) but the complexity, variability and difficulty in repeatably identifying small volumes (that is, *ca.* 1 mm$^3$) to make quantitative measurements, together with the difficulties of distinguishing between the neurons, neuroglia and vascular epithelia within the c.n.s. have consistently hampered accurate analysis. However, measurements of total cell number and cell volumes for different cell types have been achieved from statistical analysis of sample areas, and these have been expressed in percentages of different regions of the brain.

The buccal ganglia in *Planorbis* control the movements of the buccal mass during feeding. The adult pattern of feeding is displayed by the embryo in the egg case before hatching occurs and persists unchanged throughout the life span. The feeding cycle is a relatively simple, stereotyped pattern of behaviour that shows no noticeable differences between animals. The ganglia are not thought to be involved in more complex behavioural responses (for example, homing and learning, cf. the cerebral ganglia; Bullock & Horridge 1965), and are sufficiently small to enable repeated analysis with a manageable number of serial sections. The type of experiment designed to analyse the quantitative changes that may take place in nervous tissue during the life of the animal can be undertaken relatively easily in this tissue. The studies described in this section investigate the quantitative changes in the neurons and the glial in the buccal ganglia, employing the experimental labelling procedures described above.

The tritiated nucleosides adenosine and uridine (with 15 min incubation periods) were selected as the best labels for the quantitative analysis. Adenosine, because of its heavy and consistent labelling of both glial and neuronal nuclei, was employed for cell counts. Uridine was used for the volume measurements, since it accurately marked the glial cytoplasm and also resolved the connective tissue. Occasional neuronal nuclei were also labelled with this substance, but these could be corrected for by the light pen attachment of the Magiscan image analyser. Some counts of neuron numbers were also obtained from the uridine-labelled material.

#### (i) *Cell numbers*

Neuron counts, made on [$^3$H]adenosine- and [$^3$H]uridine-marked ganglia, showed that their number was almost constant throughout the size range at 298 neurons per ganglion (figure 86). The maximum variation between high and low values was 30 neurons. This variation was due to a combination of counting error (estimated at about 15–20 small neurons per ganglion, or 6–7 %) and individual variation. No significant changes in number were observed in ganglia from snails of different ages, nor in adjacent ganglia of the pair from the same animal.

Glial cell counts, made on [$^3$H]adenosine-marked ganglia, showed a statistically significant

increase (18%) in glial number with increasing size of the snail (Student's two-tailed $t$ test; $p < 0.001$), with the mean at 391 glial cells per ganglion (figure 86).

The numbers of glial cells given by this method are however, probably slightly low. Because the nuclei are relatively small (mean diameter 4μm; cf. section thickness approximately 8μm) it is possible that any nucleus lying deep within a section away from the nuclear emulsion will

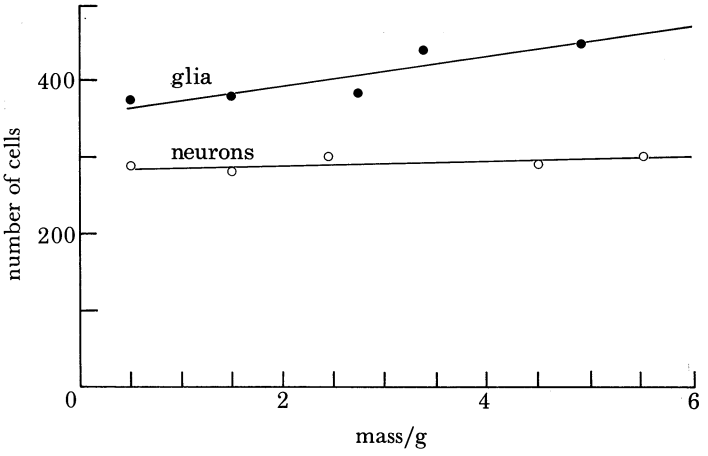


FIGURE 86. The number of glial cells increases significantly in the older animals. The increase is composed largely of the phagocytic glial cells in both the core and cortex of the ganglion. The apparent slight increase in the number of neurons is not, however, statistically significant.

not form a latent image because of scattering of the β particles by the overlying cellular material. A measure of the possible underestimation of the glial cell number was obtained by counting all of the glial nuclei in each 8μm serial section of a buccal ganglion stained with haematoxylin and eosin. Although this stain does not always mark the nuclei clearly and is impractical for a large number of sections, it did give a useful check when used with Abercrombie's formula (Abercrombie 1946) to correct for the possible recounting of nuclei. This method yielded a glial count 8% higher than that of a [$^3$H]adenosine-labelled ganglion of equivalent mass. It is possible that a similar percentage of glial cell nuclei are not detected by the radioautographic methods.

(ii) *Ganglion volumes*

Calculations of the volumes of the ganglia were obtained from planimetric measurements of photographs of the serial section radioautographs. To increase the accuracy, each photographed section was measured three times and the mean value determined. This type of calculation is also subject to several errors that should be borne in mind. First, and probably most serious, is shrinkage of the ganglion during histological processing. It has frequently been noted that fixation, dehydration and paraffin-embedding can cause significant shrinkage of nervous tissue (up to 90%, see summary by Blinkov & Glezer 1968). The buccal ganglia showed a 36% shrinkage (obtained by measuring the diameter of the ganglia with a micrometer before and after histological processing). A second source of error is section deformation during the sectioning of the block. This error was estimated by comparing the measured area of the block face to the measured area of the section. The compression for the Cambridge rocking microtome

used in this study was 17 %. Finally, section thickness (measured by micrometer) varied from 8.0 to 8.8 μm.

However, because the histological processing and equipment employed were the same for each of the buccal ganglia studied the errors were constant for each section. Therefore the results for each ganglion may be compared with one another, but not accurately with those of other material.

The volumes of the buccal ganglia were calculated in animals ranging from 0.5 to 5.5 g (figure 87). The buccal ganglia increased in volume according to the size of the snail in an approximately linear manner; from 0.05 to 0.20 $mm^3$ in the largest animals. No quantitative differences were observed between adjacent ganglia in any animal.

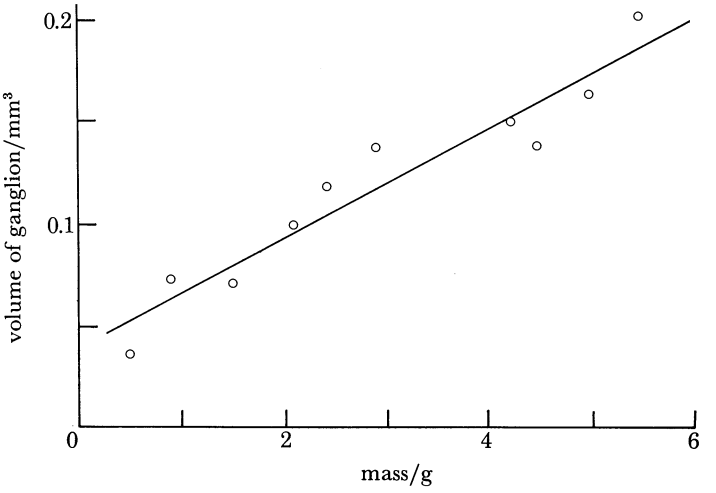


FIGURE 87. The buccal ganglia increase in volume by approximately five times (animal mass range 0.5–5.5 g).

(iii) *Core and cortical volumes*

The buccal ganglia of *Planorbis*, like those of many other invertebrates, can be divided into two main regions; a cortex that contains the neuronal perikarya and the majority of glia, and an inner core that contains groups of axons, areas of synaptic intermingling and a relatively small percentage of glia. The glial tissue in the core of the ganglion is generally associated with large axons, not with areas of neuropil (see §3.1).

There was, however, no clear physical boundary between the cortex and the inner areas of axon tracts and neuropil, and difficulties were sometimes encountered in the planimetric measurements of the cortex and core made from the radioautographs. The maximum error in judging the boundary (5 %) was estimated from analysis of measurements where it was purposely overestimated or underestimated. In addition, error may be due to different degrees of shrinkage of the cortex and core of the ganglia during histological processing, and this may vary with the age of the snail (both possibly due to as yet unknown changes in the chemical composition of the nervous system), but it is not possible to evaluate these.

Both the cortex and the core increased in size with the increase in ganglional volume. The cortex made up an average of 75 % of the ganglion and the core 25 % (see figure 88). However, these percentages both underwent a small but significant change with age. The possibility that

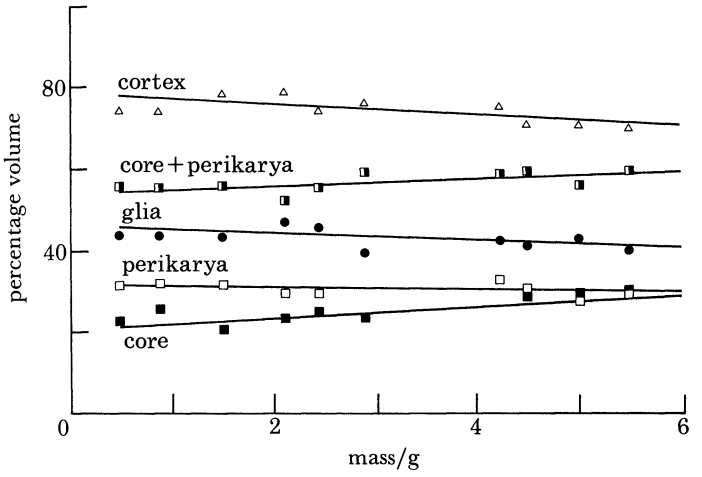


FIGURE 88. The changes in the volumes of the different components of the buccal ganglia (animal mass range 0.5–5.5 g). The core of the ganglion (axonal and dendritic processes and a small number of glial processes) increase by 6% (mean percentage volume is 25%), the cortex decreases by 6% (mean percentage volume is 75%). The disproportionate increase of the core results in the decrease of the percentage volumes of the glial cells and neuron perikarya. The volume of the core together with the neuron somata increases by approximately 5%. However many neurons project in nerves outside the core of the ganglion, and the axonal processes from other neurons in other parts of the animal terminate in the core, thus the changes for whole, individual neurons may be different.

such changes were due to the error from over- or underestimation of the boundary between them was ruled out by repeated measurements. The changes were more apparent when expressed as the ratio of cortex:core volumes (the 'cortical index', figure 89). In the smaller specimens, the cortex is three times as large as the core, but as the ganglion grows, the proportion progressively decreases until the cortex becomes only twice as large as the core. This change in the composition of the ganglion is apparently due to the relative increase in the size of the core (by a factor of seven) with that of the cortex (by a factor of five).

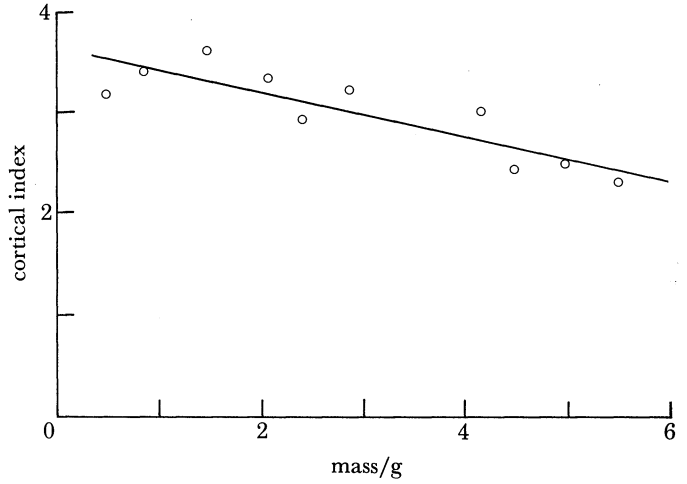


FIGURE 89. The cortical index in the buccal ganglia (the ratio of cortex volume to core volume) decreases with increasing age. This is the result of the growth and proliferation of axonal and dendritic processes.

(iv) *Glial and neuronal volumes*

The photographs of the serial section radioautographs of ganglia exposed to [$^3$H]uridine were analysed by the Magiscan image analysis system, and the percentage volumes of the glia and the neurons throughout the size range were calculated. However, there are again several sources of error that should be described. First there are the shrinkage and deformation of the ganglia by the histological processing, which have been described above. Second there are errors associated with the use of the Magiscan image analysis; the labelled glial cells are 'seen' according to a level setting, which is adjusted by the operator. Although the computed percentages varied widely between obviously high and low settings (up to 20%), careful adjustments to accurately match the radioautographs resulted in maximum errors of 10% (figure 83). Third, there are errors owing to the volume occupied by extracellular space. These spaces are not evident in light microscope radioautographs. In many tissues this error is in the region of 15%, but it can be as much as 30% (see Kuffler & Nicholls 1966). Analysis of electron micrographs selected for all levels of the buccal ganglia of *Planorbis* indicated that extracellular space could occupy up to 15% of the tissue. Much of this is composed of the narrow spaces (10–12 mm wide) between adjacent neurons, and neurons and glial cells. A significant proportion is also composed of the irregular and lacunated spaces between adjacent glial cells (§3.1), which are found in the cortex of the ganglia. Measurements made to determine possible difference in the amounts of extracellular space in the cortex and core of the ganglia showed no obvious differences. The total possible error in the quantitative analysis is thus considerable. However, standard histological and image analysis procedures were employed for all the ganglia, and therefore most of these errors were constant throughout. Furthermore, because in buccal ganglia of all sizes numbers of neurons and glia are relatively constant, and the extracellular spaces have approximately the same dimensions, it is likely that this error will also be relatively constant. In the following description the errors are considered to be constant throughout; once again the volume changes in the cellular components of ganglia of different ages can be fairly reliably compared with each other, but not with those of other material.

The glial cells and neuronal perikarya constituted a relatively constant percentage volume of the ganglia (average percentages, glia 43%; neuron perikarya 33%; figure 88). In two ganglia labelled with [$^3$H]adenosine an extensive stereological analysis of the glia was made. The values obtained (40% and 44%) fell within the range obtained from the analysis of the [$^3$H]uridine-labelled ganglia (40–48%), thus providing independent evidence of the accuracy of the image analysis. The average percentage volumes of glial cells and neuron perikarya in the cortex of the ganglia are 58% and 43% (figure 90). As described above, it was not possible to tell whether the small fluctuations are due to individual variation, or to inconsistencies in the overall error of the analysis. In addition it must be borne in mind that the percentages include the extracellular spaces. However, an important conclusion is that the relative proportions of the volumes of glial cells and neuronal perikarya in the buccal ganglia remain relatively constant throughout the life of the animal (figures 90 and 91).

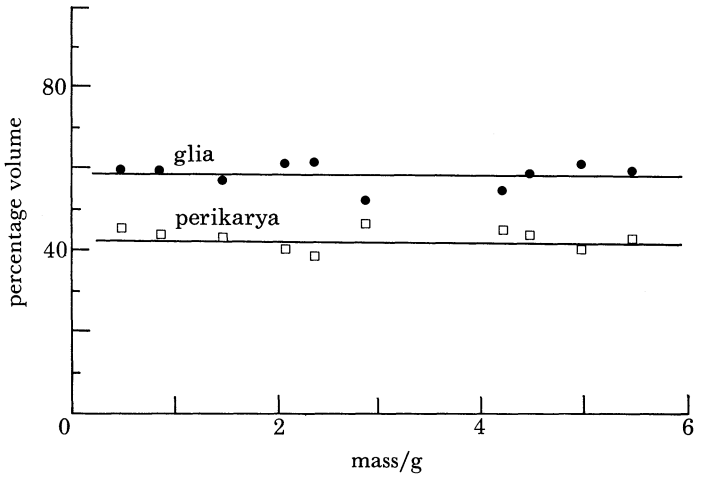


FIGURE 90. The volumes of the glial cells and neuronal perikarya (expressed as percentage volume of the cortex) remain relatively constant during the life of the animal.

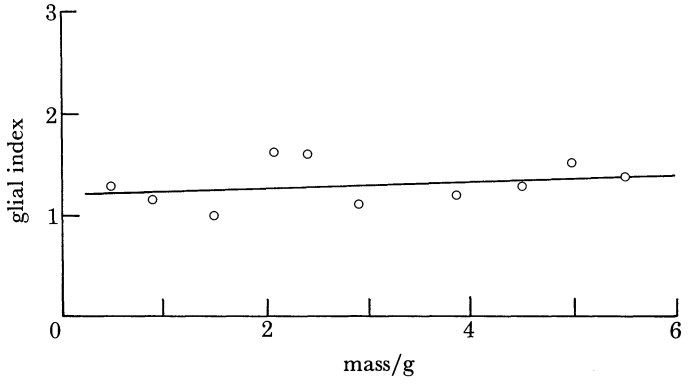


FIGURE 91. The glial index (the ratio of the volume of the glial cells to the volume of the neuron perikarya) in the buccal ganglia remains relatively constant during the life span.

## 4. DISCUSSION

The glial tissue in *Planorbis* ganglia surrounds and ensheaths the neurons. The majority of the glial processes are interwoven around the neuronal perikarya and their major axon branches. Glial cell processes form a layer between the blood and nerve perikarya, but this does not significantly interfere with the movements of many small molecules in and out of the tissue. Such movements can occur paracellularly, through the extracellular spaces, since there are no occluding junctions between the cells. This overall type of arrangement has been described in many invertebrates (reviews by Kuffler & Nicholls 1966; Johnson & Roots 1972; Radojcic & Pentreath 1979; Lane 1981), although there may be some variations in the different groups (for example, in insects peripheral junctions between the glial cells confer properties of a 'blood–brain barrier' analogous to that in mammals).

The glial cells in the buccal ganglia vary considerably in shape and contain different organelles and inclusions. However, with the exception of the phagocytic cells, the morphological differences were insufficient to justify their classification into various types; rather they

appeared to be local alterations of the same population of cells. The information obtained during this study provides a fairly complete description of several aspects of the glial tissue and the neuron–glial relations during ageing in a discrete area of nervous tissue. The findings can be constructively compared with the descriptions of the non-myelin-forming cells in other invertebrates and vertebrates, including mammals. In particular the quantitative analysis of the cellular relations in the ganglia during ageing may provide clues that are useful to similar studies in higher nervous systems.

### 4.1. *Cytological changes during development and ageing*

Several changes were observed in the glial cells in *Planorbis* with growth and ageing. First, the layering of the glial processes around the neuronal perikarya and axons increases during development. The increase appears to be directly associated with increased size of the neurons, because even in old animals the small neurons were covered by smaller numbers of thicker, shingled glial processes. In the prawn, *Palaemonetes*, there is evidence that the increased glial wrappings around the larger axons may speed impulse conduction (Heuser & Doggenweiler 1966). The wrappings are thinner and more compact than those in *Planorbis*, and in many respects are similar to vertebrate myelin. The glial wrappings around some large axons in *Planorbis* are extensive but do not appear comparable with those in crustacea. Their development around the neuronal perikarya is not obviously compatible with increased conduction velocities. A second change was an increase in dilatations of the extracellular spaces between the glial cells in some peripheral regions of the ganglia. These lacunae do not occur in embryos but increased progressively with age and were pronounced in damaged or degenerate ganglia. An obvious interpretation is that they serve to increase routes available for transfer of material between the blood and the glial cells, although evidence for this is lacking. Equivalent structures occur in other molluscs (for example, *Helix pomatia* (Reinecke 1975); *Aplysia californica* (Rosenbluth (1963); summarized in Radojcic & Pentreath (1979)) but have not to our knowledge been observed in mammals, where extracellular space has in some reports been suggested to decrease (Bondareff 1973, 1976). However, it is also possible that they may be artefactual (for example, Fahrenbech 1976), owing, for example, to the action of the fixative on other components of the glial cells that are changing with age or in a state of degeneration. Another obvious change was an increase in the fibre content of some glial cells, especially those in the nerves and the connectives. Such changes have been observed in the neuroglial cells in the rat (Vaughan & Peters 1974), monkey (Mervis 1981), and in cultured astrocytes (Aune 1976), although other reports suggest that this cellular component decreases in man (for example, Thompson 1965; Samorajski 1976).

The literature on age-related changes in mammalian nervous tissue also contains accounts of alterations in organelles such as mitochondria and Golgi structures, changes in nuclear structure, and increases in subcellular inclusions especially in the neurons (for example, neurofibrillary tangles, Hirano bodies; see Berlin & Wallace 1976). In general, the changes have not been quantified because of the difficulties in accurately comparing equivalent areas of tissue in different animals. In the buccal ganglia we observed no significant widespread changes associated with these organelles in the glial cells, but in close agreement with the descriptions in mammals, were impressed by the increase in lysosomes and lipofuscin pigment material. These topics are discussed in the following section.

### 4.2. *Nerve-ending phagocytosis, degeneration and lipofuscin accumulation*

The evidence shows that the glial cells in the central ganglia phagocytically engulf nerve endings in both the normal, apparently healthy, tissue and in cases of experimentally induced degeneration. Throughout the life of the animal there was a marked increase in lysosomal material, particularly lipofuscin and other residual bodies, as well as secondary lysosomes, including phagocytic vesicles. Most of the glial cells in the buccal ganglia showed some signs of phagocytic activity, especially after damage to the tissue, but only a small proportion of the cells appeared to be specialized for this role. Degeneration caused a significant increase in these phagocytic cells, which became actively involved in the removal of neuronal material and its apparent subsequent conversion into electron-dense granular residues (residual bodies). Some of the cells were observed to contain a spectrum of axonal processes from those that were apparently unaltered, presumably recently engulfed, through different stages of breakdown, to dense aggregates. It appeared that as the cells became packed with the end products of the breakdown process they moved out of the core of the ganglion, perhaps along axon tracts, into subcapsular areas of the cortex. No evidence was obtained for their subsequent extrusion from the ganglion. In the experiments with isolated tissues the phagocytic cells must have arisen either from the transformation of other glial cells at the edges of the ganglion, of from the few phagocytic cells normally present in the core of the ganglion.

The increased activity of the phagocytic glial cells induced by degeneration was similar to, but more extensive than, the changes that occurred during ageing. Throughout the life of the animal there were increased numbers of these cells containing lipofuscin, located in the cortex of the ganglia. The normal ageing process in *Planorbis* is evidently associated with active removal of some axonal and terminal processes. Interesting questions concern the nature of the removed terminals. For example, do they represent redundant processes, resulting perhaps from a rearrangement of neuronal connections, but which are not necessarily degenerating, or do they represent a turnover of established connections (as is indicated by some studies in higher nervous systems where no reductions in the numbers of intact synapses have been observed in severely retarded or aged tissues; Cragg 1975)? The increased incidence of phagocytosis with ageing cannot be correlated with any obvious changes in functional output from the ganglia, which remains unchanged, and this argues against rearrangement of connections, although the removed terminals may not be involved in the generation and control of the feeding cycle. The experiments with radioactive 5-HT provide some relatively direct evidence that the fate of some serotonergic terminals is to be phagocytosed by glial cells over periods of several hours. The nervous tissue was exposed to [$^3$H]5-HT, and then incubated for 10–24 h in fresh saline, which resulted in increased numbers of labelled axonal profiles, showing varying degrees of degeneration, within the glial cells (see also Pentreath & Berry 1978). A similar phenomenon has been observed in *Helix pomatia* (Pentreath 1976). In this situation the perikarya of identified serotonin-containing neurons were injected with labelled 5-HT and 15 h later regions of neuropil containing processes of the cell were studied by radioautography. Some of the labelled processes were present in glial cells, alongside other engulfed axonal processes in different states of degeneration. The glial cells resembled closely the phagocytic cells in *Planorbis*. However, it could also be argued that the injection procedure, on the presence of radioactivity within the terminals, induces their phagocytosis by the glial cells in both species.

The phagocytic activity of glial cells has been observed in some other molluscs. In the cerebral

ganglia of *Anodonta* degenerating material is removed by the glial cells (Borovyagin *et al.* 1972), and in *Helix* the removal of foreign materials such as ferritin has been recorded (Reinecke 1976), although the fate of the ingested material was not known. We have no experimental information of the possible roles of the glial cells in *Planorbis* in removal of foreign substances or other potentially damaging entities (for example, viruses), although these seem likely.

In mammals age-related phagocytosis of neuronal material, particularly of the nerve terminals by the microglia, has been described frequently (for example, Vaughan & Peters 1974; Bondareff 1980; Mervis 1981; Wisniewski *et al.* 1981). The astocytes are also capable of phagocytic activity under certain conditions (for examples, Vaughan & Peters 1974; Peters & Vaughan 1981). The increased removal of synapses, axonal processes and dendrites with age are widely assumed to be associated with decline in neuronal function and reduction in neuron numbers, although as discussed above there are great difficulties in interpreting the significances of the changes, and some studies suggest they may not be significant (Cragg 1975). One major problem is defining the extents of the differences between ageing and degeneration (that is, when should a change be considered a part of 'normal' ageing and when pathological). This subject is returned to in greater detail in §4.4. A rather different possible reason for the glial enclosure of nerve endings has been suggested in the neurohypophysis of the rat (Tweedle & Hatton 1980*a*, *b*). During water-replete conditions specialized glial elements, termed pituicytes, enclose or engulf many neurosecretory axonal processes and subsequently release them when the animal is dehydrated by water deprivation. It was suggested that the enclosure of neurosecretory terminals is involved in the inhibition of hormone release (Tweedle & Hatton 1980*b*). Although it may be said that this phenomenon, if true, is rather specifically associated with a particular type of neurosecretory terminal, it could also be argued that it offers a potential mechanism for temporary inactivation of nerve endings containing other transmitter substances, accounting perhaps for some of the phagocytosed processes observed in glial cells in the other studies.

The glial cells, and to a lesser degree the neurons in the buccal ganglia of *Planorbis* showed pronounced increases during life in the content of lipofuscin pigment and residual bodies. Similar age-related increases have been observed in the neurons of other invertebrates including insects (Herman *et al.* 1971; Sohal & Sharma 1972), nematodes (Kisiel & Zuckerman 1978) and other gastropods (Papka *et al.* 1981), and have been extensively documented in rats (see, for example, Berlin & Wallace 1976; Peters & Vaughan 1981), monkeys (Mervis 1981), humans (for example, Wisniewski & Terry 1973, 1976; Schlote & Boellaard 1983) and cultured human glial cells (Brunk 1973; Brunk *et al.* 1973). The accumulation of lipofuscin is perhaps the most consistent change associated with increasing age in the nervous system of most animals studied; some authors have, in fact, suggested that it is the only significant constantly occurring alteration (for example, Wilcox (1959) referring to guinea-pigs and man; see also Nandy (1983)). The pigment confers a yellow colour to the aged mammalian brain, and to the outer layers of the buccal ganglia from old *Planorbis*, which is an obvious feature in unstained sections. It has been called wear-and-tear pigment, senility pigment and chromolipid, and is also known to accumulate in both neurons and glial cells in a number of diseases and under various experimental conditions (for reviews see Berlin & Wallace 1976; Glees & Hasan 1976; Schlote & Boellaard 1983). The substance may be formed from the oxidation of cellular lipids by free radicals during the breakdown of material by lysosomes, thus indicating the amounts of previous lysosomal activity and active removal of cellular material (Samorajski *et al.* 1964; Armstrong

*et al.* 1978; Blomquist *et al.* 1980; Miquel *et al.* 1980; Peters & Vaughan 1981; Davies 1983). It is, however, not at all clear why the pigment is not removed from the neurons and glial cells, although some interesting studies on rats have implicated a lack of vitamin E (see Berlin & Wallace 1976). Theories concerning the roles of lipofuscin generally lie between two opposing views. First, the pigment is a harmless by-product of ageing that could prolong the optimal functioning of nervous tissue by protecting the cells from harmful metabolic breakdown products. Secondly, lipofuscin causes cellular functional impairment, aggravating and eventually causing cell loss. The properties and functional significances of lipofuscin in the nervous system of different animals is an area of great interest that is being actively researched (see Glees & Hasan 1976; Brizzee *et al.* 1983; Nandy 1983; Schlote & Boellaard 1983).

Thus the glial cells in *Planorbis* show several similarities in phagocytic activity to the glial cells in higher nervous systems. Most of the glial cells in the buccal ganglia appear capable of engulfing nerve terminals and degenerating material, but only a small proportion, residing primarily in the core of the ganglia, are specialized for this role. In the vertebrate c.n.s. the microglia are the true neuroglial phagocytes, although the astrocytes are also capable of phagocytic activity under certain conditions (Vaughan & Peters 1974; Peters & Vaughan 1981). Additional parallels between the microglia and the phagocytes in the buccal ganglia are the similar lysosome contents, with the engulfed neuronal material being converted to electron-dense pigment residues, and the cells subsequent congregation in the perivascular spaces (see also Peters *et al.* 1976; Stensaas 1977; Blakemore 1978).

### 4.3. *The significance of the labelling of the glial cells with nucleosides*

The tritium-labelled nucleosides used in this study selectively marked the glial cells in *Planorbis* ganglia, although for the purposes of the quantitative analysis uridine and adenosine were most suitable, since the cytoplasmic and nuclear components of the glial cells and neurons were distinguished. Extranuclear labelling with nucleosides has been reported to occur in several different animal cell types (for example, thymidine in human lymphocytes (Schick *et al.* 1978) and in mouse spleen (Bryant 1966); uridine into mitochondria in mouse and chick liver cells (Curgy 1969)). However, there is growing evidence that the uptake and cytoplasmic retention of nucleosides by the glial cells may be an independent and widespread phenomenon. In particular the uptake of uridine into glial cells has been observed in many vertebrates, including humans (Singer & Green 1968; Gambetti *et al.* 1973; Lange 1979; Fog & Pakkenberg 1981; see also Pevzner (1979) for a summary of some of the earlier work). We have also found, since starting the experimental work on *Planorbis*, that the property has been previously reported for gastropod nervous tissue in the Russian literature (some of which is also in Pevzner (1979). Kuzmin *et al.* (1972) have described the uptake of adenosine, guanosine, cytidine and uridine into the glial cells of *Tritonia* and *Helix*. Uridine uptake by the glial cells and neurons has also been observed in *Lymnaea*, which is closely related to *Planorbis* (Dyakonova & Veprintzev 1969). Electrical stimulation of the nervous tissue preferentially enhanced the uptake of uridine into the neurons in *Tritonia* and *Helix* (Bezruchko *et al.* 1970; Kuzmin *et al.* 1972), but in *Lymnaea* also increased its uptake and incorporation into RNA within the glial cells (Dyakonova 1972). In *Aplysia* electrical stimulation increases the incorporation of uridine and cytidine into RNA in an identified giant neuron $R_2$ (Peterson & Kernell 1970), although the possible effects on the satellite glia were not studied.

Throughout the above studies the uptake of the nucleosides was assumed to be associated

with the synthesis of DNA, RNA and protein; this was sometimes backed by experimental evidence. In contrast we could obtain no evidence for this in *Planorbis*. It is possible that even the low concentrations of exogenous nucleosides employed were significantly 'non-physiological' to inhibit DNA and RNA synthesis, as has been suggested by Angelier *et al.* (1976), but it seems more likely that the glial uptake reflects a real physiological event, especially since it appears so widespread. Several reasons could account for the uptake (see also Varon 1979). First, the glial cells may use the nucleosides for their own metabolic needs (for example, nucleotide synthesis), which are sufficiently long to be outside the time-course of our experiments. Secondly, the glial cells may 'mop-up' the nucleosides because they are not required by the neurons, as is thought to be the case with some other substances (for example, neurotransmitters), to preserve the correct neuronal environment. Thirdly, it is possible that the glial cells both store and modify the nucleosides for later use by the neurons, for example, after prolonged electrical activity or damage. In relation to these possibilities the localization of 5′-nucleotidase on the glial membranes seems interesting. The enzyme produces nucleosides from nucleotides; some of the latter substances are released from neurons during electrical activity (for reviews see Stone 1981; Schubert *et al.* 1982). In particular ATP and AMP, if released in the vicinity of the glial membrane enzyme, could provide extracellular adenosine, which in turn has been implicated in several important modulatory actions, the most important of which is probably the activation of cyclic AMP. 5′-Nucleotidase is localized predominantly on the membranes of the different glial cell types in mammalian brain (Kreutzberg & Barron 1978; Kreutzberg *et al.* 1978), and its possible role in these events has been critically evaluated by Stone (1981). Substantially more information will have to be available before any conclusions may be reached regarding the role of the enzyme or the uptake properties of the nucleosides in the buccal ganglia. However, the data can be interpreted, in the broadest sense, as providing good indication that neuron–glia cooperation is probably critical in the maintenance of the correct purine metabolic and functional balance.

The intercellular transfer of a variety of substances, especially relatively large molecules such as RNA and proteins, from glia to neurons has been extensively postulated (see Pevzner 1979; Varon & Somjen 1979), but is difficult to demonstrate convincingly in most tissues, although some firm evidence has been presented for the squid giant axon (Lasek *et al.* 1977). Dyakonova (1972) and Dyakonova & Veprintzev (1969) have suggested that their results show a transfer of labelled uridine or a metabolite from glia to neurons in *Lymnaea*, but the radioautographic data would seem to need analysis at the level of the electron microscope to provide a clear demonstration. In *Planorbis* we also obtained some radioautographic data suggestive of a redistribution of label from glial cells to neurons, but there are many possible qualifications concerning, for example, different time-dependent behaviours of the label in the two cell types, and more extensive rigorous experimental evidence will have to be found before any conclusions can be reached about this potentially important phenomenon.

### 4.4. *Quantitative analysis of neurons and glial cells during growth and ageing*

*Planorbis corneus* has been recorded to survive from two to three years in captivity and up to six years in the wild (Boycott 1936; see also Comfort 1964). Animals have been bred under laboratory conditions during the present work, and these attain a mass of 0.5 g after one year, which was the minimum size collected from the field. At this size some of the animals are sexually mature. In the source from which the animals were collected there was a continuous size range

from 0.2 to 5.5 g. Buccal ganglia in snails of mass less than 0.5 g were not analysed, because of the technical difficulties in processing tissues of such small size (less than 0.04 $mm^3$).

The major problem in all quantitative studies of nervous tissue is to obtain accurate and reliable measurements. In mammals the size and complexity of the c.n.s. necessitates statistical analysis of data obtained from sectioned material. The relatively small size and simple arrangement of the *Planorbis* buccal ganglia, together with the automated experimental procedures used in the present study has made it possible to obtain a fairly complete quantitative analysis. The buccal ganglia increase approximately fivefold in volume from animals weighing 0.5 g to those weighing 5.5 g. The number of neurons remains constant throughout the size range, but the glial cells proliferate significantly (18% increase).

'Neuron fallout', that is, the death of some of the neurons with age, did not occur in *Planorbis* buccal ganglia; the same number of neurons were present throughout the life of the animal. Similar findings have been reported for insects where the final number of neurons is reached in the pupal stage. During post-embryonic nervous development in insects only the glial cells increase in number, although neurons as well as the glial cells increase in size (Power 1952; Panov 1962; Gymer & Edwards 1967; Korr 1968; Malzacher 1968; Sohal & Sharma 1972). However, Ogawa (1939) analysed the nerve cells and nerve fibres at various stages of development of an annelid worm and found that the total number of neurons increased from 6000 to 10000 from hatching to sexual maturity. The numbers of cells in the octopus brain, neurons as well as glia, also continue to increase with age and with increase in body mass, reaching a total of $4 \times 10^8$ cells in animals of 4.5 kg body mass (Packard & Albergoni 1970; Giuditta *et al.* 1971).

The problem of neuron loss with ageing in mammals in highly controversial. The phenomenon of neuronal fallout was proposed by early workers in mammalian (especially human) tissue (see Blinkov & Glezer 1968). However, as Berlin & Wallace (1976) point out, the probable source of this conclusion in some of the quantitative studies is the use of the parameter of packing density (the number of cells per unit volume) to determine the number of cells in a part of the nervous system, without taking into account any increase or decrease in size of the cells. Because different functional regions of the mammalian nervous system are so large they cannot be completely analysed, much of the early work relied on counting the number of cells per unit volume of brain. In figure 92 the data for *Planorbis* are expressed by this means and it appears that there is a sharp decline in both neurons and glial cells, although total counts (figure 86) prove otherwise. Many other factors affect packing density; for example, cell size and number, amount of neuronal processes, and application of the sampling procedure (see Mayhew & Momoh 1973). In mammalian nervous systems changes in the vasculature may also affect packing density. It is evident from the present study that conclusions made from results expressed in this fashion may be misleading.

Some of the more recent works on mammals indicate, perhaps not surprisingly, that neuronal loss varies in different brain regions (for example, Peng & Lee 1979). In particular, regions that show obvious age-related functional decline appear to be affected by neuronal loss. These include: cerebral cortex (Henderson *et al.* 1975; Brody 1976; Terry *et al.* 1977; Henderson *et al.* 1980), hippocampus (Ball 1977; Landfield *et al.* 1977; Brizzee & Ordy 1979), cerebellum (Hall *et al.* 1975; Hirrup & Mullen 1981; Rogers *et al.* 1981) and visual and auditory cortices (Vaughan 1977; Devaney & Johnson 1980). Other regions such as the locus coeruleus (Coleman & Goldman 1981) and mammilary bodies (Wilkinson & Davies 1978) show no

apparent neuronal loss (see also Hanley 1974). It is as yet unknown whether other central ganglia of *Planorbis* suffer neuronal loss and functional decline with age. It is clear, however, that the constancy of neuronal number is consistent with the functional integrity of the buccal ganglion with age (to control the feeding buccal mass).

The number of glial cells increased by approximately 18% in the older *Planorbis*. The electron microscope studies showed that this increase occurred in response to the phagocytosis of axonal processes in the core of the ganglia, which was most apparent in the large animals. The increase did not measurably alter the glial volume:neuron perikarya volume ratio, because the extra lipofuscin-filled cells congregate in localized clumps in the periphery of the ganglia, displacing the processes of the other glial cells. Increases in glial cell number have been described in several regions of the ageing mammalian c.n.s. (see Blinkov & Glezer 1968); these are also generally associated with the removal of damaged or degenerating neuronal processes (for example, Hawkins & Olszewski 1960; Ravens & Calvo 1965; Brizzee *et al.* 1968; Dalton *et al.* 1968; Landfield *et al.* 1977). However, it also has been clearly established that there are variations in the age-related changes in glial cells at many levels in the c.n.s., ranging from the gross region (that is, white matter and grey matter) to the localized nucleus (Sturrock 1974*a–c*, 1976, 1977, 1978; Sturrock & Jew 1978). In the indusium griseum of the rat (a relatively discrete region for quantitative studies) the number of astrocytes increases by 30% and the neurons remain constant, which appears analogous to the changes in *Planorbis* buccal ganglia, although in other brain regions of the same animal the glial cells decrease (Sturrock 1977, 1978).

The factors that control the numbers of glial cells and neurons are not understood. The observation that more highly evolved brains have a higher ratio of glial cells to neurons has been used to support a long-standing concept of a phylogenetic increase in the glial:neuron ratio. For example Friede (1954) recorded that the glial:neuron ratios in all cellular layers of the mammalian cerebral cortex was 1.7 in man, 1.2 in the horse, and 0.4 in the rabbit and mouse. However, Hawkins & Olszewski (1957) reported that the mean glia:neuron ratio is 4.5 in the whale, and concluded that increase in the number of glial cells per neuron is not correlated with phylogenetic status but with the size of the brain. The results of the present work show that the mean ratio in *Planorbis* buccal ganglia ranges from 1.3 in young animals to 1.5 in old animals. Furthermore the larger neuron perikarya were surrounded by larger numbers of glial cells and glial wrappings than the smaller glial cells, which sometimes were incompletely covered, with areas of adjacent small perikarya occasionally not separated by any glial processes. This importance of neuronal size with respect to number of satellite cells was elegantly demonstrated by Reinecke (1975) in the related snail *Helix pomatia*. By using morphometric methods he measured the glial:neuron ratios in different ganglia and parts of ganglia containing neurons of varying size. The ratio ranged from 0.01 for neurons of diameter 10 μm to approximately 2.0 for neurons of diameter 50 μm. He stressed the likely importance of the glial cells in metabolic supply to the neurons. The available evidence would therefore indicate that the significance of a high glia:neuron ratio is associated with larger neurons that require more glia to support, nourish or metabolically interact with them in ways which are not yet understood (Hawkins & Olszewski 1957; Friede & van Houten 1962; Friede 1963; Reinecke 1975; see also Varon & Somjen 1979; Pentreath 1982).

The neuron–glia relations in the buccal ganglia are constant throughout the adult life of the animal. This is particularly the case with the ratio of total glial to neuron perikarya volumes in the cortex (58%:42%, that is, 4:3). It is possible that a constant ratio of glial cell volume

to neuronal perikarya volume is necessary for the normal functioning of the neurons. It is not known whether a fixed ratio of these cell volumes occurs in vertebrates or in other invertebrates. However, it has been frequently observed in many animals that during degeneration, or in pathological states, glial cells proliferate or swell, thus upsetting the glial: neuronal volume that *may* normally be constant (Nandy 1972; Matthews & Kruger 1973; Pappius 1979). In mammals an extreme form of glial cytoplasmic swelling in response to neuronal degeneration, caused by ageing and disease, or chemical and mechanical damage, sometimes occurs (for example, Roberts & Goldberg 1976). No comparable changes were observed in *Planorbis*.

The fivefold increase in the volume of the buccal ganglia is not caused by cell multiplication, but by the increases in the cell sizes, which can be calculated from the experimental data (figure 93). The increased size of the neurons and the glial cells accounts for the observed fall in packing density (figure 92). Not all the glial cells increase equally in volume; those filled with lipofuscin,

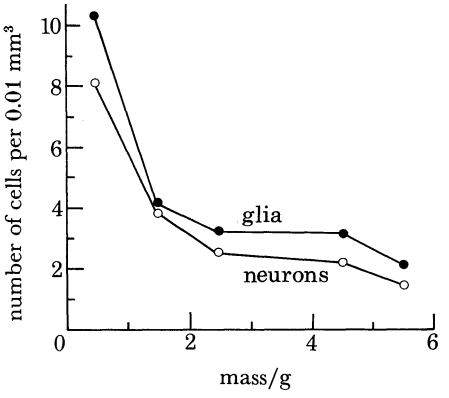


FIGURE 92. The packing densities of the glial cells and the neurons (the number of cells per 0.01 $mm^3$ of buccal ganglia) decrease with age (animal mass range 0.5–5.5 g). The data has been corrected for the small increase in glial cell number (figure 86). The declines in packing densities are due to the increase in the size of the cells (see figure 93) rather than cell loss.

located in the subcapsular regions, had reduced size compared with the other glial cells. It is not clear whether the neurons increase differently in size. However, it is evident that the increased core volume is the most significant contribution to the growth of the buccal ganglia. As far as can be ascertained this includes the axon tracts and the neuropil regions, but it is clear that it does not involve a significant increase in non-phagocytic glial cell processes. The growth of the neuron perikarya is exceeded by the mean neuronal growth (figure 93), which includes the neuronal processes. The major component of neuronal growth is thus the growth and proliferation of the axonal and dendritic processes. Existing reports on the relative changes in size of different cell types in the nervous tissue of other animals (for review see Jacobson 1978) are sometimes difficult to evaluate, and do not always seem safely comparable with the present study. It appears that different situations may exist. For example, neuronal perikarya size has been reported to increase in some regions of the rat brain (for example, Ford 1973*a*, *b*; Coleman & Goldman 1981) or spinal cord (Ford & Cohan 1968), but may decline in human brain with age (Uemura & Hartman 1981; Schultz & Hunziker 1980). In a study on ganglia of *Drosophila melanogaster* with increasing age, Herman *et al.* (1971) reported a shrinkage of the cortex. However, quantitative measurements were not made, and it seems possible that this was due to a disproportionate increase in core size.

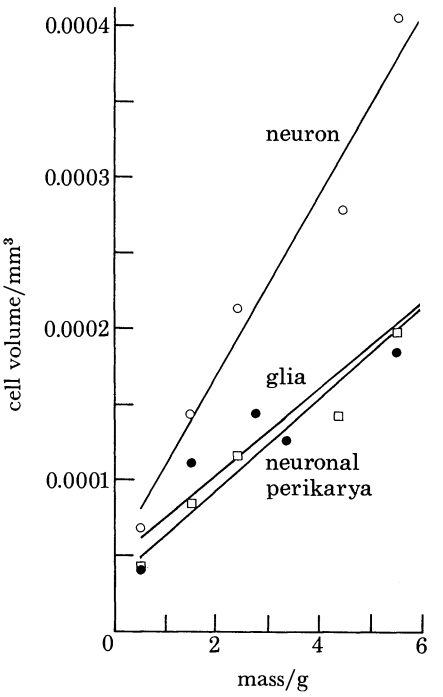


FIGURE 93. The mean cell volumes of the glial cells, the neuron perikarya, and the neurons in the buccal ganglia of *Planorbis* (mass range 0.5–5.5 g). The axons and the dendrites are the components of the ganglia that show the greatest increase in size.

The data in *Planorbis* buccal ganglia show that the glial to neuron perikarya volume relations remain constant during the life of the animal, although there are significant increases in the total tissue volume, which result chiefly from axonal and dendritic proliferation. There appears to be no neuronal redundancy in the ganglia and no significant pathological changes were observed. The alterations involved accumulation of lipofuscin and the phagocytic removal of synaptic processes by an increased population of phagocytic glial cells. The other changes appear to be associated with the growth and final size of individual neurons and the whole ganglia. None of the changes appear to be detrimental to the functioning of the ganglia; on the other hand it seems more attractive to suppose that the changes may be necessary to maintain the functioning with age. It is not known whether other ganglia of *Planorbis*, perhaps less vital to survival, show greater functional decline and associated morphological changes with age. In *Aplysia* it has been demonstrated that certain age-dependent behavioural changes may be correlated with changes in electrical activity of some central neurons (Peretz & Lukowiak 1975; Peretz *et al.* 1982; Rattan & Peretz 1981), although it is not clear what relationships, if any, these may have with their increased lipofuscin content (Papka *et al.* 1981).

The extents to which the age-related changes in *Planorbis* buccal ganglia may be considered to represent 'normal' ageing (as opposed to pathological change), and whether it has a counterpart in some regions of the mammalian c.n.s., are not understood. However, there is thought to be significant neuronal redundancy in the c.n.s. and ageing is sometimes associated with extensive morphological alterations owing to disease and degeneration (see Haymaker & Adams 1982), although corresponding functional changes are not always evident. Most nervous systems showing signs of functional impairment that have been investigated contain histologically demonstrable degenerative changes (for example, Tomlinson *et al.* 1970; Wisniewski & Terry

1976), but some similar changes may also occur in the apparent absence of functional decline (for example, Tomlinson *et al.* 1968). It may also be difficult to assess functional integrity and to correlate it with cytological change, particularly in cases of early, localized degeneration. Pathological changes in the nervous systems of higher animals may not impair function so as to affect survival, but could interfere with the quantitative analysis of ageing.

### 4.5. *Functions of the glial cells*

Glial cells have been implicated in many different activities, which generally relate to the well-being of the neurons. Principal among these are ion homeostasis (for example, potassium removal from the extracellular spaces around active neurons, perhaps by a spatial buffer mechanism), maintenance of the neurons (for example, removal of degenerating material, guidance of developing or regenerating neurons), and metabolic support (for example, supply of energy requirements) (see Varon & Somjen 1979). Some progress has been made towards providing a firmer experimental basis for these possible functions. Glial involvement in the equilibration of potassium liberated from active neurons has been demonstrated in the compound eye of the drone (honeybee; Coles & Tsacopoulos 1979, 1981; Gardner-Medwin *et al.* 1981), in the optic nerve of *Necturus* (Orkand *et al.* 1966, 1981) in the outer packet glia of leech ganglia (Kuffler & Nicholls 1966, 1976), and in mammalian cortex (see Varon & Somjen 1979; Nicholson 1980; Gardner-Medwin 1983*a*, *b*; Gardner-Medwin & Nicholson 1983). The potassium released from active neurons may also act as a signal for events in the glial cells (Kuffler 1967), stimulating their metabolism (Salem *et al.* 1975; Pentreath & Kai-Kai 1982). In particular it seems likely that glycogen synthesis and turnover may be activated within the glial cells (Pentreath 1982; Pentreath & Kai-Kai 1982). In the squid and crayfish material such as proteins may be transferred from the glial cells to support the neurons (Lasek *et al.* 1977; Bittner 1981). Glial cells may be partly responsible for GABA uptake at the arthropod neuromuscular junction (Faeder & Saltpeter 1970; Orkand & Kravitz 1971) and in the mammalian brain (Kelly & Dick 1976). During the development of relatively large volumes of nervous tissue, such as the brain of primates, some of the non-myelin-forming glial cells may form scaffold arrangements that aid neuronal migration and give directional guidance to elongating axons (Rakic 1974). The glial cells in mammals may also effect neuronal growth and other activities through trophic factors, such as nerve growth factor (see Varon & Somjen (1979) for references). In addition, there is general consensus that in most nervous systems the glial cells are involved in the removal of neuronal processes during the normal processes of development, maintenance and ageing, and in pathological and diseased states.

In the buccal ganglia of *Planorbis* 2-deoxyglucose (2-DG) is selectively incorporated into glycogen, and this property may be used in conjunction with radiolabelled 2-DG and radioautography to map the distribution and study some of the properties of glycogen within the tissue (Pentreath *et al.* 1982). Antidromic stimulation of buccal ganglion nerves (which avoids passing current across the glial cells in the ganglia) causes increased incorporation of 2-DG into glycogen in the glial cells surrounding the activated neuron perikarya, and evidence indicates that the effect is mediated by potassium released from the neurons (Pentreath & Kai-Kai 1982). It has been suggested that active neurons promote increased glycogen turnover in satellite glial cells through the potassium signal (Pentreath 1982). The results of the present study are in accord with the view that a major involvement of the glial cells is with the maintenance of the neuronal metabolism; the bulk of the glial cells are located around the

neuron perikarya, forming a layer between them and the blood. The glial cells send processes into the neurons forming a trophospongium. The glial:neuron perikarya volumes are maintained constant during the life of the animal. The glial covering of most individual perikarya of large diameter was apparently complete, although adjacent cell bodies of smaller diameter were occasionally observed unseparated by glial process. This arrangement is common in gastropods and most other invertebrates (see Radojcic & Pentreath 1979), although exceptions have been noted (for example, *Formica*, where many small-diameter neurons may come into close contact with each other (Lamparter 1966)).

Both the glial cells and the neurons contained varying amounts of glycogen. Large amounts of the substance were also present in some axonal processes and nerve terminals in the core of the buccal ganglion. Glycogen stores are prominent in the glial cells of many invertebrates and vertebrates. Large amounts are present, for example in the glial cells of the other gastropods *Aplysia* (Rosenbluth 1963) and *Helix* (Reinecke 1975). If the glycogen within glial cells acts as a store for the neurons, as many pieces of evidence indicate (see Pentreath 1982), its depolymerized product glucose-6-phosphate will have to be dephosphorylated to free glucose to be available for redistribution to other cells. The presence of an enzyme with glucose-6-phosphatase activity along glial cell membranes (except where they bordered the basement membrane) in the buccal ganglia provides evidence that is consistent with this possible role. The relative absence of the enzyme on the glial cell processes bordering the basement membrane may reduce loss of glucose from the ganglion back to the blood, and a scarce distribution of the enzyme along the neuronal membranes suggests that glucose may be more effectively trapped within these cells. Comparatively little is known about the enzyme in nervous tissue (see Anchors *et al.* 1977; Schmidley & Wissig 1983), compared with the other non-specific alkaline and acid phosphatases that have been fairly extensively studied (see Cohen 1970). Several histochemical studies have been made at both the light and electron microscope levels. In the olfactory bulb of the rat some fibres and synaptic regions show intense glucose-6-phosphatase activity, whereas the dendrites and perikarya stained weakly or moderately (Sharma 1967). Positive reacting sites have also been demonstrated in rat cerebral and trigeminal ganglion neurons, but the staining is variable; sometimes it occurs as an intense perinuclear band, in other cells it is diffused throughout the perikaryon (Tewari & Bourne 1962, 1963). Cerebellar Purkinje cells appear to contain high levels of the enzyme (Rosen 1970; Schmidley & Wissig 1983), particularly in their dendrites (Schmidley & Wissig 1983). Ultrastructural studies have shown the enzyme to be associated with smooth and rough endoplasmic reticulum in neurons and astrocytes (Stephens & Sandborn 1976; Al-Ali & Robinson 1981; Schmidley & Wissig 1983) and to be especially abundant on the endoplasmic reticulum in the endothelial cells of brain capillaries (Schmidley & Wissig 1983). In all tissues the enzyme is thought to be membrane-bound, and substantial evidence indicates that the enzyme has multiple activities, although this may in part be due to inadequate separation studies (see Ryman & Whelan 1971). The possible significance of another phosphatase enzyme, 5′-nucleotidase, also localized on the glial membranes in the buccal ganglia, has been discussed in §4.3.

The haemoglobin in the glial cells presumably acts as an oxygen store and could also facilitate the diffusion of oxygen towards the neurons. Both roles have been proposed for the respiratory pigments present in other molluscan tissues, especially the musculature involved in prolonged activity such as the radular muscles (see Read (1966) and Ghiretti & Ghiretti-Magaldi (1972,

1975) for reviews). The presence of the pigment in the nervous tissue of *Planorbis* was originally noted by Berthier (1947), who considered it to be located in the connective tissue sheath surrounding the neurons, although the presence of the glial cells around the neuron perikarya was then not understood. The only direct reference to a localization of haemoglobin within glial cells that we are aware of, is by Wittenberg *et al.* (1965), who noted that 'the large neuron cell bodies of the ganglia of *Aphrodite* (a polychaete annelid) appear in the microscope as clear areas against a red background, suggesting that the pigment is largely in the glial cells' (p. 370 in Wittenberg *et al.* 1965). In *Aplysia* the haemoprotein is present in the neuron cell bodies, concentrated within granules that have been dissected from the cells (Arvanitaki & Chalazonitis 1952, 1960). Different types of intraneuronal pigment granules thought to be involved in respiration during anaerobic conditions have been described in several other molluscs (see, for example, Zs-Nagy 1971; Benjamin & Walker 1972). A variety of granules are also located in the hillock regions of many *Planorbis* neurons, and it is possible that some of these may be additional haemoprotein stores within the neurons.

The glial cells in the buccal ganglia are located principally around the neuron perikarya and large diameter axons and dendrites, but are generally absent from areas of synaptic intermingling. This distribution has been established from the selective marking experiments and from the electron microscopic studies. Similar studies on the abdominal ganglion of the leech, *Haemopis sanguisuga*, have shown that large areas of neuropil lack glial processes in this animal (Kai-Kai & Pentreath 1981*b*). These findings are not in agreement with the widely held supposition that glial processes are prevalent in synaptic regions in invertebrates (see Radojcic & Pentreath 1979). They are also difficult to reconcile with the suggestion that glial cells are important in potassium removal from the extracellular spaces (see Varon & Somjen 1979); the surface:volume ratios of the neuronal processes are much greater in the neuropil than in the cell body regions at the periphery of the ganglia, and it might be predicted that potassium homoeostasis would be most important in the synaptic regions, and that most glial processes would be present in these regions if they were essential for potassium removal. However, some recent studies on the giant glial cells located on the central boundary of the neuropil (into which they send processes) of *Hirudo* suggest that potassium homoeostasis by glial processes in neuropil may not be as effective as previously thought (Schlue 1984). Furthermore the general absence of glial processes in the neuropil of the buccal ganglia argues against a role in the local uptake or inactivation of transmitters (see Varon & Somjen 1979). The present findings, together with those concerning increased glycogen turnover following neuronal activation (Pentreath 1982), do however consistently point direction for the majority of the glial cells having roles in the metabolic back up to the neuron perikarya, with a smaller proportion of glial cells being responsible for the removal of neuronal processes.

We thank the Wolfson Institute in the Department of Medical Biophysics, University of Manchester, for the use of the Magiscan image analysis facilities. In particular we thank Dr C. J. Taylor for devising the analysis programme. We are grateful to Pauline Riley, Heather Brown, Jane Duffy and Jackie Sastre for assistance. The work was supported by a grant from the Science and Engineering Research Council to V. W. P.

## References


Abercrombie, H. 1946 Estimation of nuclear population from microtome sections. *Anat. Rec.* **94**, 239–251.

Al-Ali, S. Y. A. & Robinson, N. 1981 Ultrastructural demonstration of glucose-6-phosphatase in cerebral cortex. *Histochemistry* **72**, 107–111.

Anchors, J. M., Haggerty, D. F. & Karnovsky, M. L. 1977 Cerebral glucose-6-phosphatase and the movement of 2-deoxy-D-glucose across cell membranes. *J. biol. Chem.* **252**, 7035–7041.

Angelier, N., Bouteille, M., Charret, R., Curgy, J. J., Delain, E., Fakan, S., Geuskens, M., Guelin, M., La Croix, J. C., Laval, M., Steinert, G. & Van Assel, S. 1976 Detection of nucleic acids by means of ultrastructural autoradiography. *J. Microsc. biol. Cellul.* **27**, 215–230.

Armstrong, D., Rinehart, R., Dixon, L. & Reigh, L. 1978 Changes of peroxidase with age in *Drosophila*. *Age* **1**, 8–12.

Aros, B., Vigh, B. & Vigh-Teichmann, I. 1977 Intra- and extra-ganglionic nerve endings formed by neurosecretory cells of the cerebral ganglia of the earthworm (*Lumbricus terrestris* L.). *Cell Tiss. Res.* **180**, 537–553.

Arvanitaki, A. & Chalazonitis, N. 1952 Répartition de quelques catalyseurs respiratoires dans l'espace cellulaire des neurons géants (*Aplysia* et *Torpedo*). *Archs Sci. physiol.* **6**, 213–232.

Arvanitaki, A. & Chalazonitis, N. 1960 Photopotentials de'excitation et d'inhibition de differents somata identifiables (*Aplysia*). Activations monochromatiques. *Bull. Inst. océanogr. Monaco* **57**, 1–83.

Aune, J. 1976 Ultrastructural changes with age. In *Interdisciplinary topics in gerontology*, vol. 10. *Cellular ageing*, part II (ed. R. G. Cutler), pp. 44–61. New York: S. Karger.

Ball, M. J. 1977 Neuronal loss, neurofibrillary tangles and granulovacuolar degeneration in the hippocampus with age and dementia: a quantitative study. *Acta Neuropathol.* **37**, 111–118.

Barka, T. & Anderson, P. J. 1963 *Histochemistry*. New York, Evanston and London: Harper and Row.

Benjamin, P. R. & Walker, T. S. 1972 Two pigments in the brain of a fresh-water pulmonate snail. *Comp. Biochem. Physiol. B* **41**, 813–823.

Berlin, M. & Wallace, R. B. 1976 Ageing and the central nervous system. *Expl Ageing Res.* **2**, 125–164.

Bernstein, H. G., Weiss, J. & Luppa, H. 1978 Cytochemical investigations on the localization of 5′-nucleotidase in the rat hippocampus with special reference to synaptic regions. *Histochemistry* **55**, 261–267.

Berry, M. S. 1972 A system of electrically coupled small cells in the buccal ganglia of the pond snail *Planorbis corneus*. *J. exp. Biol.* **56**, 621–637.

Berthier, J. 1947 Localisation de l'erythrocruorine chez les Planorbes et les Limnées. *C. r. hebd. Séanc. Acad. Sci., Paris* **225**, 957–959.

Bezruchko, S. M., Adzhimolaev, T. A., Timkin, V. N., Mezentsev, A. N. & Kozhenia, N. I. 1970 Effect of electrical stimulation on nucleic acid and protein metabolism in the nervous system of the nudibranchiate mollusc *Tritonia diomedia*. In *Neuronal mechanisms of learning*, pp. 76–77. Moscow: University Press.

Bittner, G. D. 1981 Trophic interactions of CNS giant-axons in crayfish. *Comp. Biochem. Physiol.* **68**, 299–306.

Blakemore, W. F. 1978 The ultrastructure of normal and reactive microglia. *Acta Neuropathol. (Berlin)*, suppl. VI, pp. 273–278.

Blinkov, S. M. & Glezer, I. 1968 *The human brain in figures and tables: A quantitative handbook*, trans. B. Haigh. New York: Plenum Press.

Blomquist, E., Fredriksson, B. A. & Brunk, V. 1980 Electron probe microanalysis of residual bodies in aged cultured human glia cells. *Ultrastruct. Pathol.* **1**, 11–18.

Boer, H. H., Roubos, E. W., van Dalen, H. & Groesbeek, J. R. F. Th. 1977 Neurosecretion in the basommatophoran snail *Bulinus truncatus* (Gastropoda, Pulmonata). *Cell Tiss. Res.* **176**, 56–67.

Bondareff, W. 1973 Age changes in the neuronal microenvironment. In *Development and ageing in the nervous system* (ed. M. Rockstein), pp. 128–132. New York, London: Academic Press.

Bondareff, W. 1976 Extracellular space in the ageing cerebrum. In *Ageing*, vol. 3, *Neurobiology of ageing* (ed. R. D. Terry and S. Gershon), pp. 167–175. New York: Raven Press.

Bondareff, W. 1980 Changes in synaptic structure affecting neural transmission in the senescent brain. *Advances expl. med. Biol.* **129**, 201–211.

Borovyagin, V. L., Salánki, J. & Zs.-Nagy, I. 1972 Ultrastructural alterations in the cerebral ganglion of *Anadonta cygnea* L. (Mollusca, Pelecypoda), induced by transection of the cerebrovisceral connective. *Acta biol. hung.* **23**, 31–45.

Bourne, G. H. 1973 Lipofuscin. *Prog. Brain Res.* **40**, 186–201.

Boycott, A. E. 1936 The habits of fresh water molluscs in Britain. *J. Anim. Ecol.* **5**, 116–186.

Brizzee, K. R. & Ordy, J. M. 1979 Age pigments, cell loss and hippocampal function. *Mech. Ageing Devel.* **9**, 143–162.

Brizzee, K. R., Samorajski, T., Brizzee, D. L., Ordy, J. M., Dunlap, W. & Smith, R. 1983 Age pigments and cell loss in the mammalian nervous system: functional implications. In *Ageing*, vol. 21, *Brain ageing: neuropathology and neuropharmacology* (ed. J. Cervós-Navarro and H.-I. Sarkander), pp. 211–230. New York: Raven Press.

Brizzee, K. R., Sherwood, D. N. & Timirias, P. S. 1968 A comparison of cell populations at various depth levels in cerebral cortex of young adult and aged Long–Evans rats. *J. Gerontol.* **23**, 289–301.

Brody, M. 1976 An examination of cerebral cortes and brainstem ageing. in *Neurobiology of ageing* (ed. R. D. Terry and S. Gershon), pp. 177–181. New York: Raven Press.

Brown, B. E. 1982 The form and function of metal-containing 'granules' in invertebrate tissues. *Biol. Rev.* **57**, 621–667.

Brunk, U. 1973 Distribution and shifts of ingested marker particles in residual bodies and other lysosomes. Studies on *in vitro* cultivated human glia cells in phase II and III. *Expl Ageing Res.* **79**, 15–27.

Brunk, U., Ericsson, J., Ponten, J. & Westermark, B. 1973 Residual bodies and 'ageing' in cultured human glia cells. Effect of entrance into phase III and prolonged periods of confluence. *Expl Cell Res.* **79**, 1–14.

Bryant, B. J. 1966 The incorporation of tritium from thymidine into proteins of the mouse. *J. Cell Biol.* **29**, 29–36.

Bullock, T. H. & Horridge, G. A. 1965 *Structure and function in the nervous system of invertebrates*. San Francisco and London: W. H. Freeman.

Cammer, W. & Zimmerman, T. R. 1981 Rat brain 5′-nucleotidase: Developmental changes in subcellular fractions and myelin subfractions. *Devl Brain Res.* **1**, 381–389.

Caro, L. G., Tubergen, P. P. Van & Kolb, J. A. 1962 High-resolution autoradiography. I. Methods. *J. Cell Biol.* **15**, 173–188.

Chalazonitis, N. & Arvanitaki, A. 1951 Identification et localisation de quelques catalyseurs respiratoires dans le neurone d'*Aplysia*. *Bull. Inst. océanogr. Monaco* **48**, 1–20.

Chalazonitis, N. & Arvanitaki, A. 1963 Nouvelles recherches sur l'ultrastructure et l'organisation des neurones d'*Aplysia* (grains pigmentés, cône d'origine, gliocytes). *Bull. Inst. océanogr. Monaco.* **61**, 1–16.

Cohen, S. R. 1970 Phosphatases. In *Handbook of neurochemistry*, vol. 3. *Metabolic reactions in the nervous system* (ed. A. Lajtha), pp. 87–131. New York, London: Plenum Press.

Coleman, P. D. & Goldman, G. 1981 Neuron counts in locus coeruleus of ageing rat. In *Ageing*, vol. 17 (ed. S. J. Enna, B. Samorajski and B. Beer), pp. 23–28. New York: Raven Press.

Coles, J. A. & Tsacopoulos, M. 1979 Potassium activity in photoreceptors, glial cells and extracellular space in the drone retina: Changes during photostimulation. *J. Physiol., Lond.* **290**, 524–549.

Coles, J. A. & Tsacopoulos, M. 1981 Ionic and possible metabolic interactions between sensory neurons and glial cells in the retina of the honeybee drone. *J. exp. Biol.* **95**, 75–92.

Colonnier, M., Tremblay, J. P. & McLennan, H. 1979 Synaptic contacts on glial cells in the abdominal ganglion of *Aplysia californica*. *J. comp. Neurol.* **188**, 391–400.

Comfort, A. 1964 *The biology of senescence*, 3rd edn. Edinburgh and London: Churchill-Livingstone.

Cragg, B. G. 1975 The density of synapses and neurons in normal, mentally defective ageing human brains. *Brain* **98**, 81–90.

Curgy, J. J. 1969 Incorporation *in vivo* d'uridine [$^3$H] dans l'ARN des mitochondries hepatiques du poussin et du souriceau. Étude autoradiographique au microscope electronique. *J. Microsc.* **7**, 849–864.

Dalton, M. M., Hommes, D. R. & Leblond, C. P. 1968 Correlation of glial proliferation with age in the mouse brain. *J. comp. Neurol.* **134**, 397–400.

Davies, I. 1983 Influence of age on the hypothalamo-neurohypophyseal system. In *Ageing*, vol. 21, *Brain ageing: neuropathology and neuropharmacology* (ed. J. Cervós-Navarro and H.-I. Sarkander), pp. 153–178. New York: Raven Press.

Delesse, A. 1847 Procede méchanique pour determines la composition des roches. *C. r. hebd. Séanc. Acad. Sci., Paris* **25**, 544–548.

Devaney, K. O. & Johnson, M. A. 1980 Neuron loss in the ageing visual cortex of man. *J. Gerontol.* **35**, 836–841.

Dick, F. & Kelly, J. S. 1977 Specific in vivo autoradiographic localization of [$^3$H]-β-alanine uptake sites in macro as opposed to microglial cells. *Br. J. Pharmacol.* **59**, 485*P*.

Drury, R. A. B. & Wallington, E. A. 1980 *Carlton's histological technique*, 5th edn. Oxford, New York, Toronto: Oxford University Press.

Dunn, R. C. & Thompson, E. C. 1945 A new hemoglobin stain for histological use. *Arch. Pathol.* **39**, 49–50.

Dyakonova, T. L. 1972 Activation of RNA synthesis in glial satellite cells during electrical activity of neuron. *Tsitologiya* **14**, 1147–1155.

Dyakonova, T. L. & Veprintzev, B. N. 1969 *Particularities of structural and functional organization and metabolic activity of neurons of Lymnaea*. Pushchino: U.S.S.R. Academy of Science, Department of Biophysics.

Faeder, I. R. & Saltpeter, M. M. 1970 Glutamate uptake by a stimulated insect nerve muscle preparation. *J. Cell Biol.* **46**, 300–307.

Fahrenbach, W. H. 1976 The brain of the horseshoe crab (*Limulus polyphemus*). I. Neuroglia. *Tiss. Cell* **8**, 395–410.

Fog, R. & Pakkenberg, H. 1981 Age-related changes in [$^3$H]uridine uptake in the mouse. *J. Gerontol.* **36**, 680–681.

Ford, D. H. 1973*a* Selected changes in the developing postnatal rat brain. In *Development and ageing in the nervous system* (ed. M. Rockstein), pp. 63–88. New York, London: Academic Press.

Ford, D. H. 1973*b* Selected maturational changes observed in the postnatal rat brain. *Prog. Brain Res.* **40**, 1–12.

Ford, D. H. & Cohan, G. 1968 Changes in weight and volume of rat spinal cord motor neurons with increasing age. *Acta Anat.* **71**, 311–319.

Franks, L. M., Wilson, P. D. & Whelan, R. D. 1974 The effect of age on total DNA and cell number in the mouse brain. *Gerontologia* **20**, 21–26.

Friede, R. L. 1954 Der quantitative Anteil der Glia an der Cortexentwicklung. *Acta Anat.* **20**, 290–296.

Friede, R. L. 1963 The relationship of body size, nerve cell size, axon length and glial density in the cerebellum. *Proc. natn. Acad. Sci. U.S.A.* **49**, 187–193.

Friede, R. L. & van Houten, W. H. 1962 Neuron extension and glial supply: functional significance of glia. *Proc. natn. Acad. Sci. U.S.A.* **48**, 817–821.

Gambetti, P., Autilio-Gambetti, L., Schafer, B. & Pfaff, L. 1973 Quantitative autoradiographic study of labeled RNA in rabbit optic nerve after intraocular injection of [$^3$H]uridine. *J. Cell Biol.* **59**, 677–684.

Gardner-Medwin, A. R. 1983*a* A study of the mechanisms by which potassium moves through brain tissue in the rat. *J. Physiol., Lond.* **335**, 353–374.

Gardner-Medwin, A. R. 1983*b* Analysis of potassium dynamics in mammalian brain tissue. *J. Physiol., Lond.* **335**, 393–426.

Gardner-Medwin, A. R., Coles, J. A. & Tsacopoulos, M. 1981 Clearance of extracellular potassium: evidence for spatial buffering by glial cells in the retina of the drone. *Brain Res.* **209**, 452–457.

Gardner-Medwin, A. R. & Nicholson, C. 1983 Changes of extracellular potassium activity induced by electric current through brain tissue in the rat. *J. Physiol., Lond.* **335**, 375–392.

Ghiretti, F. & Ghiretti-Magaldi, A. 1972 Respiratory proteins in molluscs. In *Chemical zoology*, vol. 7, *Mollusca* (ed. M. Florkin and B. T. Scheer), pp. 201–217. New York and London: Academic Press.

Ghiretti, F. & Ghiretti-Magaldi, A. 1975 Respiration. In *Pulmonates*, vol. 1, *Functional anatomy and physiology* (ed. V. Fretter and J. Peake), pp. 33–52. London, New York, San Francisco: Academic Press.

Giuditta, A., Libonati, M., Packard, A. & Prozzo, N. 1971 Nuclear counts in the brain lobes of *Octopus vulgaris* as a function of body size. *Brain Res.* **25**, 55–62.

Glauert, A. M. 1975 *Practical methods in electron microscopy*, vol. 3. *Fixation, dehydration and embedding of biological specimens*. Amsterdam, New York and Oxford: North-Holland.

Glees, P. & Hasan, M. 1976 *Lipofuscin in neuronal ageing and disease*. Stuttgart: Thieme.

Gymer, A. & Edwards, J. S. 1967 The development of the insect nervous system. I. An analysis of postembryonic growth in the terminal ganglion of *Acheta domesticus*. *J. Morphol.* **123**, 191–198.

Hall, T. C., Miller, A. K. H. & Corsellis, J. A. N. 1975 Variations in the human Purkinje cell population according to age and sex. *Neuropathol. appl. Neurobiol.* **1**, 267–292.

Hanley, T. 1974 'Neuronal fallout' in the ageing brain: a critical review of the quantitative data. *Age Ageing* **3**, 133–151.

Hawkins, A. & Olszewski, J. 1957 Glia/nerve cell index for cortex of the whale. *Science, Wash.* **126**, 76–77.

Hawkins, A. & Olszewski, J. 1960 Quantitative study of gliosis in degenerating pyramidal tracts. *J. Neuropathol. expl. Neurol.* **19**, 130–134.

Haymaker, W. & Adams, R. D. 1982 *Histology and histopathology of the nervous system*. Springfield, U.S.A.: Charles C. Thomas.

Henderson, G., Tomlinson, B. E. & Gibson, P. H. 1980 Cell counts in human cerebral cortex in normal adults throughout life using an image analysing computer. *J. neurol. Sci.* **35**, 351–373.

Henderson, G., Tomlinson, B. E. & Weightman, D. 1975 Cell counts in the human cerebral cortex using a traditional and an automated method. *J. neurol. Sci.* **25**, 129–144.

Herman, M. M., Miquel, J. & Johnson, M. 1971 Insect brain as a model for the study of ageing. *Acta Neuropathol.* **19**, 167–183.

Heuser, J. E. & Doggenweiler, C. F. 1966 The fine structural organization of nerve fibres, sheaths and glial cells in the prawn, *Palaemonetes vulgaris*. *J. Cell Biol.* **30**, 381–403.

Hirrup, K. & Mullen, R. J. 1981 Role of the staggerer gene in determining Purkinje cell number in the cerebellar cortex of mouse chimeras. *Devel. Brain Res.* **1**, 475–485.

Holtzman, E. 1976 *Lysosomes: A survey*. Cell Biology Monographs, vol. 3. Wien, New York: Springer-Verlag.

Howard, E. 1973 DNA content of rodent brains during maturation and ageing and autoradiography of postnatal DNA synthesis in monkey brain. In *Progress in brain research*, vol. 40. *Neurobiological aspects of maturation and ageing* (ed. D. H. Ford), pp. 91–114. Amsterdam, London, New York: Elsevier.

Jacobson, M. 1978 *Developmental neurobiology*, 2nd edn. New York and London: Plenum Press.

Johnson, H. A. & Erner, S. 1972 Neuron survival in the ageing mouse. *Expl Gerontol.* **7**, 111–117.

Johnston, P. V. & Roots, B. I. 1972 *Nerve membranes: A study of the biological and chemical aspects of neuron–glia relationships*. Int. Series Monographs Pure Appl. Biol., vol. 46. Oxford, New York: Pergamon Press.

Jones, J. D. 1961 Aspects of respiration in *Planorbis corneus* L. and *Lymnaea stagnalis* L. (Gastropoda: Pulmonata). *Comp. Biochem. Physiol.* **4**, 1–29.

Jones, J. D. 1964 The role of haemoglobin in the aquatic pulmonate, *Planorbis corneus*. *Comp. Biochem. Physiol.* **12**, 283–295.

Kai-Kai, M. A. & Pentreath, V. W. 1981*a* High resolution analysis of [$^3$H]2-deoxyglucose incorporation into neurons and glial cells in invertebrate ganglia: histological processing of nervous tissue for selective marking of glycogen. *J. Neurocytol.* **10**, 693–708.

Kai-Kai, M. A. & Pentreath, V. W. 1981*b* The structure, distribution, and quantitative relationships of the glia in the abdominal ganglia of the horse leech, *Haemopis sanguisuga*. *J. comp. Neurol.* **202**, 193–210.

Kelly, J. S. & Dick, F. 1976 Differential labelling of glial cells and GABA inhibitory interneurons and nerve terminals following the micro-injection of β-[$^3$H]alanine, [$^3$H]DABA and [$^3$H]GABA into single folia of the cerebellum. *Cold Spring Harb. Symp. quant. Biol.* **40**, 93–106.

Kisiel, M. J. & Zuckerman, B. M. 1978 Effects of centrophenoxine on the nematode *Caenorhabditis briggsae*. *Age* **1**, 17–20.

Kornguth, M. L. & Stubbs, E. A. 1965 Hydrolysis of phosphohydroxypyruvate and β-glycerophosphate by a phosphatase preparation from beef brain. *Archs Biochem. Biophys.* **109**, 104–169.

Korr, H. 1968 Das postembryonale Wachstum verschiedener Hirnbereiche *Orchesella villosa* L. (Ins. Collembola). *Z. Morphol. Oekol. Tiere* **62**, 389–422.

Kraus-Ruppert, R., Laissue, J., Bürki, H. & Odartchenko, N. 1973 Proliferation and turnover of glial cells in the forebrain of young adult mice as studied by the repeated injections of [$^3$H]thymidine over a prolonged period of time. *J. comp. Neurol.* **148**, 211–216.

Kreutzberg, G. W. & Barron, K. D. 1978 5′-Nucleotidase of microglial cells in the facial nucleus during axonal reaction. *J. Neurocytol.* **7**, 601–610.

Kreutzberg, G. W., Barron, K. D. & Schubert, P. 1978 Cytochemical localization of 5′-nucleotidase in glial plasma membranes. *Brain Res.* **158**, 247–257.

Kuffler, S. W. 1967 Neuroglial cells: physiological properties and a potassium mediated effect of neuronal activity on the glial membrane potential. *Proc. R. Soc. Lond.* B **168**, 1–21.

Kuffler, S. W. & Nicholls, J. G. 1966 The physiology of neuroglial cells. *Ergebn. Physiol.* **57**, 1–90.

Kuffler, S. W. & Nicholls, J. G. 1976 *From neuron to brain.* Sunderland, Massachusetts: Sinauer.

Kuzmin, S. M., Timkin, V. N., Bezruchko, S. M. & Adzhimolaev, T. A. 1972 Dynamic aspects of RNA metabolism in mollusc ganglia during electrical effects. *Zh. Evol. Biokhim. I Fiziol.* **II**, 274–281.

Lamparter, J. E. 1966 Die strukturelle Organization des Prothorakalganglions bei der Waldameise (*Formica lugubris*, Zett.). *Z. Zellforsch. mikrosk. Anat.* **74**, 198–231.

Landfield, P. W., Rose, G., Sandles, L., Wahlstadter, J. C. & Lynch, G. 1977 Patterns of astroglial hypertrophy and neuronal degeneration in the hippocampus of aged, memory deficient rats. *J. Gerontol.* **32**, 3–12.

Lane, N. J. 1981 Invertebrate neuroglia-junctional structure and development. *J. exp. Biol.* **95**, 7–33.

Lange, P. W. 1979 Nucleic acids and proteins. In *Dynamic properties of glia cells* (ed. E. Schoffeniels, G. Franck, L. Hertz and D. B. Tower), pp. 231–246. New York: Pergamon Press.

Lasek, R. J., Gainer, H. & Barker, J. L. 1977 Cell-to-cell transfer of glial proteins to the squid giant axon. The glia-neuron protein transfer hypothesis. *J. Cell Biol.* **74**, 501–523.

Lasek, R. J. & Tytell, M. A. 1981 Macromolecular transfer from glia to the axon. *J. exp. Biol.* **95**, 153–165.

Lemkey-Johnson, N., Butler, V. & Reynold, W. A. 1976 Glial changes in the progress of a chemical lesion. An electron microscopic study. *J. comp. Neurol.* **167**, 481–501.

Lewis, P. R. & Knight, D. P. 1977 *Practical methods in electron microscopy*, vol. 5, part II (ed. A. M. Glauert). Amsterdam, New York and Oxford: North Holland.

Mačela, I. & Seliškar, A. 1925 The influence of temperature on the equilibrium between oxygen and haemoglobin of various forms of life. *J. Physiol. Lond.* **60**, 428–442.

Malzacher, P. 1968 Die Embryogenese des Gehirns paurometaboler Insekten. Untersuchungen an *Carausius morosus* und *Periplaneta americana*. *Z. Morphol. Oekol. Tiere* **62**, 103–161.

Matthews, M. A. & Kruger, L. 1973 Electron microscopy of non-neuronal cellular changes accompanying neural degeneration in thalamic nuclei of the rabbit. II. Reactive elements within the neuropile. *J. comp. Neurol.* **148**, 313–346.

Mayhew, T. M. & Momoh, C. K. 1973 Contribution to the quantitative analysis of neuronal parameters: The effect of biased sampling procedures on estimates of neuronal volume, surface area and packing density. *J. comp. Neurol.* **148**, 217–228.

Mervis, R. 1981 Cytomorphological alterations in the aging animal brain with emphasis on Golgi structures. In *Aging and cell structure*, vol. 1 (ed. J. E. Johnson), pp. 143–186. New York, London: Plenum Press.

Miguel, J., Economos, A. C., Fleming, J. & Johnson, J. E. 1980 Mitochondrial role in cell aging. *Expl Gerontol.* **15**, 575–591.

Nandy, M. 1972 Neuronal degeneration in aging and after experimental injury. *Expl Gerontol.* **7**, 301–311.

Nandy, K. 1983 Aging neurons and pharmacological agents. In *Ageing*, vol. 21, *Brain ageing: neuropathology and neuropharmacology* (ed. J. Cervós-Navarro and H.-I. Sarkander), pp. 401–413. New York: Raven Press.

Nicaise, G. 1967 Description d'un 'systeme glio-interstitial' chez *Glossodoris* (Gastéropode: Opisthobranche). *C. r. hebd. Séanc. Acad. Sci., Paris* **246**, 2793–2795.

Nicaise, G. 1973 The gliointerstitial system of molluscs. *Int. Rev. Cytol.* **34**, 251–332.

Nicholson, C. 1980 Dynamics of brain cell microenvironment. *Neurosci. Res. Prog. Bull.* **18**, 177–322.

Ogawa, F. 1939 The nervous system of earthworm (*Pheretima communissima*) in different ages. *Sci. Rep. Tohoku Univ. Fourth Ser.* **13**, 395–488.

Ogur, M. & Rosen, G. 1950 Nucleic acids of plant tissues. I. Extraction and estimation of deoxypentose nucleic acid and pentose nucleic acid. *Archs Biochem.* **25**, 262–270.

Orkand, P. M. & Kravitz, E. A. 1971 Localization of the sites of γ-aminobutyric acid (GABA) uptake in lobster nerve-muscle preparations. *J. Cell Biol.* **49**, 75–89.

Orkand, R. K., Nicholls, J. G. & Kuffler, S. W. 1966 Effect of nerve impulses on the membrane potential of glial cells in the central nervous system of amphibia. *J. Neurophysiol.* **19**, 788–806.

Orkand, R. K., Orkand, P. M. & Tang, C.-M. 1981 Membrane properties of neuroglia in the optic nerve of *Necturus*. *J. exp. Biol.* **95**, 49–59.

Packard, A. & Albergoni, V. 1970 Relative growth, nucleic acid content and cell numbers of the brain in *Octopus vulgaris* (Lamarck). *J. exp. Biol.* **52**, 539–552.

Panov, A. A. 1962 The nature of cell reproduction in the central nervous system of the house cricket. (*G. domesticus*, Orthoptera, Insects) (Transl.). *Dokl. Akad. Nauk SSR (Biol. Sci. Sect.)* **145**, 904–907.

Papka, R., Peretz, B. G., Tudor, J. & Becker, J. 1981 Age-dependent anatomical changes in an identified neuron in the CNS of *Aplysia californica*. *J. Neurobiol.* **12**, 455–468.

Pappius, H. M. 1979 Cerebral edema. In *Dynamic properties of glia cells* (ed. E. Schoffeniels, G. Franck, L. Hertz and D. B. Tower), pp. 397–402. New York: Pergamon Press.

Peng, M. T. & Lee, L. R. 1979 Regional differences of neuron loss of rat brain in old age. *Gerontology* **25**, 205–211.

Pentreath, V. W. 1976 Ultrastructure of the terminals of an identified serotonin-containing neurone marked by intracellular injection of radioactive serotonin. *J. Neurocytol.* **5**, 43–61.

Pentreath, V. W. 1982 Potassium signalling of metabolic interactions between neurons and glial cells. *Trends Neurosci.* **5**, 339–345.

Pentreath, V. W. & Berry, M. S. 1978 Radioautographic study of 5-hydroxytryptamine-containing nerve terminals in central ganglia of *Planorbis corneus*: comparison with other species and characteristics of the serotonergic nerve terminal. *J. Neurocytol.* **7**, 433–459.

Pentreath, V. W., Berry, M. S. & Osborne, N. N. 1982 The serotonergic cells in gastropods. In *Biology of serotonergic transmission* (ed. N. N. Osborne), pp. 457–513. Chichester, New York, Brisbane, Toronto, Singapore: John Wiley.

Pentreath, V. W. & Cottrell, G. A. 1970 The blood supply to the central nervous system of *Helix pomatia*. *Z. Zellforsch. mikrosk. Anat.* **111**, 160–178.

Pentreath, V. W. & Kai-Kai, M. A. 1982 Significance of the potassium signal from neurones to glial cells. *Nature, Lond.* **295**, 59–61.

Pentreath, V. W., Seal, L. H. & Kai-Kai, M. A. 1982 Incorporation of [$^3$H]2-deoxyglucose into glycogen in nervous tissues. *Neuroscience* **7**, 759–767.

Peretz, B. G. & Lukowiak, K. 1975 Age dependent CNS control of the habituating gill withdrawal reflex and of correlated activity in identified neurons in *Aplysia*. *J. comp. Physiol.* **103**, 1–17.

Peretz, B., Ringham, G. & Wilson, R. 1982 Age diminished neuronal function of central neuron L7 in *Aplysia*. *J. Neurobiol.* **13**, 141–151.

Peters, A., Palay, S. L. & Webster, H. de F. 1976 *The fine structure of the nervous system. The neurons and supporting cells*. Philadelphia: Saunders.

Peters, A. & Vaughan, D. W. 1981 Central nervous system. In *Aging and cell structure* (ed. J. E. Johnson, Jr), pp. 1–34. New York, London: Plenum Press.

Petersen, R. P. & Kernell, D. 1970 Effect of nerve stimulation of the metabolism of ribonucleic acid in a molluscan giant neurone. *J. Neurochem.* **17**, 1075–1085.

Pevzner, L. Z. 1979 *Functional biochemistry of the neuroglia*, transl. B. Tiplady. New York and London: Consultants Bureau.

Pipa, R. L., Nishioka, R. S. & Bern, H. A. 1962 Studies on the hexapod nervous system. V. The ultrastructure of cockroach gliosomes. *J. ultrastruct. Res.* **6**, 164–170.

Power, M. E. 1952 A quantitative study of the growth of the central nervous system of a holometabolous insect. *Drosophila melanogaster*. *J. Morphol.* **91**, 389–411.

Radojcic, T. & Pentreath, V. W. 1979 Invertebrate glia. *Progr. Neurobiol.* **12**, 115–179.

Radojcic, T. & Pentreath, V. W. 1981 Quantitative analysis of neuron-glial relationships in the buccal ganglion of *Planorbis*: life constancy in the absence of changes in functional output. *Brain Res.* **211**, 468–475.

Rakic, P. 1974 Intrinsic and extrinsic factors influencing the shape of neurons and their assembly into neuronal circuits. In *Frontiers in neurology and neuroscience research* (ed. P. Seeman and G. M. Brown), pp. 112–132. Toronto: University of Toronto Press.

Rattan, K. S. & Peretz, B. 1981 Age-dependent behavioural changes and physiological changes in identified neurons in *Aplysia californica*. *J. Neurobiol.* **12**, 469–478.

Ravens, J. R. & Calvo, W. 1965 Neuroglial changes in the senile brain. In *Proc. Fifth Int. congr. Neuropathology*, Zurich (ed. F. Luthy and A. Bischoff), pp. 506–512. International Congress Serial no. 100, Amsterdam, New York, London: Excerpta Medica Foundation.

Read, K. R. H. 1966 Molluscan hemoglobin and myoglobin. In *Physiology of Mollusca*, vol. 2 (ed. K. M. Wilbur and C. M. Yonge), pp. 209–232. New York and London: Academic Press.

Reinecke, M. 1975 Die Gliazellen der Cerebralganglien von *Helix pomatia* L. (Gastropoda: Pulmonata). I. Ultrastruktur und Organisation. *Zoomorphology* **82**, 105–136.

Reinecke, M. 1976 The glial cells of the cerebral ganglia of *Helix pomatia* L. (Gastropoda: Pulmonata). II. Uptake of ferritin and [$^3$H]glutamate. *Cell Tiss. Res.* **169**, 361–382.

Roberts, J. & Goldberg, P. B. 1976 Some aspects of the CNS of the rat during aging. *Expl Aging Res.* **2**, 531–542.

Rogers, J., Zornetzer, S. & Bloom, F. E. 1981 Senescent pathology of cerebellum: Purkinje neurons and their parallel fiber afferents. *Neurobiol. Aging* **2**, 15–25.

Roots, B. I. 1981 Comparative studies on glial markers. *J. exp. Biol.* **95**, 167–180.

Rosen, S. I. 1970 Glucose-6-phosphate hydrolysing activity in the cerebellum of the mouse, rat, marmoset and hamster. *Acta histochem.* **36**, 44–53.

Rosenbluth, J. 1963 The visceral ganglion of *Aplysia californica*. *Z. Zellforsch. mikrosk. Anat.* **60**, 213–236.

Roubos, E. W. & Moorer-van Delft, C. M. 1979 Synaptology of the central nervous system of the freshwater snail *Lymnaea stagnalis* (L.), with particular reference to neurosecretion. *Cell Tiss. Res.* **198**, 217–235.

Ryman, B. E. & Whelan, W. J. 1971 New aspects of glycogen metabolism. *Adv. Enzymol.* **34**, 285–443.

Salem, R. D., Hammerschlag, R., Bracho, H. & Orkand, R. K. 1975 Influence of potassium ions on accumulation and metabolism of $^{14}C$ glucose by glial cells. *Brain Res.* **86**, 499–503.

Samorajski, T. 1976 How the human brain responds to aging. *J. Am. Ger. Soc.* **24**, 4–11.

Samorajski, T., Keefe, J. R. & Ordy, J. M. 1964 Intracellular localization of lipofuscin age pigments in the nervous system. *J. Gerontol.* **19**, 262–276.

Samorajski, T., Ordy, J. M. & Keefe, J. R. 1965 The fine structure of lipofuscin age pigment in the nervous system of aged rats. *J. Cell Biol.* **26**, 779–795.

Scharrer, B. C. J. 1939 The differentiation between neuroglia and the connective tissue sheath in the cockroach (*Periplaneta americana*). *J. comp. Neurol.* **70**, 77–88.

Schick, P., Trepel, F., Maisel, K. H., Past, W., Reisert, I., Bergeman, H. & Pilgrim, C. H. 1978 Labelling of human resting lymphocytes by continuous infusion of [$^3$H]thymidine. I. Characterization of cytoplasmic label. *J. Cell Sci.* **33**, 351–362.

Schlote, W. & Boellaard, J. W. 1983 Role of lipopigment during aging of nerve and glial cells in the human central nervous system. In *Ageing*, vol. 21, *Brain ageing: neuropathology and neuropharmacology* (ed. J. Cervós-Navarro and H.-I. Sarkander), pp. 27–74. New York: Raven Press.

Schlue, W. R. 1984 Electrophysiology of neuropile glial cells in the central nervous system of the leech. A model system for potassium homeostasis in the brain. *Advan. Cell. Neurobiol.* **5**. (In the press.)

Schmechel, D. 1978 Brain enolases as specific markers of neuronal and glial cells. *Science, Wash.* **199**, 313–314.

Schmidley, J. W. & Wissig, S. L. 1983 Abundant, uniquely oriented endoplasmic reticulum in capillaries of the CNS: demonstration using reduced-osmium and glucose-6-phosphatase cytochemistry. *Brain Res.* **262**, 9–15.

Schon, F. & Kelly, J. S. 1975 Selective uptake of [$^3$H]β-alanine by glia: association with the glial uptake system for GABA. *Brain Res.* **86**, 243–257.

Schubert, P., Lee, K. & Kreutzberg, G. W. 1982 Neuronal release of adenosine derivatives and modulation of signal processing in the CNS. *Prog. Brain Res.* **55**, 225–237.

Schultz, U. & Hunziker, D. 1980 Comparative study of neuronal perikaryon size and shape in the aging cerebral cortex. *J. Gerontol.* **35**, 483–491.

Scott, T. G. 1965 The specificity of 5′-nucleotidase in the brain of the mouse. *J. Histochem. Cytochem.* **13**, 657–667.

Sears, T. A. (ed.) 1982 *Neuron–glial cell interrelationships.* Dahlem Konferenzen. Berlin, Heidelberg, New York: Springer-Verlag.

Sharma, N. N. 1967 Studies on the histochemical distribution of glucose-6-phosphatase, glucose-6-phosphate dehydrogenase, β-glucoronidase and glucosan phosphorylase in olfactory bulb of rat. *Acta histochem.* **27**, 165–171.

Singer, M. & Green, M. 1968 Autoradiographic studies of the ribonucleic acid in the peripheral nerve of the newt *Triturus*. *J. Morphol.* **124**, 321–344.

Smart, I. & Leblond, C. P. 1961 Evidence for division and transformation of neuroglia cells in the mouse brain as derived from radioautography after injection of thymidine-[$^3$H]. *J. comp. Neurol.* **116**, 349–367.

Snyder, D. S., Zimmerman, T. R., Farooq, M., Norton, W. T. & Cammer, W. 1983 Carbonic anhydrase, R′-nucleotidase, and 2′, 3′-cyclic nucleotide -3′-phosphodiesterase activities in oligodendrocytes, astrocytes and neurons isolated from the brains of developing rats. *J. Neurochem.* **40**, 120–127.

Sohal, R. S. & Sharma, S. P. 1972 Age-related changes in the fine structure and number of neurones in the brain of the housefly, *Musca domestica*. *Expl Gerontol.* **7**, 243–249.

Solyom, A. & Trams, E. G. 1973 Enzyme markers in characterization of isolated plasma membranes. *Enzyme* **13**, 329–372.

Soreide, A. J., Torvik, A., Dick, F. & Kelly, J. S. 1978 Lack of labelling of microglial cells following microinjection of [$^3$H]β-alanine: an electron microscope autoradiographic study. *J. Neurocytol.* **7**, 3–9.

Stensaas, L. J. 1977 The ultrastructure of astrocytes, oligodendrocytes and microglia in the optic nerve of urodele amphibians (*A. punctatum*, *T. pyrrhogaster*, *T. viridescens*). *J. Neurocytol.* **6**, 269–286.

Stephens, H. R. & Sandborn, E. B. 1976 Cytochemical localization of glucose-6-phosphatase activity in the central nervous system of the rat. *Brain Res.* **113**, 127–146.

Stone, T. W. 1981 Physiological roles for adenosine and adenosine 5′-triphosphate in the nervous system. *Neuroscience* **6**, 523–555.

Sturrock, R. R. 1974*a* Histogenesis of the anterior limb of the anterior commissure of the mouse brain. I. A quantitative study of changes in the glial population with age. *J. Anat.* **117**, 17–25.

Sturrock, R. R. 1974*b* Histogenesis of the anterior limb of the anterior commissure of the mouse brain. II. A quantitative study of pre and post-natal mitosis. *J. Anat.* **117**, 27–35.

Sturrock, R. R. 1974*c* A light microscope study of glial necrosis with age in the interior limb of the anterior commissure of the pre and post-natal mouse. *J. Anat.* **117**, 469–474.

Sturrock, R. R. 1976 Changes in neuroglia and myelin in white matter of ageing mice. *J. Gerontol.* **31**, 513–522.

Sturrock, R. R. 1977 Quantitative changes in neuroglia in different areas of the ageing mouse brain. *J. Anat.* **124**, 501.

Sturrock, R. R. 1978 Development of the indusium griseum. I. A quantitative light microscope study of neurons and glia. *J. Anat.* **125**, 293–298.

Sturrock, R. R. & Jew, J. Y. 1978 A quantitative histological study of changes in neurons and glia in the Gunn rat brain. *Neuropathol. appl. Neurobiol.* **4**, 209–224.

Svedberg, I. 1933 Sedimentation constants, molecular weights, and isoelectric points of the respiratory proteins. *J. biol. Chem.* **103**, 311–325.

Svedberg, T. & Hedenius, A. 1934 The sedimentation constants of the respiratory proteins. *Biol. Bull. mar. Biol. Lab., Woods Hole* **66**, 191–223.

Swindale, N. V. & Benjamin, P. R. 1976*a* Peripheral neurosecretion in the pond snail *Lymnaea stagnalis* (L.). In *Neurobiology of invertebrates*, vol. 3. Budapest: Publishing House of the Hungarian Academy of Sciences.

Swindale, N. V. & Benjamin, P. R. 1976*b* The anatomy of neurosecretory neurons in the pond snail *Lymnaea stagnalis* (L.). *Phil. Trans. R. Soc. Lond.* B **274**, 169–202.

Szabo, I. 1935 Senescence and death in invertebrate animals. *Riv. Biol.* **19**, 377–436.

Terry, R. D., Fitzgerald, C., Peck, A., Milner, J. & Farmer, P. 1977 Cortical cell units in senile dementia. *J. Neuropathol. exp. Neurol.* **36**, 633.

Tewari, H. B. & Bourne, G. H. 1962 Histochemical evidence of metabolic cycles in spinal ganglion cells of rat. *J. Histochem. Cytochem.* **10**, 42–64.

Tewari, H. B. & Bourne, G. H. 1963 On the intracellular distribution of glucose-6-phosphatase in the neurons of cerebrum and trigeminal ganglion of the rat. *J. Histochem. Cytochem.* **11**, 121–122.

Thompson, A. F. 1965 The ependymo-venticular glia in normal ageing. In *Proc. Fifth Int. cong. Neuropathology*, Zurich (ed. F. Luthy and A. Bischoff), pp. 95–105. International Congress Serial, no. 100. Amsterdam, New York, London: Excerpta Medica Foundation.

Tomlinson, B. E., Blessed, G. & Roth, M. 1968 Observations on the brains of non-demented old people. *J. neurol. Sci.* **7**, 331–356.

Tomlinson, B. E., Blessed, G. & Roth, M. 1970 Observations on the brains of demented old people. *J. neurol. Sci.* **11**, 205–242.

Treherne, J. E. (ed.) 1981 Glial–neurone interactions. *J. exp. Biol.* **95**, 1–240.

Treherne, J. E. & Schofield, P. K. 1981 Mechanisms of ionic homeostasis in the central nervous system of an insect. *J. exp. Biol.* **95**, 61–73.

Tweedle, C. D. & Hatton, G. I. 1980*a* Evidence for dynamic interaction between pituicytes and neurosecretory axons in the rat. *Neuroscience* **5**, 661–667.

Tweedle, C. D. & Hatton, G. I. 1980*b* Glial cell enclosure of neurosecretory endings in the neurohypophysis of the rat. *Brain Res.* **192**, 555–559.

Uemura, E. & Hartman, H. A. 1981 RNA content and volume of nerve cell bodies in human brain. *Expl Neurol.* **65**, 107–117.

Veron, S. S. 1979 Macromolecular glial cell markers. In *Dynamic properties of glia cells* (ed. E. Schoffeniels, G. Franck, L. Hertz and D. B. Tower), pp. 93–104. New York: Pergamon Press.

Varon, S. S. & Somjen, G. G. 1979 Neuron-glia interactions. *Neurosci. Res. Prog. Bull.* **17**, 6–239.

Vaughan, D. W. 1977 Age-related deterioration of pyramidal cell basal dendrites in rat auditory cortex. *J. comp. Neurol.* **171**, 501–516.

Vaughan, D. W. & Peters, A. 1974 Neuroglial cells in the cerebral cortex of rats from young adulthood to old age: an electron microscope study. *J. Neurocytol.* **3**, 405–429.

Vercelli-Retta, J., Silveira, R., Dajas, F. & Rodriquez, D. 1976 Enzyme histochemistry of rat interfascicular oligodendroglia, with special reference to 5′-nucleotidase. *Acta Anat.* **96**, 534–536.

Villegas, J. 1981 Axon/Schwann-cell relationships in the giant nerve fibre of the squid. *J. exp. Biol.* **95**, 135–151.

Wachstein, M. & Meisel, E. 1957 Histochemistry of hepatic phosphatases at a physiologic pH with special reference to the demonstration of bile canaliculi. *Am. J. clin. Path.* **27**, 13–23.

Wendelaar Bonga, S. E. 1970 Ultrastructure and histochemistry of neurosecretory cells and neurohaemal areas in the pond snail *Lymnaea stagnalis* (L.). *Z. Zellforsch. mikrosk. Anat.* **108**, 190–224.

Wilcox, H. H. 1959 Structural changes in the nervous system related to the process of aging. In *The process of aging in the nervous system* (ed. J. F. Birren, H. A. Imus and W. F. Windle), pp. 16–23. Springfield, Illinois: Charles C. Thomas.

Wilkinson, A. & Davies, I. 1978 The influence of age and dementia on the neuron population of the mammillary bodies. *Age Ageing* **7**, 151–160.

Williams, M. A. 1977 *Quantitative methods in biology. Practical methods in electron microscopy*, vol. 6. Amsterdam: North Holland.

Wisniewski, H. M. & Terry, R. D. 1973 Morphology of the aging brain, human and animal. In *Progress in brain research*, vol. 40 (ed. D. H. Ford), pp. 167–188. Amsterdam, New York, London: Elsevier.

Wisniewski, H. M. & Terry, R. D. 1976 Neuropathology of the aging brain. In *Ageing*, vol. 3, *Neurobiology of ageing* (ed. R. D. Terry and S. Gershon), pp. 265–280. New York: Raven Press.

Wisniewski, H. M., Sinatra, R. S., Iqbal, K. & Grundke-Iqbal, I. 1981 Neurofibrillary and synaptic pathology in the aged brain. In *Aging and cell structure* (ed. J. E. Johnson Jr), pp. 105–142. New York, London: Plenum Press.

Wittenberg, J. B. 1966 The molecular mechanisms of hemoglobin-facilitated oxygen diffusion. *J. biol. Chem.* **241**, 104–114.

Wittenberg, B. A., Briehl, R. W. & Wittenberg, J. B. 1965 Haemoglobins of invertebrate tissues. *Biochem. J.* **96**, 363–371.

Zs-Nagy, I. 1971 Pigmentation and energy dependent $Sr^{++}$-accumulation of molluscan neurons under anaerobic conditions. *Ann. Biol. Tihany* **38**, 117–129.

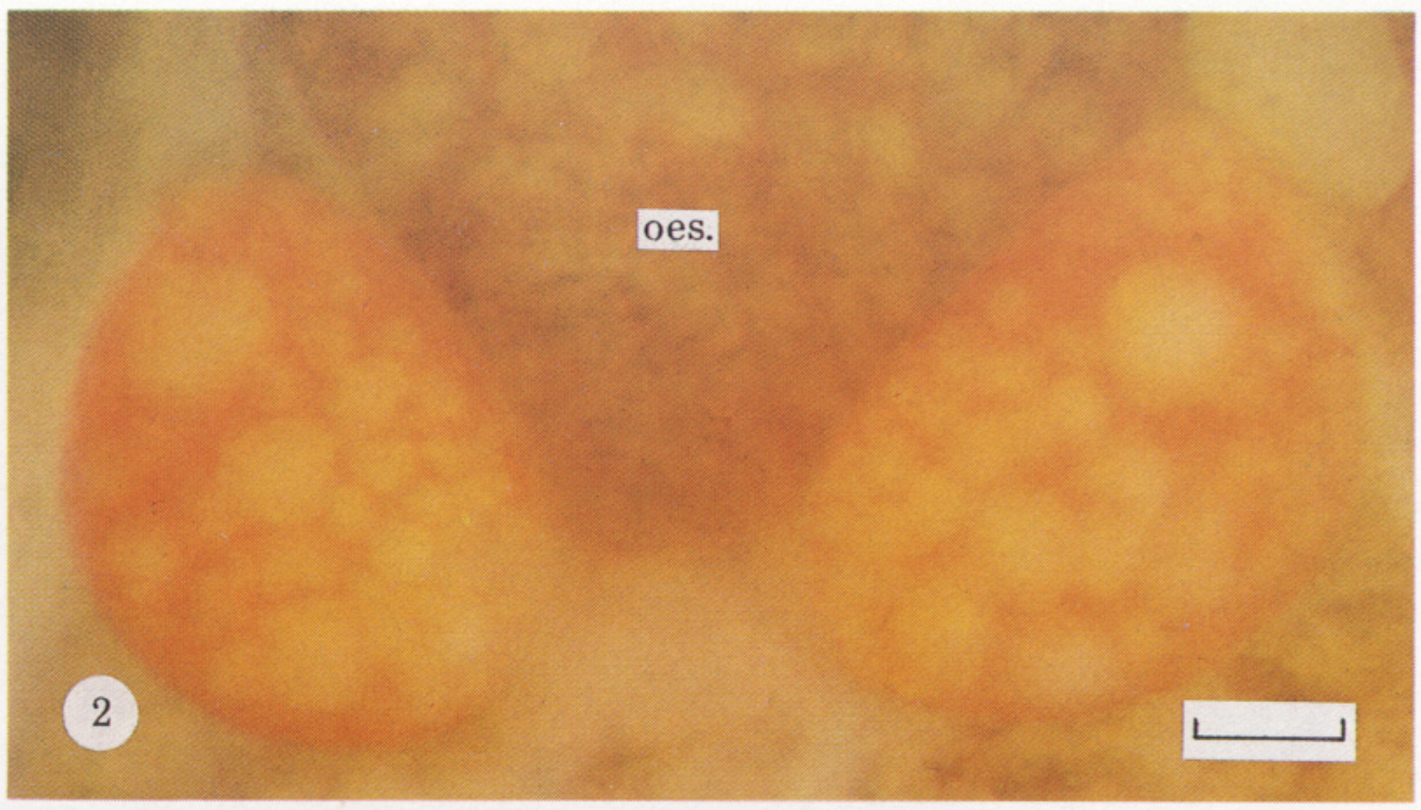


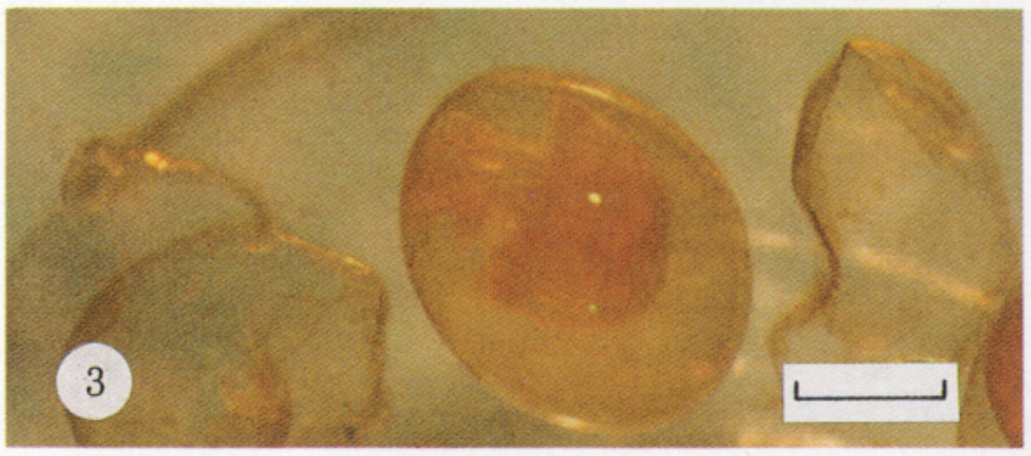

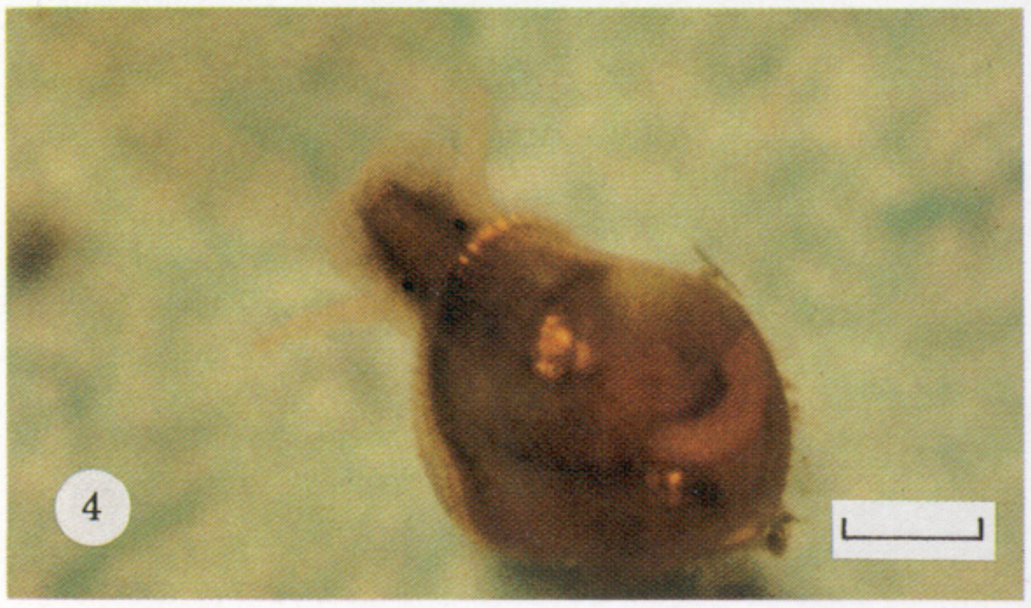


FIGURES 1–6. For description see opposite.

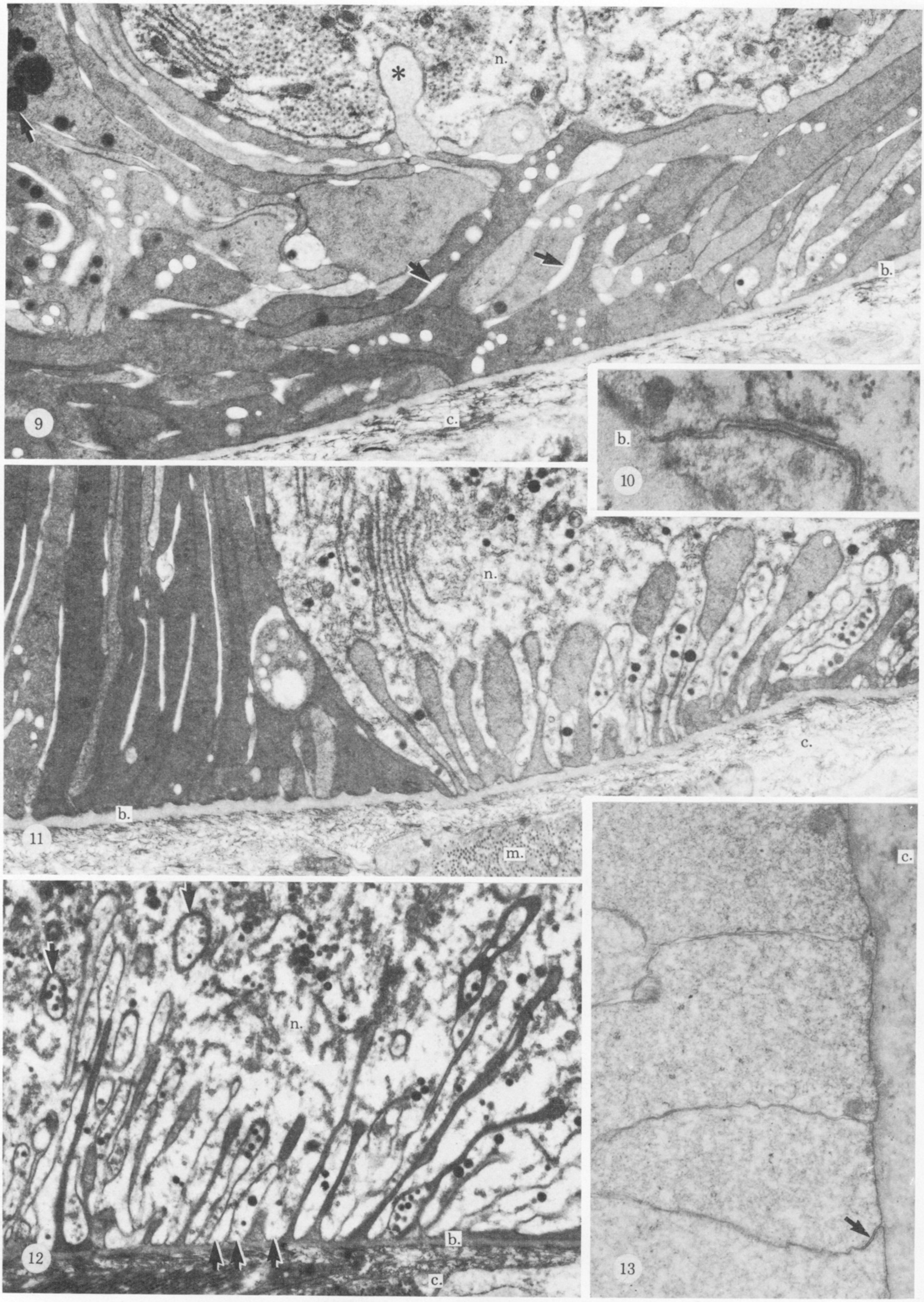


FIGURES 9–13. For description see p. 410.

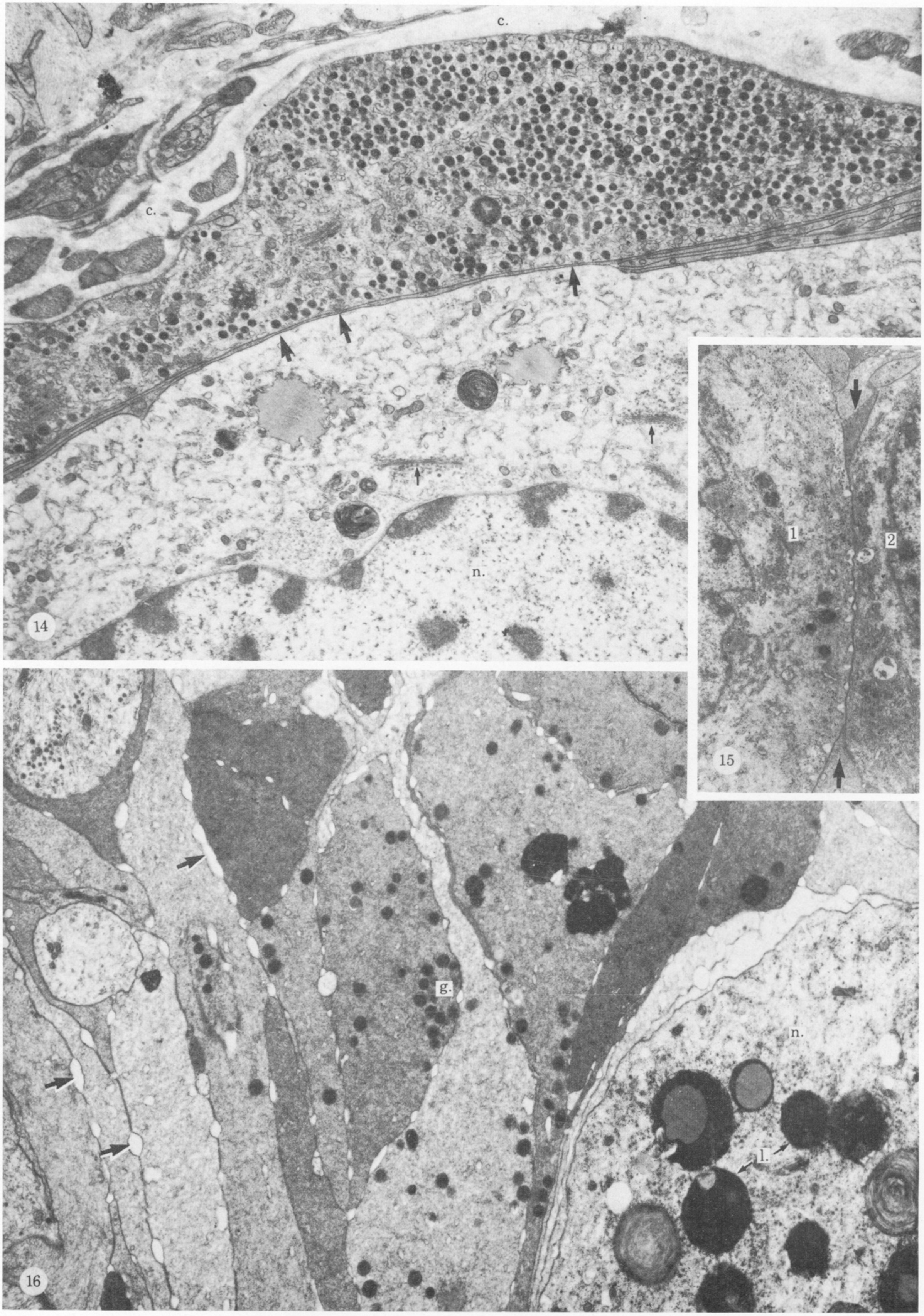


FIGURES 14–16. For description see p. 411.

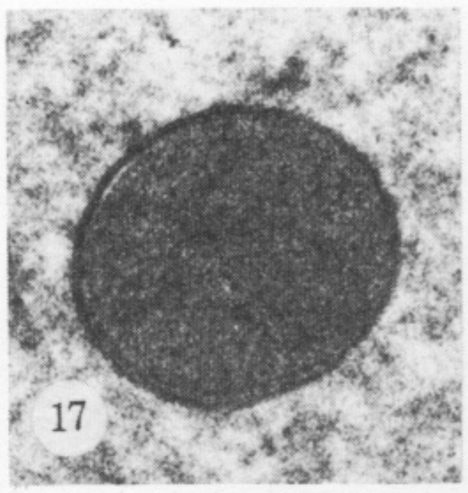






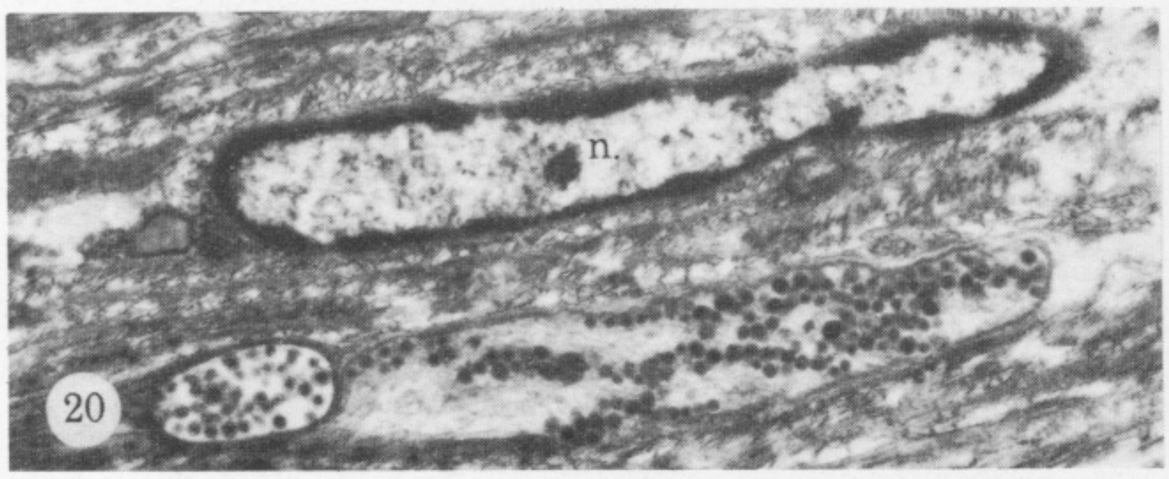


FIGURES 17–21. For description see opposite.

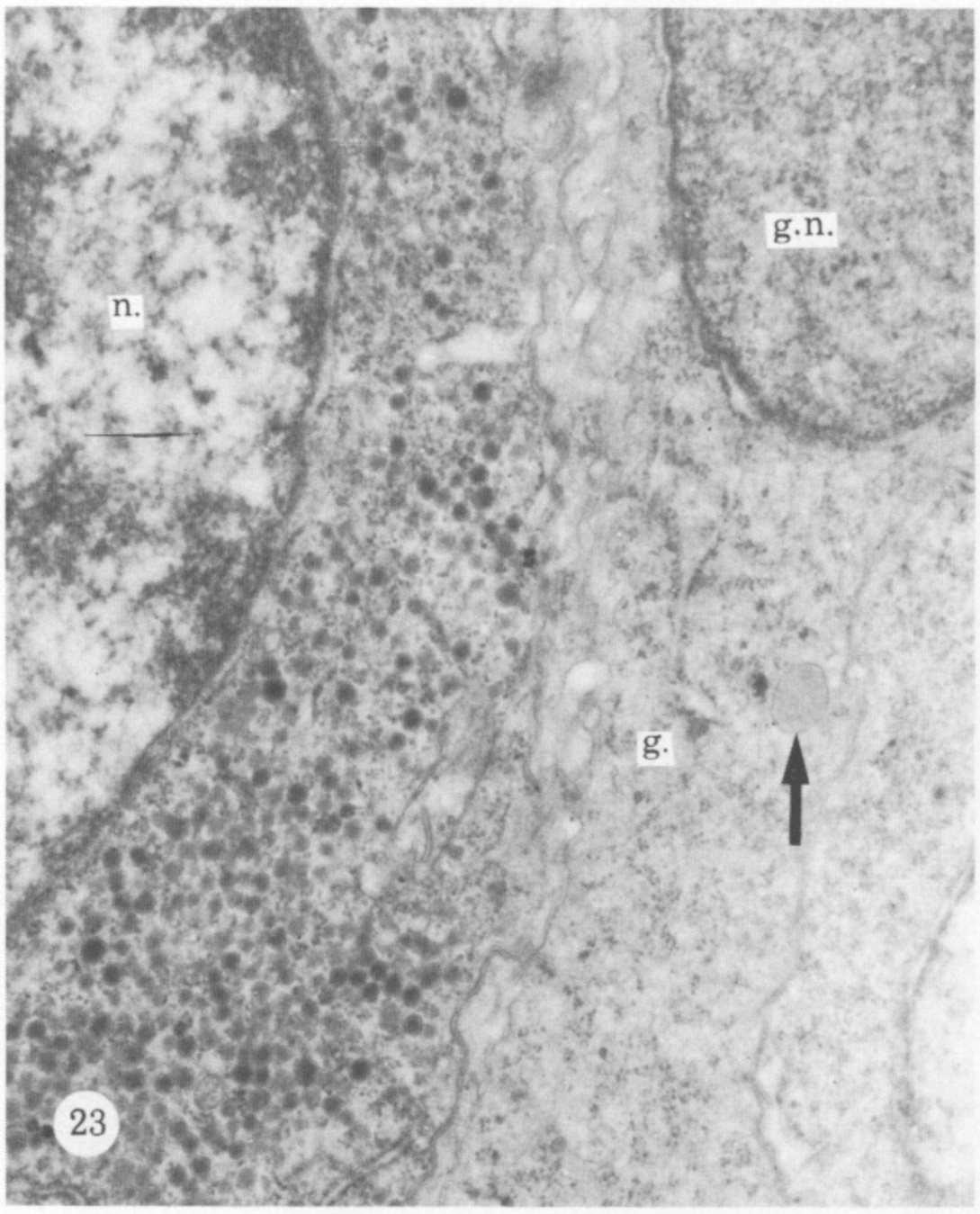


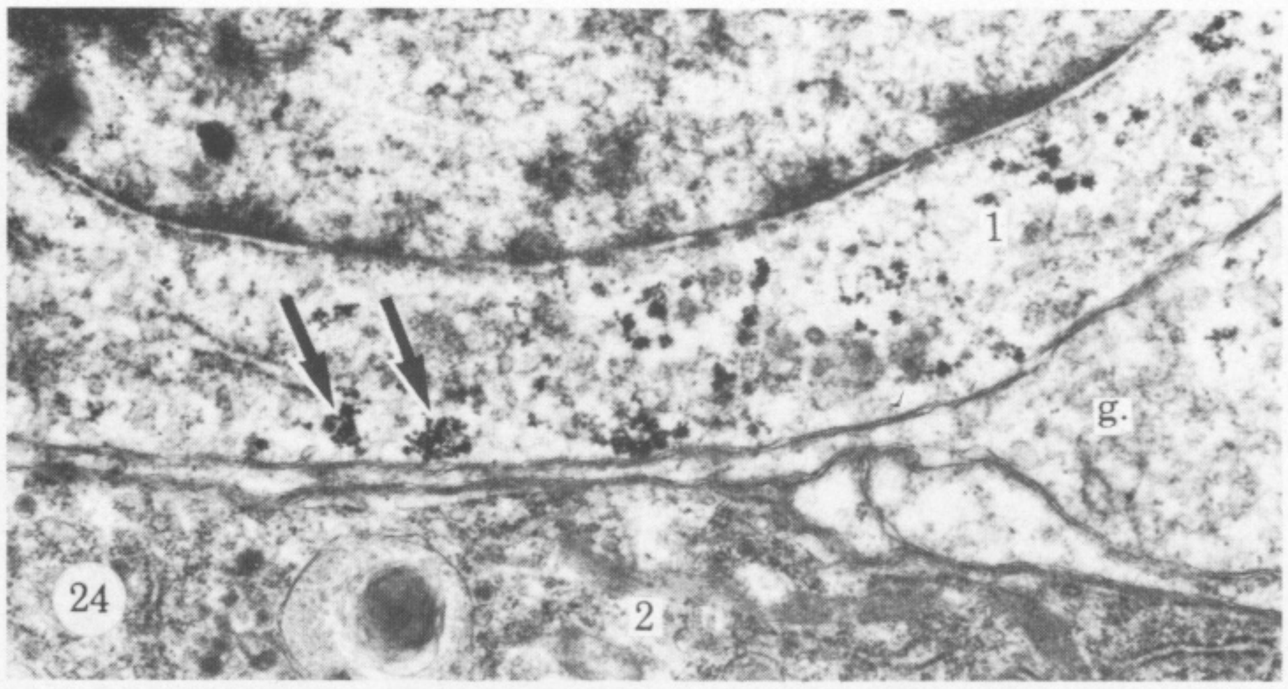


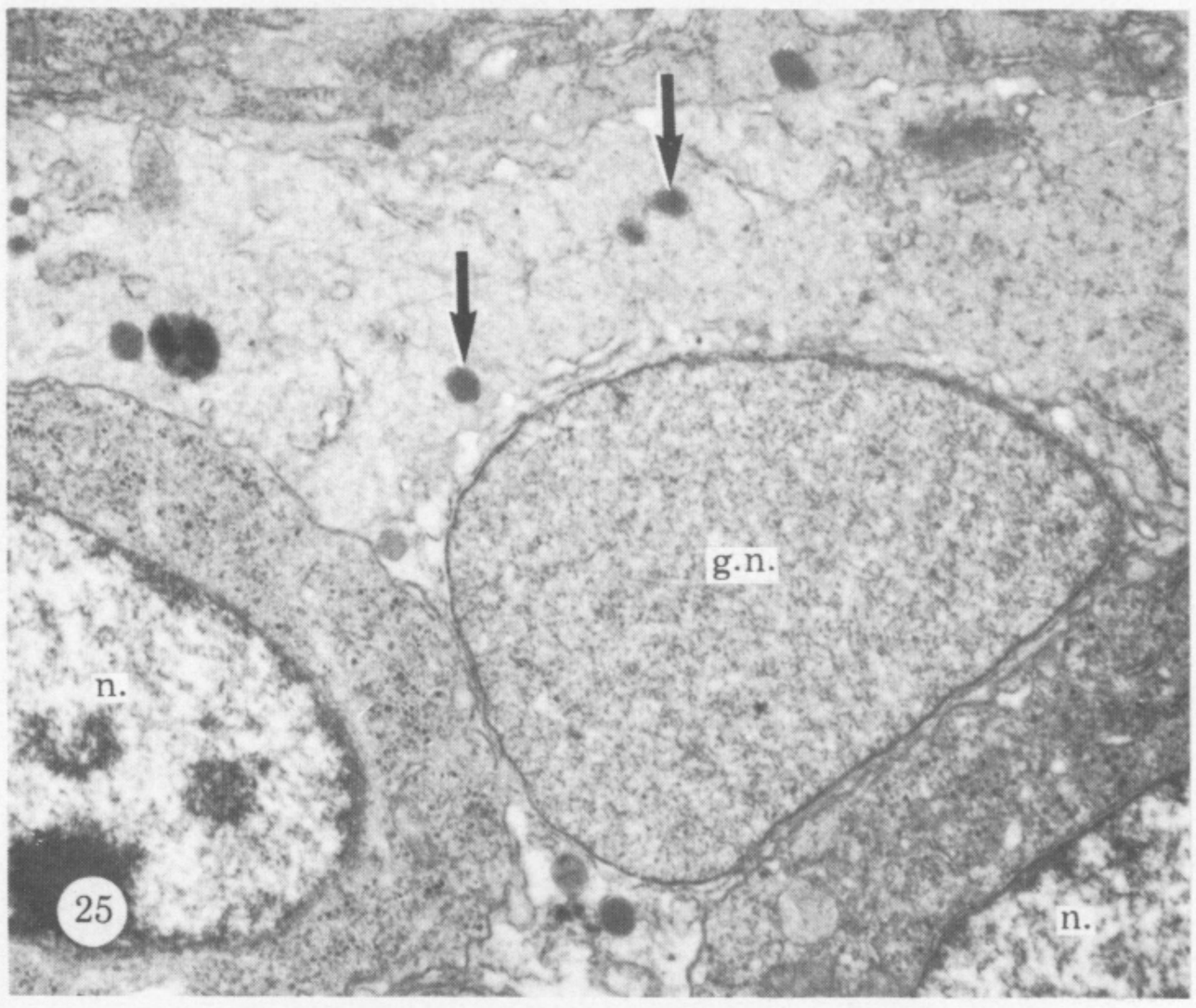


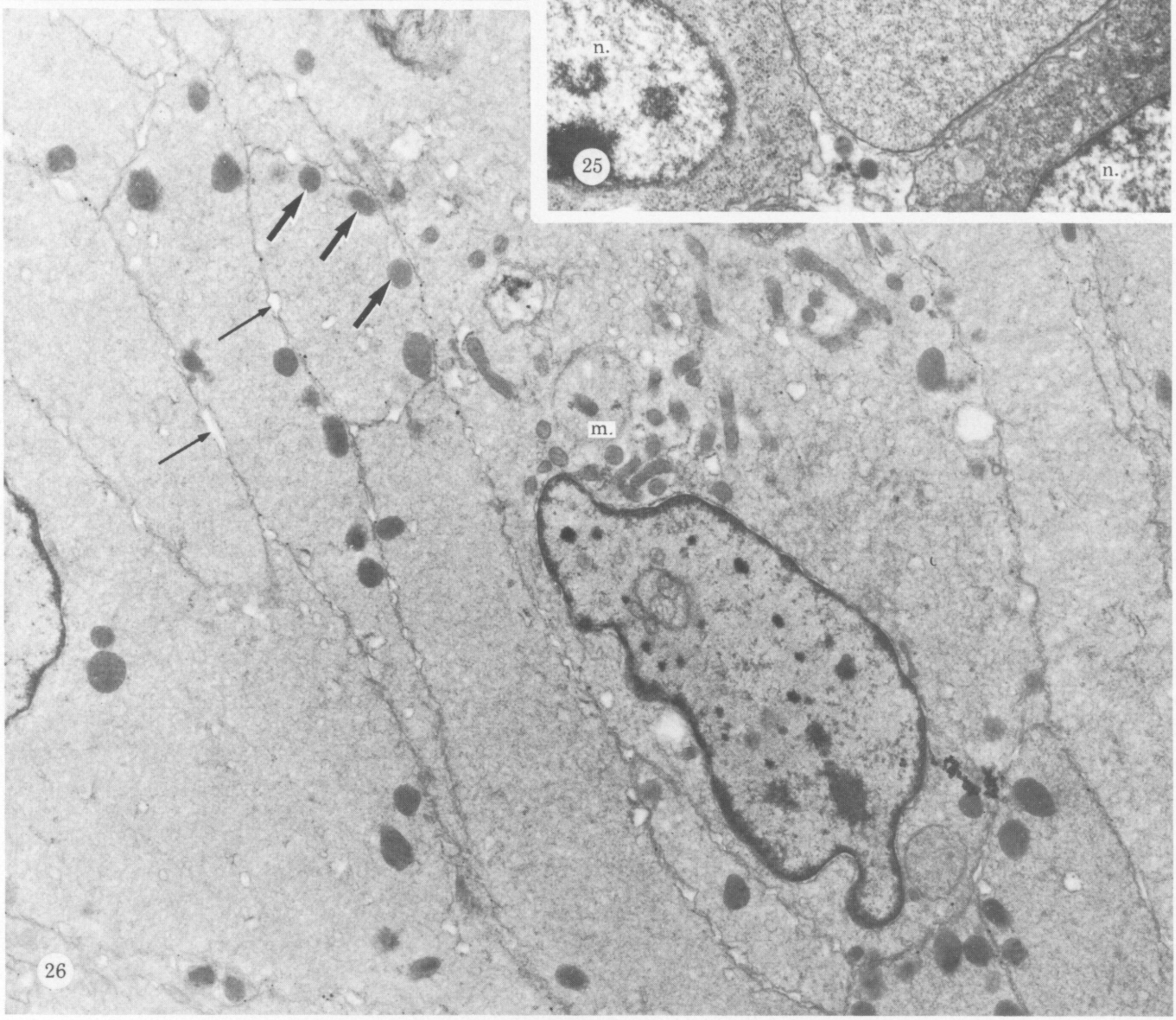


FIGURES 23–26. For description see opposite.

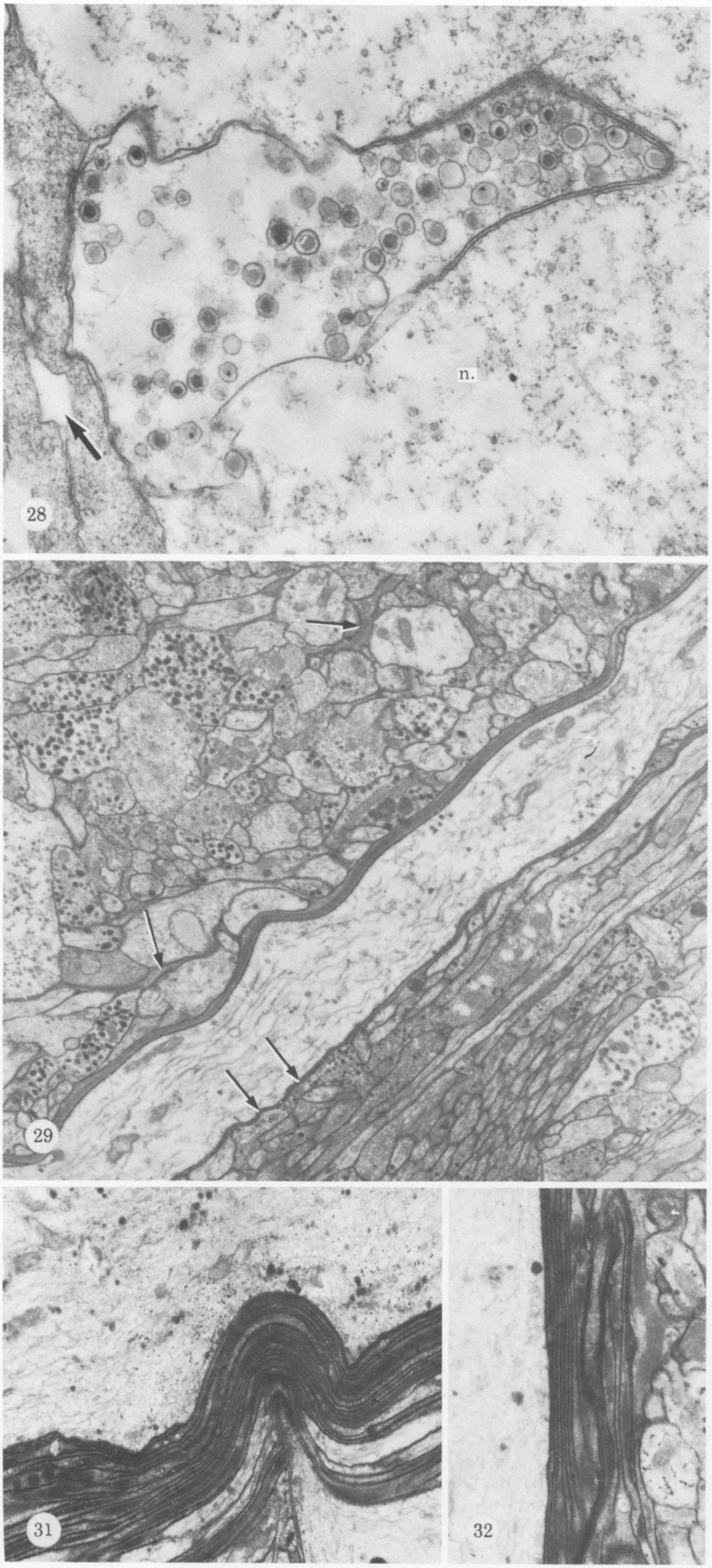


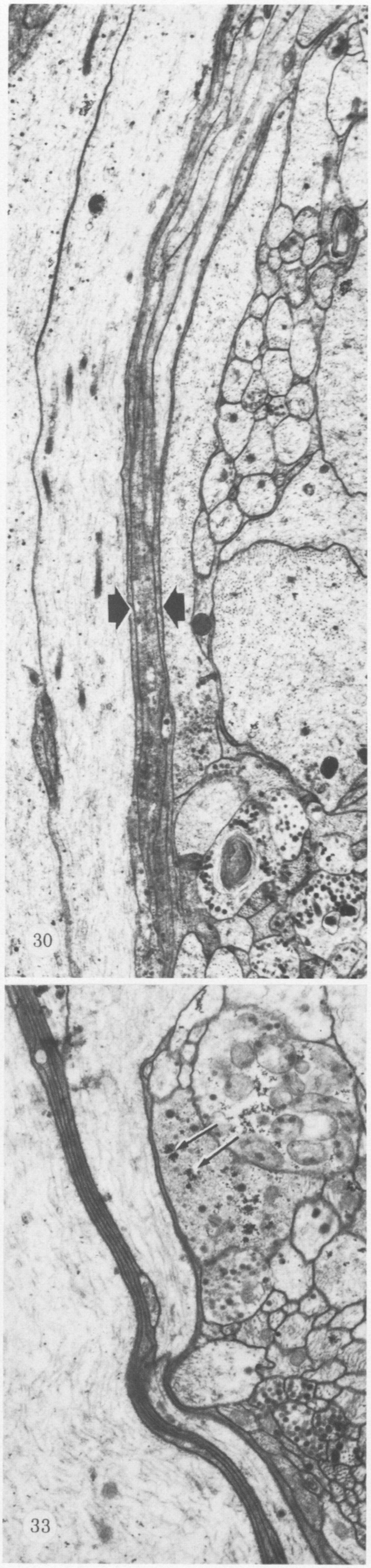











FIGURES 28–33. For description see p. 418.

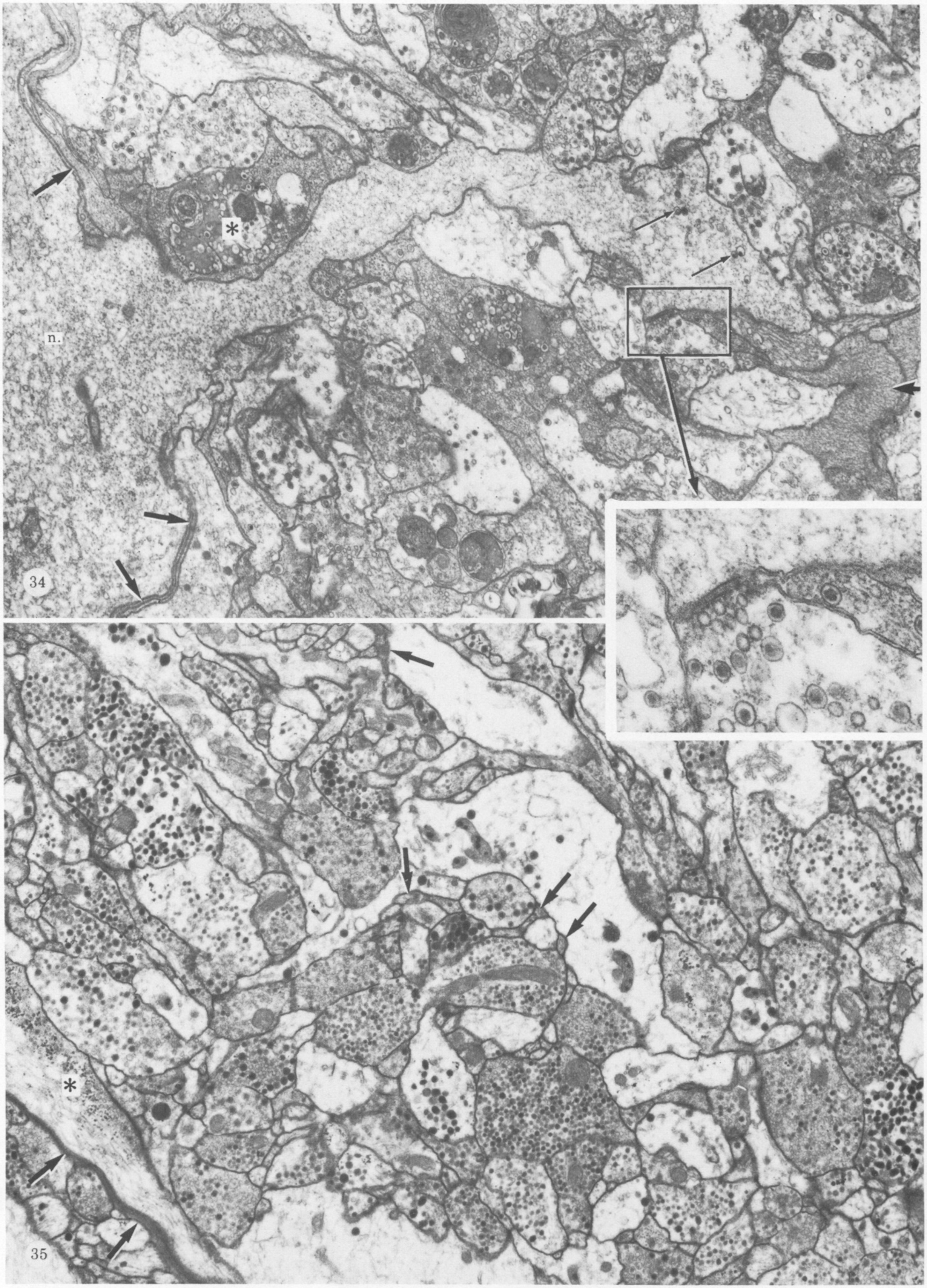


FIGURES 34 AND 35. For description see opposite plate 8.

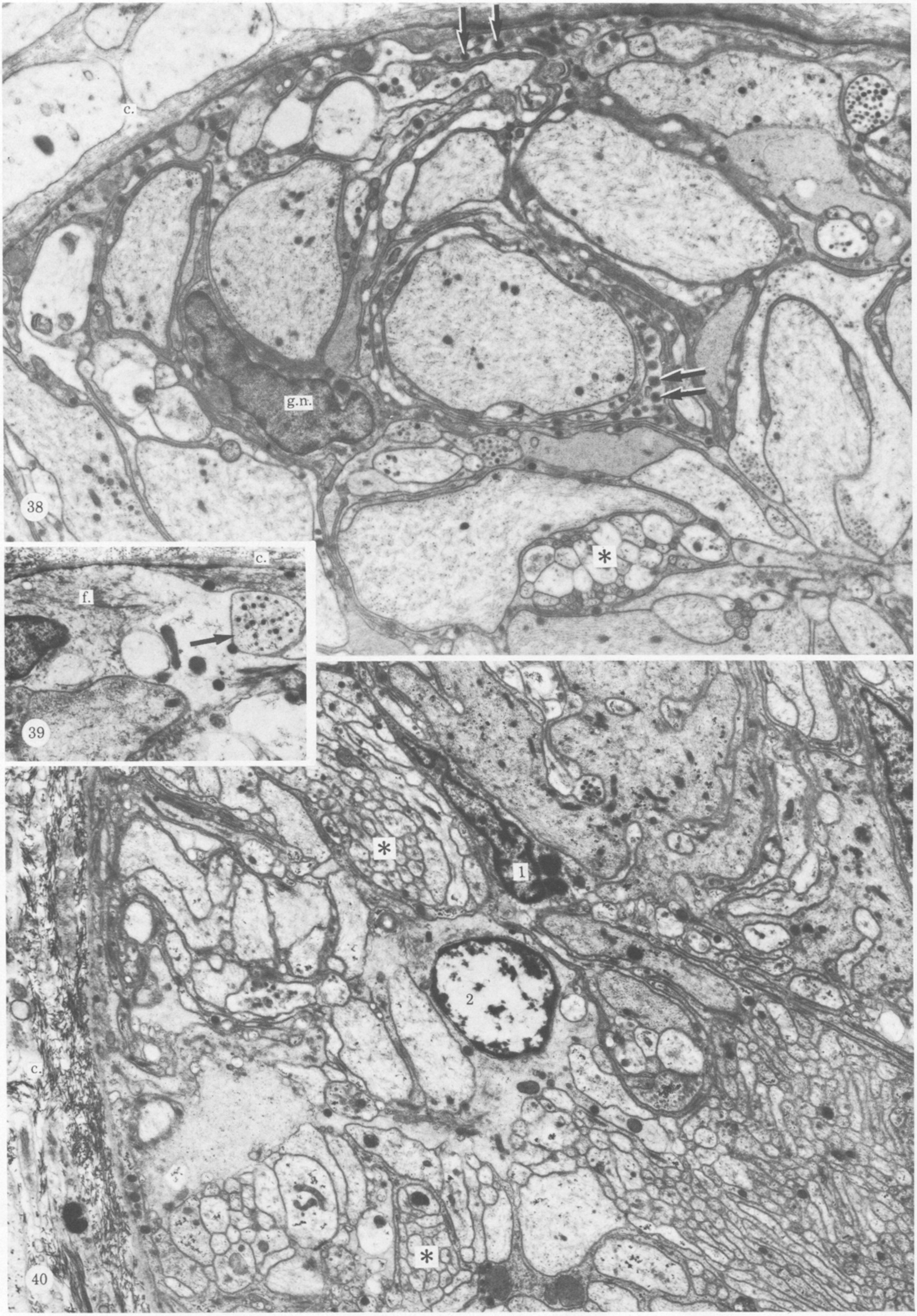


FIGURES 38–40. For description see opposite.

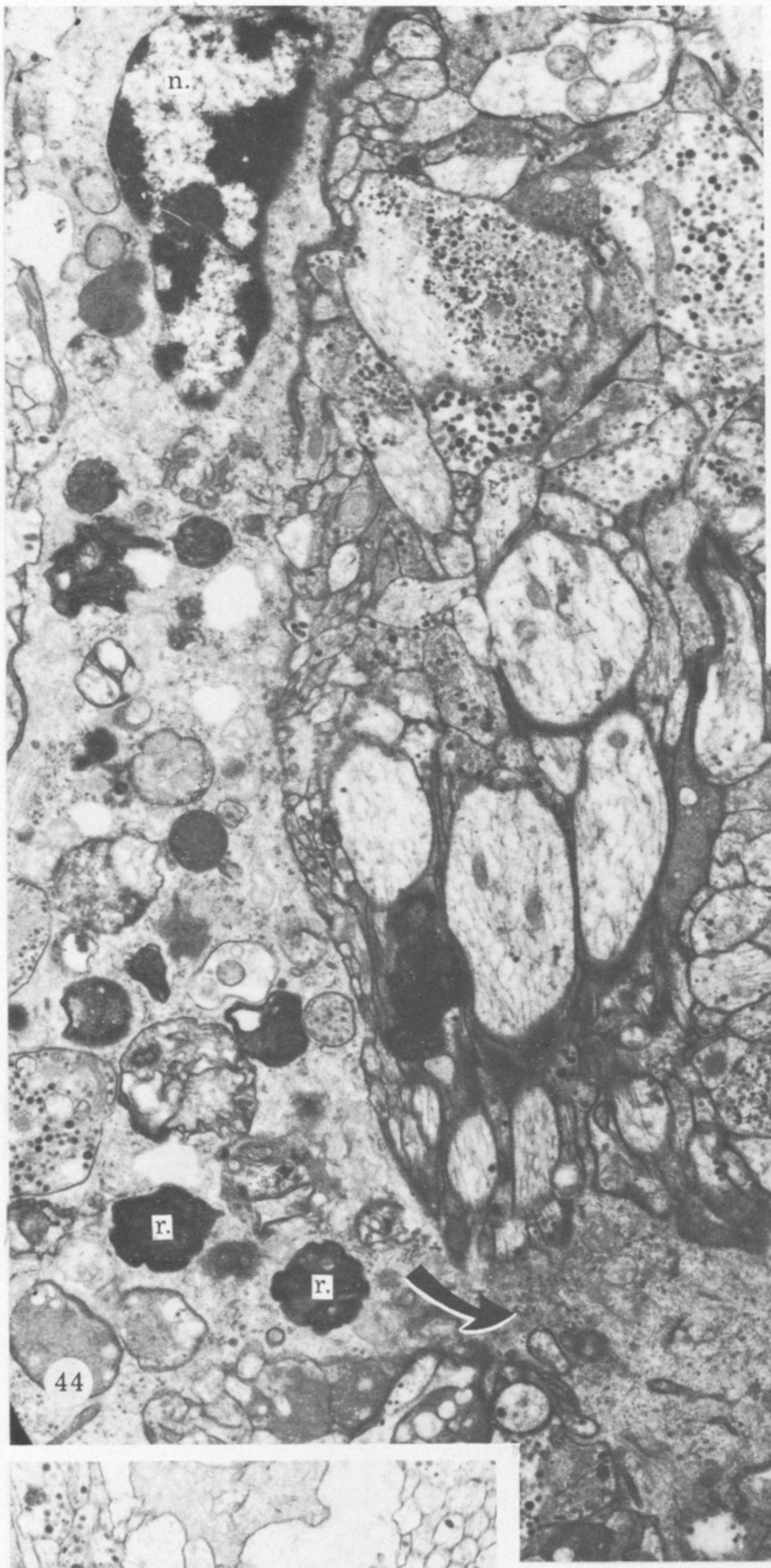


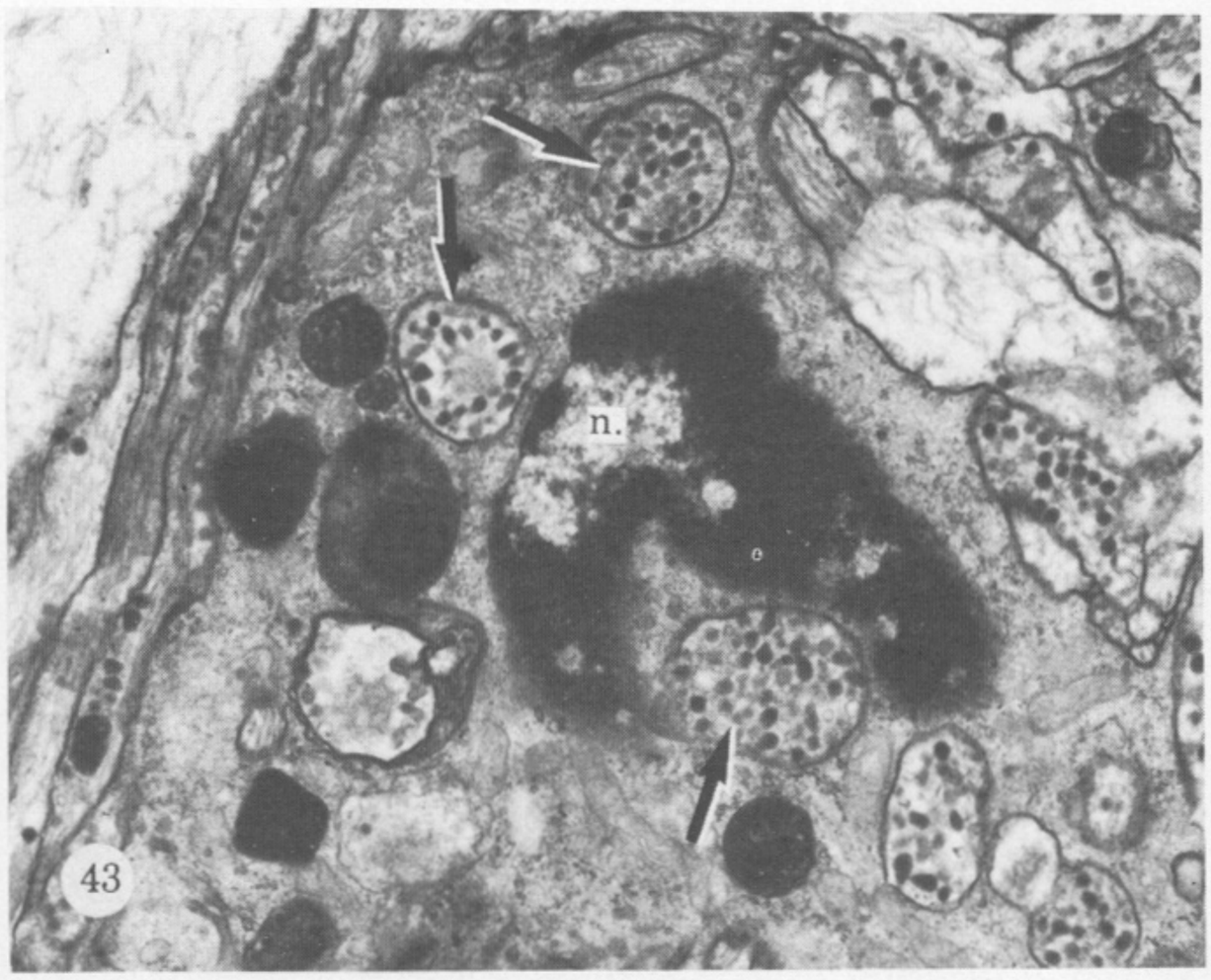






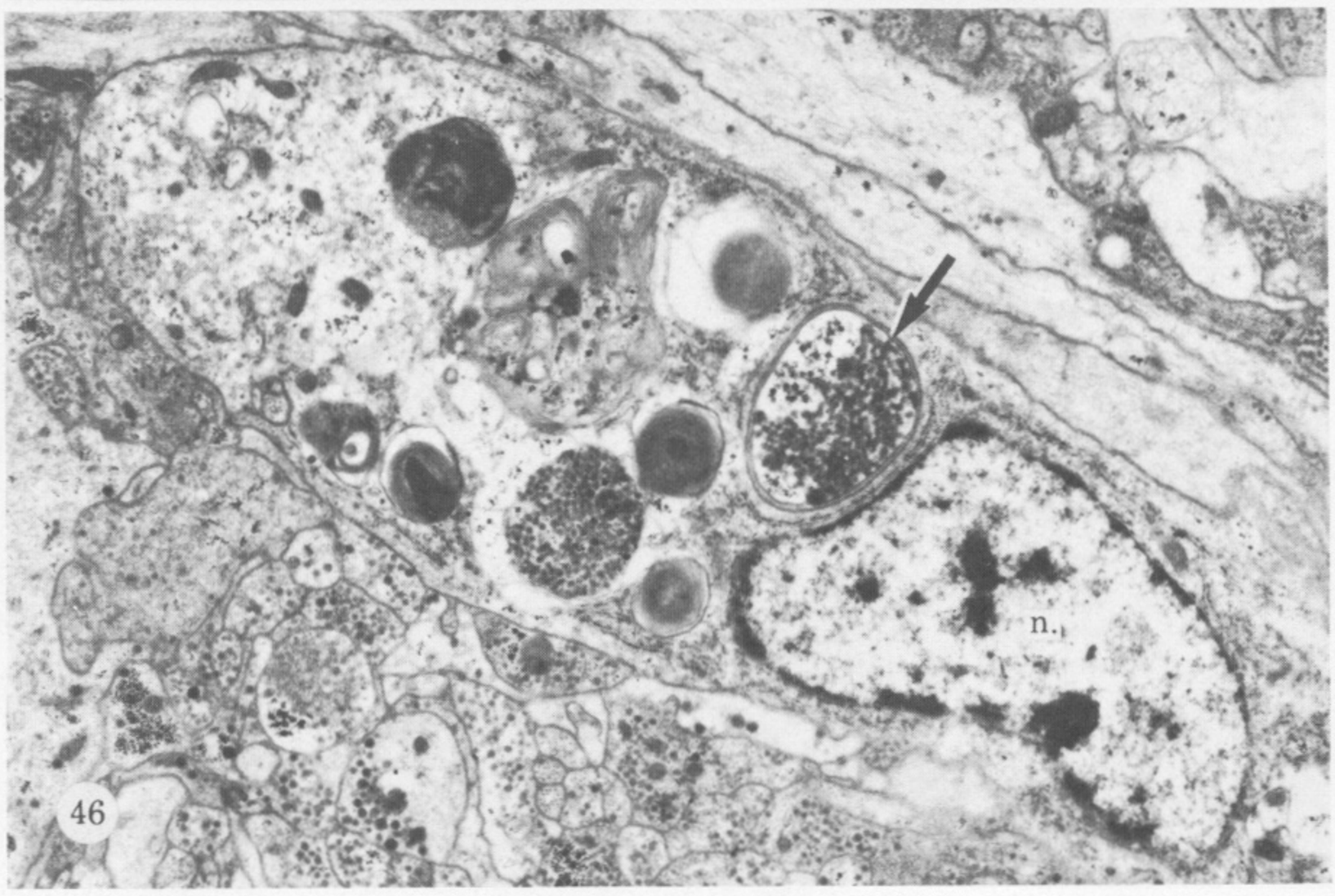


FIGURES 43–46. For description see opposite plate 8.

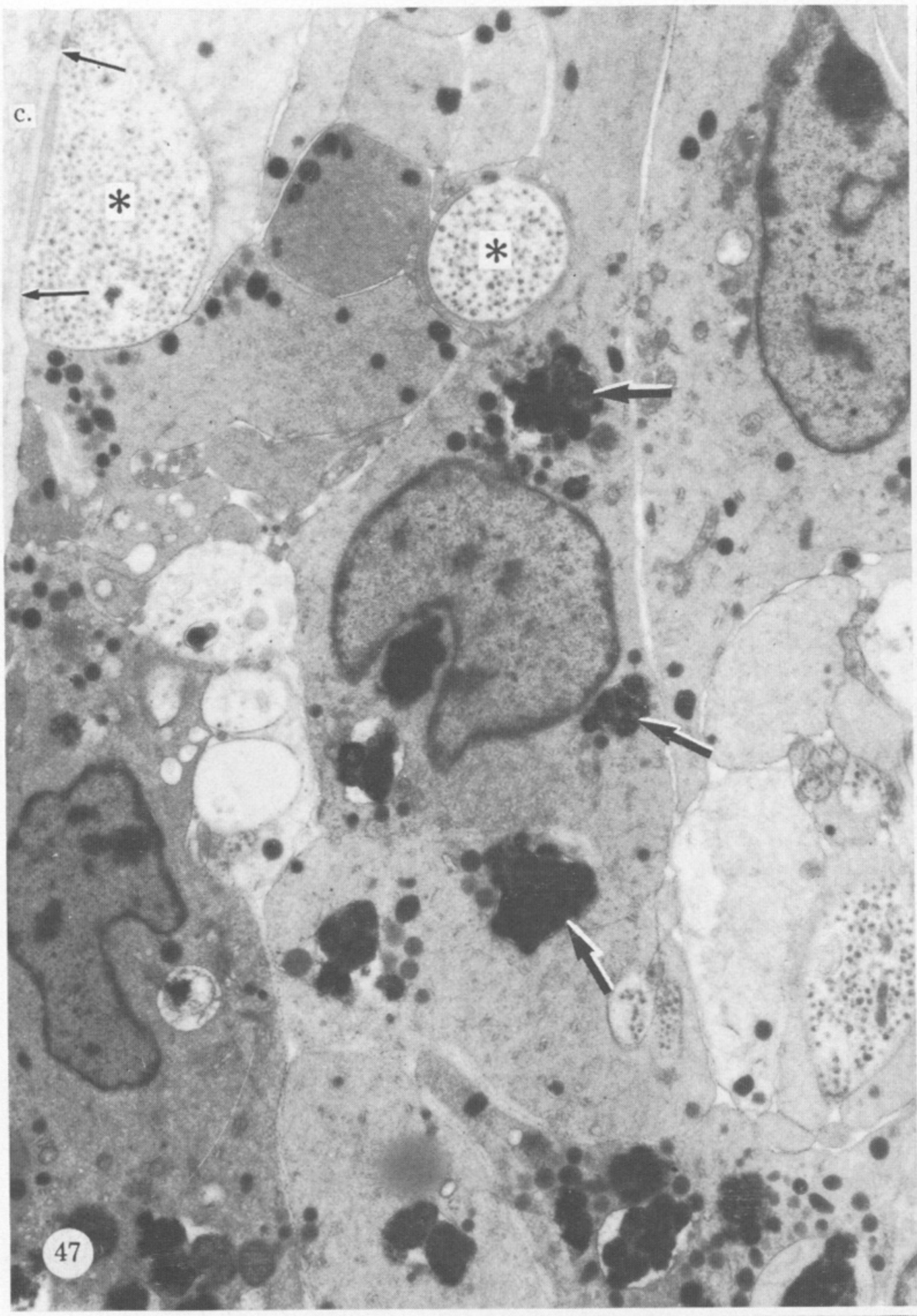


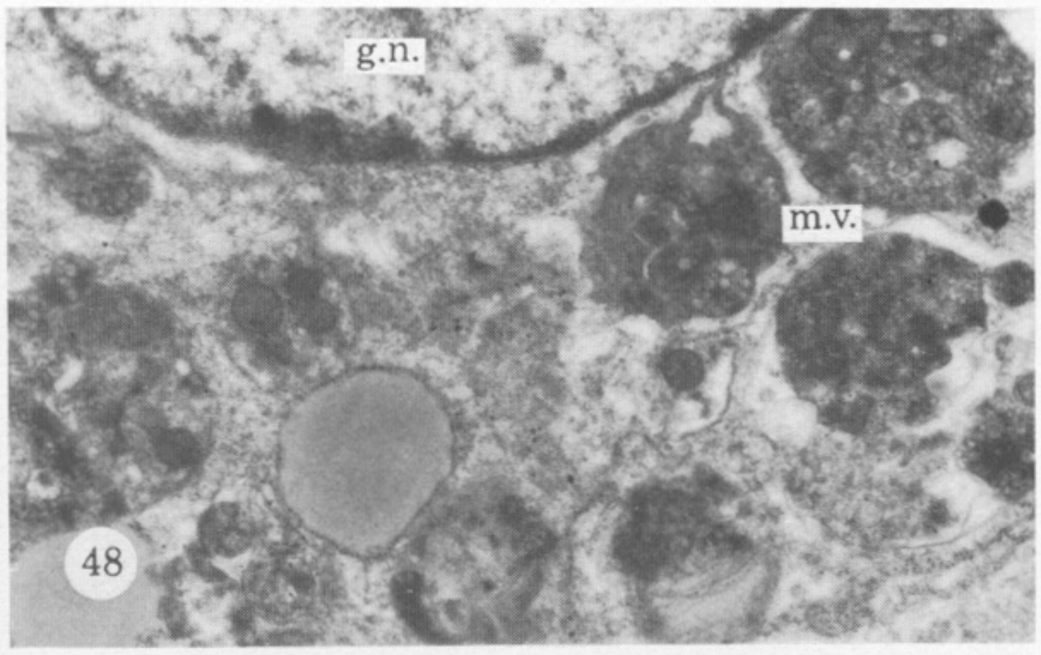


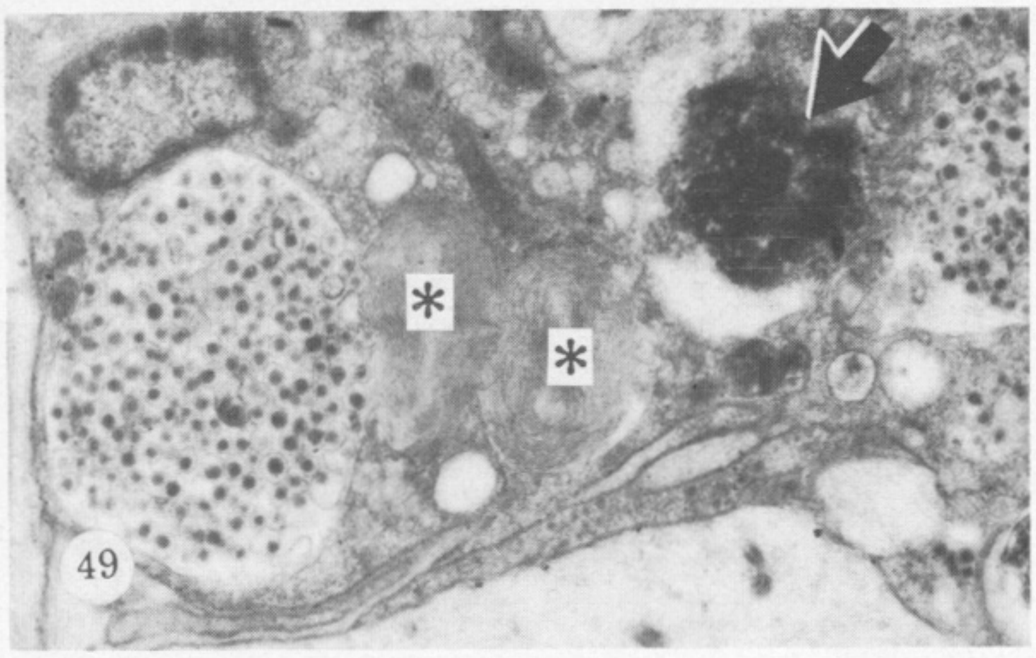




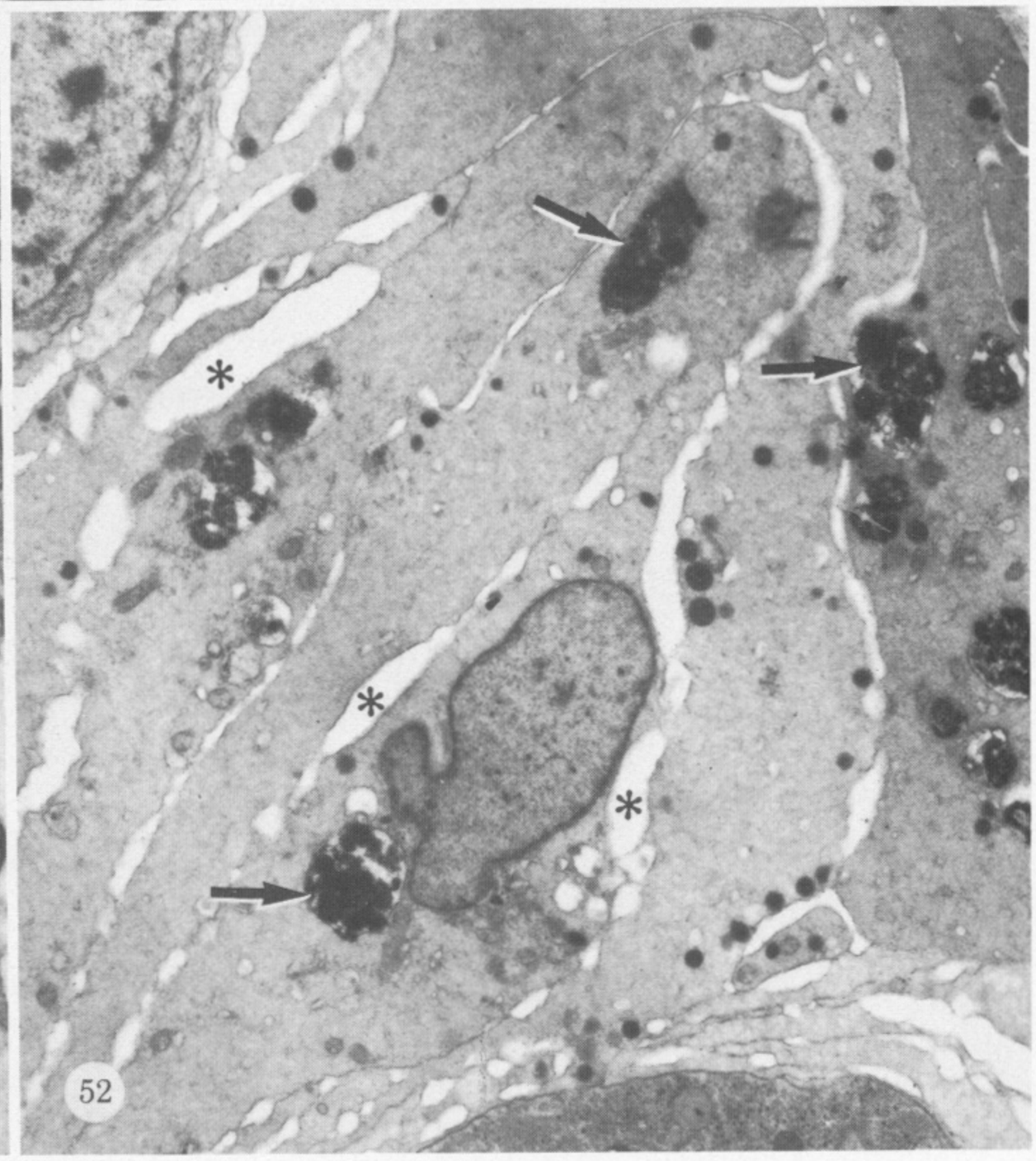


FIGURES 47–52. For description see p. 419.

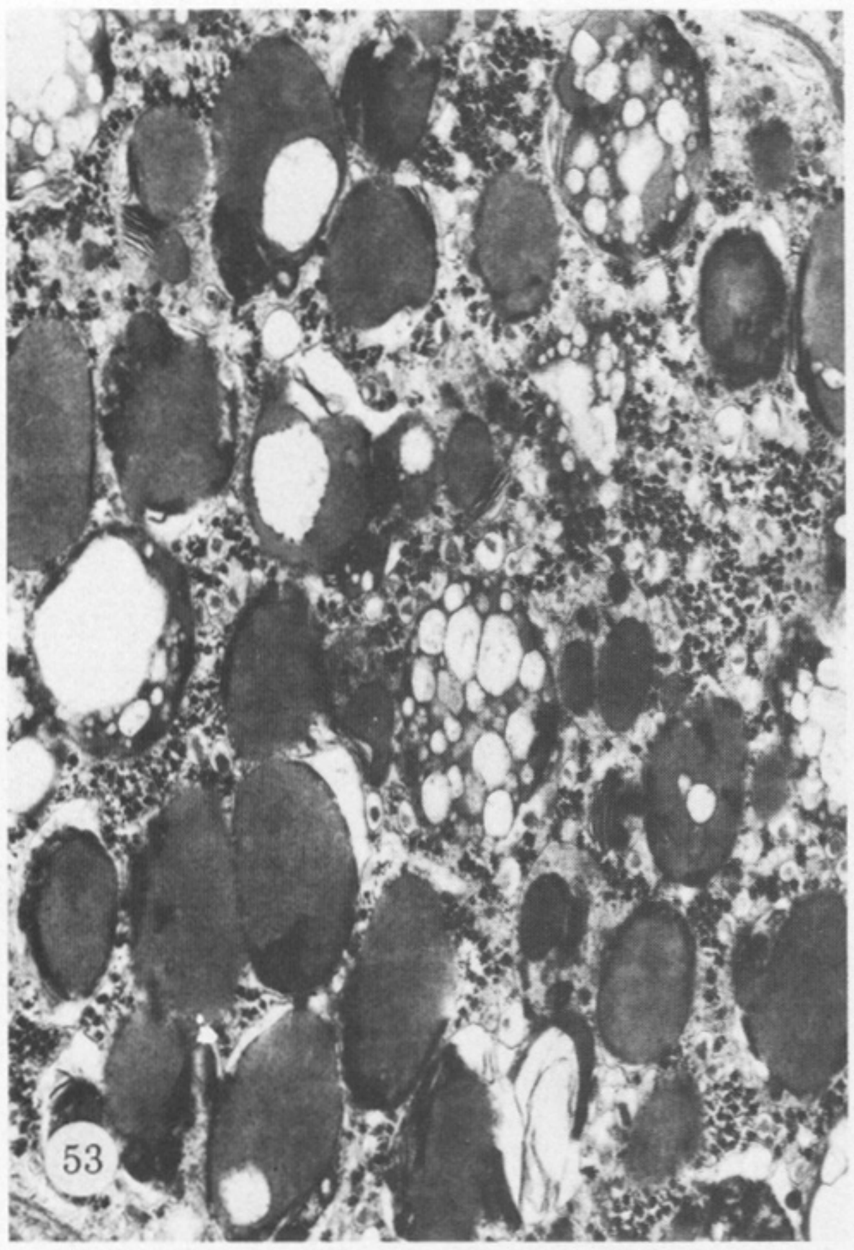
53


54

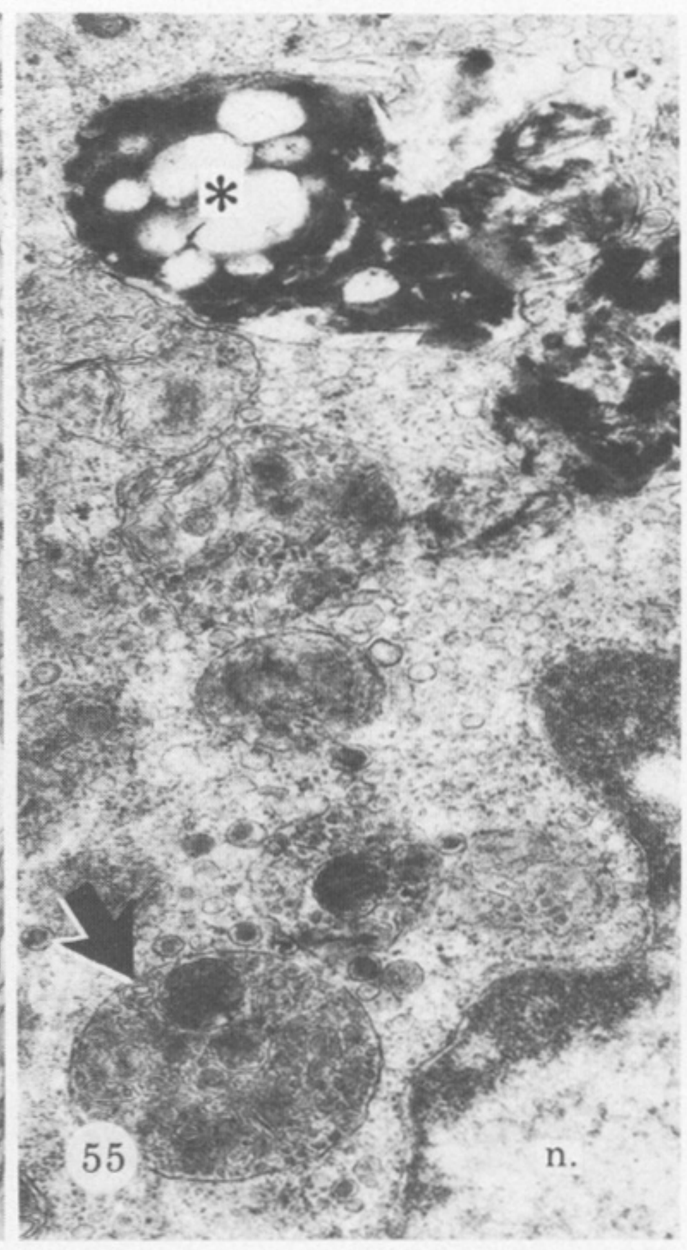

55

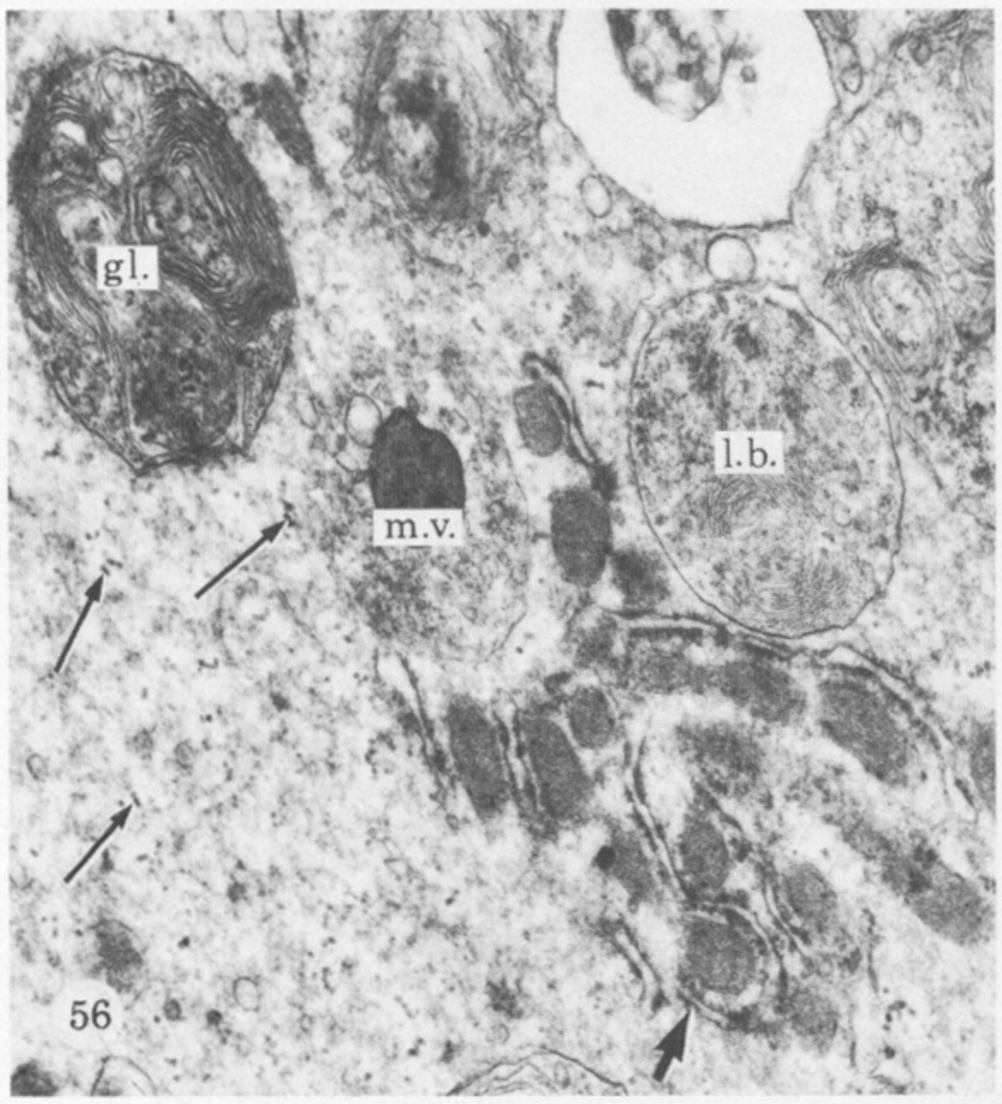

56

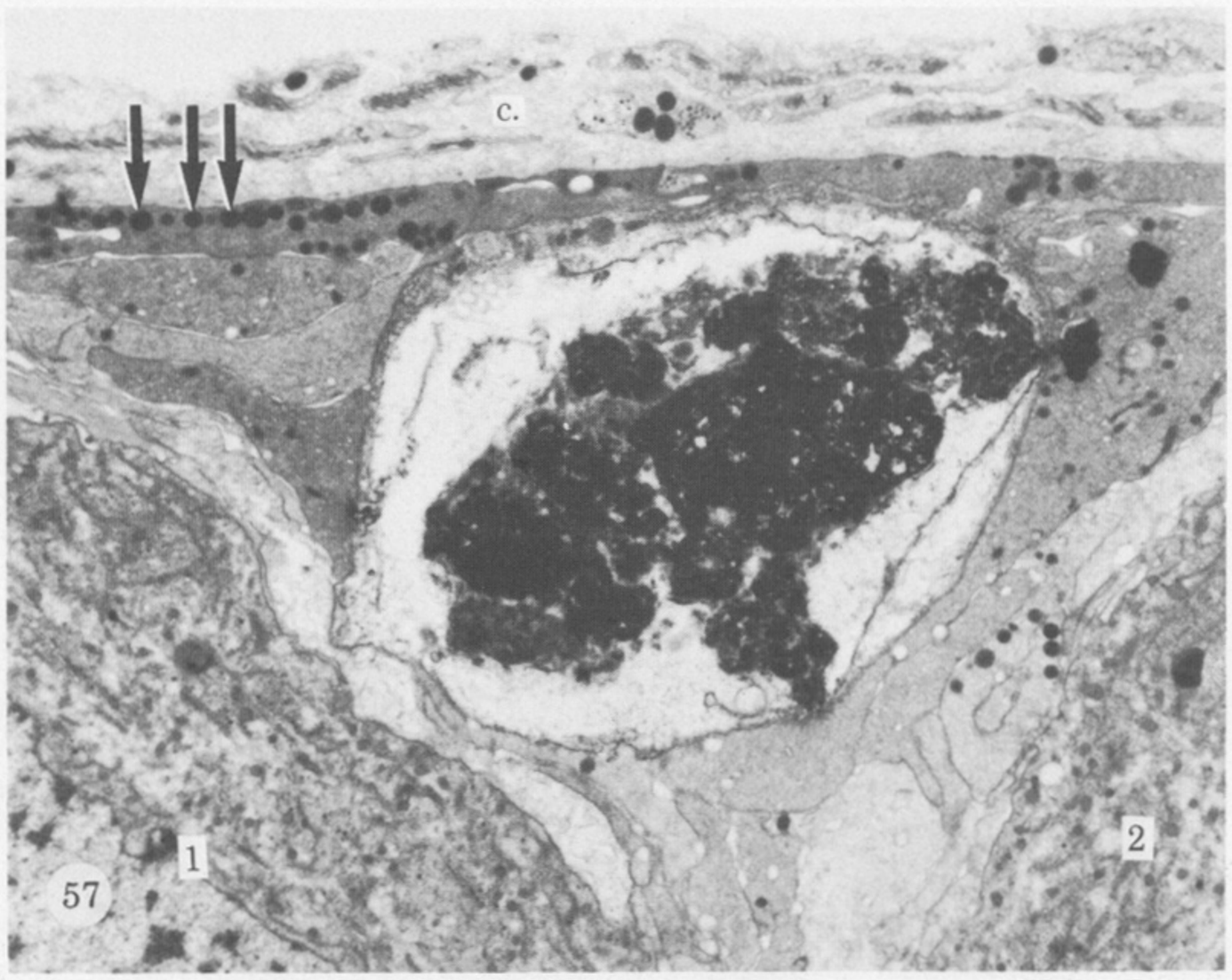

57

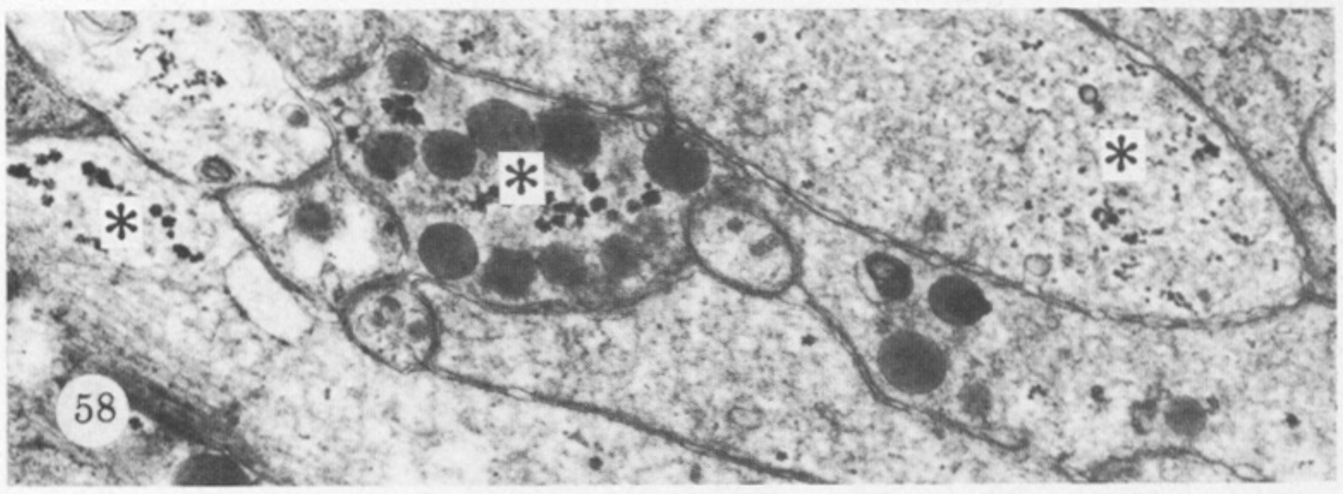

58

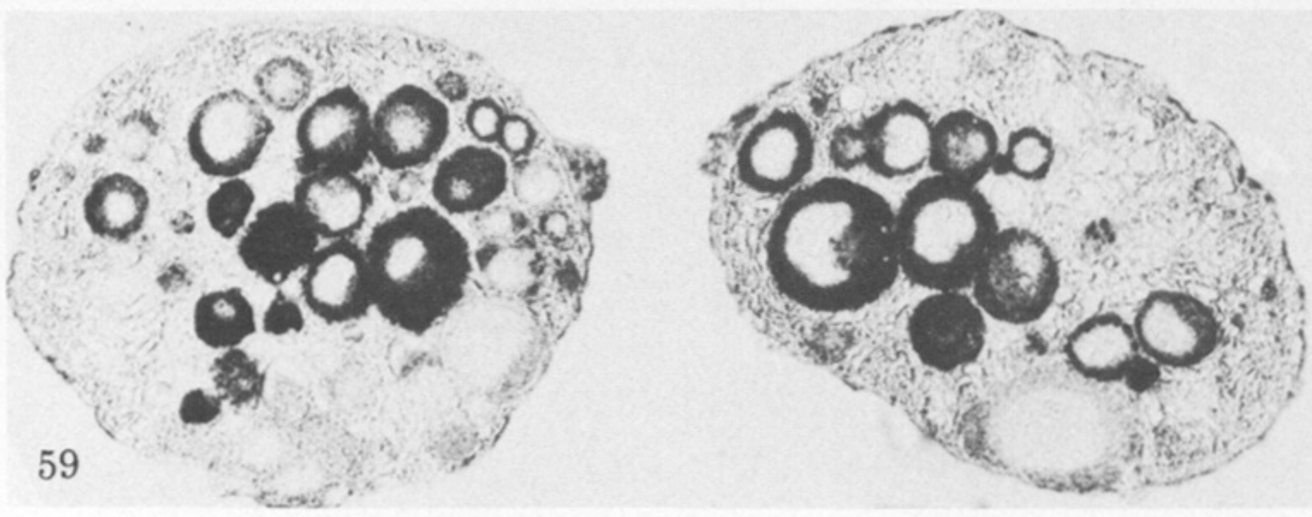
59

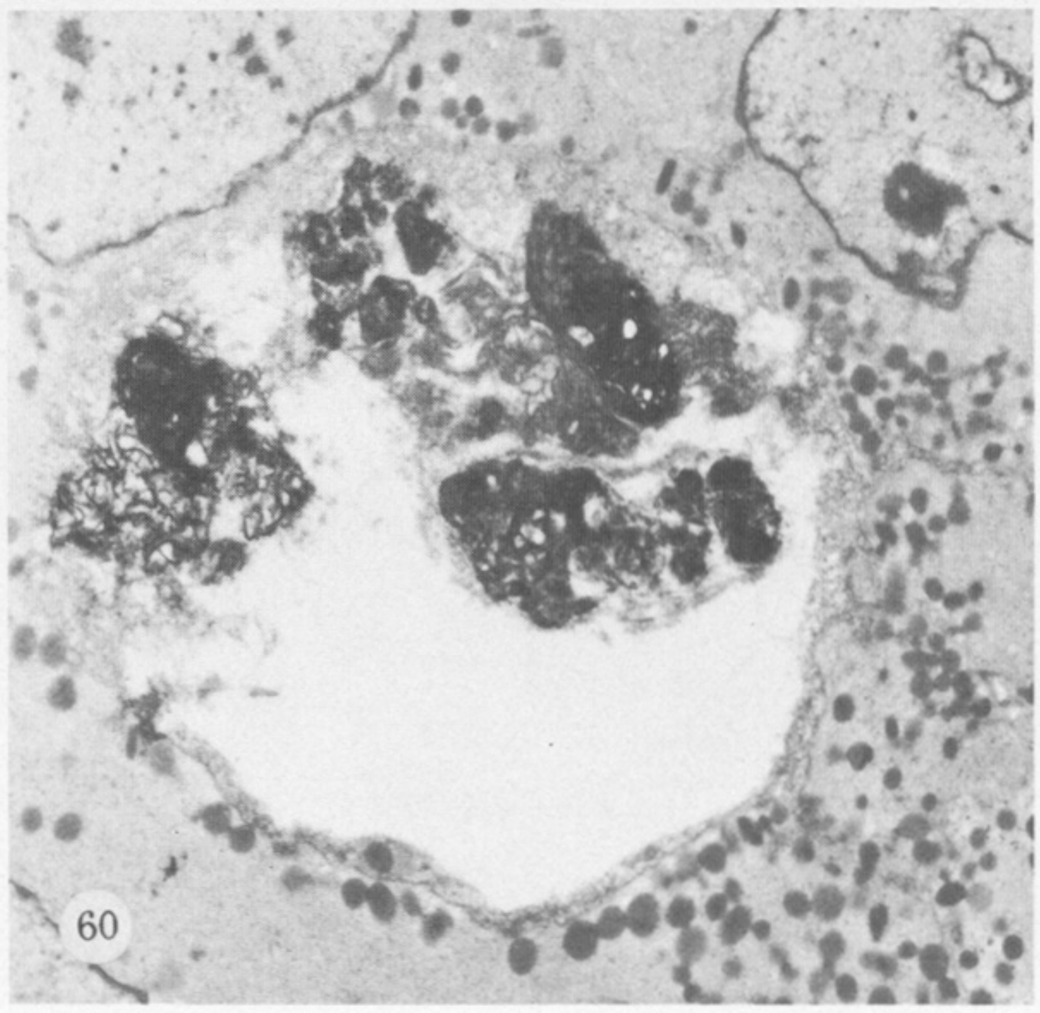
60

FIGURES 53–60. For description see opposite.

61

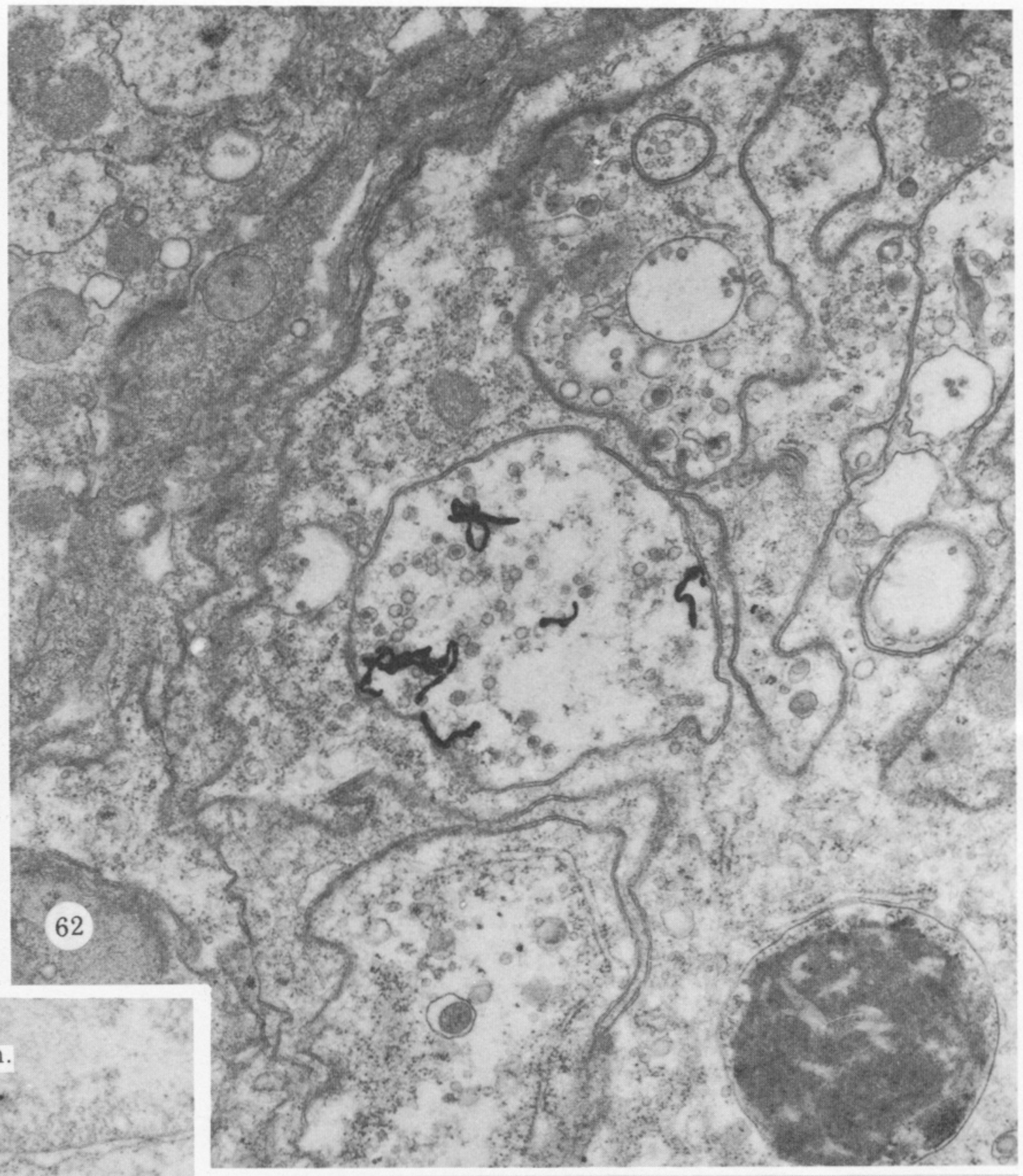

62

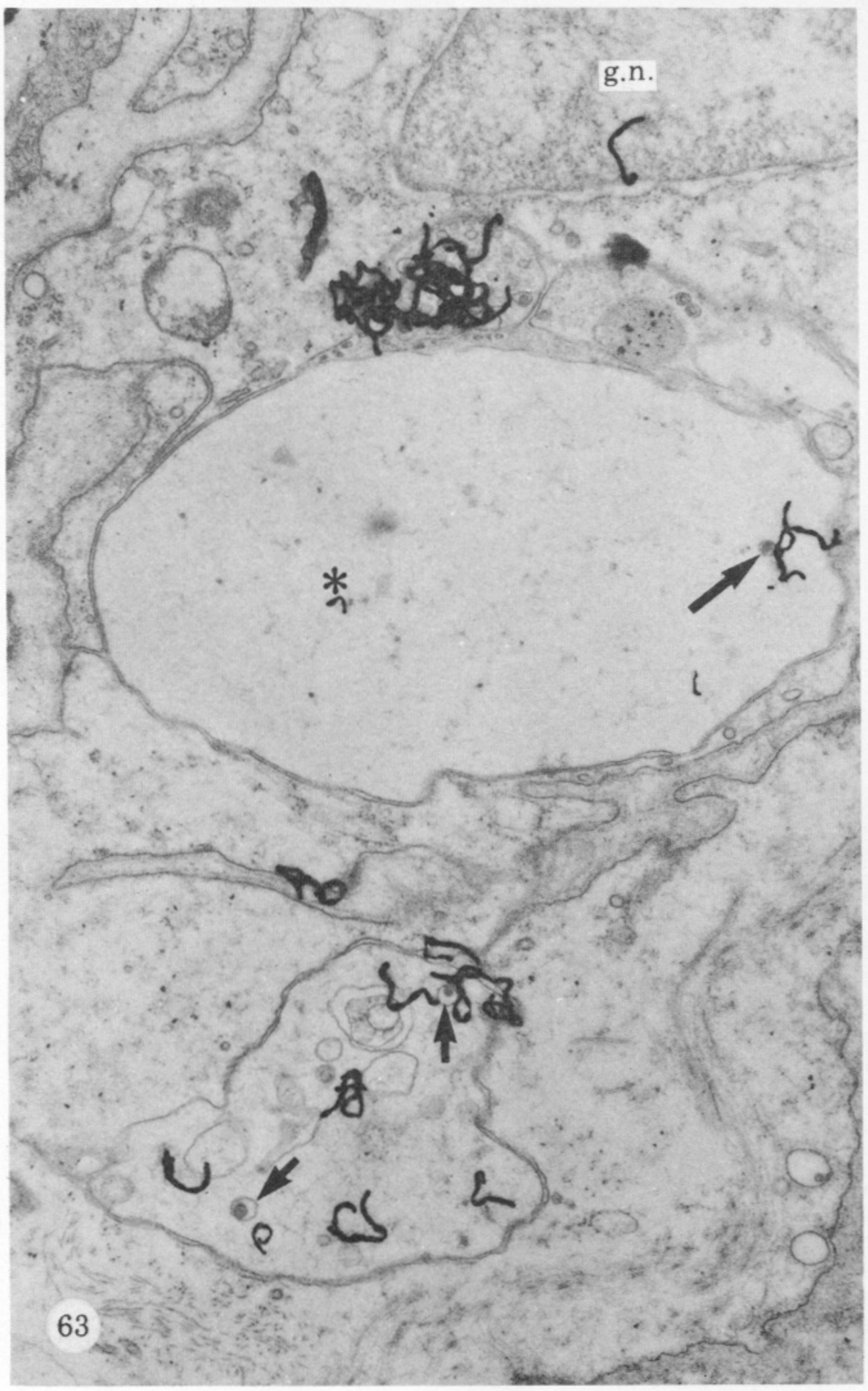


63

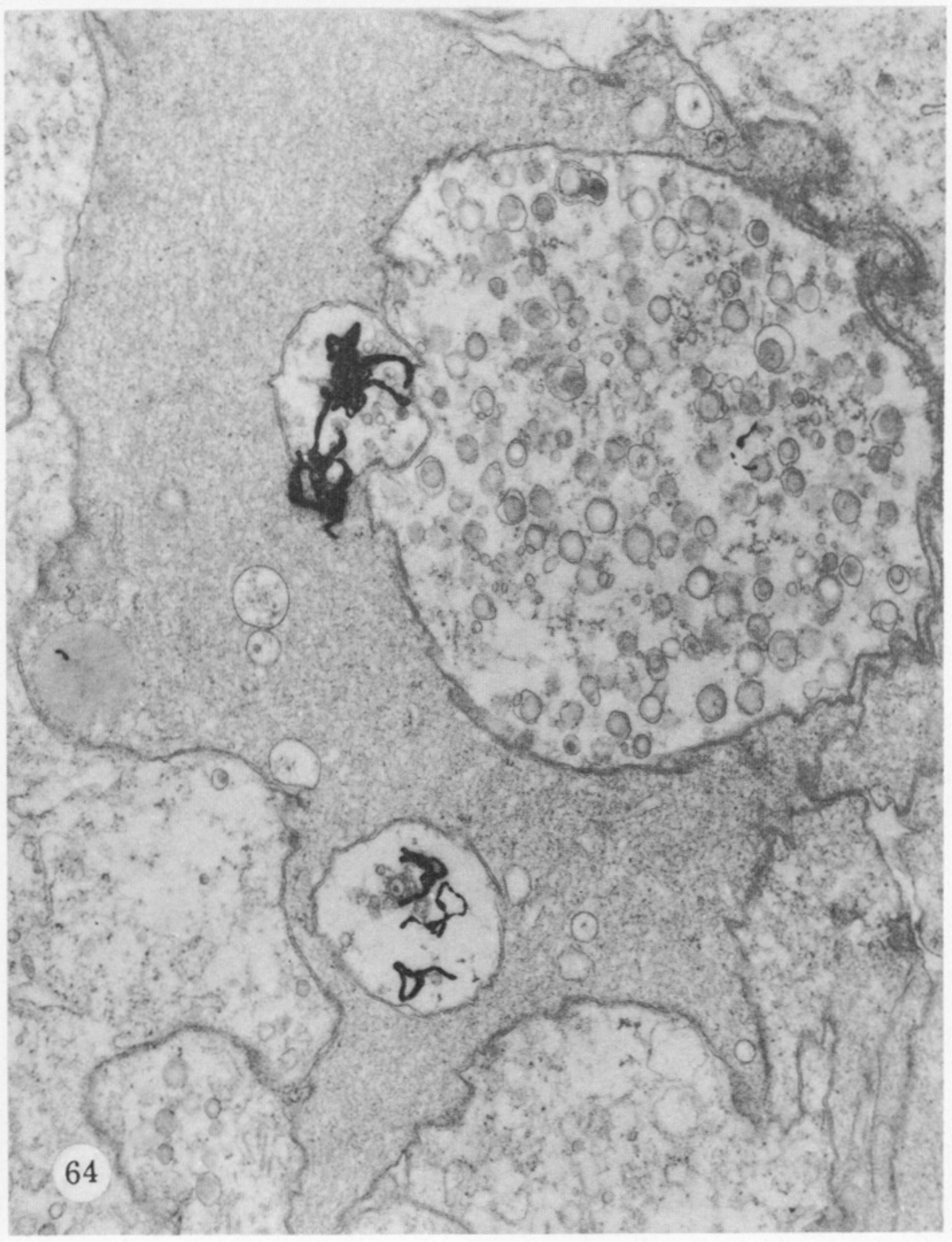

64

FIGURES 61–64. For description see opposite.

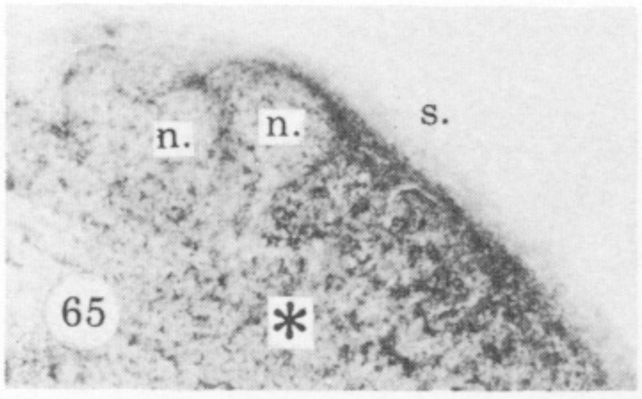


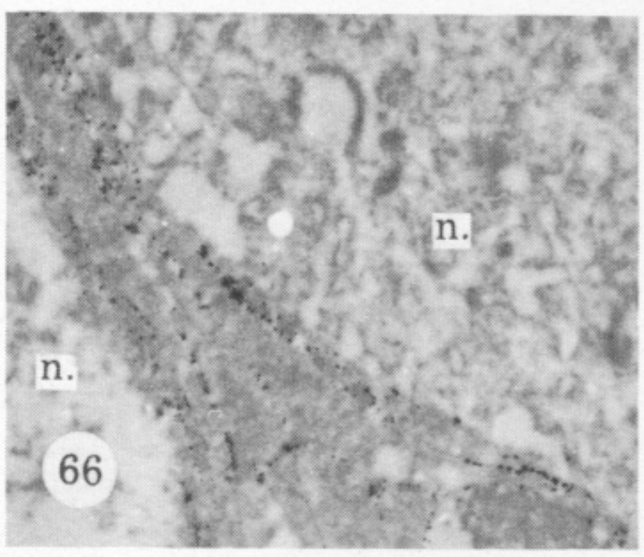


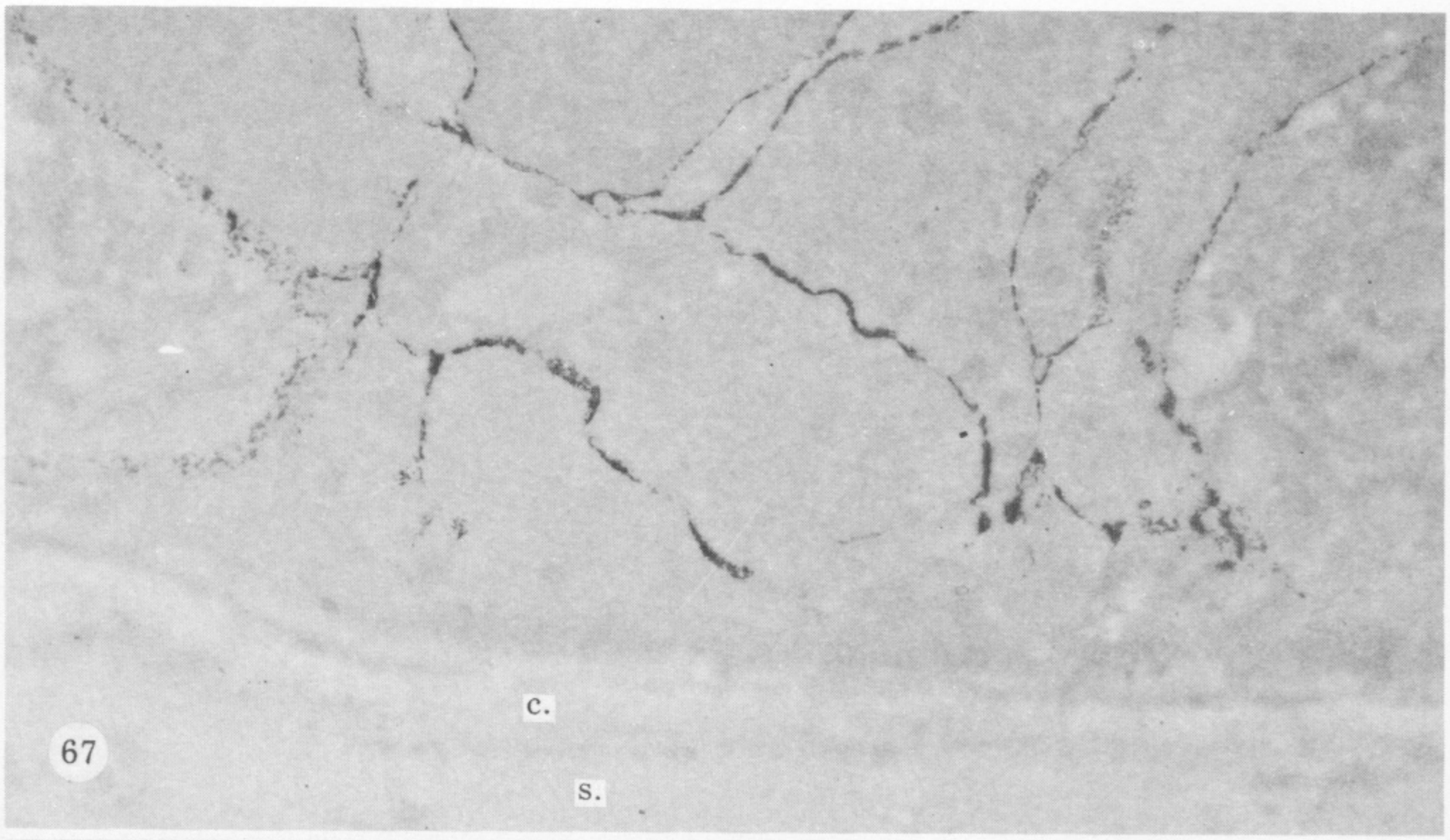


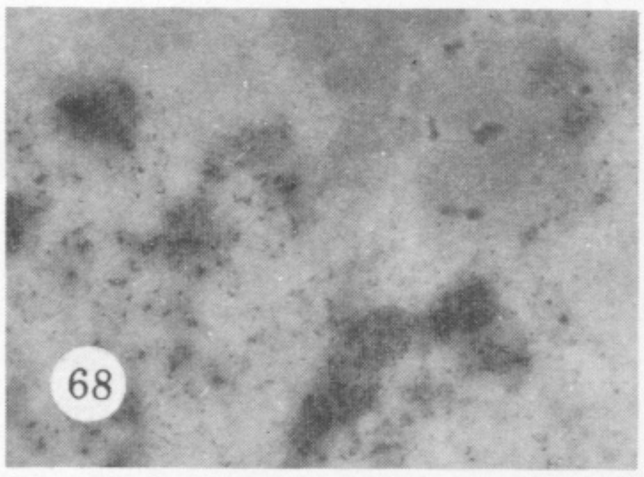


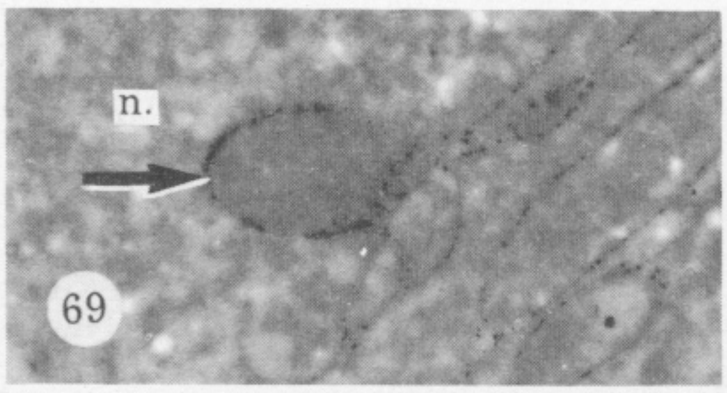


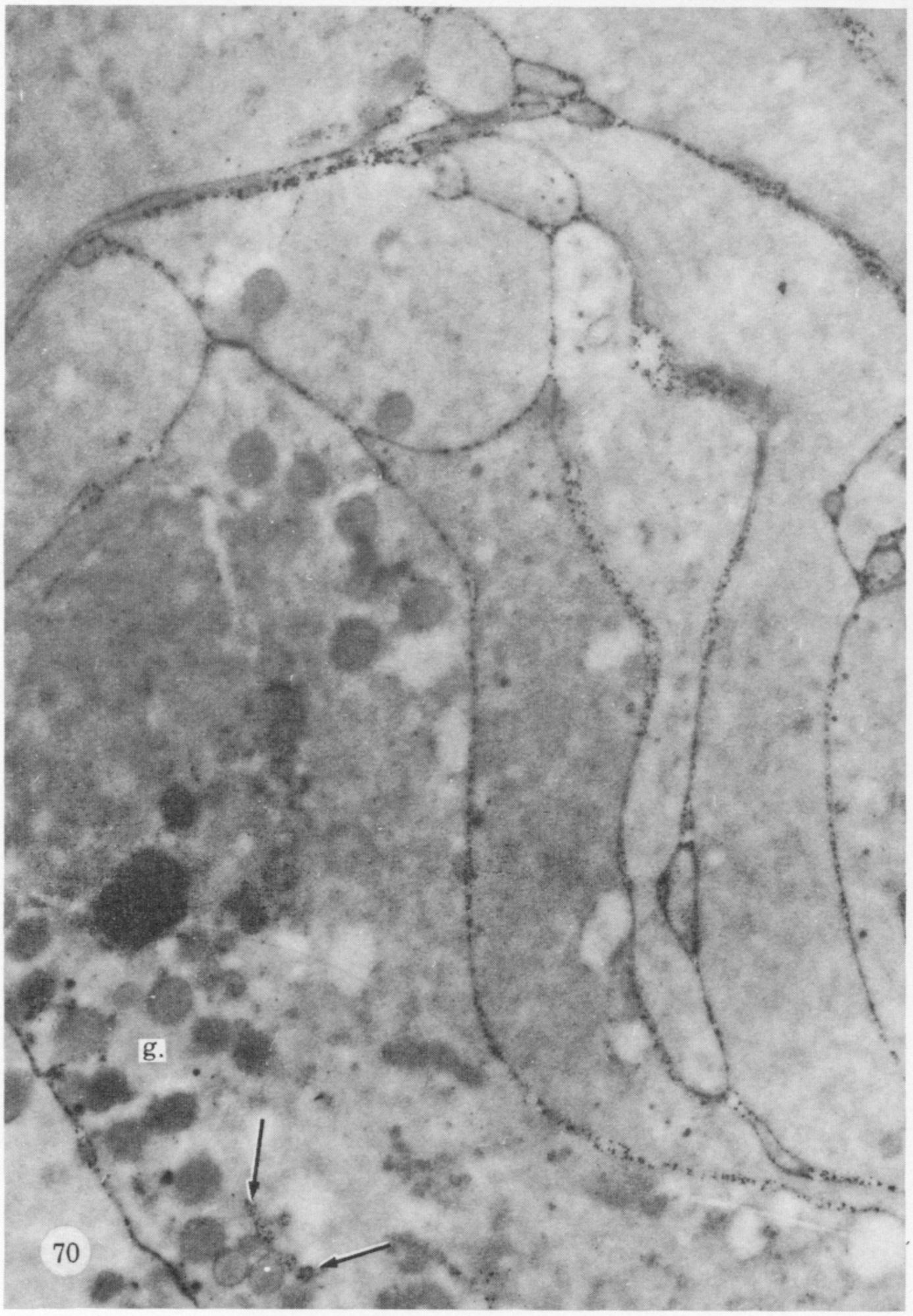


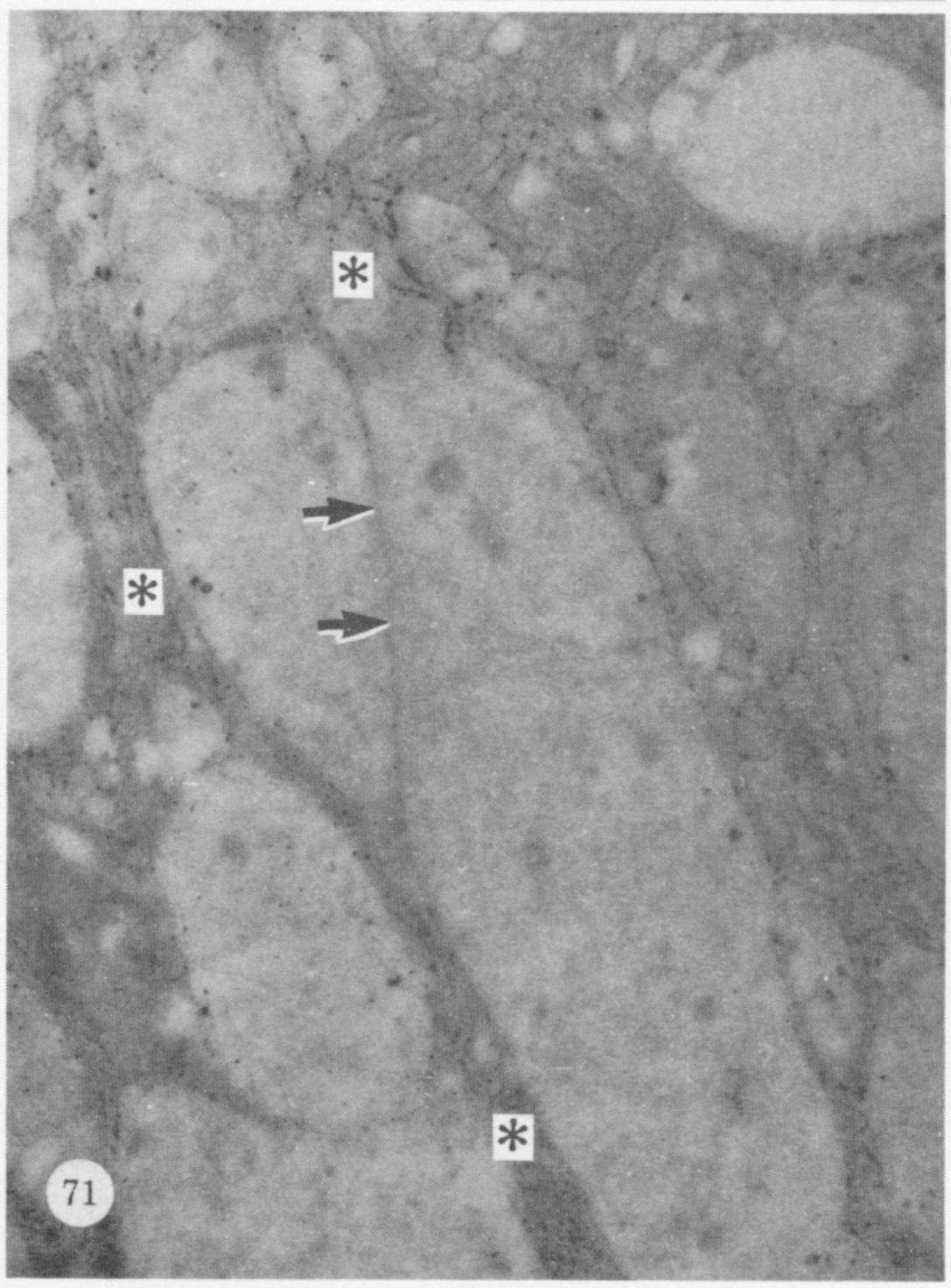


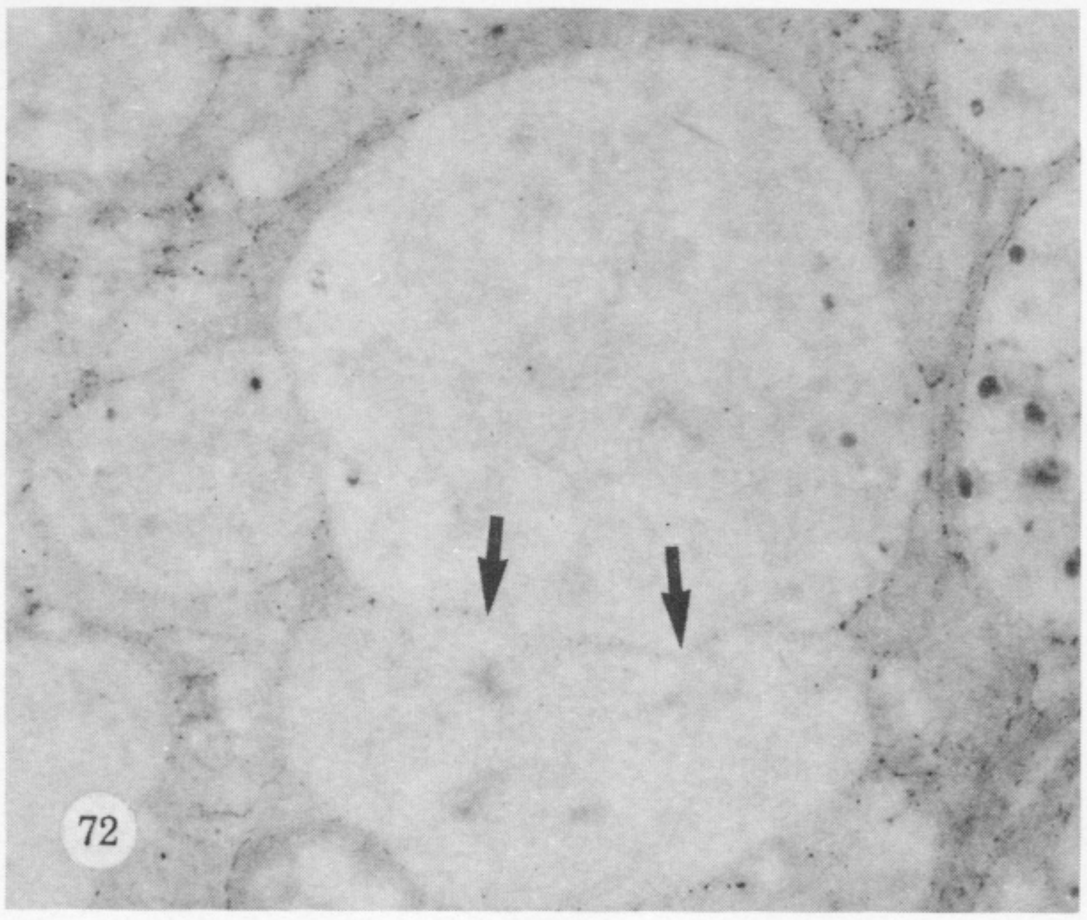


FIGURES 65–72. For description see p. 424.

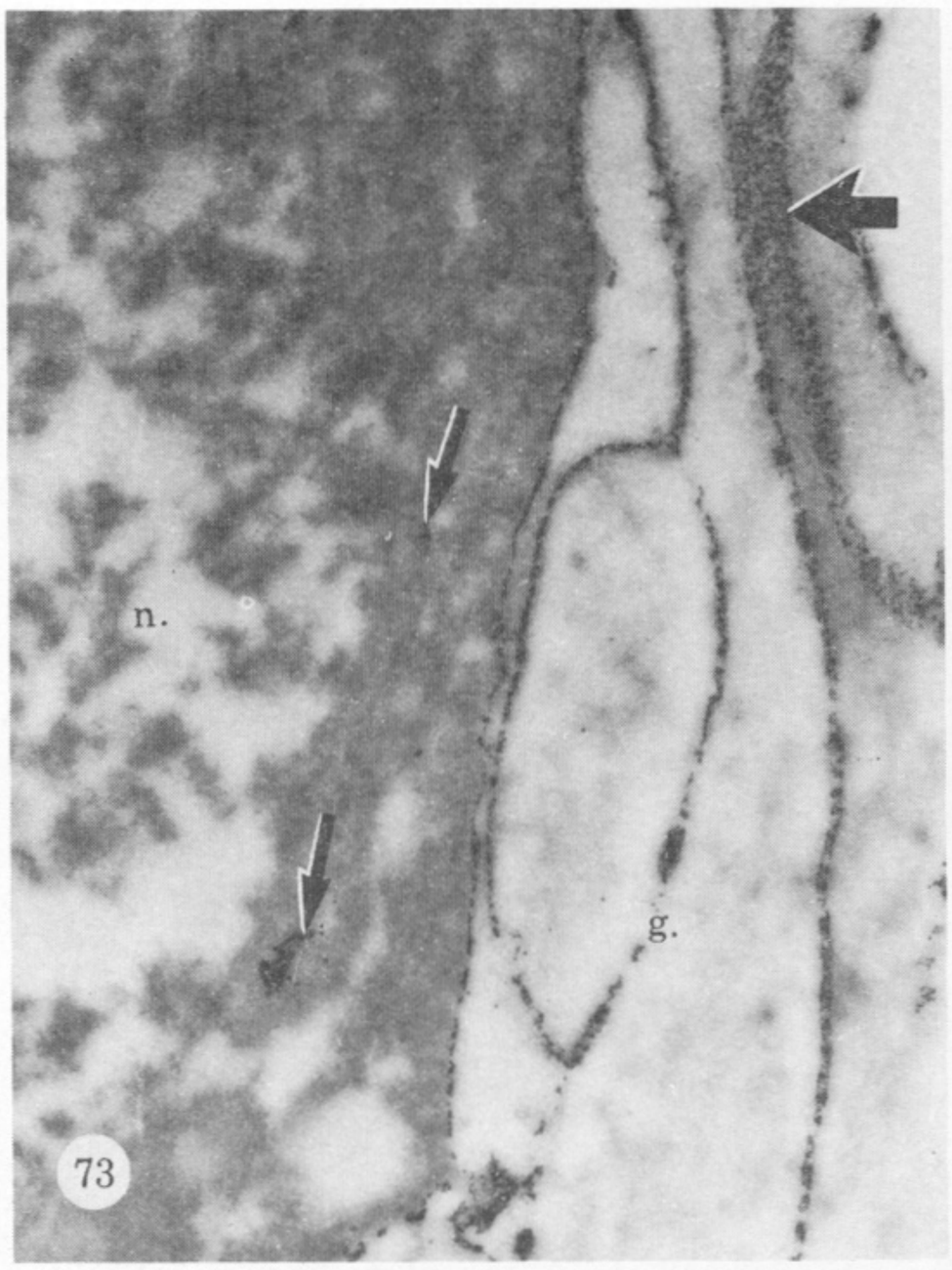


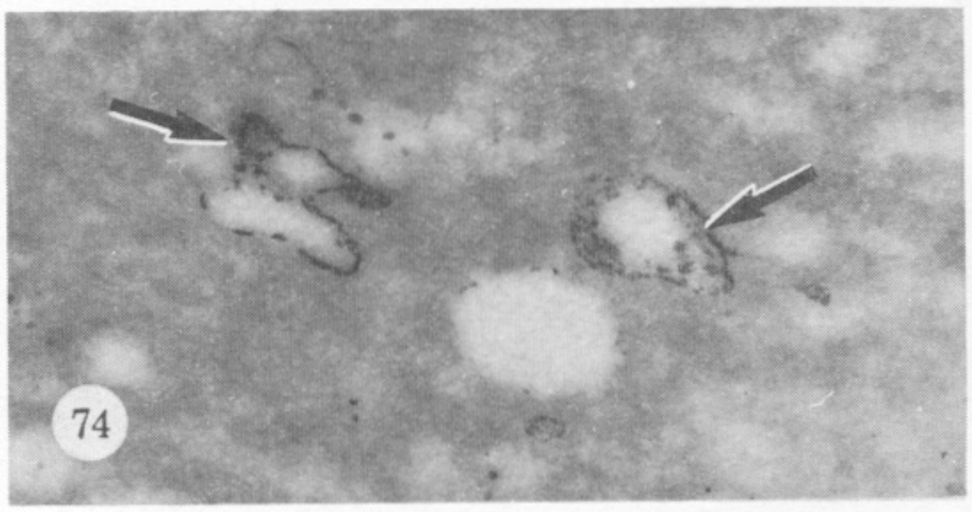


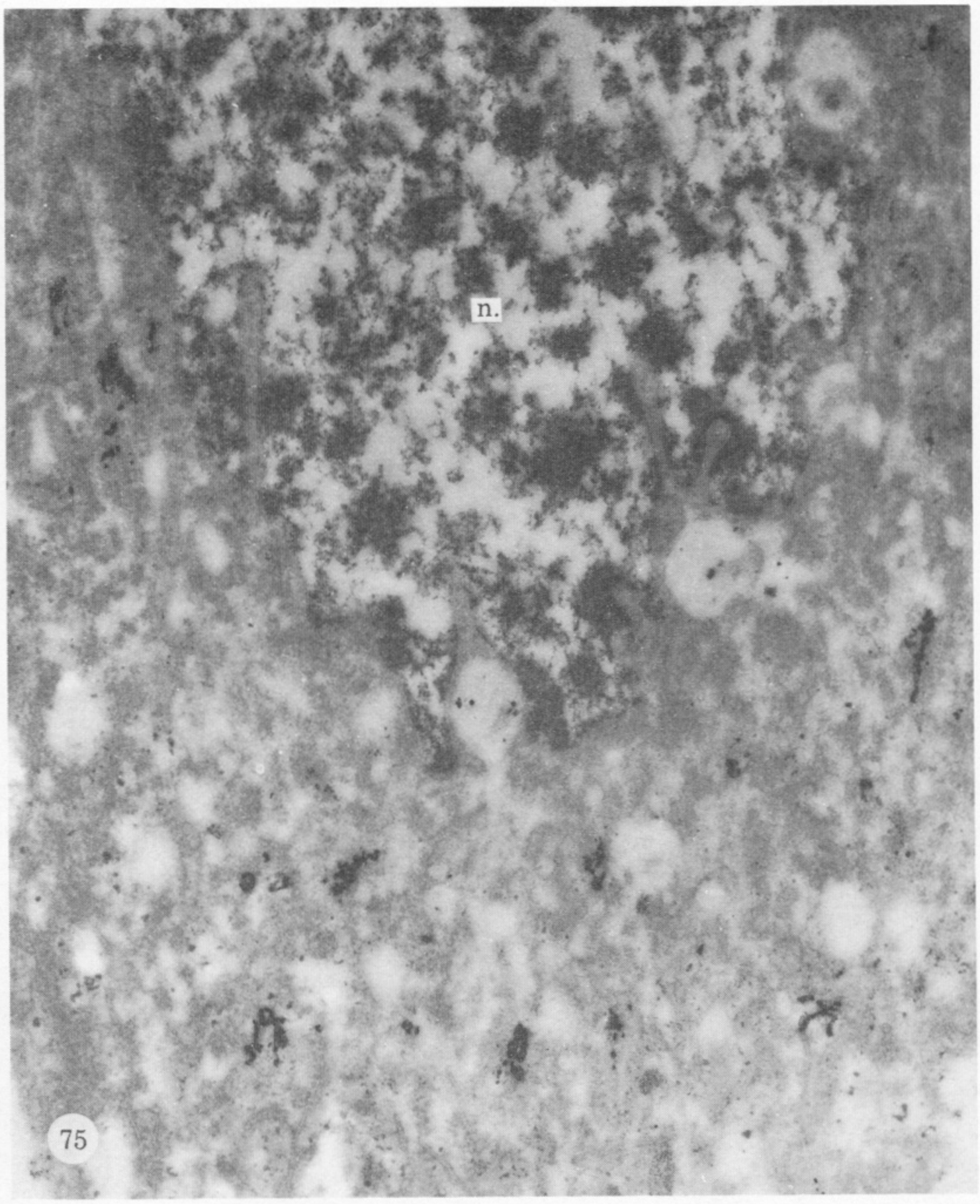


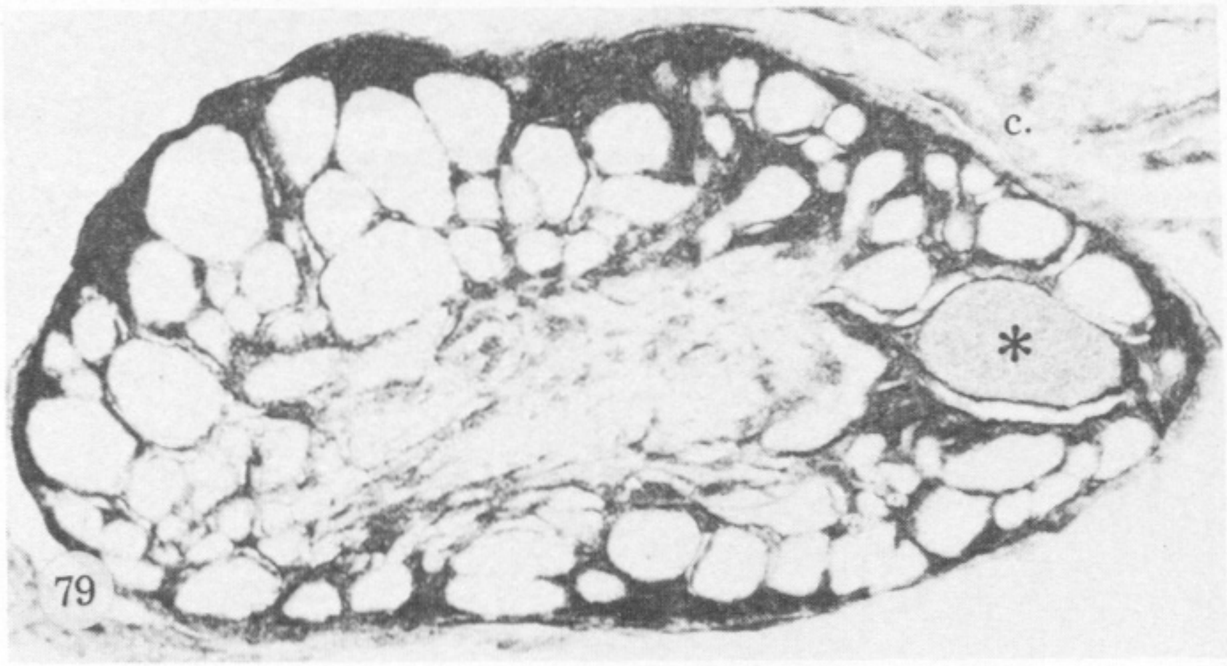


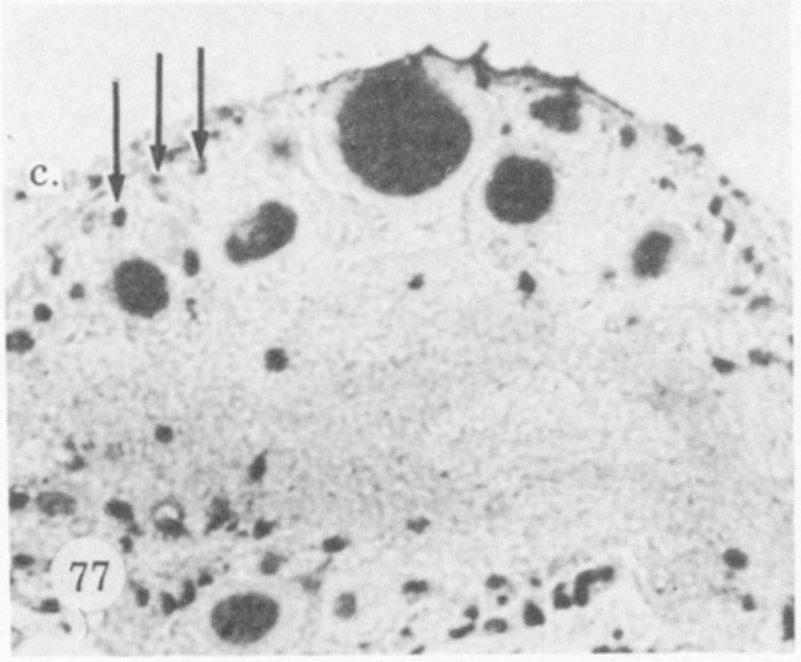


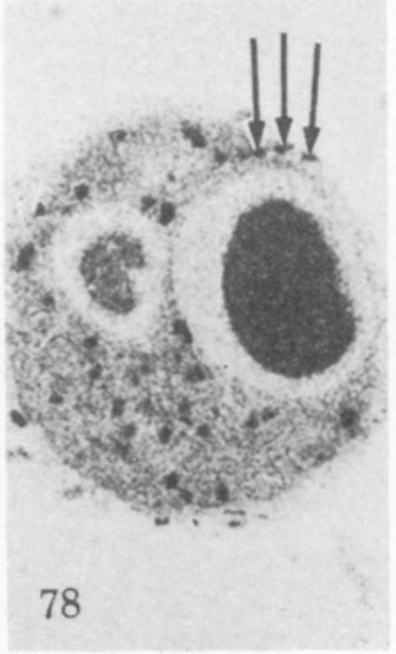



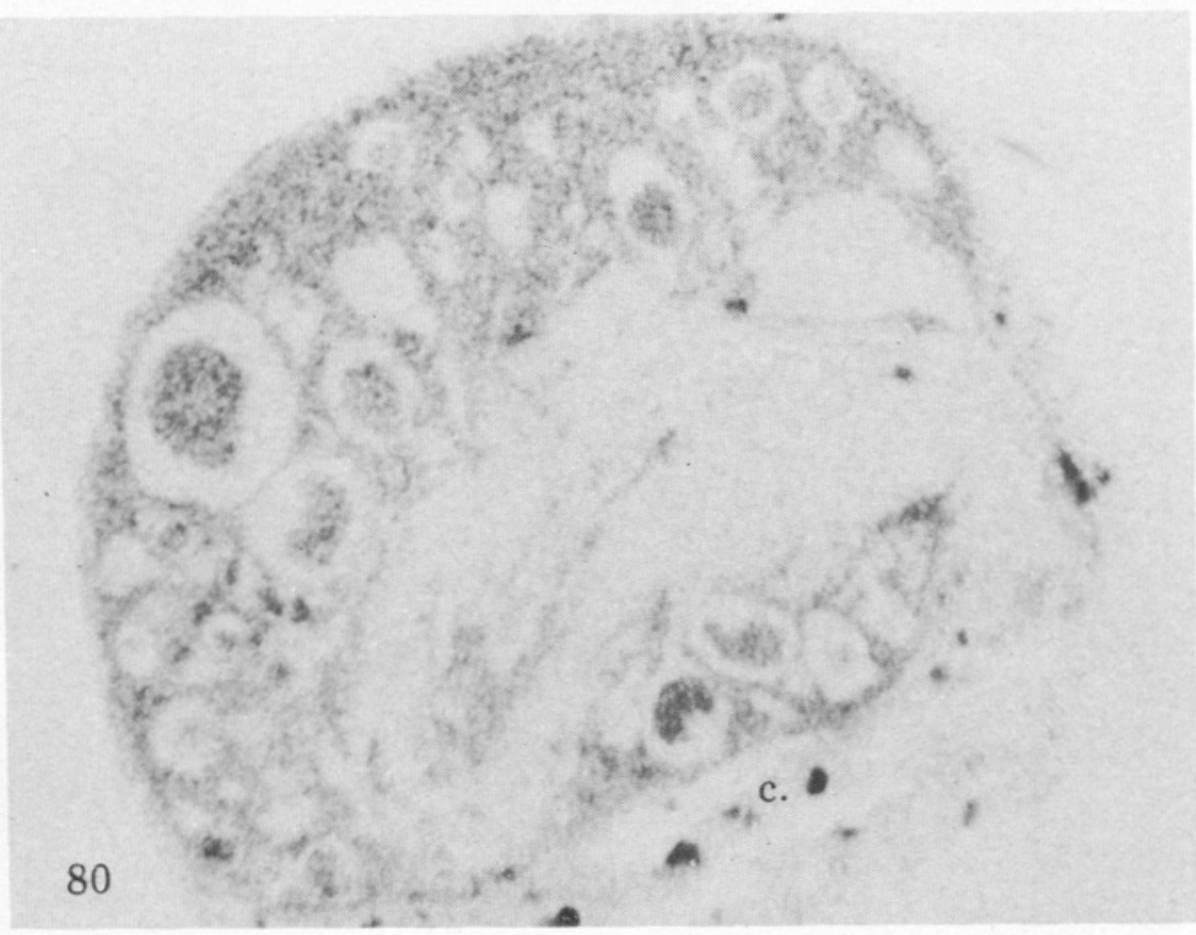


FIGURES 73–80. For description see p. 425.

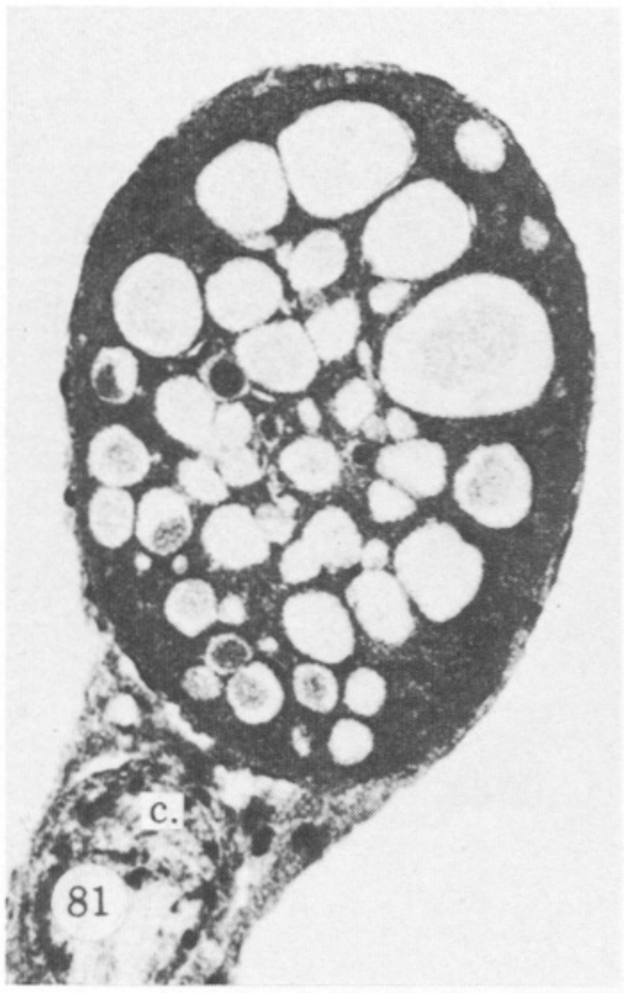



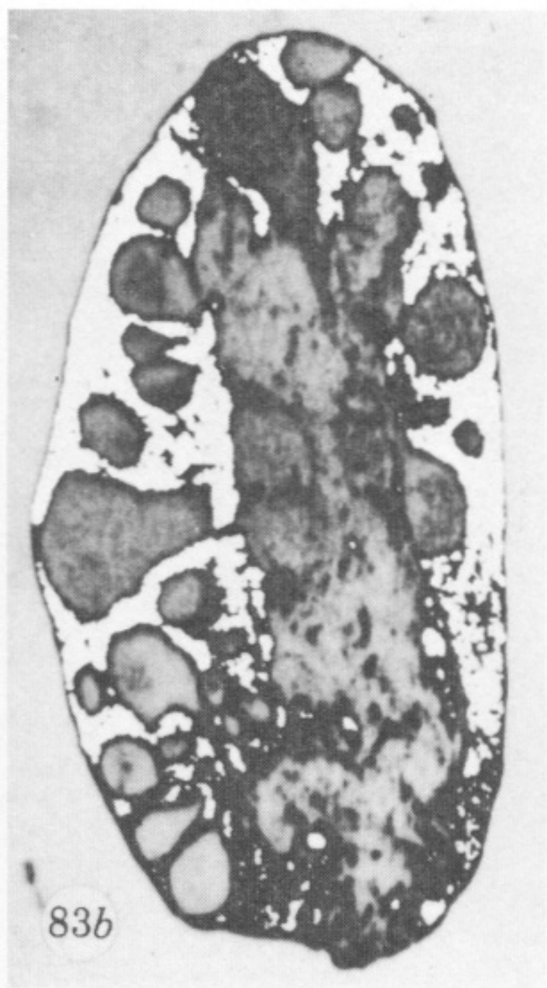


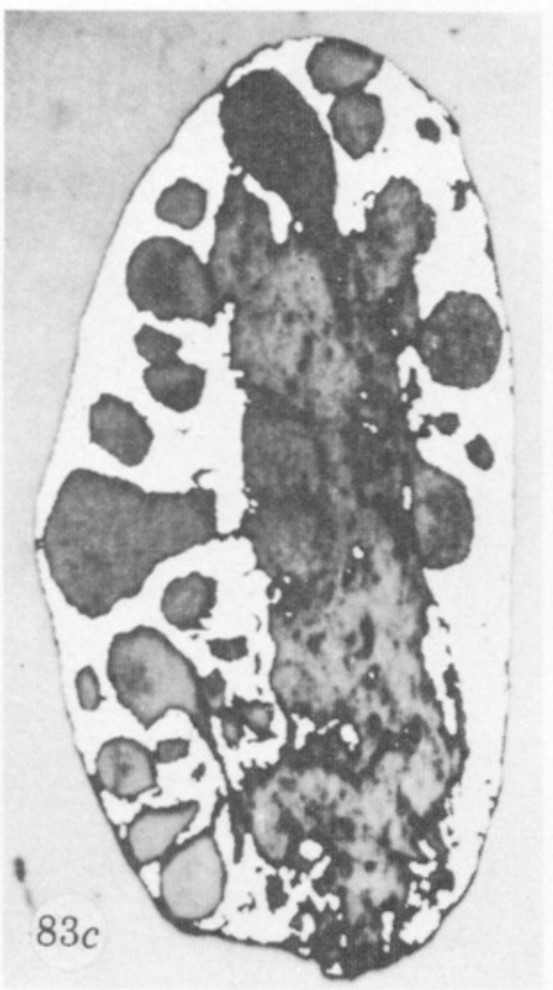


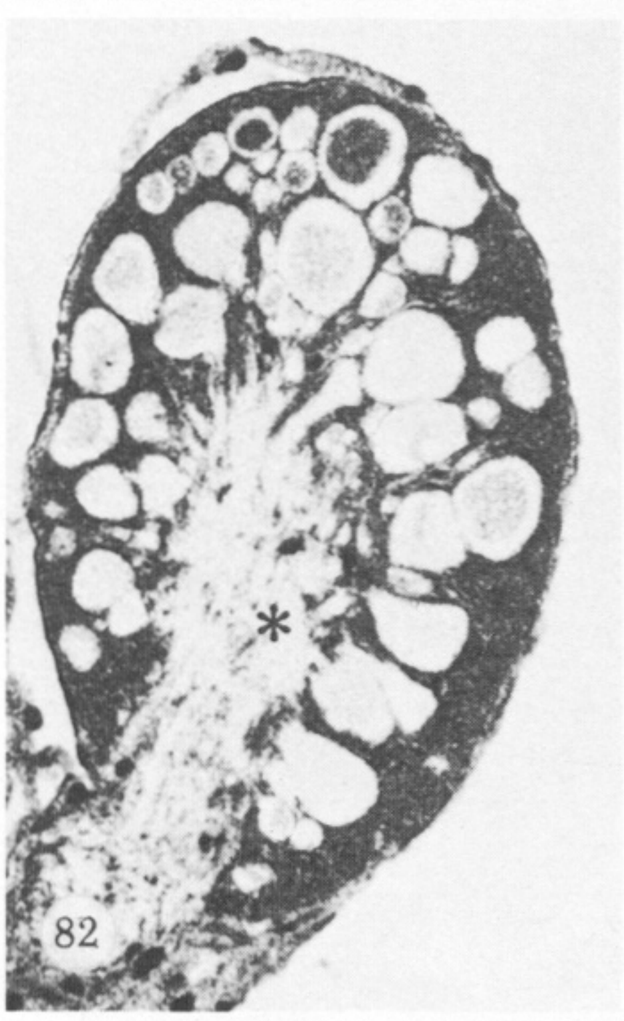


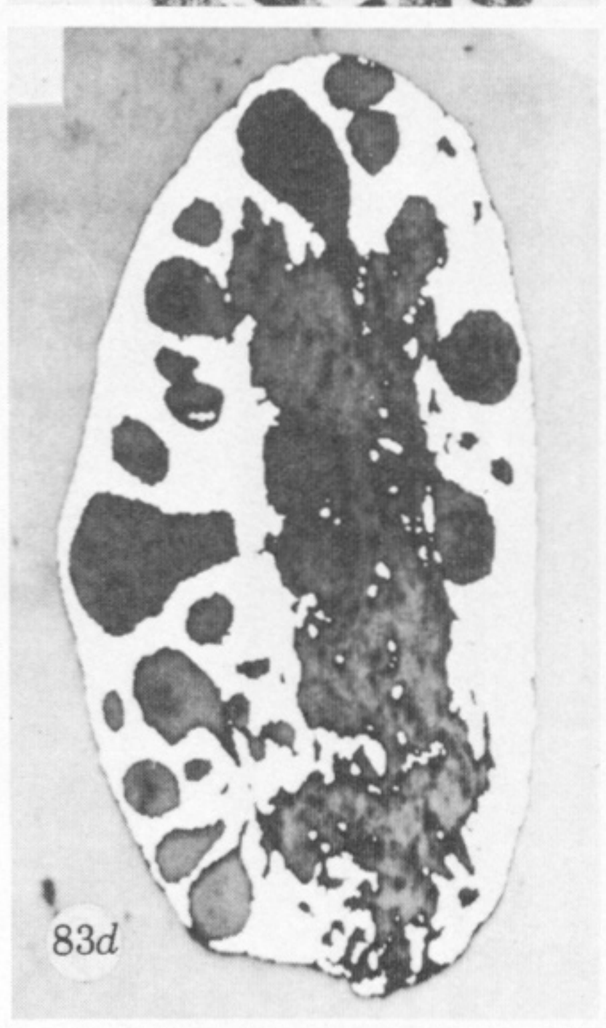


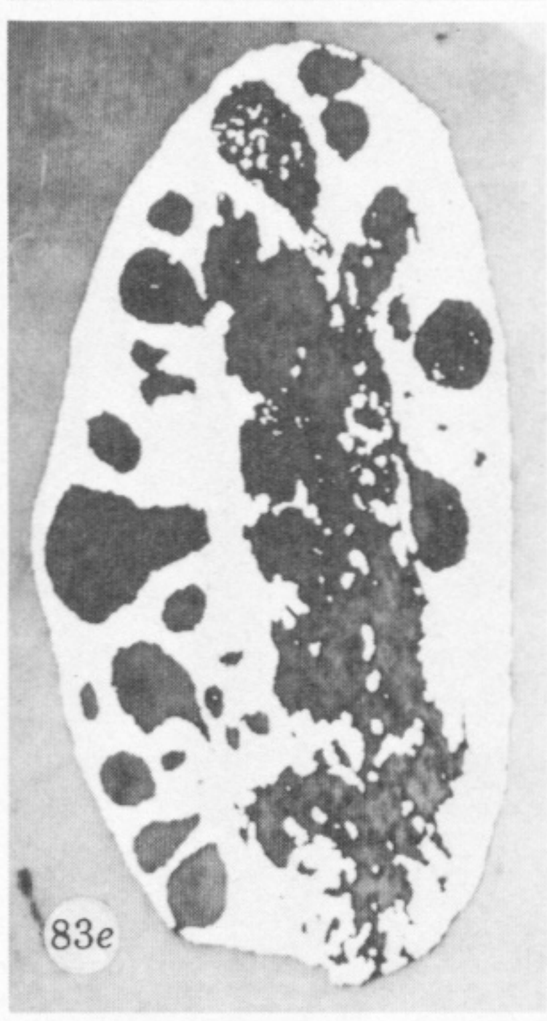



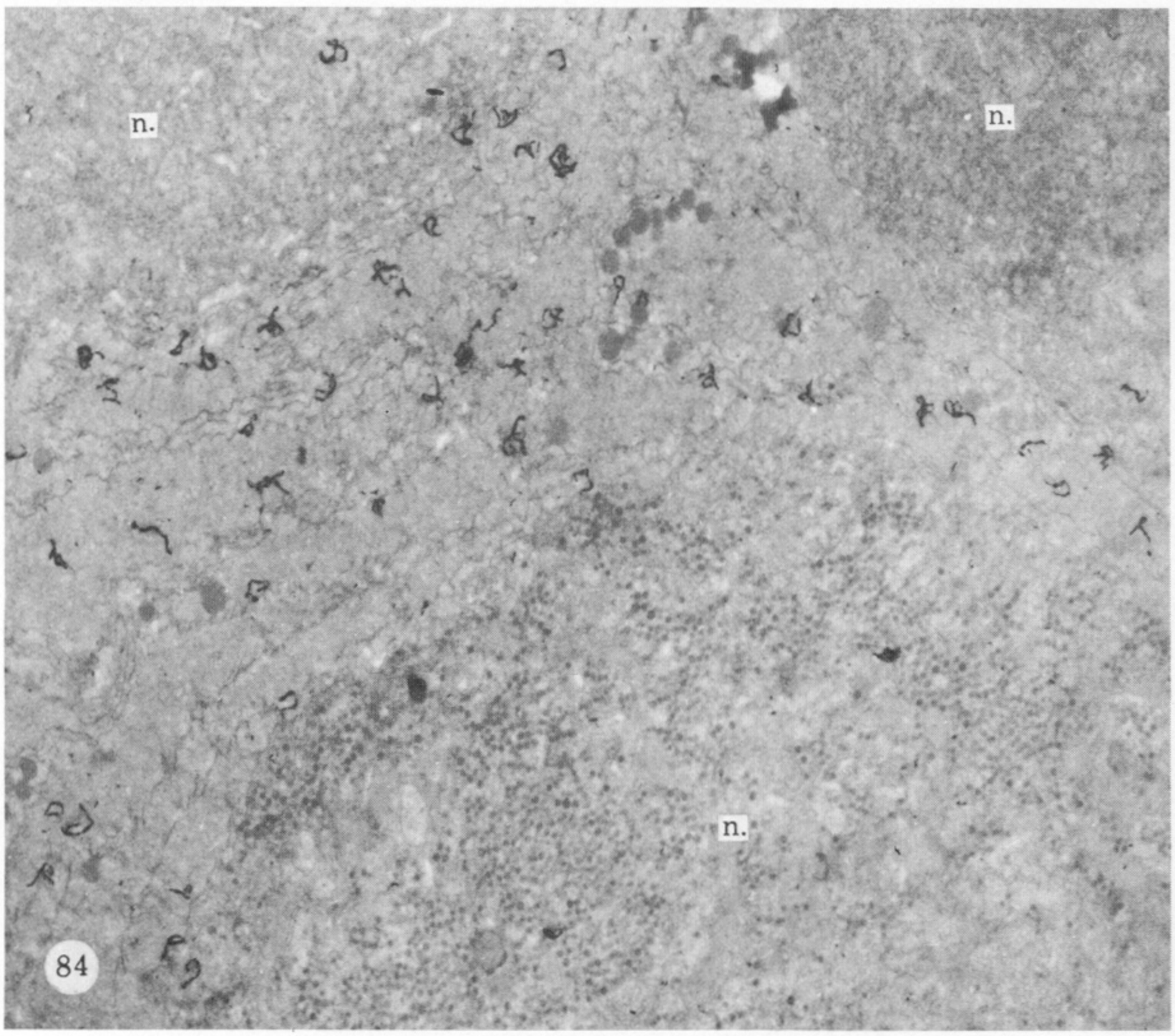


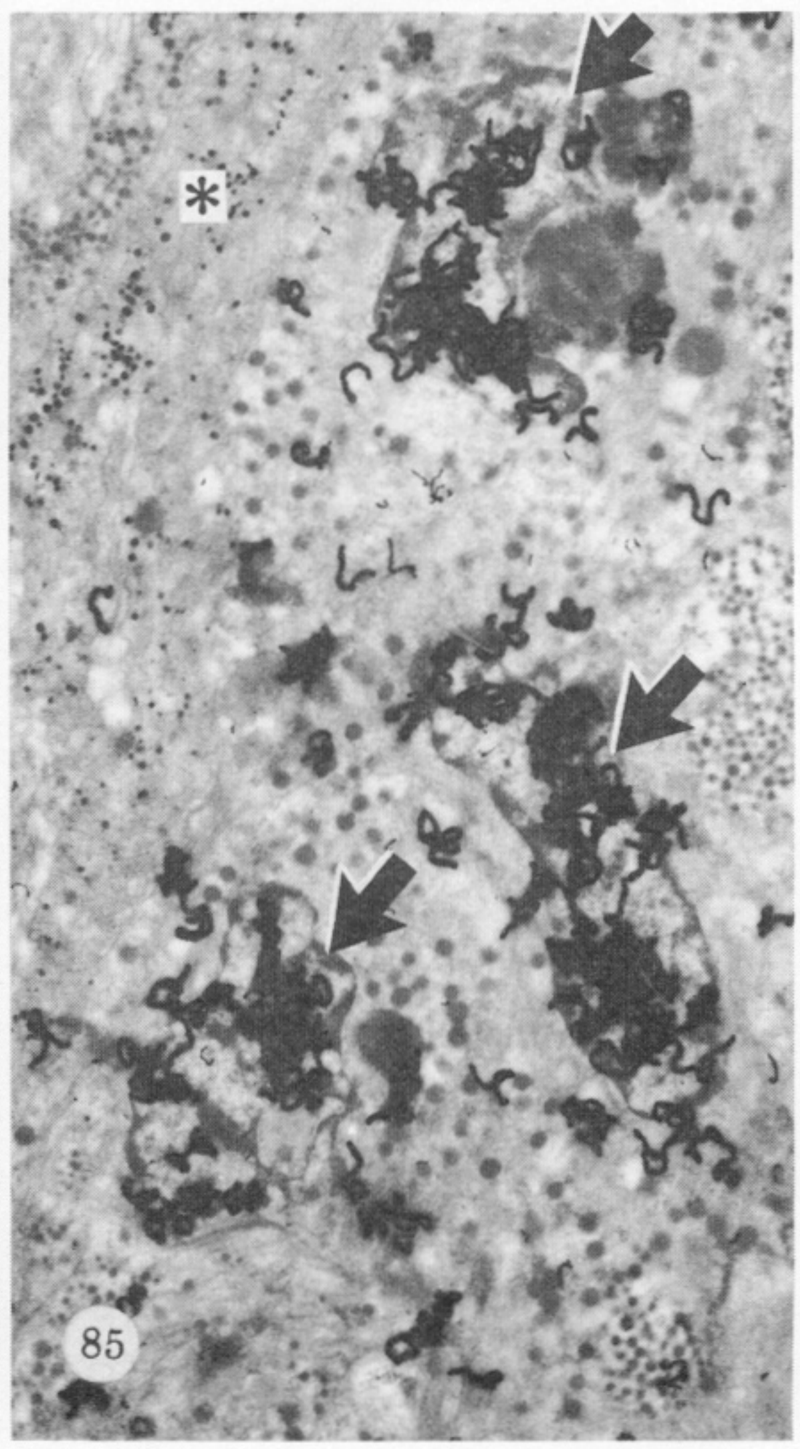


FIGURES 81–85. For description see opposite.